

Figure 6-32. Predicted Z-displacement, liner section, pretest elastic model, 6 months of heating.

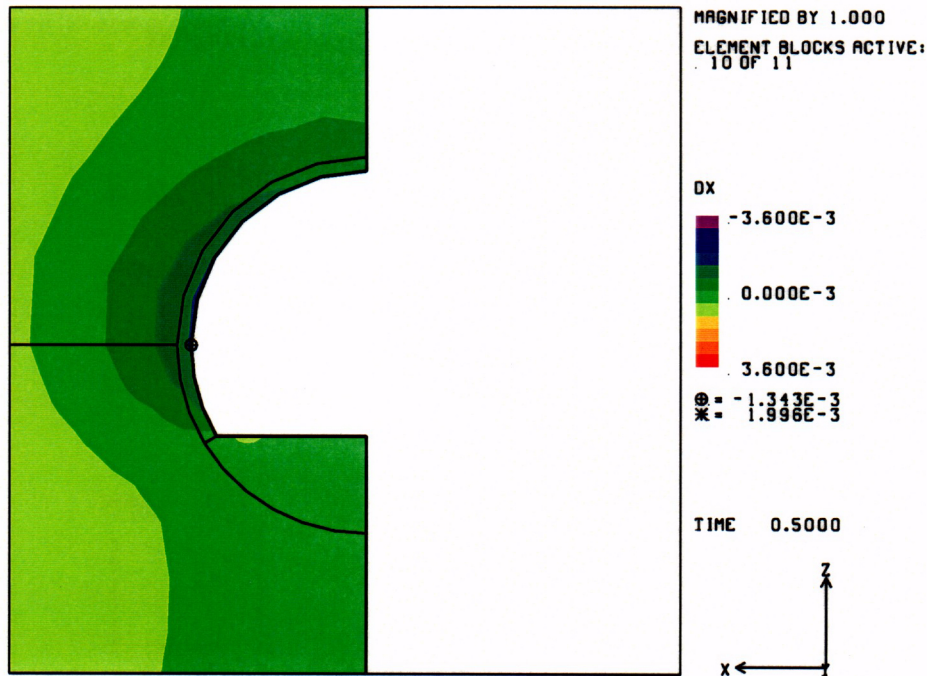


Figure 6-33. Predicted X-displacement, liner section, pretest elastic model, 6 months of heating.

C71

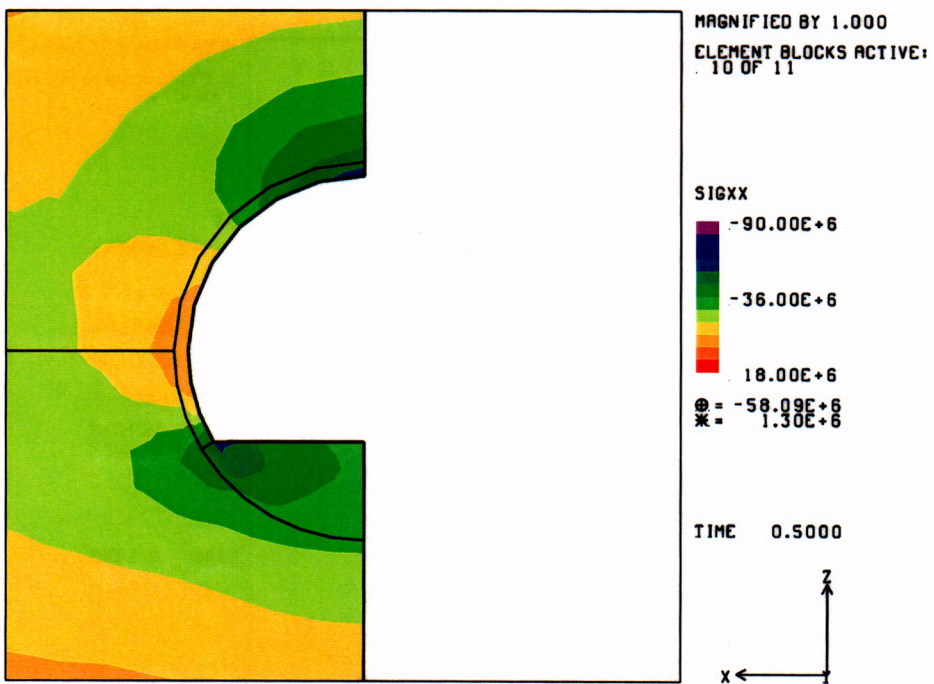


Figure 6-34. Predicted σ_x (horizontal), liner section, pretest elastic model, 6 months of heating.

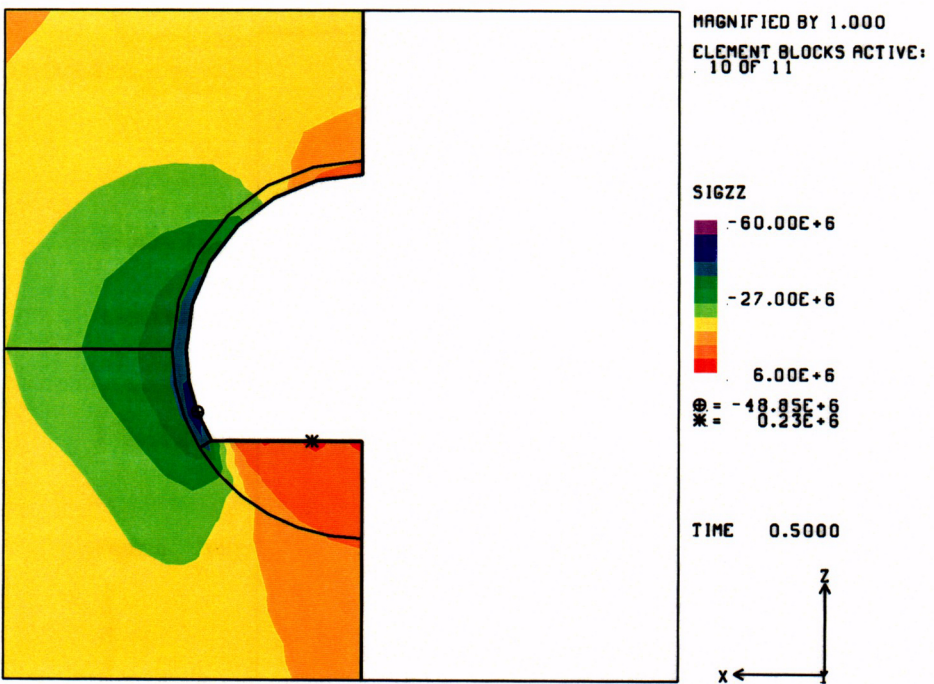


Figure 6-35. Predicted σ_z (vertical), liner section, pretest elastic model, 6 months of heating.

072

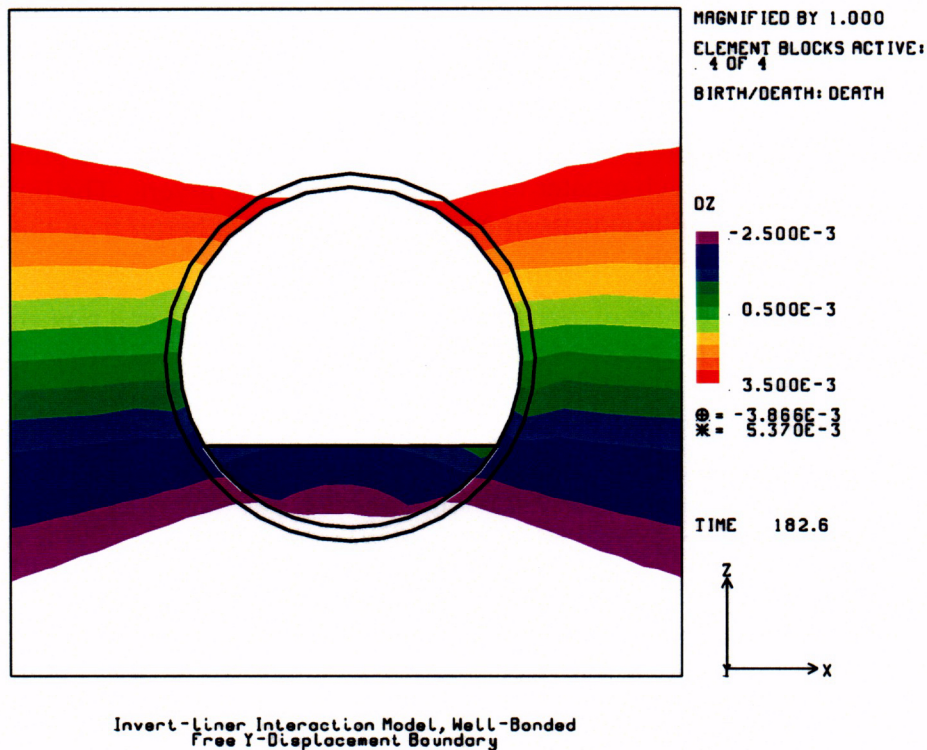


Figure 6-36. Predicted Z-displacement, invert/liner model, free boundary, 6 months of heating.

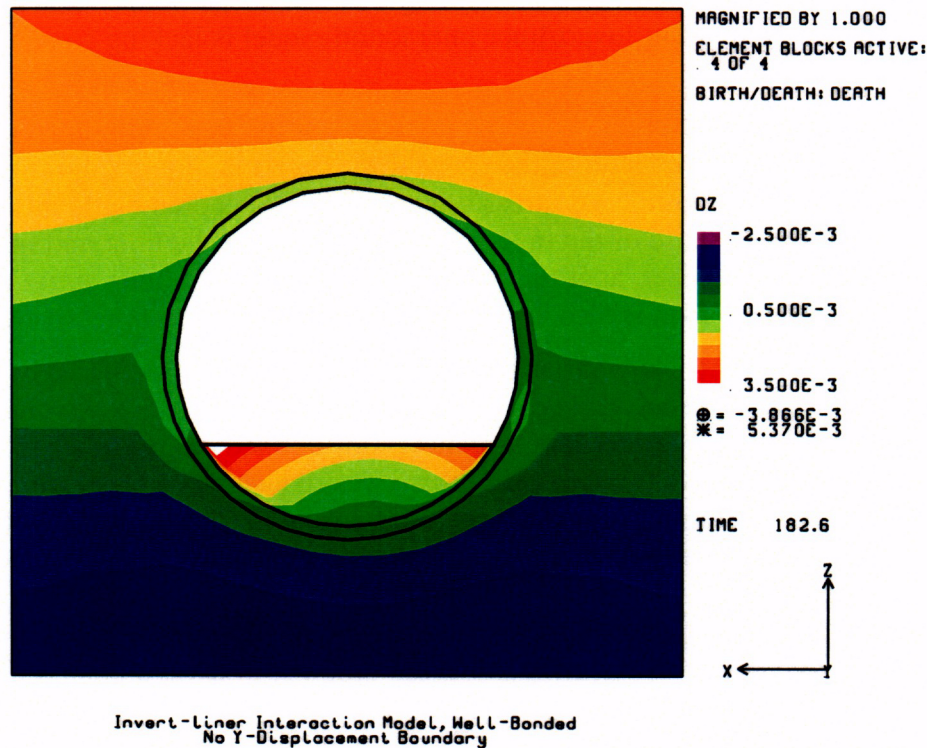


Figure 6-37. Predicted Z-displacement, invert/liner model, pinned boundary, 6 months of heating.

C73

This bowing is better illustrated in Figures 6-38 and 6-39, where the mesh deformations have been magnified by a factor of 100. The free boundary shows a much larger displacement gradient through a vertical cross-section through the rock surrounding the drift than the pinned boundary or the pretest analyses, but a smaller gradient in just the invert section. The gradient through the invert at the pinned boundary is a little greater than the pretest model at the middle of the invert, but much greater toward the sides of the invert. The invert/liner model seems to predict the displacements of MPBX-14 somewhat better than the pretest model, but the improvement is not obvious.

Figures 6-40 and 6-41 show the predicted X displacements at the free and pinned boundaries of the model. A comparison with the pretest model in Figure 6-30 shows some interesting differences. The rock and liner displacements at the pinned boundary are nearly identical to those predicted by the pretest model, whereas the invert displacements are somewhat higher, probably due to the predicted bending of the invert. The predicted displacements at the free boundary are nearly twice those at the pinned boundary. This is due in part to the ability of the liner and invert to expand past the end of the modeled rock.

Figures 6-42 and 6-43 show the predicted horizontal stresses at the free and pinned boundaries of the model. The hoop stress at the crown is of particular interest here. The predicted stress at the crown of the free end is about 48 MPa (ignore the symbol at the top—the plotting program is picking up the maximum at the pinned end). This value is about 10 MPa less than the predicted value from the pretest analyses. Also note the high tension (12 MPa) at the bottom of the invert, indicative of bending. The maximum hoop stress at the pinned boundary is 81 MPa, exceeding the unconfined compressive strength measured in the lab. No failure has yet been detected by the periodic video scanning in the Heated Drift, so this large stress probably indicates that the current invert/liner interaction model is lacking some necessary physics.

Figures 6-44 and 6-45 show the predicted vertical stresses at the free and pinned boundaries of the model. The hoop stress in the liner at the rib near the invert is of particular interest here. For the free boundary, a maximum hoop stress of about 21 MPa is predicted. Also note the tensile stress of 4 MPa in the base of the invert; this indicates that the liner and invert are being pulled away from each other, as if they were well-bonded. The hoop stress at the pinned boundary is about 65 MPa, which is also larger than the unconfined compressive strength.

The invert/liner interaction model, as described above, does not necessarily predict a separation between invert and liner. However, as Figures 6-44 and 6-45 make clear, the input parameters used for these calculations approximate a well-bonded interface. A second calculation was performed where the separation force was reduced to 3 MPa, which is less than the 4.21 MPa tensile stress shown in Figures 6-44 and 6-45. In these calculations, the invert and liner separated, and the calculations did not converge. The unconverged solution's predictions for Z-displacement are shown in Figure 6-46. With no magnification, there is visible separation between the invert and liner (about 90 mm). The elastic-only model used for the rock and concrete cause the invert to “ride” on the liner at two points in this view. This representation of a poorly bonded interface between invert and liner indicates that the behavior shown in the MPBX14 data is probably debonding at the invert/liner interface (though certainly not to the magnitude predicted here!).

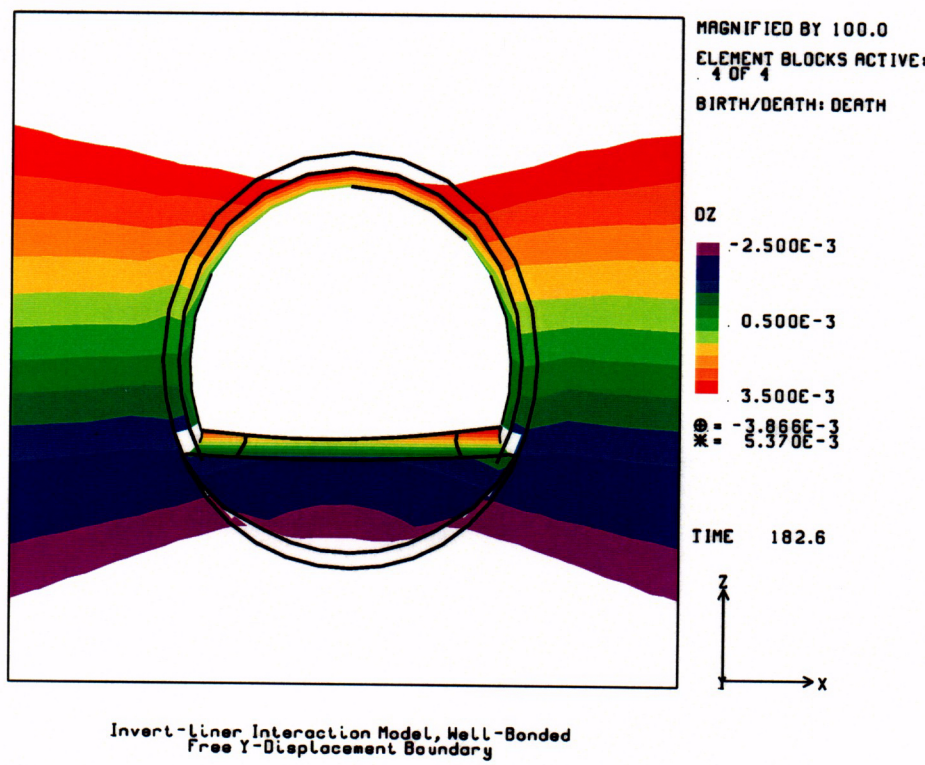


Figure 6-38. Predicted Z-displacement, invert/liner model, free boundary, magnified mesh deformation.

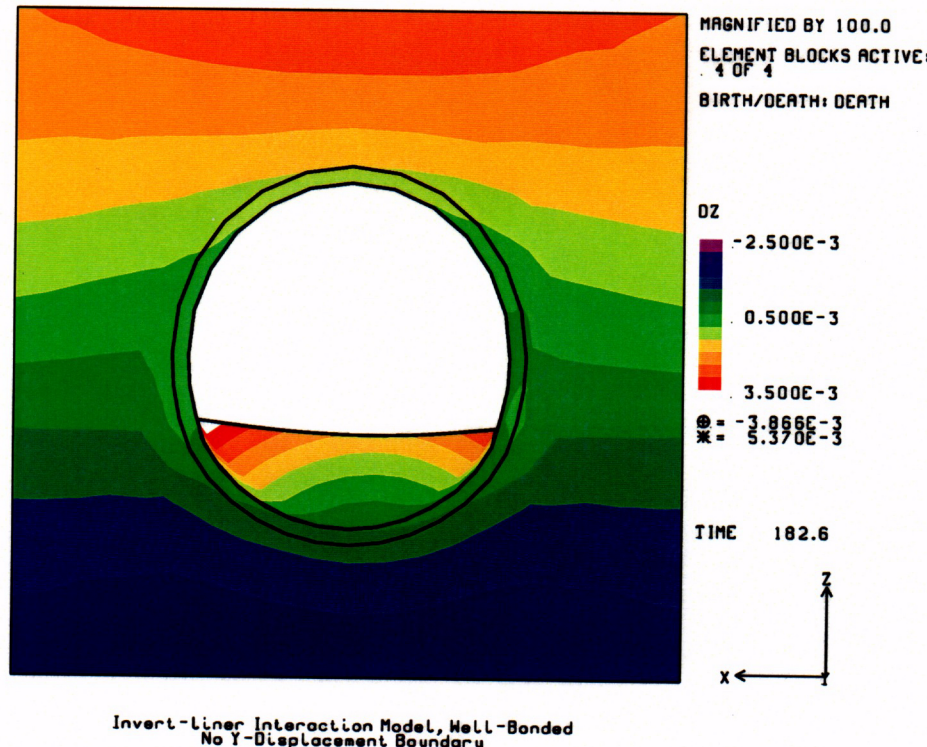


Figure 6-39. Predicted Z-displacement, invert/liner model, pinned boundary, magnified mesh deformation.

⑦4

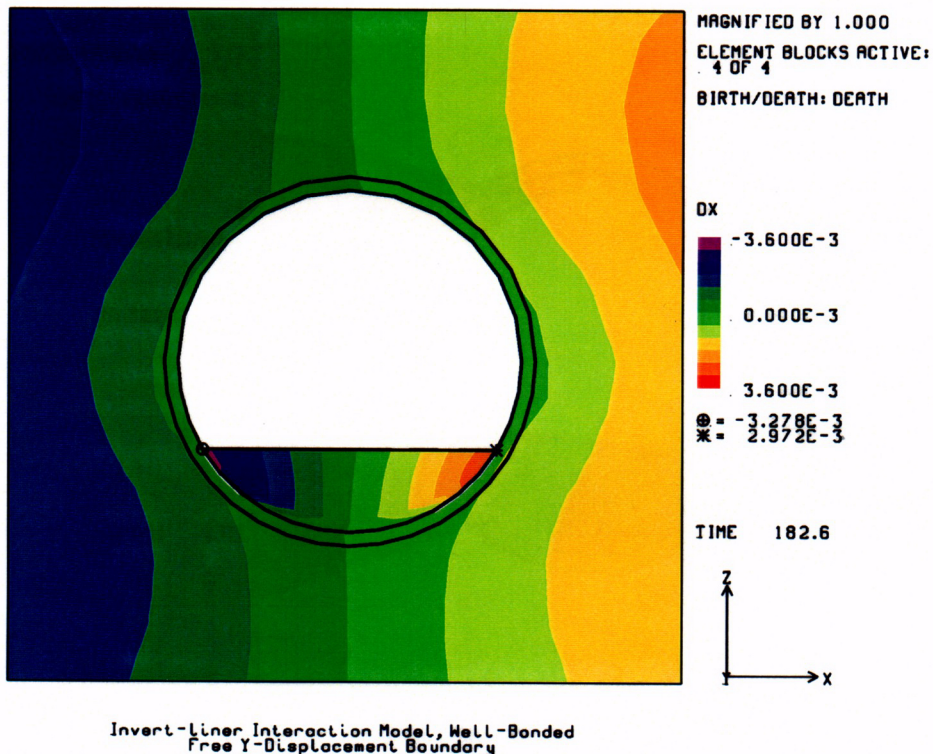


Figure 6-40. Predicted X-displacement, invert/liner model, free boundary, 6 months of heating.

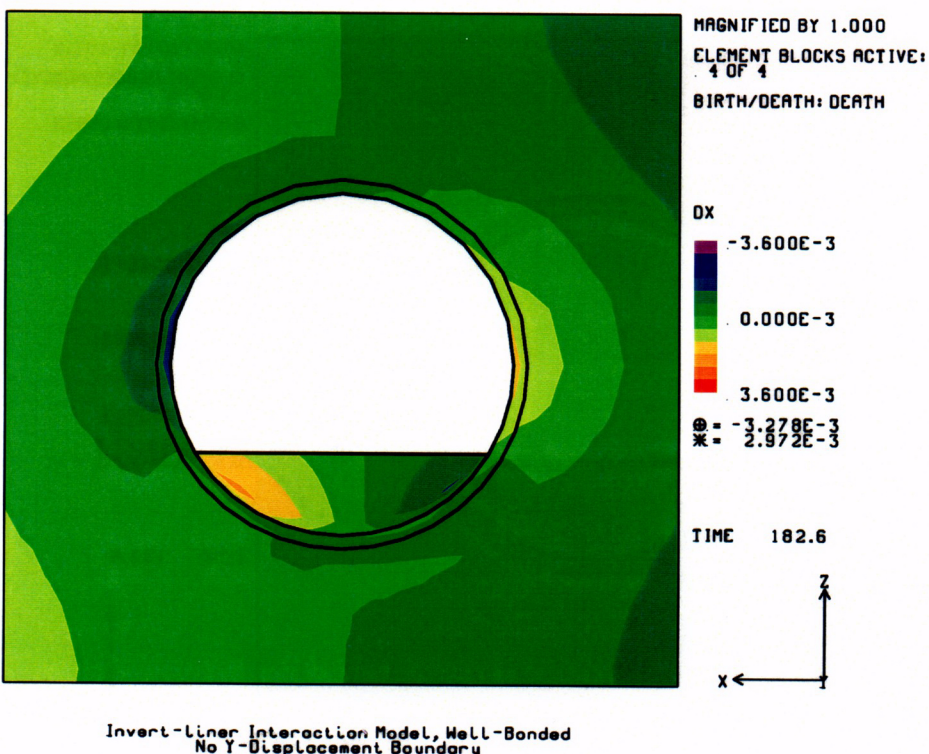


Figure 6-41. Predicted X-displacement, invert/liner model, pinned boundary, 6 months of heating.

C 75

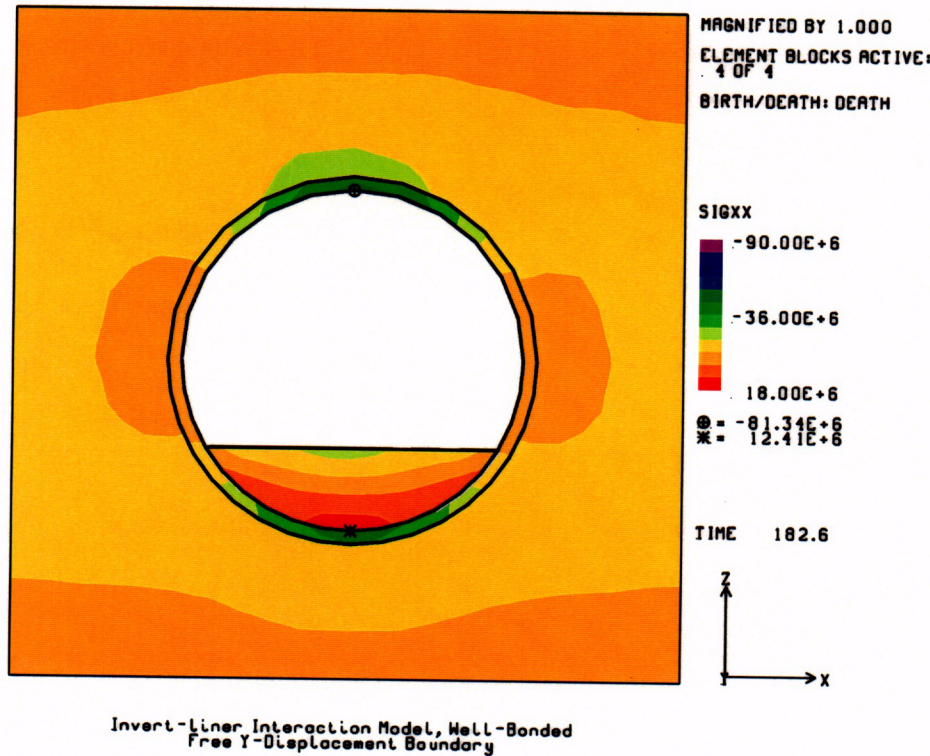


Figure 6-42. Predicted σ_x (horizontal), invert/liner model, free boundary, 6 months of heating.

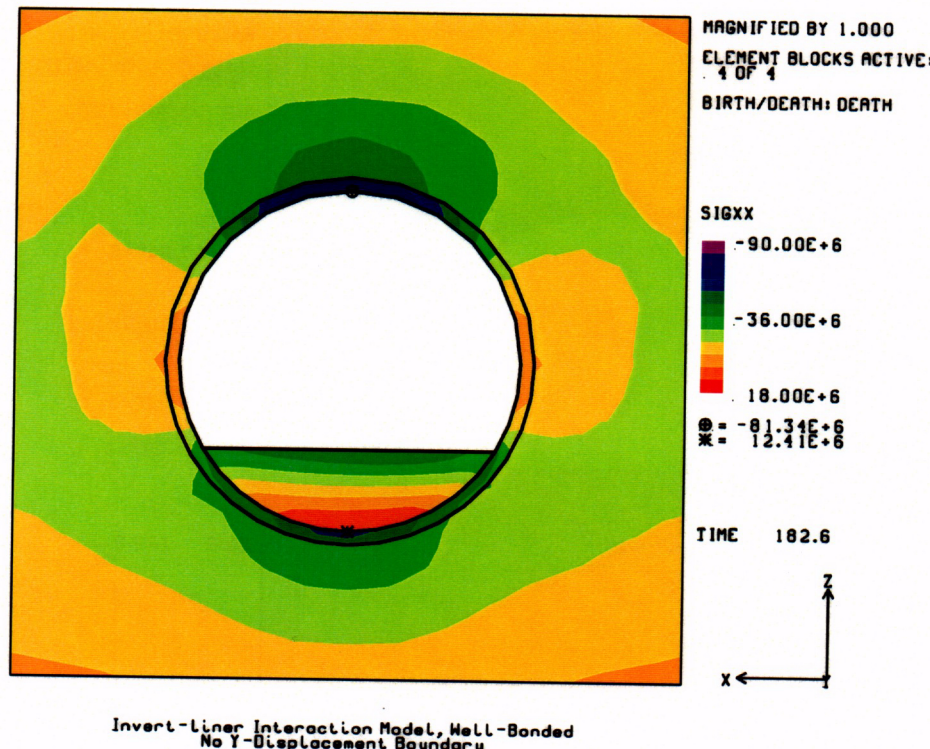


Figure 6-43. Predicted σ_x (horizontal), invert/liner model, pinned boundary, 6 months of heating.

⑦6

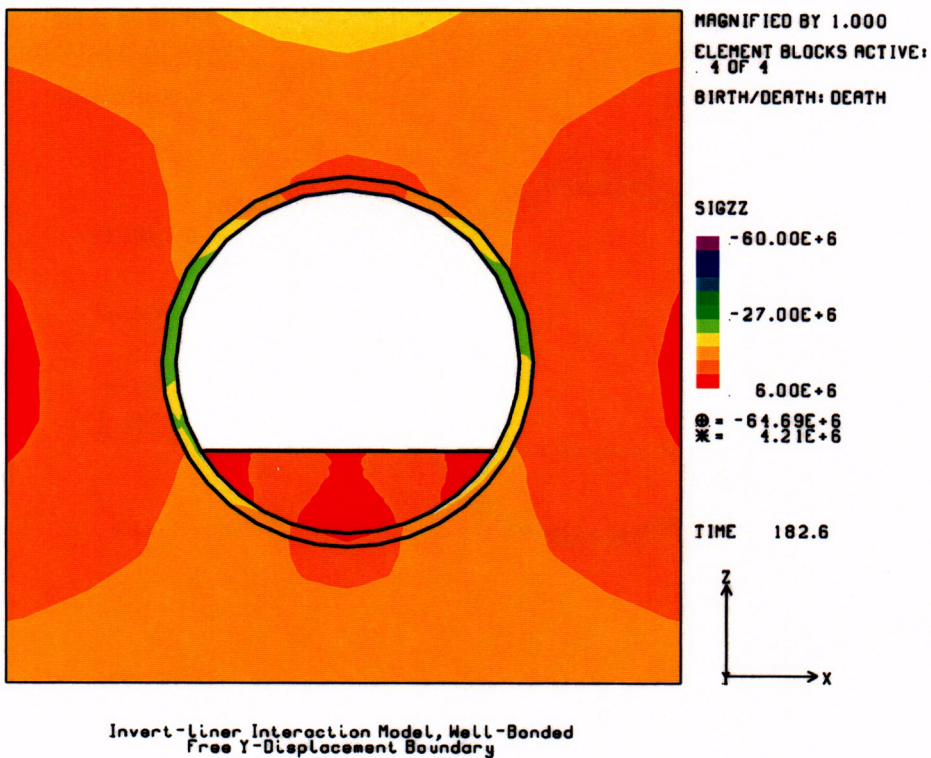


Figure 6-44. Predicted σ_z (vertical), invert/liner model, free boundary, 6 months of heating.

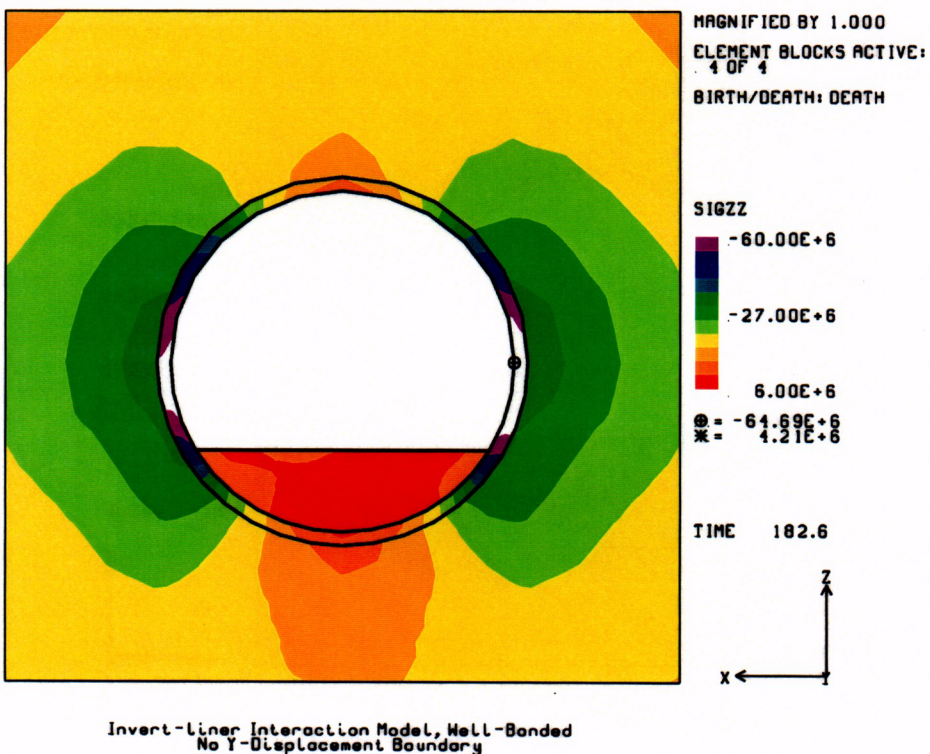


Figure 6-45. Predicted σ_z (vertical), invert/liner model, pinned boundary, 6 months of heating.

C77

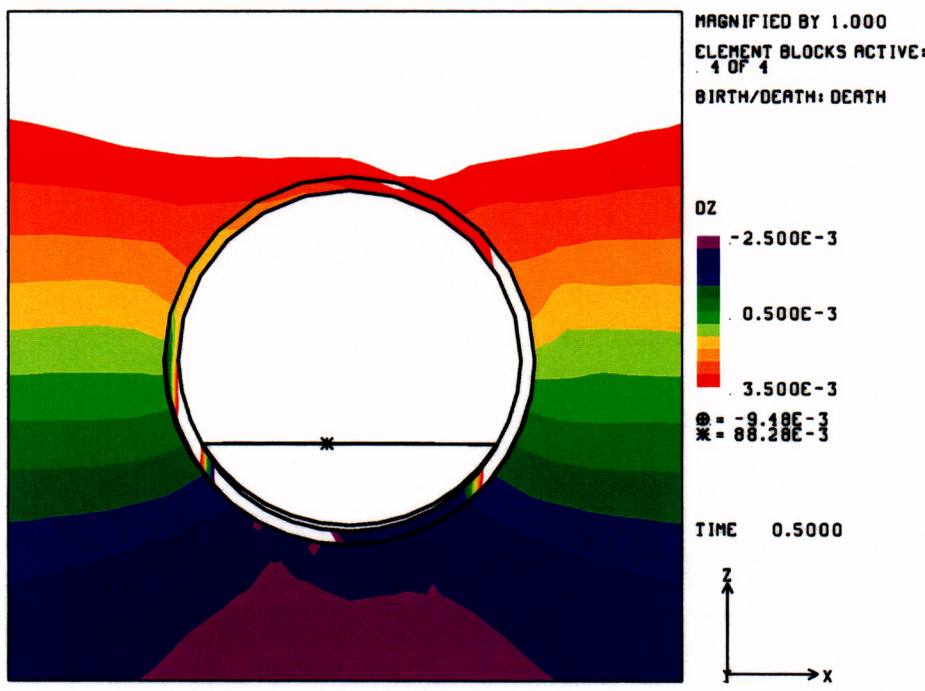


Figure 6-46. Predicted Z-displacement, invert/liner model, poorly bonded, 6 months of heating.

The measured displacement behavior of the invert is somewhere between that characterized by the well-bonded and poorly bonded models discussed here. Also, the strain gage data indicate the liner stresses appear to be less than predicted in any of the models described thus far. The physical representation of the invert/liner interaction in this model can be improved in several ways; these improvements will be developed in the near future:

- realistic stress boundaries at the ends of the modeled tunnel
- implementation of an elastic/plastic model with supporting data, to allow deformation of the invert during debonding and possibly increase the likelihood of convergence
- implementation of a creep model for concrete with laboratory data at elevated temperature and load (a preliminary implementation is discussed in the next section).

6.2.4 Potential Effects of Creep on Stresses in the Concrete Liner

Because of concerns about possible overstressing of the concrete liner in the Heated Drift, it was decided to perform a revised analysis using the models developed for the pre-experiment analysis (Francis et al., 1997) and the JAC3D code (Biffle, 1983) taking into account creep of the concrete liner. This section describes a preliminary creep model for the concrete liner for use with JAC3D. Because there are no test data available at the present time for the creep behavior of the concrete used in the tunnel liner and invert, information available in the literature on creep of concrete is

C 78

used as the basis for the concrete liner and invert model. (An interim report on laboratory creep measurements of concrete samples can be found in Appendix E.)

One of the standard material models available in JAC3D is a temperature-dependent secondary creep model (Material Type 3). In this model the effective creep strain rate, D_c , is represented by the scalar equation:

$$D_c = A_1 \cdot \sigma_c^{A_2} \cdot e^{\left(-\frac{A_3}{\theta}\right)} \quad (6-4)$$

where

A_1	=	the creep constant
A_2	=	the stress exponent
A_3	=	the thermal constant
σ_c	=	the effective stress, and
θ	=	the absolute temperature

This relationship can also be expressed as follows:

$$D_c = A \bar{\sigma}^n \exp(-Q/RT) \quad (6-5)$$

where

D_c	=	the creep strain rate
A, n	=	constants obtained from fitting the model to creep data (equal to A_1 and A_2)
Q	=	the effective activation energy (kcal/mole)
R	=	the universal gas constant (1.987 cal/mole-K)
T	=	the absolute temperature, and
σ	=	the effective von Mises stress

A , n and Q are obtained experimentally and have not been determined for the concrete drift liner and invert.

Unconfined compression tests on the liner and invert concrete (DTN SNL23030598001.001, TDIF No. 306714) yielded the results presented in Table 6-2. In lieu of creep test data, the literature was surveyed for data that could be used for a preliminary evaluation of the effect of creep on the DST liner response. Creep tests of concrete with comparable strength and at the range of temperatures of interest were conducted by the Portland Cement Association for Hanford concrete (Henager et al., 1988). Strains were measured for concrete specimens at three load/temperature combinations: 1500psi/250°F, 500psi/350°F and 1500psi/350°F. These data were used to develop an equation for predicted strain:

$$\hat{\epsilon}_{cr} = a_0 - \hat{\epsilon} \quad (6-6)$$

$$\hat{\epsilon} = 3064.152 - 0.863 L - 6.125 T - 127.526 \log_e(t+1) \quad (6-7)$$

where

\hat{e}_{cr}	=	the computed creep strain at t days (in millionths)
a_0	=	the initial strain at 0 days (in millionths)
e	=	the measured strain at t days (millionths)
L	=	the load (or effective stress) (in psi)
T	=	the temperature (in °F)
t	=	the time (in days)

The creep strain and creep strain rates predicted by these equations are shown in Figures 6-47 and 6-48. A comparison of Equations 6-4 or 6-5 with the PCA data fit (Equations 6-6 and 6-7) indicates the difference in the form of the equations and also shows that the JAC3D secondary creep model assumes a constant creep rate at steady state conditions (constant load and temperature) while the PCA test data show a time-dependent creep rate, independent of load and temperature. Given this apparent inconsistency between the test data and the constraint to use the standard creep model in JAC3D for preliminary evaluation of creep effects, it was decided to develop piece-wise approximations of the PCA data using the JAC3D material model. This approximation is also shown in the figures.

This approximation, using the JAC3D secondary creep model, was made by setting A_2 and A_3 in Equation 6-4 equal to 0 (i.e. the creep strain rate is independent of stress and temperature) and selecting A_1 so that the total creep strain approximates the strain predicted by the PCA data. For each of the heating periods, the value of A_1 is given in Table 6-3 below.

Table 6-3. Creep Equation Constants

Time	A_1
0 – 6 months	5.70773 E-11
6 - 12 months	4.63862 E-12
12 - 18 months	2.94321 E-12
18 - 24 months	2.15675 E-12
24 - 30 months	1.70227 E-12
30 – 36 months	1.40609 E-12
36 – 42 months	1.19774 E-12
42 – 48 months	1.04319 E-12
48 – 54 months	9.23975 E-12
54 – 60 months	8.29218 E-12

Figure 6-49 shows the predicted Z displacement using the creep model. In comparison with the pretest model in Figure 6-32, there is little difference between the two models. However, a more significant difference exists in the X displacement in Figure 6-50. The displacement at the rib is greater for the creep model than the pretest elastic case.

The primary differences between the creep and elastic models are expected to be shown in the predicted stresses. Figures 6-51 and 6-52 show the horizontal and vertical stress components using the creep model; these may be compared with the pretest model in figures 6-34 and 6-35. For both components, there is a significant reduction (nearly 16 MPa) in the maximum hoop stresses using the creep model. The decreased stresses are also expressed in the invert and the surrounding rock.

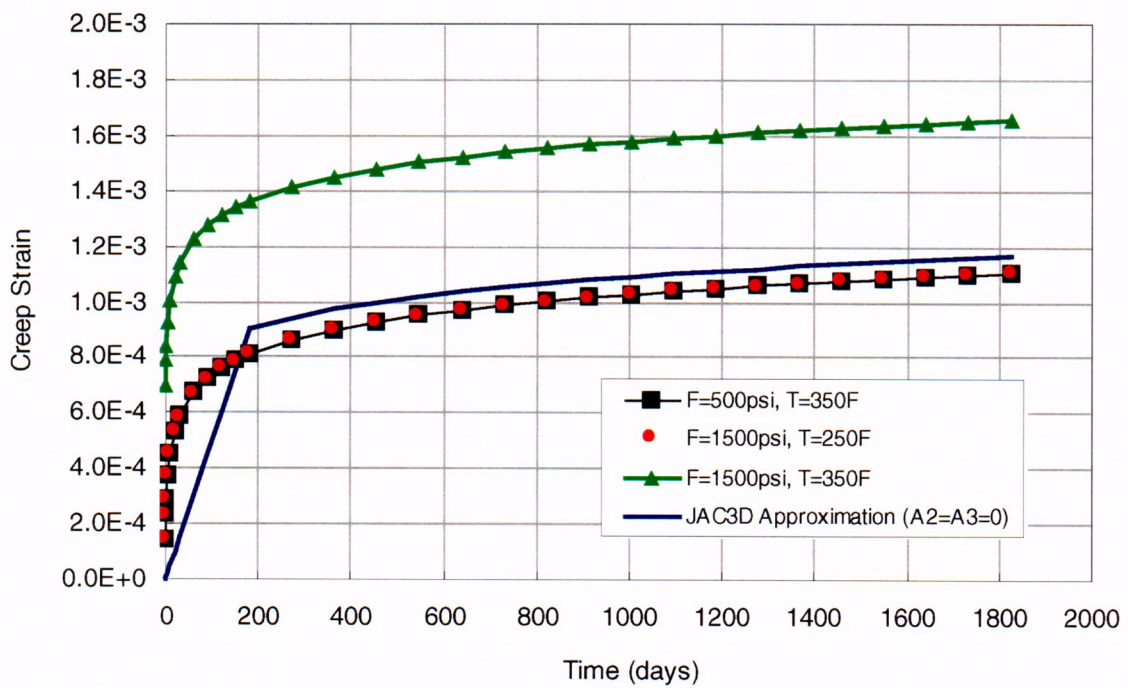


Figure 6-47. PCA concrete creep data.

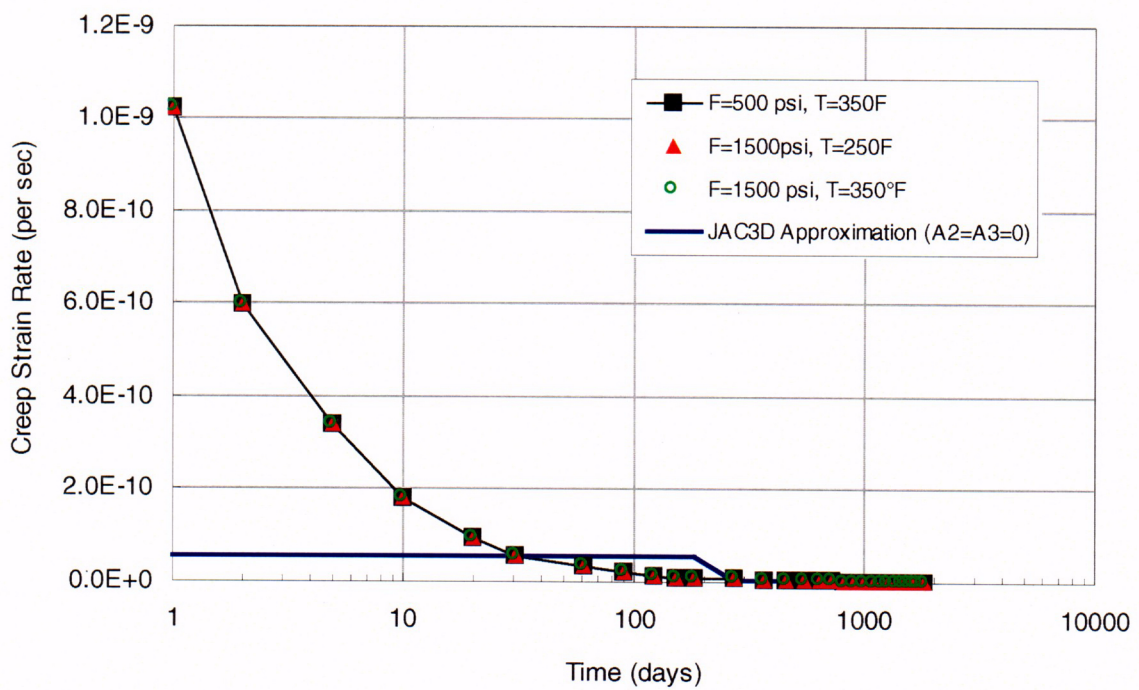


Figure 6-48. PCA concrete creep data, 4500 psi.

C 79

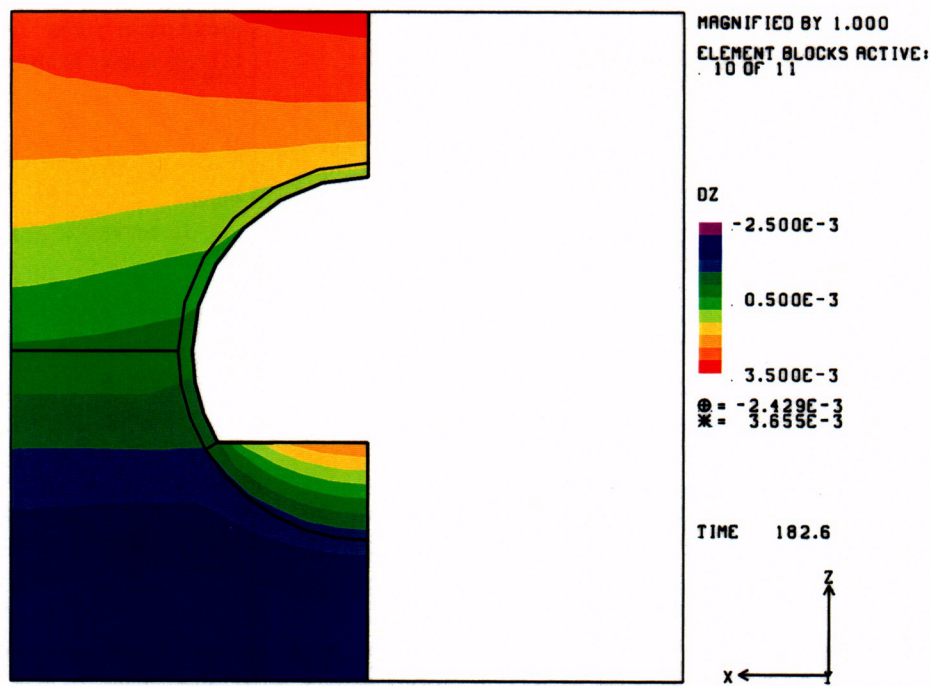


Figure 6-49. Predicted Z-displacement, liner section, creep model, 6 months of heating.

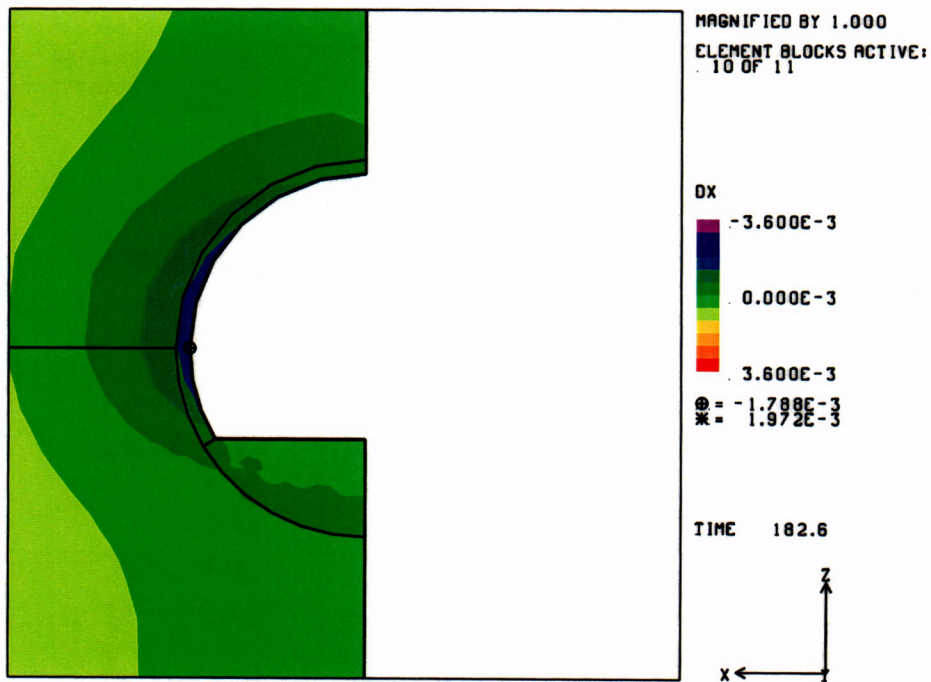


Figure 6-50. Predicted X-displacement, liner section, creep model, 6 months of heating.

C 80

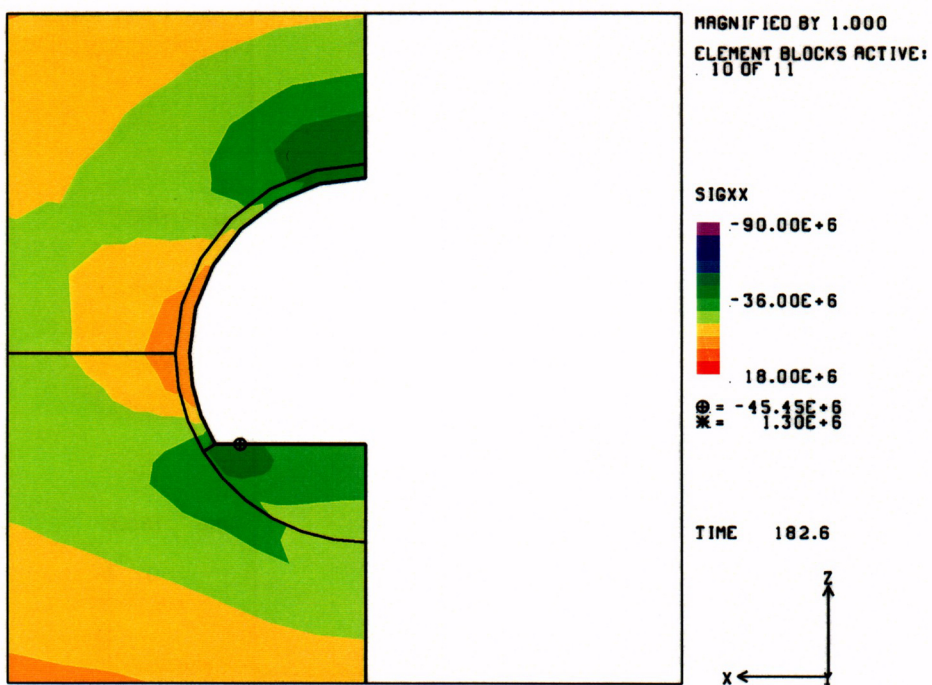


Figure 6-51. Predicted σ_x (horizontal), liner section, creep model, 6 months of heating.

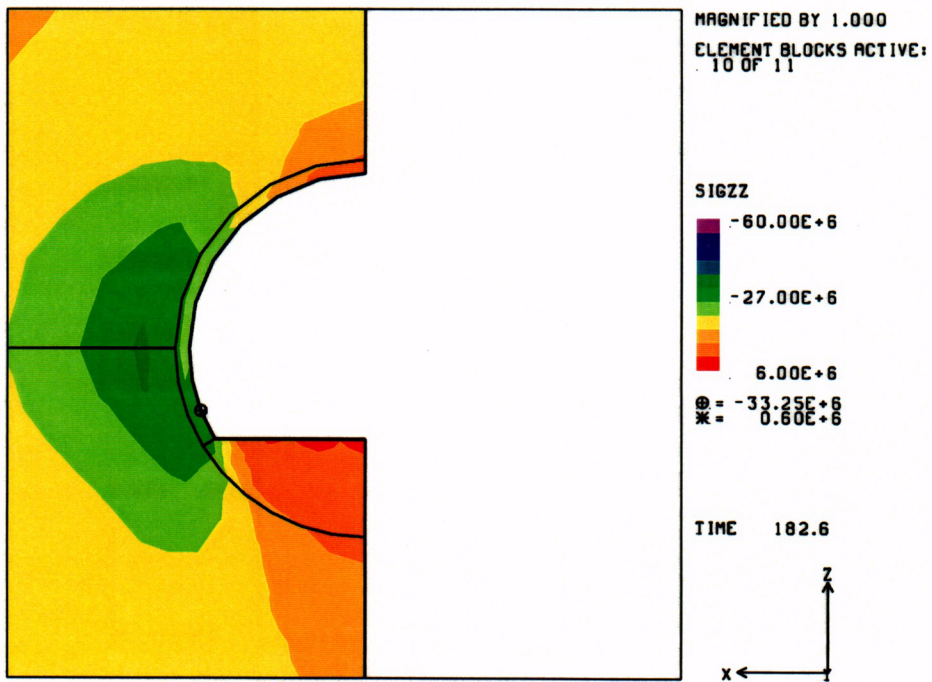


Figure 6-52. Predicted σ_z (vertical), liner section, creep model, 6 months of heating.

C 81

Additional calculations not presented here using the invert/liner interaction model also show an ~16 MPa reduction in hoop stresses from the elastic predictions.

The results of the creep model indicate that concrete creep plays a potentially significant role in stress reduction in the elevated temperature environment of the Heated Drift. Laboratory creep testing currently under way will attempt to characterize concrete creep as a function of temperature and load. These data, in conjunction with this or another creep model, plastic deformation of the concrete, and realistic invert/liner bonding and friction parameters, can be used in a comprehensive T-M model that can be tested with the results of the DST. Such a model will be an important contribution toward the design of engineered concrete structures in a potential future repository. Future analyses will incorporate creep data obtained from SNL laboratory creep testing.

Page intentionally blank

7. Summary and Recommendations

The Drift Scale Test was initiated on December 3, 1997, and the experimental results after six months of heating are included in this report. The results of the DST are to be used to evaluate and/or propose conceptual models that best describe the observed thermal-hydrological-mechanical response of the rock mass to thermal input. The DST data has been evaluated, analyzed, and compared to pretest modeling predictions, and the following results have been observed:

- Temperature data indicate that the rock mass surrounding the DST has a higher bulk permeability (perhaps on the order of 10^{-13} m^2) than did the Single Heater Test (which was on the order of 10^{-15} m^2). This conclusion is based on the observed leveling of temperature profiles at the local boiling point of water, 96°C, for extended periods of time. This behavior is indicative of a permeable, nonpressurizing system that allows convective heat transfer from the region of phase change.
- The borehole displacement data indicate that the heated rock mass is trying to expand toward the open drifts, and that the mechanical behavior to this point is elastic in nature. Ongoing analysis of the data will examine whether a nonelastic, stick-slip behavior as seen in the Single Heater Test will also occur for the DST.
- The cross-drift displacement data indicate that the Heated Drift is being ovalized by horizontal compressive forces driven by the wing heaters. This conclusion is partially verified by the strain data from gages on the concrete liner.
- The strain gages placed on the concrete liner and on unconstrained concrete samples in the Heated Drift show the combined effects of thermal expansion, dehydration-induced shrinkage, and mechanical stress imposed by the interaction of the concrete with the heated rock surrounding the drift. The results from the strain gages on the unconstrained samples exhibit behavior indicative of drying shrinkage due to dehydration, a phenomenon seen elsewhere in engineering literature. The circumferential strain gages on the liner consistently show that the crown of the liner is in compression while the rest of the liner experiences smaller magnitudes of compression and tension. Drying shrinkage was not included in the pretest thermal-mechanical model; efforts are under way to understand this phenomenon better for inclusion in the model.
- New thermal-hydrologic and thermal-mechanical modeling presented in this report examine several potential processes that are suggested by the DST data: accumulation of water under the Heated Drift; stress reduction in the concrete liner due to creep; invert-liner debonding due to the combination of thermal and mechanical stresses. These analysis techniques are being continuously refined with more physically realistic models and new material property data.
- The Plate Loading Test data suggest a rock mass modulus (using simplified analytical techniques) ranging from 11.5 GPa to 29.7 GPa at the Plate Loading Niche. These data show that the higher values for modulus are obtained on the hot side of the Plate Loading Niche (i.e., the side closer to the Heated Drift). Additional evaluation of the video and core logs as well as the surface fracture exposure in the PLT will be performed to determine whether heterogeneities in either side of the PLT have contributed to these modulus estimates.

- A CIP concrete laboratory testing program is being conducted to assess the magnitude of the projected creep strains and the impact of these strains on the thermally induced stresses. Specimens of concrete were cast into specimen molds during emplacement of the cast-in-place concrete liner used in the Drift Scale Test. Thermal expansion measurements and constant load (creep) tests have been initiated on these specimens at temperatures up to 200°C and at axial loads of up to 30% of the unconfined compressive strength. The results of these tests are given in this report.

The data results highlight areas where our current modeling efforts are inadequate to describe the observed behavior. Examples of analyses performed and described in this report include the following:

- Updated T-H calculations based on actual heater power output, higher bulk permeability of $\sim 10^{-13} \text{ m}^2$, and improved boundary conditions. These calculations also will be used to simulate heater ramp-down scenarios to maintain a 200°C maximum temperature at the drift wall. The current heater output, if held constant, will cause the wall temperature to reach 200°C after 18 months of heating, and 320°C after 4 years of heating. A heater ramp down scenario to 60% of the current output after 18 months would cause the wall temperature to just reach 200°C at 4 years of heating.
- Displacement and strain data were compared with the pretest elastic calculations using rock mass properties based on both intact rock and in situ measurements. The calculations using intact rock values for elastic modulus and thermal expansion match the data very well, both in general trends and in magnitudes. The pretest calculations indicate that the rock mass to this point is behaving as an elastic medium, and with properties very much like those measured in the lab with intact rock samples.
- A new T-M model was created for which the concrete liner and invert are modeled as independent structures with the potential for frictional sliding and separation. This model predicts displacements at the invert-liner interface of magnitudes like those measured by MPBX14; and given certain parameters predicts a separation, or debonding, of the invert and liner. Unrealistic boundary conditions in the axial direction cause predictions of hoop stresses that are higher than those indicated by strain gage data; this model will be modified to include better boundary conditions.
- T-M calculations were performed using the pretest conceptual model and mesh, and employing a creep model for the concrete liner and invert. Input parameters for the creep model were obtained from concrete testing in the general literature; later calculations will use data currently being obtained from the SNL testing program. The creep model indicates a significant reduction (about 16 MPa) in compressive stresses in the concrete liner.

Examples of calculations to be performed for future reports include:

- T-H calculations employing a dual permeability model for matrix-fracture interaction.
- T-M calculations employing a compliant joint model, which is a continuum model for joints and fractures. Such a model is capable of integrating the behavior of individual fractures over large volumes, and thus should be evaluated by tests such as the Drift Scale Test for potential use in performance assessment applications.

The instrumentation for the Drift Scale Test is performing very well. The canister and wing heaters have performed reliably. Only six heater problems have been registered to date, and the power output for nearly all the heaters has varied from the mean by no more than 3%. Data noise has been a minor problem, although it has become more significant beginning in April 1998; the causes of the noise (and there appear to be several) are currently being investigated. To date, only ~4% of the installed thermal and mechanical gages have failed or are suspect.

Page intentionally blank

8. References

- ASTM (American Society for Testing and Materials). 1970. *Determination of the In Situ Modulus of Deformation of Rock*, ASTM STP-477. Philadelphia, Pennsylvania: American Society for Testing and Materials. TIC Catalog Number: 210409.
- ASTM (American Society for Testing and Materials). 1996. *Standard Test Method for Determining the In Situ Modulus of Deformation of Rock Using the Diametrically Loaded 76-mm (3-in.) Borehole Jack*, ASTM D4971-89. Philadelphia, Pennsylvania: American Society for Testing and Materials.
- ASTM (American Society for Testing and Materials). 1994a. *Standard Test Method for Determining the In Situ Modulus of Deformation of Rock Mass Using the Rigid Plate Loading Method*, ASTM D4394-84. (Reapproved 1989) Philadelphia, Pennsylvania: American Society for Testing and Materials.
- ASTM (American Society for Testing and Materials). 1994b. *Standard Test Method for Determining the In Situ Modulus of Deformation of Rock Mass Using the Flexible Plate Loading Method*, ASTM D4395-84. (Reapproved 1989) Philadelphia, Pennsylvania: American Society for Testing and Materials.
- Barton, N.R., Lien, R., and Lunde, J. 1974. "Engineering Classification of Rock Masses for the Design of Tunnel Support." *Rock Mechanics*, 6, 4, 189-236.
- Barton, N.R. 1983. "Application of Q System and Index Tests to Estimate Shear Strength and Deformability of Rock Masses." *Proceedings of the International Symposium On Engineering Geology and Underground Construction*, 2, 2, 51-70. Lisbon, Portugal.
- Bieniawski, Z.T. 1974. "Geomechanics Classification of Rock Masses and its Application in Tunnelling," *Proceedings of the Third International Congress on Rock Mechanics*. ISRM, Vol. IIA, 27-32. Denver, CO.
- Bieniawski, Z.T. 1978. "Determining Rock Mass Deformability: Experience from Case Histories." *International Journal of Rock Mechanics, Mineral Science, & Geomechanical Abstracts*. 15, 5, 237-247. TIC Catalog Number: 218740.
- Biffle, J.H. 1993. *JAC3D - A Three-Dimensional Finite Element Computer Program for the Nonlinear Quasi-static Response of Solids with the Conjugate Gradient Method*, SAND87-1305, Albuquerque, New Mexico: Sandia National Laboratories. TIC Catalog Number: 206132.
- Bowles, J.E. 1982. *Foundation Analysis and Design*, New York, New York: McGraw Hill.
- Boyle, W.J. 1992. "Interpretation of Plate Load Test Data." *International Journal Of Rock Mechanics Science & Geomechanical Abstracts*, 29, 2, 133-141.
- Brown, E.T. (ed.). 1981. *Rock Characterization, Testing, and Monitoring*, Oxford, England: Pergamon Press. TIC Catalog Number: 9663.
- CRWMS M&O. 1997a. "Drift Scale Test Design and Forecast Results." BAB000000-01717-4600-00007 Rev.00, July 16, 1997. Las Vegas, Nevada: TRW Environmental Safety Systems. MOL.19980119.0021.

- CRWMS M&O. 1997b. "Ambient Characterization of the Drift Scale Test Block." BADD00000-01717-5705-00001, Rev. 1, December 11, 1997. Las Vegas, Nevada: TRW Environmental Safety Systems. MOL.19980425.0151.
- DOE (United States Department of Energy). 1988. "Site Characterization Plan, Yucca Mountain Site, Nevada Research and Development Area, Nevada." DOE/RW-0199. Las Vegas, Nevada: United States Department of Energy. HQO.19881201.0002.
- DOE (United States Department of Energy). 1995. "In Situ Thermal Testing Program Strategy." DOE/YMSCO-003. Las Vegas, Nevada: United States Department of Energy. TIC Catalog Number: 215726.
- Francis, N.D.; Sobolik, S.R.; Ho, C.K.; Eaton, R.R.; and Preece, D. 1997. "Pre-Experiment Thermal-Hydrologic-Mechanical Analyses for the ESF Heated Drift Test." Sandia Letter Report SLTR97-0002. Data Tracking Number (DTN) SNF35110695002.001. Technical Data Information Form (TDIF) No. 306151. Albuquerque, New Mexico: Sandia National Laboratories. MOL.19980128.0366.
- Goodman, R.E. 1980. *Introduction to Rock Mechanics*, New York, New York: John Wiley & Sons. TIC Catalog Number: 218828.
- Goodman, R.E.; Van, T.K.; and Heuze, F.W. 1968. "The Measurement of Rock Deformability in Boreholes." *Proceedings of the 10th U.S. Symposium on Rock Mechanics*, Austin, Texas.
- Hansen, W. and Almudaiheem, J.A. 1987. "Ultimate Drying Shrinkage of Concrete - Influence of Major Parameters." *ACI Materials Journal*, 84, 3, 217-223. TIC Catalog Number: 236450.
- Henager, C. H.; Piepel, G.F.; Anderson, W. E.; Koehmstedt, P. L.; and Simonen, F. A. 1988. "Modeling of Time-Variant Concrete Properties At Elevated Temperatures." 51-65. Pacific Northwest Laboratory for Kaiser Engineers Hanford.
- Heuze, F.W. 1984. "Suggested Method for Estimating the In-Situ Modulus of Deformation of Rock Using the NX-Borehole Jack." *Geotechnical Testing Journal GTJODJ*, 7, 4. TIC Catalog Number: 234090. MOL.19940718.0003.
- Heuze, F.E. and Amadei, B. 1985. "The NX Borehole Jack: A Lesson in Trials and Errors." *International Journal of Rock Mechanics and Mining Sciences*, 22, 105-112. TIC Catalog Number: 218975.
- Hustrulid, W.A. and Schrauf, T.W. 1979. "Borehole Modulus Measurements with the CSM Cell in Swedish Granite." *Proceedings of the 20th U.S. Symposium on Rock Mechanics*, Austin, Texas. NNA.19940629.0027.
- Lawrence Berkeley National Laboratory (LBNL). 1996. *Letter Report on Hydrological Characterization of the Single Heater Test Area in the ESF*, Data Tracking Number (DTN) LB960500834244.001. Technical Data Information Form (TDIF) No. 305605. MOL.19971119.0548; MOL.19971119.0553; MOL.19971119.0554.
- Lawrence Berkeley National Laboratory (LBNL). 1997. *DKM BaseCase Parameter Set for UZ Model with Mean Fracture Alpha, Present Day Infiltration, and Estimated Welded and Non Welded and Zeolitic FMX*, Data Tracking Number (DTN) LB971212001254.001. Technical Data Information Form (TDIF) No. 306527. MOL.19980518.0232.

- Lawrence Berkeley National Laboratory (LBNL). 1998. *Base Case Thermal Property Data for TSPA-VA*, Data Tracking Number (DTN) SNT05071897001.002. Technical Data Information Form (TDIF) No. 306664. MOL.19980501.0475.
- Lawrence Berkeley National Laboratory (LBNL). 1998. *ESF Drift Scale Test As-built Data and Baseline Measurements; Air Permeability Data of Boreholes in the Heated Drift*, Data Tracking Number (DTN) LB980120123142.005. Technical Data Information Form (TDIF) No. 306574. MOL.19980527.0249; MOL.19980527.0252; MOL.19980527.0260.
- Lin, W. and Wagoner, J. 1998. "DST As-Built TDIF SPY195M4: XYZ Coordinates of the Sensors in the Drift Scale Test." Level 4 Deliverable dated January 16, 1998. Livermore, California: Lawrence Livermore National Laboratory. MOL.19980203.0221.
- Neville, A. M. 1997. *Properties of Concrete*, Fourth Edition. New York, New York: John Wiley and Sons, Inc. TIC Catalog Number: 236567.
- Nicholson, G.A. and Bieniawski, Z.T. 1986. "An Empirical Constitutive Relationship for Rock Masses." *Proceedings of the 27th U.S. Rock Mechanics Symposium*, Littleton, Colorado: University of Alabama, SME.
- Olsson, W.A. 1987. "NNWSI Project Rock Joint Compliance Studies." SAND86-0177. Albuquerque, New Mexico: Sandia National Laboratories. NNA.19870511.0131.
- Pratt, H.R.; Schrauf, T.W.; Bills, L.A.; and Hustrulid, W.A. 1977. "Thermal and Mechanical Properties of Granite: Stripa, Sweden." *Terra Tek Summary Report*, TR-77-92. Salt Lake City, Utah. NNA.19900607.0178.
- Pruess, K. 1991. *TOUGH2--A General-Purpose Simulator for Multiphase Fluid and Heat Flow*, LBL-29400. Berkeley, California: Lawrence Berkeley Laboratory. TIC Catalog Number: 213489. NNA.19940202.0088.
- Rocha, M. 1964. "Mechanical Behaviour of Rock Foundations in Concrete Dams." *Transactions of the Eighth Congress on Large Dams*, Edinburgh, Scotland. MOL.19941128.0062.
- Sandia National Laboratories (SNL). 1997. *Evaluation of Single Heater Test, Thermal and Thermomechanical Data: Second Quarter Results*, Data Tracking Number (DTN) SNF35110695001.004. Technical Data Information Form (TDIF) No. 306088. MOL.19971111.0187; MOL.19971111.0188.
- Sandia National Laboratories (SNL). 1997. *Thermal Expansion of Carbon Fiber and Invar Rods*, Data Tracking Number (DTN) SNL22100196001.003. Technical Data Information Form (TDIF) No. 306356. MOL.19980210.0198.
- Sandia National Laboratories (SNL). 1998. *Heated Drift Test: SNL As-Built Gauge Table [Thermomechanical Gauges Only]*, Data Tracking Number (DTN) SNF38040197001.001. Technical Data Information Form (TDIF) No. 306548. Albuquerque, New Mexico: Sandia National Laboratories. MOL.19980323.0466.
- Sandia National Laboratories (SNL). 1998. *Evaluation and Comparative Analysis of Single Heater Test Thermal and Thermomechanical Data: First Quarter FY98 Results*, Data Tracking Number (DTN) SNF35110695001.008. Technical Data Information Form (TDIF) No. 306549. MOL.19980429.0940; MOL.19980429.0941.

- Sandia National Laboratories (SNL). 1998. *Unconfined Compression Tests on Cast-in-Place Concrete Specimens from the Drift Scale Test Area of the Exploratory Studies Facility at Yucca Mountain, Nevada*, Data Tracking Number (DTN) SNL23030598001.001. Technical Data Information Form (TDIF) No. 306714. MOL.19980518.0273; MOL.19980518.0276.
- Serafim, J.L. and Periera, J.P. 1983. "Considerations of the Geomechanics Classification of Bieniawski." *Proceedings of the First International Symposium on Engineering Geology and Underground Construction*, Lisbon, Portugal: 2. NNA.19910327.0063.
- Troxell, G.E.; Davis, H.E.; and Kelly, J.W. 1968. *Composition and Properties of Concrete*, New York, New York: McGraw-Hill Book Company.
- Tsang, Y.W. and Cook, P. 1997. "Ambient Characterization of the ESF Drift Scale Test Area by Field Air Permeability Measurements." *YM Site Project Milestone Report SP9512M4*, Data Tracking Number (DTN) LB970600123142.001. Technical Data Information Form (TDIF) No. 306164. Berkeley, California: Lawrence Berkeley National Laboratory. MOL.19971201.0829; MOL.19971201.0835.0837.
- Van Genuchten, M. 1980. "A Closed-Form Equation for Predicting the Hydraulic Conductivity of Unsaturated Soils." *Soil Science Society of America Journal*, 44, 892- 898. NNA.19890522.0287.
- Zimmerman, R.M. and Finley, R.E. 1987. "Summary of Geomechanical Measurements Taken in and Around the G-Tunnel Underground Facility, NTS." SAND86-1015, Albuquerque, New Mexico: Sandia National Laboratories. NNA.19870526.0015.
- Zimmerman, R.M.; Schuch, R.L.; Mason, D.S.; Wilson, M.L.; Hall, M.E.; Board, M.P.; Bellman, R.P.; and Blanford, M.L. 1986. "Final Report: G-Tunnel Heated Block Experiment." SAND84-2620, Albuquerque, New Mexico: Sandia National Laboratories. MOL.19961217.0085.

Appendix A

Available DCS-Acquired Data for the DST (through May 31, 1998)

All DST data acquired from the Data Collection System were previously submitted in CD-ROM format to YMP Records by the Test Coordinator prior to the production of this report. The data presented in this report is a subset of all the data on those previous CD-ROMs. Table A-1 lists the CD-ROMs issued by the Test Coordinator Office. Copies of these previous CD-ROMs may be obtained from Fred Homuth, LANL-TCO, at (702) 295-4900.

Table A-1. Drift Scale Test Data Submitted on CD-ROM

CD-ROM Title: ESF Drift Scale Test, ESF DCS Data, Los Alamos National Lab, TCO Data Management Distribution Data Set	
CD-ROM ID	Time period for data on CD-ROM
CD1DST, Batch 1, Rev 0	pre-November 1997 (including measurements from the Sequential Drift Mine-By gages)
CD2DST, Batch 1, Rev 0.00	Nov 97 - Feb 98
CD3DST, Batch 1, Rev 0.00	March 98
CD4DST, Batch 1, Rev 0.00	April 98
CD5DST, Batch 1, Rev 0.00	May 98

Note that the CD-ROM included with this report contains a subset of all the DST data in the CD-ROMs listed in Table A-1.

Page intentionally blank

Appendix B

Thermomechanical Gage Specifications for the DST

Summary of SNL-Installed Measurement System Specifications

Measurement System	Manufacturer	Gage Accuracy, Range, Precision	Comments
Type-K Thermocouples	Watlow ARI, Inc. (probes)	$\pm 2.2^\circ\text{C}$ max 1280°C	Chromel-Alumel
Vibrating Wire Displacement Transducers	Geokon	1 in. full range Accuracy: 0.02% of full range	
High Temperature LVDTs (Heated Drift)	RDP Electrosense, Inc.	± 1 in. full range 0.5% linearity full range calibrated from ambient to 350°C	AC-LVDT's
High Temperature LVDTs (High Temperature Side, PLT)	RDP Electrosense, Inc.	± 1 in. full range 0.5% linearity full range calibrated from ambient to 200°C	Model ACW-1000-595
High Temperature LVDTs (Ambient Temperature Side, PLT)	RDP Electrosense, Inc.	± 1 in. full range 0.5% linearity full range calibrated from ambient to 90°C	Model ACW-1000-596
CIP Strain Gages	BLH Electronics	Karma Foil 4-in gages with gage factor of 2 Temperature range limited by bonding epoxy and extension wire	
Pressure Transducers (PLT)	Dynisco, Model S861-310-10M	Range: 0-10,000 psi Accuracy: $\pm 0.5\%$ Full scale from 1,000-10,000 psi	
Yo-Yo Gages (Wire Displacement, PLT)	Houston Scientific Inc., #1950-002	Range: 0.0-2.0 inches Accuracy: 0.1% full scale	

Note: Additional gage information can be found in the SNL Scientific Notebook covering this work.

Because of an ongoing quality assurance (QA) Deficiency Report YM-97-C-004 regarding procurement and issues with the manufacturer (GEOKON) of the C-ring anchors, vibrating wire transducers, and linear variable displacement transducers, the displacement measurements from all the MPBXs and CDEXs are currently not qualified per YMP QA procedures. It is anticipated that the data will be qualified upon resolution of the QA issues.

Page intentionally blank

Appendix C

As-Built Gage Locations and Selected Data

As-Built Heater and Gage Locations Tabulated Strain Gage Data

The gage locations presented in this appendix are identified by a unique designation based on borehole (if used), gage type, and gage location along the hole. The gage identification for the DST begins with ESF (for Exploratory Studies Facility), and either HD (for Heated Drift) or SDM (for Sequential Drift Mining). This is followed by the borehole ID (see Table 2-1) and number as follows:

WH1 through WH50	= Wing heaters (WH1-1 designates "inner" heater closest to drift wall, and WH1-2 designates "outer" heater deeper in the borehole)
CAN1 through CAN9	= Canister heaters (each canister has 9 heaters, which are lumped together as one unit)
TC-1, 2, 3, etc.	= Thermocouples (in wing heater boreholes, on canisters, in MPBX boreholes, on the drift and bulkhead surfaces)
SURF	= Rock or liner surface in the Heated Drift
BHSF	= Bulkhead surface
MPBX1 through MPBX14	= Multi-point borehole extensometer (using either linear variable displacement transformers [LVDTs] or vibrating wire transducers)
CDEX-1 and CDEX-2	= Cross-drift MPBXs (using LVDTs)
ANC-1 through ANC-6	= MPBX anchor location
THRM	= Thermistor (at SDM MPBX heads)
RTD	= Resistance Temperature Device
RSG-1 through RSG-18	= Rosette strain gage (RSG-16, 17, and 18 are not rosettes, but the name stuck)
AXL	= Axial strain gage in the rosette
CIR	= Circumferential strain gage in the rosette
DIA	= Diagonal strain gage in the rosette
EVL	= Evaluation strain gage

The gage locations are given in x,y,z coordinates in Tables C-1 through C-4. The gage location tables in Appendix C present each gage relative to the assigned origin (x,y,z=0) for the Drift Scale Test coordinate system, which is a point on the axis of the heated drift on the hot (i.e., west) surface of the bulkhead. The x-axis is aligned with the axis of the Heated Drift, with positive from the bulkhead towards the heaters; the z-axis is vertical, positive upwards. All

locations are expressed in meters. The gage locations for all SNL-installed gages (wing heaters, MPBXs, CDEXs, thermocouples, strain gages) have previously been reviewed by SNL and submitted under TDIF #306548 (DTN: SNF38040197001.001). The RTDs were installed by Lawrence Livermore National Laboratories and submitted as a Level 4 Deliverable (Lin and Wagoner, 1998).

All the DST data presented in this report have been previously submitted to YMP Records in CD-ROM form by the Test Coordination Office (see Appendix A). Typically, all gages are scanned every six hours, providing four data points per day. The data presented in tabular form here in Appendix C is a small subset of the DST data; the graphs presented in the text of this report are representative of all the data for each individual gage. Of this set of DST data, all are "Q" data (that is, qualified under approved QA procedures) with two exceptions: the heater power for individual heaters represented in Table C-1, and the displacements measured by the MPBXs. The total power for the wing heaters and canisters in that table are correct and qualified; the individual heater powers in the table are based on non-qualified current measurements and represent an over-estimation of the actual power output of heaters. The individual heater powers are valuable, though, for qualitative assessment of individual heater performance, and are presented for that reason. Because of an ongoing quality assurance (QA) Deficiency Report YM-97-C-004 regarding procurement and issues with the manufacturer (GEOKON) of the C-ring anchors, vibrating wire transducers, and linear variable displacement transducers, the displacement measurements from all the MPBXs and CDEXs are currently not qualified per YMP QA procedures. It is anticipated that the data will be qualified upon resolution of the QA issues. Additionally, the MPBX displacement data presented in this report have been modified from the values on the DST CD-ROM. When the deficiency report on GEOKON has been completed, the values on the CD-ROM will be "Q" values representing the displacement measured by the LVDT or vibrating wire transducer. However, the gage is measuring total displacement caused by two effects: the thermal expansion of the rock itself (the desired value), and the thermal expansion of the Invar rods connecting the anchors to the MPBX heads. Using measured thermal expansion coefficients for Invar and measured temperatures along the lengths of the MPBXs, SNL has calculated thermal corrections to convert the measured displacement value to the displacement due only to rock thermal expansion. The DST engineering data are the actual measured displacements of the gages, and the values in this report have been corrected for temperature and have been technically reviewed. The values in Table C-3 are those including the thermal correction.

The data presented in Table C-4 include strain measurements at selected times. Table C-4 in this report completely supersedes Table C-4 in the April 1998 DST data report. As described in Section 4.4, analysis of the strain data resulted in the realization that a correction for the thermal expansion of the strain gage must be included in obtaining the true strain measurement. In Table C-4 in this report, we have included data points from 7, 14, etc. days from heater activation, to the last data point for the quarter. As we will be submitting quarterly reports for at least four years for this test, we do not wish the size of the report to become intimidatingly large. Therefore, in each subsequent report, only the as-built locations will be tabulated in Appendix C. The entire set of data used for the data report for each quarter will be submitted electronically on the CD-ROM accompanying each report. A detailed description of the contents of the CD-ROM is contained in the Preface.

Table C-1. Gage Locations for the DST Heater Power Gages

Gage ID	x	y	z	Gage ID	x	y	z	
ESF-HD-WH-PWR				ESF-HD-92-WH10-2	-14.066	18.171	-0.342	
ESF-HD-CAN-PWR				ESF-HD-93-WH11-2	-13.955	20.104	-0.475	
Individual Heaters				ESF-HD-94-WH12-2	-13.864	22.087	-0.237	
ESF-HD-83-WH1-1	-4.263	1.839	-0.269	ESF-HD-95-WH13-2	-14.085	23.777	-0.293	
ESF-HD-84-WH2-1	-4.208	3.650	-0.231	ESF-HD-96-WH14-2	-14.060	25.653	-0.549	
ESF-HD-85-WH3-1	-4.250	5.503	-0.249	ESF-HD-97-WH15-2	-13.519	27.611	-0.345	
ESF-HD-86-WH4-1	-4.081	7.293	-0.265	ESF-HD-98-WH16-2	-13.945	29.154	-0.254	
ESF-HD-87-WH5-1	-4.175	9.179	-0.249	ESF-HD-99-WH17-2	-14.013	31.267	-0.263	
ESF-HD-88-WH6-1	-4.137	10.979	-0.243	ESF-HD-100-WH18-2	-14.015	33.022	-0.311	
ESF-HD-89-WH7-1	-4.348	12.825	-0.243	ESF-HD-101-WH19-2	-14.045	34.660	-0.281	
ESF-HD-90-WH8-1	-4.267	14.588	-0.286	ESF-HD-102-WH20-2	-14.029	36.407	-0.622	
ESF-HD-91-WH9-1	-4.292	16.507	-0.227	ESF-HD-103-WH21-2	-14.097	38.457	-0.161	
ESF-HD-92-WH10-1	-4.237	18.264	-0.272	ESF-HD-104-WH22-2	-14.142	40.306	-0.099	
ESF-HD-93-WH11-1	-4.127	20.107	-0.303	ESF-HD-105-WH23-2	-13.847	42.230	-0.247	
ESF-HD-94-WH12-1	-4.035	21.976	-0.245	ESF-HD-106-WH24-2	-14.090	43.911	-0.155	
ESF-HD-95-WH13-1	-4.255	23.777	-0.259	ESF-HD-107-WH25-2	-14.096	45.795	-0.383	
ESF-HD-96-WH14-1	-4.233	25.622	-0.317	ESF-HD-108-WH26-2	14.091	45.805	-0.489	
ESF-HD-97-WH15-1	-3.691	27.468	-0.246	ESF-HD-109-WH27-2	14.041	43.790	-0.302	
ESF-HD-98-WH16-1	-4.115	29.228	-0.240	ESF-HD-110-WH28-2	14.032	42.121	-0.216	
ESF-HD-99-WH17-1	-4.184	31.146	-0.260	ESF-HD-111-WH29-2	14.055	40.278	-0.133	
ESF-HD-100-WH18-1	-4.186	32.946	-0.257	ESF-HD-112-WH30-2	14.141	38.316	-0.269	
ESF-HD-101-WH19-1	-4.215	34.722	-0.265	ESF-HD-113-WH31-2	14.126	36.476	-0.212	
ESF-HD-102-WH20-1	-4.204	36.548	-0.331	ESF-HD-114-WH32-2	14.279	34.969	-0.276	
ESF-HD-103-WH21-1	-4.267	38.416	-0.234	ESF-HD-115-WH33-2	14.060	32.668	-0.194	
ESF-HD-104-WH22-1	-4.313	40.241	-0.228	ESF-HD-116-WH34-2	13.848	31.031	-0.229	
ESF-HD-105-WH23-1	-4.018	42.109	-0.269	ESF-HD-117-WH35-2	13.775	29.165	-0.129	
ESF-HD-106-WH24-1	-4.260	43.880	-0.227	ESF-HD-118-WH36-2	14.048	27.390	-0.050	
ESF-HD-107-WH25-1	-4.267	45.743	-0.278	ESF-HD-119-WH37-2	14.097	25.657	-0.406	
ESF-HD-108-WH26-1	4.263	45.747	-0.309	ESF-HD-120-WH38-2	13.838	23.830	-0.376	
ESF-HD-109-WH27-1	4.211	43.864	-0.258	ESF-HD-121-WH39-2	14.081	21.945	-0.299	
ESF-HD-110-WH28-1	4.202	42.073	-0.252	ESF-HD-122-WH40-2	12.992	20.121	-0.234	
ESF-HD-111-WH29-1	4.226	40.225	-0.221	ESF-HD-123-WH41-2	13.960	18.275	-0.297	
ESF-HD-112-WH30-1	4.311	38.375	-0.263	ESF-HD-124-WH42-2	14.155	16.278	-0.517	
ESF-HD-113-WH31-1	4.296	36.548	-0.240	ESF-HD-125-WH43-2	14.127	14.678	-0.526	
ESF-HD-114-WH32-1	4.450	34.813	-0.273	ESF-HD-126-WH44-2	13.960	12.864	-0.340	
ESF-HD-115-WH33-1	4.233	32.878	-0.227	ESF-HD-127-WH45-2	14.114	10.704	-0.442	
ESF-HD-116-WH34-1	4.018	31.075	-0.251	ESF-HD-128-WH46-2	13.944	9.212	-0.418	
ESF-HD-117-WH35-1	3.946	29.221	-0.228	ESF-HD-129-WH47-2	13.750	7.114	-0.271	
ESF-HD-118-WH36-1	4.219	27.416	-0.185	ESF-HD-130-WH48-2	13.990	5.350	-0.177	
ESF-HD-119-WH37-1	4.268	25.611	-0.279	ESF-HD-131-WH49-2	12.897	3.702	-0.321	
ESF-HD-120-WH38-1	4.009	23.782	-0.281	ESF-HD-132-WH50-2	14.114	1.581	-0.446	
ESF-HD-121-WH39-1	4.251	21.941	-0.276	Canister Heaters				
ESF-HD-122-WH40-1	3.162	20.114	-0.248	ESF-HD-CAN1: East end	0.006	0.543	-1.273	
ESF-HD-123-WH41-1	4.130	18.285	-0.255	West end	-0.001	3.968	-1.287	
ESF-HD-124-WH42-1	4.328	16.410	-0.311	ESF-HD-CAN2: East end	-0.006	5.826	-1.292	
ESF-HD-125-WH43-1	4.299	14.648	-0.325	West end	-0.008	9.247	-1.298	
ESF-HD-126-WH44-1	4.131	12.810	-0.259	ESF-HD-CAN3: East end	0.011	10.991	-1.291	
ESF-HD-127-WH45-1	4.287	10.913	-0.297	West end	0.005	14.417	-1.304	
ESF-HD-128-WH46-1	4.115	9.151	-0.282	ESF-HD-CAN4: East end	-0.027	16.283	-1.305	
ESF-HD-129-WH47-1	3.922	7.290	-0.248	West end	-0.030	19.714	-1.291	
ESF-HD-130-WH48-1	4.161	5.482	-0.223	ESF-HD-CAN5: East end	-0.015	21.522	-1.306	
ESF-HD-131-WH49-1	3.067	3.673	-0.279	West end	-0.001	24.951	-1.285	
ESF-HD-132-WH50-1	4.287	1.782	-0.290	ESF-HD-CAN6: East end	-0.026	26.870	-1.301	
ESF-HD-83-WH1-2	-14.093	1.848	-0.326	West end	-0.026	30.300	-1.298	
ESF-HD-84-WH2-2	-14.038	3.676	-0.182	ESF-HD-CAN7: East end	-0.017	32.055	-1.292	
ESF-HD-85-WH3-2	-14.080	5.529	-0.255	West end	-0.022	35.486	-1.273	
ESF-HD-86-WH4-2	-13.910	7.190	-0.353	ESF-HD-CAN8: East end	0.002	37.353	-1.280	
ESF-HD-87-WH5-2	-14.004	9.335	-0.233	West end	-0.003	40.783	-1.284	
ESF-HD-88-WH6-2	-13.967	10.946	-0.249	ESF-HD-CAN9: East end	-0.013	42.642	-1.290	
ESF-HD-89-WH7-2	-14.178	12.882	-0.270	West end	-0.030	46.074	-1.254	
ESF-HD-90-WH8-2	-14.096	14.507	-0.381					
ESF-HD-91-WH9-2	-14.121	16.645	-0.187					

Table C-2. Gage Locations for the DST Temperature Gages

Gage ID	x	y	z	Gage ID	x	y	z
Canister Thermocouples							
ESF-HD-CAN1-TC-1	-0.144	1.719	0.605	ESF-HD-CAN6-TC-6	-0.756	29.216	-0.673
ESF-HD-CAN1-TC-2	0.736	1.719	-0.645	ESF-HD-CAN6-TC-7	-0.176	30.386	0.577
ESF-HD-CAN1-TC-3	-0.724	1.719	-0.645	ESF-HD-CAN6-TC-8	0.704	30.386	-0.673
ESF-HD-CAN1-TC-4	-0.144	2.889	0.605	ESF-HD-CAN6-TC-9	-0.756	30.386	-0.673
ESF-HD-CAN1-TC-5	0.736	2.889	-0.645	ESF-HD-CAN7-TC-1	-0.167	33.231	0.586
ESF-HD-CAN1-TC-6	-0.724	2.889	-0.645	ESF-HD-CAN7-TC-2	0.713	33.231	-0.664
ESF-HD-CAN1-TC-7	-0.144	4.059	0.605	ESF-HD-CAN7-TC-3	-0.747	33.231	-0.664
ESF-HD-CAN1-TC-8	0.736	4.059	-0.645	ESF-HD-CAN7-TC-4	-0.167	34.401	0.586
ESF-HD-CAN1-TC-9	-0.724	4.059	-0.645	ESF-HD-CAN7-TC-5	0.713	34.401	-0.664
ESF-HD-CAN2-TC-1	-0.156	7.002	0.586	ESF-HD-CAN7-TC-6	-0.747	34.401	-0.664
ESF-HD-CAN2-TC-2	0.724	7.002	-0.664	ESF-HD-CAN7-TC-7	-0.167	35.571	0.586
ESF-HD-CAN2-TC-3	-0.736	7.002	-0.664	ESF-HD-CAN7-TC-8	0.713	35.571	-0.664
ESF-HD-CAN2-TC-4	-0.156	8.172	0.586	ESF-HD-CAN7-TC-9	-0.747	35.571	-0.664
ESF-HD-CAN2-TC-5	0.724	8.172	-0.664	ESF-HD-CAN8-TC-1	-0.148	38.529	0.598
ESF-HD-CAN2-TC-6	-0.736	8.172	-0.664	ESF-HD-CAN8-TC-2	0.732	38.529	-0.652
ESF-HD-CAN2-TC-7	-0.156	9.342	0.586	ESF-HD-CAN8-TC-3	-0.728	38.529	-0.652
ESF-HD-CAN2-TC-8	0.724	9.342	-0.664	ESF-HD-CAN8-TC-4	-0.148	39.699	0.598
ESF-HD-CAN2-TC-9	-0.736	9.342	-0.664	ESF-HD-CAN8-TC-5	0.732	39.699	-0.652
ESF-HD-CAN3-TC-1	-0.139	12.167	0.587	ESF-HD-CAN8-TC-6	-0.728	39.699	-0.652
ESF-HD-CAN3-TC-2	0.741	12.167	-0.663	ESF-HD-CAN8-TC-7	-0.148	40.869	0.598
ESF-HD-CAN3-TC-3	-0.719	12.167	-0.663	ESF-HD-CAN8-TC-8	0.732	40.869	-0.652
ESF-HD-CAN3-TC-4	-0.139	13.337	0.587	ESF-HD-CAN8-TC-9	-0.728	40.869	-0.652
ESF-HD-CAN3-TC-5	0.741	13.337	-0.663	ESF-HD-CAN9-TC-1	-0.163	43.818	0.588
ESF-HD-CAN3-TC-6	-0.719	13.337	-0.663	ESF-HD-CAN9-TC-2	0.717	43.818	-0.662
ESF-HD-CAN3-TC-7	-0.139	14.507	0.587	ESF-HD-CAN9-TC-3	-0.743	43.818	-0.662
ESF-HD-CAN3-TC-8	0.741	14.507	-0.663	ESF-HD-CAN9-TC-4	-0.163	44.988	0.588
ESF-HD-CAN3-TC-9	-0.719	14.507	-0.663	ESF-HD-CAN9-TC-5	0.717	44.988	-0.662
ESF-HD-CAN4-TC-1	-0.177	17.459	0.573	ESF-HD-CAN9-TC-6	-0.743	44.988	-0.662
ESF-HD-CAN4-TC-2	0.703	17.459	-0.677	ESF-HD-CAN9-TC-7	-0.163	46.158	0.588
ESF-HD-CAN4-TC-3	-0.757	17.459	-0.677	ESF-HD-CAN9-TC-8	0.717	46.158	-0.662
ESF-HD-CAN4-TC-4	-0.177	18.629	0.573	ESF-HD-CAN9-TC-9	-0.743	46.158	-0.662
ESF-HD-CAN4-TC-5	0.703	18.629	-0.677	Wing Heater Thermocouples			
ESF-HD-CAN4-TC-6	-0.757	18.629	-0.677	ESF-HD-83-WH1-TC-1	-5.353	1.840	-0.275
ESF-HD-CAN4-TC-7	-0.177	19.799	0.573	ESF-HD-83-WH1-TC-2	-7.363	1.842	-0.287
ESF-HD-CAN4-TC-8	0.703	19.799	-0.677	ESF-HD-83-WH1-TC-3	-9.243	1.843	-0.298
ESF-HD-CAN4-TC-9	-0.757	19.799	-0.677	ESF-HD-83-WH1-TC-4	-10.843	1.845	-0.307
ESF-HD-CAN5-TC-1	-0.165	22.698	0.572	ESF-HD-83-WH1-TC-5	-13.843	1.848	-0.324
ESF-HD-CAN5-TC-2	0.715	22.698	-0.678	ESF-HD-84-WH2-TC-1	-5.298	3.653	-0.225
ESF-HD-CAN5-TC-3	-0.745	22.698	-0.678	ESF-HD-84-WH2-TC-2	-7.308	3.658	-0.215
ESF-HD-CAN5-TC-4	-0.165	23.868	0.572	ESF-HD-84-WH2-TC-3	-9.188	3.663	-0.206
ESF-HD-CAN5-TC-5	0.715	23.868	-0.678	ESF-HD-84-WH2-TC-4	-10.788	3.667	-0.198
ESF-HD-CAN5-TC-6	-0.745	23.868	-0.678	ESF-HD-84-WH2-TC-5	-13.788	3.675	-0.183
ESF-HD-CAN5-TC-7	-0.165	25.038	0.572	ESF-HD-85-WH3-TC-1	-5.340	5.506	-0.250
ESF-HD-CAN5-TC-8	0.715	25.038	-0.678	ESF-HD-85-WH3-TC-2	-7.350	5.511	-0.251
ESF-HD-CAN5-TC-9	-0.745	25.038	-0.678	ESF-HD-85-WH3-TC-3	-9.230	5.516	-0.252
ESF-HD-CAN6-TC-1	-0.176	28.046	0.577	ESF-HD-85-WH3-TC-4	-10.830	5.520	-0.253
ESF-HD-CAN6-TC-2	0.704	28.046	-0.673	ESF-HD-85-WH3-TC-5	-13.830	5.528	-0.255
ESF-HD-CAN6-TC-3	-0.756	28.046	-0.673	ESF-HD-86-WH4-TC-1	-5.171	7.282	-0.275
ESF-HD-CAN6-TC-4	-0.176	29.216	0.577	ESF-HD-86-WH4-TC-2	-7.181	7.261	-0.293
ESF-HD-CAN6-TC-5	0.704	29.216	-0.673	ESF-HD-86-WH4-TC-3	-9.060	7.241	-0.310

Table C-2. Gage Locations for the DST Temperature Gages (continued)

Gage ID	x	y	z	Gage ID	x	y	z
ESF-HD-86-WH4-TC-4	-10.660	7.224	-0.324	ESF-HD-96-WH14-TC-4	-10.811	25.643	-0.472
ESF-HD-86-WH4-TC-5	-13.660	7.193	-0.351	ESF-HD-96-WH14-TC-5	-13.810	25.652	-0.543
ESF-HD-87-WH5-TC-1	-5.265	9.196	-0.247	ESF-HD-97-WH15-TC-1	-4.781	27.484	-0.257
ESF-HD-87-WH5-TC-2	-7.274	9.228	-0.244	ESF-HD-97-WH15-TC-2	-6.790	27.513	-0.277
ESF-HD-87-WH5-TC-3	-9.154	9.258	-0.241	ESF-HD-97-WH15-TC-3	-8.670	27.540	-0.296
ESF-HD-87-WH5-TC-4	-10.754	9.283	-0.238	ESF-HD-97-WH15-TC-4	-10.270	27.564	-0.312
ESF-HD-87-WH5-TC-5	-13.754	9.331	-0.233	ESF-HD-97-WH15-TC-5	-13.269	27.608	-0.342
ESF-HD-88-WH6-TC-1	-5.227	10.975	-0.244	ESF-HD-98-WH16-TC-1	-5.205	29.220	-0.242
ESF-HD-88-WH6-TC-2	-7.237	10.968	-0.245	ESF-HD-98-WH16-TC-2	-7.215	29.205	-0.245
ESF-HD-88-WH6-TC-3	-9.117	10.962	-0.246	ESF-HD-98-WH16-TC-3	-9.095	29.191	-0.248
ESF-HD-88-WH6-TC-4	-10.717	10.957	-0.247	ESF-HD-98-WH16-TC-4	-10.695	29.178	-0.250
ESF-HD-88-WH6-TC-5	-13.717	10.947	-0.249	ESF-HD-98-WH16-TC-5	-13.695	29.156	-0.254
ESF-HD-89-WH7-TC-1	-5.438	12.831	-0.246	ESF-HD-99-WH17-TC-1	-5.274	31.159	-0.261
ESF-HD-89-WH7-TC-2	-7.448	12.843	-0.252	ESF-HD-99-WH17-TC-2	-7.284	31.184	-0.261
ESF-HD-89-WH7-TC-3	-9.328	12.854	-0.257	ESF-HD-99-WH17-TC-3	-9.164	31.207	-0.262
ESF-HD-89-WH7-TC-4	-10.928	12.863	-0.262	ESF-HD-99-WH17-TC-4	-10.763	31.227	-0.262
ESF-HD-89-WH7-TC-5	-13.928	12.881	-0.270	ESF-HD-99-WH17-TC-5	-13.763	31.264	-0.263
ESF-HD-90-WH8-TC-1	-5.357	14.579	-0.296	ESF-HD-100-WH18-TC-1	-5.276	32.955	-0.263
ESF-HD-90-WH8-TC-2	-7.367	14.562	-0.316	ESF-HD-100-WH18-TC-2	-7.286	32.970	-0.274
ESF-HD-90-WH8-TC-3	-9.246	14.547	-0.334	ESF-HD-100-WH18-TC-3	-9.166	32.985	-0.284
ESF-HD-90-WH8-TC-4	-10.846	14.534	-0.350	ESF-HD-100-WH18-TC-4	-10.766	32.997	-0.293
ESF-HD-90-WH8-TC-5	-13.846	14.509	-0.379	ESF-HD-100-WH18-TC-5	-13.765	33.020	-0.310
ESF-HD-91-WH9-TC-1	-5.382	16.522	-0.222	ESF-HD-101-WH19-TC-1	-5.305	34.716	-0.266
ESF-HD-91-WH9-TC-2	-7.391	16.550	-0.214	ESF-HD-101-WH19-TC-2	-7.315	34.703	-0.270
ESF-HD-91-WH9-TC-3	-9.271	16.577	-0.206	ESF-HD-101-WH19-TC-3	-9.195	34.691	-0.273
ESF-HD-91-WH9-TC-4	-10.871	16.599	-0.200	ESF-HD-101-WH19-TC-4	-10.795	34.681	-0.276
ESF-HD-91-WH9-TC-5	-13.871	16.641	-0.188	ESF-HD-101-WH19-TC-5	-13.795	34.662	-0.281
ESF-HD-92-WH10-TC-1	-5.327	18.254	-0.280	ESF-HD-102-WH20-TC-1	-5.294	36.532	-0.363
ESF-HD-92-WH10-TC-2	-7.337	18.235	-0.294	ESF-HD-102-WH20-TC-2	-7.302	36.503	-0.423
ESF-HD-92-WH10-TC-3	-9.217	18.217	-0.308	ESF-HD-102-WH20-TC-3	-9.181	36.476	-0.478
ESF-HD-92-WH10-TC-4	-10.816	18.202	-0.319	ESF-HD-102-WH20-TC-4	-10.781	36.453	-0.526
ESF-HD-92-WH10-TC-5	-13.816	18.173	-0.340	ESF-HD-102-WH20-TC-5	-13.779	36.410	-0.614
ESF-HD-93-WH11-TC-1	-5.217	20.107	-0.322	ESF-HD-103-WH21-TC-1	-5.357	38.420	-0.225
ESF-HD-93-WH11-TC-2	-7.226	20.106	-0.357	ESF-HD-103-WH21-TC-2	-7.367	38.429	-0.211
ESF-HD-93-WH11-TC-3	-9.106	20.106	-0.390	ESF-HD-103-WH21-TC-3	-9.247	38.437	-0.197
ESF-HD-93-WH11-TC-4	-10.706	20.105	-0.418	ESF-HD-103-WH21-TC-4	-10.847	38.443	-0.185
ESF-HD-93-WH11-TC-5	-13.705	20.104	-0.470	ESF-HD-103-WH21-TC-5	-13.847	38.456	-0.162
ESF-HD-94-WH12-TC-1	-5.125	21.988	-0.244	ESF-HD-104-WH22-TC-1	-5.403	40.248	-0.213
ESF-HD-94-WH12-TC-2	-7.135	22.011	-0.242	ESF-HD-104-WH22-TC-2	-7.412	40.262	-0.187
ESF-HD-94-WH12-TC-3	-9.015	22.032	-0.241	ESF-HD-104-WH22-TC-3	-9.292	40.274	-0.162
ESF-HD-94-WH12-TC-4	-10.614	22.050	-0.240	ESF-HD-104-WH22-TC-4	-10.892	40.285	-0.141
ESF-HD-94-WH12-TC-5	-13.614	22.084	-0.237	ESF-HD-104-WH22-TC-5	-13.892	40.304	-0.102
ESF-HD-95-WH13-TC-1	-5.345	23.777	-0.263	ESF-HD-105-WH23-TC-1	-5.108	42.123	-0.266
ESF-HD-95-WH13-TC-2	-7.355	23.777	-0.270	ESF-HD-105-WH23-TC-2	-7.118	42.147	-0.262
ESF-HD-95-WH13-TC-3	-9.235	23.777	-0.276	ESF-HD-105-WH23-TC-3	-8.998	42.170	-0.258
ESF-HD-95-WH13-TC-4	-10.835	23.777	-0.282	ESF-HD-105-WH23-TC-4	-10.597	42.190	-0.254
ESF-HD-95-WH13-TC-5	-13.835	23.777	-0.292	ESF-HD-105-WH23-TC-5	-13.597	42.227	-0.247
ESF-HD-96-WH14-TC-1	-5.322	25.626	-0.342	ESF-HD-106-WH24-TC-1	-5.350	43.884	-0.219
ESF-HD-96-WH14-TC-2	-7.332	25.632	-0.390	ESF-HD-106-WH24-TC-2	-7.360	43.890	-0.204
ESF-HD-96-WH14-TC-3	-9.211	25.638	-0.434	ESF-HD-106-WH24-TC-3	-9.240	43.896	-0.191

Table C-2. Gage Locations for the DST Temperature Gages (continued)

Gage ID	x	y	z	Gage ID	x	y	z
ESF-HD-106-WH24-TC-4	-10.840	43.901	-0.179	ESF-HD-116-WH34-TC-4	10.598	31.046	-0.236
ESF-HD-106-WH24-TC-5	-13.840	43.910	-0.157	ESF-HD-116-WH34-TC-5	13.598	31.032	-0.230
ESF-HD-107-WH25-TC-1	-5.357	45.749	-0.290	ESF-HD-117-WH35-TC-1	5.036	29.215	-0.217
ESF-HD-107-WH25-TC-2	-7.367	45.759	-0.311	ESF-HD-117-WH35-TC-2	7.046	29.203	-0.197
ESF-HD-107-WH25-TC-3	-9.247	45.769	-0.332	ESF-HD-117-WH35-TC-3	8.926	29.193	-0.178
ESF-HD-107-WH25-TC-4	-10.846	45.778	-0.349	ESF-HD-117-WH35-TC-4	10.525	29.184	-0.162
ESF-HD-107-WH25-TC-5	-13.846	45.793	-0.381	ESF-HD-117-WH35-TC-5	13.525	29.167	-0.132
ESF-HD-108-WH26-TC-1	5.352	45.753	-0.329	ESF-HD-118-WH36-TC-1	5.309	27.413	-0.170
ESF-HD-108-WH26-TC-2	7.362	45.765	-0.366	ESF-HD-118-WH36-TC-2	7.319	27.408	-0.142
ESF-HD-108-WH26-TC-3	9.242	45.776	-0.400	ESF-HD-118-WH36-TC-3	9.198	27.403	-0.116
ESF-HD-108-WH26-TC-4	10.841	45.786	-0.429	ESF-HD-118-WH36-TC-4	10.798	27.399	-0.094
ESF-HD-108-WH26-TC-5	13.841	45.804	-0.485	ESF-HD-118-WH36-TC-5	13.798	27.391	-0.053
ESF-HD-109-WH27-TC-1	5.301	43.856	-0.263	ESF-HD-119-WH37-TC-1	5.358	25.616	-0.293
ESF-HD-109-WH27-TC-2	7.311	43.841	-0.272	ESF-HD-119-WH37-TC-2	7.368	25.626	-0.319
ESF-HD-109-WH27-TC-3	9.191	43.827	-0.280	ESF-HD-119-WH37-TC-3	9.247	25.634	-0.343
ESF-HD-109-WH27-TC-4	10.791	43.815	-0.287	ESF-HD-119-WH37-TC-4	10.847	25.642	-0.364
ESF-HD-109-WH27-TC-5	13.791	43.792	-0.301	ESF-HD-119-WH37-TC-5	13.847	25.656	-0.403
ESF-HD-110-WH28-TC-1	5.292	42.078	-0.248	ESF-HD-120-WH38-TC-1	5.099	23.788	-0.292
ESF-HD-110-WH28-TC-2	7.302	42.088	-0.241	ESF-HD-120-WH38-TC-2	7.109	23.797	-0.311
ESF-HD-110-WH28-TC-3	9.182	42.097	-0.234	ESF-HD-120-WH38-TC-3	8.989	23.807	-0.329
ESF-HD-110-WH28-TC-4	10.782	42.105	-0.228	ESF-HD-120-WH38-TC-4	10.589	23.814	-0.344
ESF-HD-110-WH28-TC-5	13.782	42.119	-0.217	ESF-HD-120-WH38-TC-5	13.588	23.829	-0.373
ESF-HD-111-WH29-TC-1	5.316	40.231	-0.212	ESF-HD-121-WH39-TC-1	5.341	21.941	-0.279
ESF-HD-111-WH29-TC-2	7.326	40.242	-0.194	ESF-HD-121-WH39-TC-2	7.351	21.942	-0.283
ESF-HD-111-WH29-TC-3	9.206	40.252	-0.177	ESF-HD-121-WH39-TC-3	9.231	21.943	-0.288
ESF-HD-111-WH29-TC-4	10.806	40.260	-0.162	ESF-HD-121-WH39-TC-4	10.831	21.944	-0.291
ESF-HD-111-WH29-TC-5	13.805	40.276	-0.136	ESF-HD-121-WH39-TC-5	13.831	21.945	-0.298
ESF-HD-112-WH30-TC-1	5.401	38.368	-0.264	ESF-HD-122-WH40-TC-1	4.252	20.115	-0.246
ESF-HD-112-WH30-TC-2	7.411	38.356	-0.265	ESF-HD-122-WH40-TC-2	6.262	20.117	-0.243
ESF-HD-112-WH30-TC-3	9.291	38.345	-0.266	ESF-HD-122-WH40-TC-3	8.142	20.118	-0.241
ESF-HD-112-WH30-TC-4	10.891	38.336	-0.267	ESF-HD-122-WH40-TC-4	9.742	20.119	-0.238
ESF-HD-112-WH30-TC-5	13.891	38.318	-0.269	ESF-HD-122-WH40-TC-5	12.742	20.121	-0.234
ESF-HD-113-WH31-TC-1	5.386	36.540	-0.237	ESF-HD-123-WH41-TC-1	5.220	18.284	-0.260
ESF-HD-113-WH31-TC-2	7.396	36.526	-0.231	ESF-HD-123-WH41-TC-2	7.230	18.282	-0.268
ESF-HD-113-WH31-TC-3	9.276	36.512	-0.226	ESF-HD-123-WH41-TC-3	9.110	18.280	-0.276
ESF-HD-113-WH31-TC-4	10.876	36.500	-0.221	ESF-HD-123-WH41-TC-4	10.710	18.278	-0.283
ESF-HD-113-WH31-TC-5	13.876	36.478	-0.213	ESF-HD-123-WH41-TC-5	13.710	18.275	-0.296
ESF-HD-114-WH32-TC-1	5.540	34.830	-0.274	ESF-HD-124-WH42-TC-1	5.418	16.395	-0.334
ESF-HD-114-WH32-TC-2	7.549	34.862	-0.274	ESF-HD-124-WH42-TC-2	7.427	16.368	-0.376
ESF-HD-114-WH32-TC-3	9.429	34.892	-0.275	ESF-HD-124-WH42-TC-3	9.307	16.343	-0.415
ESF-HD-114-WH32-TC-4	11.029	34.917	-0.275	ESF-HD-124-WH42-TC-4	10.906	16.322	-0.449
ESF-HD-114-WH32-TC-5	14.029	34.965	-0.276	ESF-HD-124-WH42-TC-5	13.905	16.282	-0.511
ESF-HD-115-WH33-TC-1	5.322	32.855	-0.223	ESF-HD-125-WH43-TC-1	5.388	14.652	-0.347
ESF-HD-115-WH33-TC-2	7.332	32.812	-0.216	ESF-HD-125-WH43-TC-2	7.398	14.658	-0.388
ESF-HD-115-WH33-TC-3	9.211	32.772	-0.210	ESF-HD-125-WH43-TC-3	9.278	14.664	-0.427
ESF-HD-115-WH33-TC-4	10.811	32.738	-0.205	ESF-HD-125-WH43-TC-4	10.877	14.669	-0.459
ESF-HD-115-WH33-TC-5	13.810	32.674	-0.195	ESF-HD-125-WH43-TC-5	13.877	14.678	-0.521
ESF-HD-116-WH34-TC-1	5.108	31.070	-0.249	ESF-HD-126-WH44-TC-1	5.221	12.816	-0.268
ESF-HD-116-WH34-TC-2	7.118	31.061	-0.244	ESF-HD-126-WH44-TC-2	7.231	12.827	-0.284
ESF-HD-116-WH34-TC-3	8.998	31.053	-0.240	ESF-HD-126-WH44-TC-3	9.111	12.837	-0.300

Table C-2. Gage Locations for the DST Temperature Gages (continued)

Gage ID	x	y	z	Gage ID	x	y	z
ESF-HD-126-WH44-TC-4	10.711	12.846	-0.313	ESF-HD-SURF-TC-18	2.442	21.642	-0.049
ESF-HD-126-WH44-TC-5	13.710	12.863	-0.338	ESF-HD-SURF-TC-19	0.174	25.183	2.652
ESF-HD-127-WH45-TC-1	5.377	10.889	-0.313	ESF-HD-SURF-TC-20	2.504	25.170	-0.071
ESF-HD-127-WH45-TC-2	7.386	10.847	-0.343	ESF-HD-SURF-TC-21	-2.387	25.238	-0.995
ESF-HD-127-WH45-TC-3	9.266	10.807	-0.370	ESF-HD-SURF-TC-22	-0.042	28.938	2.470
ESF-HD-127-WH45-TC-4	10.865	10.773	-0.394	ESF-HD-SURF-TC-23	-2.483	28.853	-0.142
ESF-HD-127-WH45-TC-5	13.864	10.709	-0.438	ESF-HD-SURF-TC-24	2.614	28.807	-0.131
ESF-HD-128-WH46-TC-1	5.205	9.158	-0.297	ESF-HD-SURF-TC-25	0.081	32.209	2.367
ESF-HD-128-WH46-TC-2	7.214	9.170	-0.325	ESF-HD-SURF-TC-26	2.524	32.380	-0.092
ESF-HD-128-WH46-TC-3	9.094	9.182	-0.351	ESF-HD-SURF-TC-27	-2.394	32.358	-0.711
ESF-HD-128-WH46-TC-4	10.694	9.192	-0.373	ESF-HD-SURF-TC-28	0.024	34.709	2.710
ESF-HD-128-WH46-TC-5	13.694	9.210	-0.415	ESF-HD-SURF-TC-29	-2.703	34.740	-0.104
ESF-HD-129-WH47-TC-1	5.012	7.270	-0.251	ESF-HD-SURF-TC-30	2.783	34.584	-0.254
ESF-HD-129-WH47-TC-2	7.021	7.234	-0.255	ESF-HD-SURF-TC-31	0.442	36.825	2.530
ESF-HD-129-WH47-TC-3	8.901	7.200	-0.260	ESF-HD-SURF-TC-32	2.345	36.927	1.150
ESF-HD-129-WH47-TC-4	10.501	7.172	-0.264	ESF-HD-SURF-TC-33	2.353	36.951	-1.014
ESF-HD-129-WH47-TC-5	13.500	7.118	-0.271	ESF-HD-SURF-TC-34	-2.314	36.846	-1.074
ESF-HD-130-WH48-TC-1	5.251	5.468	-0.218	ESF-HD-SURF-TC-35	-2.417	36.886	1.013
ESF-HD-130-WH48-TC-2	7.261	5.441	-0.208	ESF-HD-SURF-TC-36	0.438	41.548	2.553
ESF-HD-130-WH48-TC-3	9.140	5.416	-0.200	ESF-HD-SURF-TC-37	2.373	41.695	1.128
ESF-HD-130-WH48-TC-4	10.740	5.394	-0.192	ESF-HD-SURF-TC-38	2.303	41.738	-1.018
ESF-HD-130-WH48-TC-5	13.740	5.354	-0.178	ESF-HD-SURF-TC-39	-2.333	41.600	-1.051
ESF-HD-131-WH49-TC-1	4.157	3.677	-0.284	ESF-HD-SURF-TC-40	-2.358	41.699	1.169
ESF-HD-131-WH49-TC-2	6.167	3.682	-0.292	ESF-HD-SURF-TC-41	0.080	44.524	2.600
ESF-HD-131-WH49-TC-3	8.047	3.688	-0.300	ESF-HD-SURF-TC-42	2.396	44.566	1.075
ESF-HD-131-WH49-TC-4	9.647	3.692	-0.307	ESF-HD-SURF-TC-43	2.326	44.605	-1.010
ESF-HD-131-WH49-TC-5	12.647	3.701	-0.320	ESF-HD-SURF-TC-44	-2.305	44.474	-1.063
ESF-HD-132-WH50-TC-1	5.377	1.760	-0.307	ESF-HD-SURF-TC-45	-2.357	44.559	1.124
ESF-HD-132-WH50-TC-2	7.386	1.719	-0.339	ESF-HD-SURF-TC-46	-0.010	47.548	1.431
ESF-HD-132-WH50-TC-3	9.266	1.680	-0.369	ESF-HD-SURF-TC-47	-0.004	47.613	0.227
ESF-HD-132-WH50-TC-4	10.865	1.647	-0.394	ESF-HD-SURF-TC-48	-0.006	5.826	-1.292
ESF-HD-132-WH50-TC-5	13.864	1.586	-0.442	ESF-HD-SURF-TC-49	-0.026	26.870	-1.301
Surface Thermocouples				ESF-HD-SURF-TC-50	-0.013	42.642	-1.290
ESF-HD-SURF-TC-1	0.065	3.433	2.441	Bulkhead Thermocouples			
ESF-HD-SURF-TC-2	2.559	3.600	-0.127	ESF-HD-BHSF-TC-1	0.185	0.000	2.320
ESF-HD-SURF-TC-3	-2.351	3.639	-0.491	ESF-HD-BHSF-TC-2	1.920	0.000	-1.095
ESF-HD-SURF-TC-4	-0.027	7.162	2.525	ESF-HD-BHSF-TC-3	1.815	0.000	-1.120
ESF-HD-SURF-TC-5	-2.435	7.203	-0.148	ESF-HD-BHSF-TC-4	0.000	0.000	-1.120
ESF-HD-SURF-TC-6	2.567	7.066	-0.068	ESF-HD-BHSF-TC-5	-1.815	0.000	-1.120
ESF-HD-SURF-TC-7	-0.121	10.832	2.501	ESF-HD-BHSF-TC-6	-1.920	0.000	1.095
ESF-HD-SURF-TC-8	2.478	10.789	-0.081	ESF-HD-BHSF-TC-7	1.065	0.000	1.655
ESF-HD-SURF-TC-9	-2.431	10.830	-0.843	ESF-HD-BHSF-TC-8	-1.065	0.000	1.655
ESF-HD-SURF-TC-10	-0.154	14.317	2.566	ESF-HD-BHSF-TC-9	0.000	0.000	0.300
ESF-HD-SURF-TC-11	-2.545	14.417	-0.115	Lateral MPBX Thermocouples			
ESF-HD-SURF-TC-12	2.467	14.303	-0.096	ESF-HD-81-MPBX1-TC-20	6.994	-11.130	3.463
ESF-HD-SURF-TC-13	-0.105	17.832	2.583	ESF-HD-81-MPBX1-TC-3	6.973	-6.630	3.450
ESF-HD-SURF-TC-14	2.515	18.043	-0.130	ESF-HD-81-MPBX1-TC-5	6.959	-3.630	3.441
ESF-HD-SURF-TC-15	-2.421	17.773	-0.380	ESF-HD-81-MPBX1-TC-6	6.934	1.870	3.424
ESF-HD-SURF-TC-16	-0.413	21.372	2.529	ESF-HD-81-MPBX1-TC-8	6.925	3.870	3.418
ESF-HD-SURF-TC-17	-2.445	21.586	-0.130	ESF-HD-81-MPBX1-TC-10	6.920	4.870	3.415

Table C-2. Gage Locations for the DST Temperature Gages (continued)

Gage ID	x	y	z	Gage ID	x	y	z
ESF-HD-81-MPBX1-TC-14	6.837	22.869	3.362	ESF-HD-149-MPBX5-TC-1	-0.028	13.697	2.484
ESF-HD-81-MPBX1-TC-17	6.804	29.869	3.341	ESF-HD-149-MPBX5-TC-2	-0.033	13.691	3.524
ESF-HD-81-MPBX1-TC-18	6.798	31.369	3.337	ESF-HD-149-MPBX5-TC-3	-0.037	13.685	4.524
ESF-HD-81-MPBX1-TC-19	6.786	33.869	3.329	ESF-HD-149-MPBX5-TC-4	-0.041	13.681	5.234
ESF-HD-81-MPBX1-TC-2	Not installed or lost			ESF-HD-149-MPBX5-TC-5	-0.047	13.673	6.564
ESF-HD-81-MPBX1-TC-4	Not installed or lost			ESF-HD-149-MPBX5-TC-6	-0.058	13.659	8.984
ESF-HD-81-MPBX1-TC-7	Not installed or lost			ESF-HD-149-MPBX5-TC-7	-0.069	13.644	11.484
ESF-HD-81-MPBX1-TC-9	Not installed or lost			ESF-HD-149-MPBX5-TC-8	-0.096	13.609	17.434
ESF-HD-81-MPBX1-TC-11	Not installed or lost			ESF-HD-150-MPBX6-TC-1	0.006	13.693	-1.639
ESF-HD-81-MPBX1-TC-12	Not installed or lost			ESF-HD-150-MPBX6-TC-2	0.024	13.708	-3.739
ESF-HD-81-MPBX1-TC-13	Not installed or lost			ESF-HD-150-MPBX6-TC-3	0.032	13.715	-4.739
ESF-HD-81-MPBX1-TC-15	Not installed or lost			ESF-HD-150-MPBX6-TC-4	0.038	13.719	-5.389
ESF-HD-81-MPBX1-TC-16	Not installed or lost			ESF-HD-150-MPBX6-TC-5	0.049	13.729	-6.739
ESF-HD-82-MPBX2-TC-1	-7.028	-10.958	3.451	ESF-HD-150-MPBX6-TC-6	0.061	13.738	-8.139
ESF-HD-82-MPBX2-TC-2	-7.049	-9.458	3.441	ESF-HD-150-MPBX6-TC-7	0.087	13.759	-11.138
ESF-HD-82-MPBX2-TC-3	-7.084	-6.958	3.423	ESF-HD-150-MPBX6-TC-8	0.138	13.802	-17.238
ESF-HD-82-MPBX2-TC-4	-7.119	-4.459	3.406	ESF-HD-154-MPBX7-TC-1	1.285	21.020	2.186
ESF-HD-82-MPBX2-TC-5	-7.154	-1.959	3.388	ESF-HD-154-MPBX7-TC-2	1.842	21.019	3.135
ESF-HD-82-MPBX2-TC-6	-7.185	0.241	3.373	ESF-HD-154-MPBX7-TC-3	2.348	21.019	3.997
ESF-HD-82-MPBX2-TC-7	-7.217	2.540	3.357	ESF-HD-154-MPBX7-TC-4	2.804	21.018	4.773
ESF-HD-82-MPBX2-TC-8	-7.252	5.040	3.339	ESF-HD-154-MPBX7-TC-5	3.336	21.018	5.678
ESF-HD-82-MPBX2-TC-9	-7.283	7.240	3.324	ESF-HD-154-MPBX7-TC-6	4.323	21.016	7.360
ESF-HD-82-MPBX2-TC-10	-7.308	9.040	3.311	ESF-HD-154-MPBX7-TC-7	6.095	21.014	10.378
ESF-HD-82-MPBX2-TC-11	-7.343	11.539	3.294	ESF-HD-154-MPBX7-TC-8	8.804	21.011	14.992
ESF-HD-82-MPBX2-TC-12	-7.381	14.239	3.275	ESF-HD-155-MPBX8-TC-1	-1.317	21.006	2.270
ESF-HD-82-MPBX2-TC-13	-7.441	18.538	3.245	ESF-HD-155-MPBX8-TC-2	-1.867	21.000	3.199
ESF-HD-82-MPBX2-TC-14	-7.479	21.238	3.226	ESF-HD-155-MPBX8-TC-3	-2.372	20.994	4.051
ESF-HD-82-MPBX2-TC-15	-7.504	23.038	3.213	ESF-HD-155-MPBX8-TC-4	-2.846	20.989	4.851
ESF-HD-82-MPBX2-TC-16	-7.539	25.538	3.196	ESF-HD-155-MPBX8-TC-5	-3.381	20.983	5.755
ESF-HD-82-MPBX2-TC-17	-7.577	28.237	3.177	ESF-HD-155-MPBX8-TC-6	-4.375	20.971	7.432
ESF-HD-82-MPBX2-TC-18	-7.602	30.037	3.164	ESF-HD-155-MPBX8-TC-7	-5.904	20.954	10.013
ESF-HD-82-MPBX2-TC-20	-7.665	34.536	3.133	ESF-HD-155-MPBX8-TC-8	-8.757	20.922	14.832
ESF-HD-82-MPBX2-TC-19	Not installed or lost			ESF-HD-156-MPBX9-TC-1	-0.013	21.001	2.504
Heated Drift MPBX Thermocouples				ESF-HD-156-MPBX9-TC-2	-0.010	20.997	3.604
ESF-HD-147-MPBX3-TC-1	1.284	13.706	2.213	ESF-HD-156-MPBX9-TC-3	-0.007	20.993	4.604
ESF-HD-147-MPBX3-TC-2	1.827	13.702	3.169	ESF-HD-156-MPBX9-TC-4	-0.005	20.990	5.504
ESF-HD-147-MPBX3-TC-3	2.321	13.699	4.039	ESF-HD-156-MPBX9-TC-5	-0.002	20.985	6.604
ESF-HD-147-MPBX3-TC-4	2.766	13.695	4.821	ESF-HD-156-MPBX9-TC-6	0.003	20.978	8.504
ESF-HD-147-MPBX3-TC-5	3.309	13.691	5.778	ESF-HD-156-MPBX9-TC-7	0.013	20.965	12.004
ESF-HD-147-MPBX3-TC-6	4.792	13.681	8.386	ESF-HD-156-MPBX9-TC-8	0.028	20.944	17.354
ESF-HD-147-MPBX3-TC-7	5.854	13.673	10.255	ESF-HD-157-MPBX10-TC-1	-0.004	21.037	-1.624
ESF-HD-147-MPBX3-TC-8	8.595	13.654	15.081	ESF-HD-157-MPBX10-TC-2	0.000	21.034	-3.684
ESF-HD-148-MPBX4-TC-1	-1.390	13.725	2.387	ESF-HD-157-MPBX10-TC-3	0.003	21.033	-4.674
ESF-HD-148-MPBX4-TC-2	-1.945	13.723	3.337	ESF-HD-157-MPBX10-TC-4	0.005	21.031	-5.624
ESF-HD-148-MPBX4-TC-3	-2.425	13.722	4.157	ESF-HD-157-MPBX10-TC-5	0.007	21.030	-6.674
ESF-HD-148-MPBX4-TC-4	-2.904	13.720	4.977	ESF-HD-157-MPBX10-TC-6	0.011	21.027	-8.624
ESF-HD-148-MPBX4-TC-5	-3.434	13.718	5.883	ESF-HD-157-MPBX10-TC-7	0.018	21.023	-11.624
ESF-HD-148-MPBX4-TC-6	-3.661	13.717	6.272	ESF-HD-157-MPBX10-TC-8	0.029	21.015	-16.924
ESF-HD-148-MPBX4-TC-7	-5.932	13.710	10.157	ESF-HD-178-MPBX11-TC-1	1.297	41.138	2.249
ESF-HD-148-MPBX4-TC-8	-8.758	13.700	14.991	ESF-HD-178-MPBX11-TC-2	1.813	41.136	3.163

Table C-2. Gage Locations for the DST Temperature Gages (continued)

Gage ID	x	y	z	Gage ID	x	y	z
ESF-HD-178-MPBX11-TC-3	2.310	41.133	4.043	ESF-SDM-42-MPBX1-TC-12	-5.745	13.699	0.054
ESF-HD-178-MPBX11-TC-4	2.773	41.131	4.861	ESF-SDM-42-MPBX1-TC-13	-5.254	13.697	-0.041
ESF-HD-178-MPBX11-TC-5	3.412	41.128	5.993	ESF-SDM-42-MPBX1-TC-14	-4.763	13.694	-0.136
ESF-HD-178-MPBX11-TC-6	4.248	41.124	7.473	ESF-SDM-43-MPBX2-THRM-1	-29.166	21.062	5.073
ESF-HD-178-MPBX11-TC-7	5.724	41.117	10.085	ESF-SDM-43-MPBX2-TC-1	-25.232	21.013	4.352
ESF-HD-178-MPBX11-TC-8	8.581	41.104	15.144	ESF-SDM-43-MPBX2-TC-2	-21.298	20.964	3.631
ESF-HD-179-MPBX12-TC-1	-1.319	41.143	2.279	ESF-SDM-43-MPBX2-TC-3	-17.363	20.916	2.910
ESF-HD-179-MPBX12-TC-2	-1.832	41.138	3.183	ESF-SDM-43-MPBX2-TC-4	-13.429	20.867	2.189
ESF-HD-179-MPBX12-TC-3	-2.326	41.133	4.053	ESF-SDM-43-MPBX2-TC-5	-12.446	20.855	2.009
ESF-HD-179-MPBX12-TC-4	-2.800	41.128	4.888	ESF-SDM-43-MPBX2-TC-6	-11.462	20.843	1.829
ESF-HD-179-MPBX12-TC-5	-3.308	41.123	5.784	ESF-SDM-43-MPBX2-TC-7	-10.479	20.830	1.649
ESF-HD-179-MPBX12-TC-6	-4.281	41.113	7.497	ESF-SDM-43-MPBX2-TC-8	-9.495	20.818	1.468
ESF-HD-179-MPBX12-TC-7	-5.761	41.098	10.106	ESF-SDM-43-MPBX2-TC-9	-8.511	20.806	1.288
ESF-HD-179-MPBX12-TC-8	-8.758	41.067	15.385	ESF-SDM-43-MPBX2-TC-10	-7.528	20.794	1.108
ESF-HD-180-MPBX13-TC-1	0.010	41.134	2.597	ESF-SDM-43-MPBX2-TC-11	-6.544	20.782	0.928
ESF-HD-180-MPBX13-TC-2	0.020	41.129	3.897	ESF-SDM-43-MPBX2-TC-12	-5.561	20.769	0.748
ESF-HD-180-MPBX13-TC-3	0.025	41.127	4.637	ESF-SDM-43-MPBX2-TC-13	-5.069	20.763	0.657
ESF-HD-180-MPBX13-TC-4	0.032	41.123	5.597	ESF-SDM-43-MPBX2-TC-14	-4.577	20.757	0.567
ESF-HD-180-MPBX13-TC-5	0.040	41.119	6.657	ESF-SDM-44-MPBX3-THRM-1	-29.539	32.079	5.137
ESF-HD-180-MPBX13-TC-6	0.054	41.112	8.597	ESF-SDM-44-MPBX3-TC-1	-25.039	32.099	4.181
ESF-HD-180-MPBX13-TC-7	0.080	41.099	12.097	ESF-SDM-44-MPBX3-TC-2	-22.105	32.111	3.558
ESF-HD-180-MPBX13-TC-8	0.119	41.080	17.377	ESF-SDM-44-MPBX3-TC-3	-17.801	32.130	2.644
ESF-HD-181-MPBX14-TC-1	0.035	41.194	-1.658	ESF-SDM-44-MPBX3-TC-4	-13.888	32.147	1.813
ESF-HD-181-MPBX14-TC-2	0.040	41.196	-3.458	ESF-SDM-44-MPBX3-TC-5	-12.910	32.151	1.605
ESF-HD-181-MPBX14-TC-3	0.044	41.197	-4.708	ESF-SDM-44-MPBX3-TC-6	-11.932	32.156	1.398
ESF-HD-181-MPBX14-TC-4	0.047	41.198	-5.658	ESF-SDM-44-MPBX3-TC-7	-10.954	32.160	1.190
ESF-HD-181-MPBX14-TC-5	0.050	41.199	-6.718	ESF-SDM-44-MPBX3-TC-8	-9.976	32.164	0.982
ESF-HD-181-MPBX14-TC-6	0.055	41.201	-8.658	ESF-SDM-44-MPBX3-TC-9	-8.997	32.168	0.774
ESF-HD-181-MPBX14-TC-7	0.064	41.204	-11.658	ESF-SDM-44-MPBX3-TC-10	-8.019	32.173	0.567
ESF-HD-181-MPBX14-TC-8	0.081	41.210	-17.458	ESF-SDM-44-MPBX3-TC-11	-7.041	32.177	0.359
Cross Drift MPBX Thermocouples				ESF-SDM-44-MPBX3-TC-12	-6.063	32.181	0.151
ESF-HD-CDEX-TC1	0.424	42.357	1.870	ESF-SDM-44-MPBX3-TC-13	-5.574	32.183	0.047
ESF-HD-CDEX-TC2	0.418	42.357	0.570	ESF-SDM-44-MPBX3-TC-14	-5.085	32.186	-0.057
ESF-HD-CDEX-TC3	0.411	42.357	-0.750	Heated Drift RTD Probes			
ESF-HD-CDEX-TC4	1.967	42.269	-0.016	ESF-HD-79-TEMP1-RTD-1	9.460	-17.522	3.866
ESF-HD-CDEX-TC5	-0.183	42.273	-0.003	ESF-HD-79-TEMP1-RTD-2	9.460	-16.522	3.849
ESF-HD-CDEX-TC6	-2.103	42.276	0.008	ESF-HD-79-TEMP1-RTD-3	9.460	-15.522	3.831
Access Observation Drift MPBX Thermocouples and Thermistors				ESF-HD-79-TEMP1-RTD-4	9.460	-14.522	3.814
ESF-SDM-42-MPBX1-THRM-1	-29.304	13.820	4.631	ESF-HD-79-TEMP1-RTD-5	9.460	-13.522	3.796
ESF-SDM-42-MPBX1-TC-1	-25.377	13.800	3.868	ESF-HD-79-TEMP1-RTD-6	9.460	-12.522	3.778
ESF-SDM-42-MPBX1-TC-2	-21.451	13.780	3.105	ESF-HD-79-TEMP1-RTD-7	9.460	-11.522	3.761
ESF-SDM-42-MPBX1-TC-3	-17.524	13.760	2.343	ESF-HD-79-TEMP1-RTD-8	9.460	-10.522	3.743
ESF-SDM-42-MPBX1-TC-4	-13.598	13.739	1.580	ESF-HD-79-TEMP1-RTD-9	9.460	-9.522	3.726
ESF-SDM-42-MPBX1-TC-5	-12.616	13.734	1.389	ESF-HD-79-TEMP1-RTD-10	9.460	-8.522	3.708
ESF-SDM-42-MPBX1-TC-6	-11.635	13.729	1.199	ESF-HD-79-TEMP1-RTD-11	9.460	-7.522	3.690
ESF-SDM-42-MPBX1-TC-7	-10.653	13.724	1.008	ESF-HD-79-TEMP1-RTD-12	9.460	-6.522	3.673
ESF-SDM-42-MPBX1-TC-8	-9.671	13.719	0.817	ESF-HD-79-TEMP1-RTD-13	9.460	-5.522	3.655
ESF-SDM-42-MPBX1-TC-9	-8.690	13.714	0.626	ESF-HD-79-TEMP1-RTD-14	9.460	-4.522	3.638
ESF-SDM-42-MPBX1-TC-10	-7.708	13.709	0.436	ESF-HD-79-TEMP1-RTD-15	9.460	-3.522	3.620
ESF-SDM-42-MPBX1-TC-11	-6.726	13.704	0.245	ESF-HD-79-TEMP1-RTD-16	9.460	-2.522	3.603

Table C-2. Gage Locations for the DST Temperature Gages (continued)

Gage ID	x	y	z	Gage ID	x	y	z
ESF-HD-79-TEMP1-RTD-17	9.460	-1.522	3.585	ESF-HD-80-TEMP2-RTD-7	-9.533	-4.381	3.220
ESF-HD-79-TEMP1-RTD-18	9.460	-0.522	3.567	ESF-HD-80-TEMP2-RTD-8	-9.540	-3.383	3.219
ESF-HD-79-TEMP1-RTD-19	9.460	0.478	3.550	ESF-HD-80-TEMP2-RTD-9	-9.547	-2.385	3.218
ESF-HD-79-TEMP1-RTD-20	9.460	1.478	3.532	ESF-HD-80-TEMP2-RTD-10	-9.554	-1.387	3.217
ESF-HD-79-TEMP1-RTD-21	9.460	2.478	3.515	ESF-HD-80-TEMP2-RTD-11	-9.561	-0.389	3.216
ESF-HD-79-TEMP1-RTD-22	9.460	3.478	3.497	ESF-HD-80-TEMP2-RTD-12	-9.568	0.609	3.215
ESF-HD-79-TEMP1-RTD-23	9.460	4.478	3.480	ESF-HD-80-TEMP2-RTD-13	-9.575	1.608	3.214
ESF-HD-79-TEMP1-RTD-24	9.460	5.478	3.462	ESF-HD-80-TEMP2-RTD-14	-9.582	2.606	3.213
ESF-HD-79-TEMP1-RTD-25	9.460	6.478	3.444	ESF-HD-80-TEMP2-RTD-15	-9.589	3.604	3.212
ESF-HD-79-TEMP1-RTD-26	9.460	7.478	3.427	ESF-HD-80-TEMP2-RTD-16	-9.596	4.602	3.211
ESF-HD-79-TEMP1-RTD-27	9.460	8.478	3.409	ESF-HD-80-TEMP2-RTD-17	-9.603	5.600	3.209
ESF-HD-79-TEMP1-RTD-28	9.460	9.478	3.392	ESF-HD-80-TEMP2-RTD-18	-9.610	6.598	3.208
ESF-HD-79-TEMP1-RTD-29	9.460	10.478	3.374	ESF-HD-80-TEMP2-RTD-19	-9.616	7.596	3.207
ESF-HD-79-TEMP1-RTD-30	9.460	11.478	3.356	ESF-HD-80-TEMP2-RTD-20	-9.623	8.594	3.206
ESF-HD-79-TEMP1-RTD-31	9.460	12.478	3.339	ESF-HD-80-TEMP2-RTD-21	-9.630	9.592	3.205
ESF-HD-79-TEMP1-RTD-32	9.460	13.478	3.321	ESF-HD-80-TEMP2-RTD-22	-9.637	10.591	3.204
ESF-HD-79-TEMP1-RTD-33	9.460	14.478	3.304	ESF-HD-80-TEMP2-RTD-23	-9.644	11.589	3.203
ESF-HD-79-TEMP1-RTD-34	9.460	15.478	3.286	ESF-HD-80-TEMP2-RTD-24	-9.651	12.587	3.202
ESF-HD-79-TEMP1-RTD-35	9.460	16.478	3.269	ESF-HD-80-TEMP2-RTD-25	-9.658	13.585	3.201
ESF-HD-79-TEMP1-RTD-36	9.460	17.478	3.251	ESF-HD-80-TEMP2-RTD-26	-9.665	14.583	3.200
ESF-HD-79-TEMP1-RTD-37	9.460	18.478	3.233	ESF-HD-80-TEMP2-RTD-27	-9.672	15.581	3.198
ESF-HD-79-TEMP1-RTD-38	9.459	19.478	3.216	ESF-HD-80-TEMP2-RTD-28	-9.679	16.579	3.197
ESF-HD-79-TEMP1-RTD-39	9.459	20.478	3.198	ESF-HD-80-TEMP2-RTD-29	-9.686	17.577	3.196
ESF-HD-79-TEMP1-RTD-40	9.459	21.478	3.181	ESF-HD-80-TEMP2-RTD-30	-9.693	18.576	3.195
ESF-HD-79-TEMP1-RTD-41	9.459	22.478	3.163	ESF-HD-80-TEMP2-RTD-31	-9.700	19.574	3.194
ESF-HD-79-TEMP1-RTD-42	9.459	23.478	3.145	ESF-HD-80-TEMP2-RTD-32	-9.707	20.572	3.193
ESF-HD-79-TEMP1-RTD-43	9.459	24.478	3.128	ESF-HD-80-TEMP2-RTD-33	-9.714	21.570	3.192
ESF-HD-79-TEMP1-RTD-44	9.459	25.478	3.110	ESF-HD-80-TEMP2-RTD-34	-9.721	22.568	3.191
ESF-HD-79-TEMP1-RTD-45	9.459	26.478	3.093	ESF-HD-80-TEMP2-RTD-35	-9.728	23.566	3.190
ESF-HD-79-TEMP1-RTD-46	9.459	27.478	3.075	ESF-HD-80-TEMP2-RTD-36	-9.735	24.564	3.188
ESF-HD-79-TEMP1-RTD-47	9.459	28.478	3.058	ESF-HD-80-TEMP2-RTD-37	-9.742	25.562	3.187
ESF-HD-79-TEMP1-RTD-48	9.459	29.478	3.040	ESF-HD-80-TEMP2-RTD-38	-9.749	26.561	3.186
ESF-HD-79-TEMP1-RTD-49	9.459	30.478	3.022	ESF-HD-80-TEMP2-RTD-39	-9.756	27.559	3.185
ESF-HD-79-TEMP1-RTD-50	9.459	31.478	3.005	ESF-HD-80-TEMP2-RTD-40	-9.763	28.557	3.184
ESF-HD-79-TEMP1-RTD-51	9.459	32.478	2.987	ESF-HD-80-TEMP2-RTD-41	-9.770	29.555	3.183
ESF-HD-79-TEMP1-RTD-52	9.459	33.478	2.970	ESF-HD-80-TEMP2-RTD-42	-9.777	30.553	3.182
ESF-HD-79-TEMP1-RTD-53	9.459	34.478	2.952	ESF-HD-80-TEMP2-RTD-43	-9.784	31.551	3.181
ESF-HD-79-TEMP1-RTD-54	9.459	35.478	2.935	ESF-HD-80-TEMP2-RTD-44	-9.791	32.549	3.180
ESF-HD-79-TEMP1-RTD-55	9.459	36.478	2.917	ESF-HD-80-TEMP2-RTD-45	-9.798	33.547	3.179
ESF-HD-79-TEMP1-RTD-56	9.459	37.478	2.899	ESF-HD-80-TEMP2-RTD-46	-9.805	34.545	3.177
ESF-HD-79-TEMP1-RTD-57	9.459	38.478	2.882	ESF-HD-80-TEMP2-RTD-47	-9.812	35.544	3.176
ESF-HD-79-TEMP1-RTD-58	9.459	39.478	2.864	ESF-HD-80-TEMP2-RTD-48	-9.819	36.542	3.175
ESF-HD-79-TEMP1-RTD-59	9.459	40.478	2.847	ESF-HD-80-TEMP2-RTD-49	-9.826	37.540	3.174
ESF-HD-79-TEMP1-RTD-60	9.459	41.478	2.829	ESF-HD-80-TEMP2-RTD-50	-9.833	38.538	3.173
ESF-HD-80-TEMP2-RTD-1	-9.491	-10.370	3.227	ESF-HD-80-TEMP2-RTD-51	-9.840	39.536	3.172
ESF-HD-80-TEMP2-RTD-2	-9.498	-9.372	3.226	ESF-HD-80-TEMP2-RTD-52	-9.847	40.534	3.171
ESF-HD-80-TEMP2-RTD-3	-9.505	-8.374	3.225	ESF-HD-80-TEMP2-RTD-53	-9.854	41.532	3.170
ESF-HD-80-TEMP2-RTD-4	-9.512	-7.376	3.224	ESF-HD-80-TEMP2-RTD-54	-9.861	42.530	3.169
ESF-HD-80-TEMP2-RTD-5	-9.519	-6.377	3.223	ESF-HD-80-TEMP2-RTD-55	-9.868	43.529	3.168
ESF-HD-80-TEMP2-RTD-6	-9.526	-5.379	3.222	ESF-HD-80-TEMP2-RTD-56	-9.875	44.527	3.166

Table C-2. Gage Locations for the DST Temperature Gages (continued)

Gage ID	x	y	z	Gage ID	x	y	z
ESF-HD-80-TEMP2-RTD-57	-9.882	45.525	3.165	ESF-HD-133-TEMP3-RTD-47	0.839	2.804	16.344
ESF-HD-80-TEMP2-RTD-58	-9.889	46.523	3.164	ESF-HD-133-TEMP3-RTD-48	0.841	2.805	16.645
ESF-HD-80-TEMP2-RTD-59	-9.896	47.521	3.163	ESF-HD-133-TEMP3-RTD-49	0.843	2.807	16.946
ESF-HD-80-TEMP2-RTD-60	-9.903	48.519	3.162	ESF-HD-133-TEMP3-RTD-50	0.845	2.808	17.247
ESF-HD-133-TEMP3-RTD-1	0.750	2.736	2.497	ESF-HD-133-TEMP3-RTD-51	0.846	2.810	17.548
ESF-HD-133-TEMP3-RTD-2	0.752	2.738	2.798	ESF-HD-133-TEMP3-RTD-52	0.848	2.811	17.849
ESF-HD-133-TEMP3-RTD-3	0.754	2.739	3.099	ESF-HD-133-TEMP3-RTD-53	0.850	2.813	18.150
ESF-HD-133-TEMP3-RTD-4	0.756	2.741	3.400	ESF-HD-133-TEMP3-RTD-54	0.852	2.814	18.451
ESF-HD-133-TEMP3-RTD-5	0.758	2.742	3.701	ESF-HD-133-TEMP3-RTD-55	0.854	2.816	18.752
ESF-HD-133-TEMP3-RTD-6	0.759	2.743	4.002	ESF-HD-133-TEMP3-RTD-56	0.856	2.817	19.053
ESF-HD-133-TEMP3-RTD-7	0.761	2.745	4.303	ESF-HD-133-TEMP3-RTD-57	0.858	2.819	19.354
ESF-HD-133-TEMP3-RTD-8	0.763	2.746	4.604	ESF-HD-133-TEMP3-RTD-58	0.860	2.820	19.655
ESF-HD-133-TEMP3-RTD-9	0.765	2.748	4.905	ESF-HD-133-TEMP3-RTD-59	0.862	2.822	19.956
ESF-HD-133-TEMP3-RTD-10	0.767	2.749	5.206	ESF-HD-133-TEMP3-RTD-60	0.864	2.823	20.258
ESF-HD-133-TEMP3-RTD-11	0.769	2.751	5.507	ESF-HD-133-TEMP3-RTD-61	0.866	2.825	20.559
ESF-HD-133-TEMP3-RTD-12	0.771	2.752	5.808	ESF-HD-133-TEMP3-RTD-62	0.868	2.826	20.860
ESF-HD-133-TEMP3-RTD-13	0.773	2.754	6.109	ESF-HD-133-TEMP3-RTD-63	0.870	2.828	21.161
ESF-HD-133-TEMP3-RTD-14	0.775	2.755	6.410	ESF-HD-133-TEMP3-RTD-64	0.872	2.829	21.462
ESF-HD-133-TEMP3-RTD-15	0.777	2.757	6.711	ESF-HD-133-TEMP3-RTD-65	0.873	2.831	21.763
ESF-HD-133-TEMP3-RTD-16	0.779	2.758	7.013	ESF-HD-133-TEMP3-RTD-66	0.875	2.832	22.064
ESF-HD-133-TEMP3-RTD-17	0.781	2.760	7.314	ESF-HD-133-TEMP3-RTD-67	0.877	2.834	22.365
ESF-HD-133-TEMP3-RTD-18	0.783	2.761	7.615	ESF-HD-134-TEMP4-RTD-1	0.739	2.732	-0.919
ESF-HD-133-TEMP3-RTD-19	0.785	2.763	7.916	ESF-HD-134-TEMP4-RTD-2	0.738	2.733	-1.235
ESF-HD-133-TEMP3-RTD-20	0.787	2.764	8.217	ESF-HD-134-TEMP4-RTD-3	0.736	2.734	-1.550
ESF-HD-133-TEMP3-RTD-21	0.788	2.766	8.518	ESF-HD-134-TEMP4-RTD-4	0.735	2.734	-1.866
ESF-HD-133-TEMP3-RTD-22	0.790	2.767	8.819	ESF-HD-134-TEMP4-RTD-5	0.733	2.735	-2.182
ESF-HD-133-TEMP3-RTD-23	0.792	2.769	9.120	ESF-HD-134-TEMP4-RTD-6	0.732	2.736	-2.497
ESF-HD-133-TEMP3-RTD-24	0.794	2.770	9.421	ESF-HD-134-TEMP4-RTD-7	0.730	2.737	-2.813
ESF-HD-133-TEMP3-RTD-25	0.796	2.772	9.722	ESF-HD-134-TEMP4-RTD-8	0.729	2.738	-3.129
ESF-HD-133-TEMP3-RTD-26	0.798	2.773	10.023	ESF-HD-134-TEMP4-RTD-9	0.727	2.738	-3.444
ESF-HD-133-TEMP3-RTD-27	0.800	2.774	10.324	ESF-HD-134-TEMP4-RTD-10	0.726	2.739	-3.760
ESF-HD-133-TEMP3-RTD-28	0.802	2.776	10.625	ESF-HD-134-TEMP4-RTD-11	0.724	2.740	-4.076
ESF-HD-133-TEMP3-RTD-29	0.804	2.777	10.926	ESF-HD-134-TEMP4-RTD-12	0.723	2.741	-4.392
ESF-HD-133-TEMP3-RTD-30	0.806	2.779	11.227	ESF-HD-134-TEMP4-RTD-13	0.721	2.742	-4.707
ESF-HD-133-TEMP3-RTD-31	0.808	2.780	11.528	ESF-HD-134-TEMP4-RTD-14	0.720	2.742	-5.023
ESF-HD-133-TEMP3-RTD-32	0.810	2.782	11.829	ESF-HD-134-TEMP4-RTD-15	0.718	2.743	-5.339
ESF-HD-133-TEMP3-RTD-33	0.812	2.783	12.130	ESF-HD-134-TEMP4-RTD-16	0.717	2.744	-5.654
ESF-HD-133-TEMP3-RTD-34	0.814	2.785	12.431	ESF-HD-134-TEMP4-RTD-17	0.715	2.745	-5.970
ESF-HD-133-TEMP3-RTD-35	0.816	2.786	12.732	ESF-HD-134-TEMP4-RTD-18	0.714	2.746	-6.286
ESF-HD-133-TEMP3-RTD-36	0.817	2.788	13.033	ESF-HD-134-TEMP4-RTD-19	0.712	2.746	-6.602
ESF-HD-133-TEMP3-RTD-37	0.819	2.789	13.334	ESF-HD-134-TEMP4-RTD-20	0.711	2.747	-6.917
ESF-HD-133-TEMP3-RTD-38	0.821	2.791	13.635	ESF-HD-134-TEMP4-RTD-21	0.709	2.748	-7.233
ESF-HD-133-TEMP3-RTD-39	0.823	2.792	13.936	ESF-HD-134-TEMP4-RTD-22	0.708	2.749	-7.549
ESF-HD-133-TEMP3-RTD-40	0.825	2.794	14.237	ESF-HD-134-TEMP4-RTD-23	0.706	2.749	-7.864
ESF-HD-133-TEMP3-RTD-41	0.827	2.795	14.538	ESF-HD-134-TEMP4-RTD-24	0.705	2.750	-8.180
ESF-HD-133-TEMP3-RTD-42	0.829	2.797	14.839	ESF-HD-134-TEMP4-RTD-25	0.703	2.751	-8.496
ESF-HD-133-TEMP3-RTD-43	0.831	2.798	15.140	ESF-HD-134-TEMP4-RTD-26	0.702	2.752	-8.811
ESF-HD-133-TEMP3-RTD-44	0.833	2.800	15.441	ESF-HD-134-TEMP4-RTD-27	0.700	2.753	-9.127
ESF-HD-133-TEMP3-RTD-45	0.835	2.801	15.742	ESF-HD-134-TEMP4-RTD-28	0.699	2.753	-9.443
ESF-HD-133-TEMP3-RTD-46	0.837	2.803	16.043	ESF-HD-134-TEMP4-RTD-29	0.697	2.754	-9.759

Table C-2. Gage Locations for the DST Temperature Gages (continued)

Gage ID	x	y	z	Gage ID	x	y	z
ESF-HD-134-TEMP4-RTD-30	0.696	2.755	-10.074	ESF-HD-137-TEMP5-RTD-13	0.793	11.905	5.903
ESF-HD-134-TEMP4-RTD-31	0.694	2.756	-10.390	ESF-HD-137-TEMP5-RTD-14	0.795	11.904	6.202
ESF-HD-134-TEMP4-RTD-32	0.693	2.757	-10.706	ESF-HD-137-TEMP5-RTD-15	0.796	11.903	6.501
ESF-HD-134-TEMP4-RTD-33	0.691	2.757	-11.021	ESF-HD-137-TEMP5-RTD-16	0.798	11.902	6.801
ESF-HD-134-TEMP4-RTD-34	0.690	2.758	-11.337	ESF-HD-137-TEMP5-RTD-17	0.799	11.900	7.100
ESF-HD-134-TEMP4-RTD-35	0.688	2.759	-11.653	ESF-HD-137-TEMP5-RTD-18	0.801	11.899	7.400
ESF-HD-134-TEMP4-RTD-36	0.687	2.760	-11.968	ESF-HD-137-TEMP5-RTD-19	0.803	11.898	7.699
ESF-HD-134-TEMP4-RTD-37	0.685	2.760	-12.284	ESF-HD-137-TEMP5-RTD-20	0.804	11.897	7.998
ESF-HD-134-TEMP4-RTD-38	0.684	2.761	-12.600	ESF-HD-137-TEMP5-RTD-21	0.806	11.896	8.298
ESF-HD-134-TEMP4-RTD-39	0.682	2.762	-12.916	ESF-HD-137-TEMP5-RTD-22	0.807	11.895	8.597
ESF-HD-134-TEMP4-RTD-40	0.681	2.763	-13.231	ESF-HD-137-TEMP5-RTD-23	0.809	11.893	8.896
ESF-HD-134-TEMP4-RTD-41	0.679	2.764	-13.547	ESF-HD-137-TEMP5-RTD-24	0.810	11.892	9.196
ESF-HD-134-TEMP4-RTD-42	0.678	2.764	-13.863	ESF-HD-137-TEMP5-RTD-25	0.812	11.891	9.495
ESF-HD-134-TEMP4-RTD-43	0.676	2.765	-14.178	ESF-HD-137-TEMP5-RTD-26	0.813	11.890	9.795
ESF-HD-134-TEMP4-RTD-44	0.675	2.766	-14.494	ESF-HD-137-TEMP5-RTD-27	0.815	11.889	10.094
ESF-HD-134-TEMP4-RTD-45	0.673	2.767	-14.810	ESF-HD-137-TEMP5-RTD-28	0.817	11.888	10.393
ESF-HD-134-TEMP4-RTD-46	0.672	2.768	-15.125	ESF-HD-137-TEMP5-RTD-29	0.818	11.886	10.693
ESF-HD-134-TEMP4-RTD-47	0.670	2.768	-15.441	ESF-HD-137-TEMP5-RTD-30	0.820	11.885	10.992
ESF-HD-134-TEMP4-RTD-48	0.669	2.769	-15.757	ESF-HD-137-TEMP5-RTD-31	0.821	11.884	11.291
ESF-HD-134-TEMP4-RTD-49	0.667	2.770	-16.073	ESF-HD-137-TEMP5-RTD-32	0.823	11.883	11.591
ESF-HD-134-TEMP4-RTD-50	0.666	2.771	-16.388	ESF-HD-137-TEMP5-RTD-33	0.824	11.882	11.890
ESF-HD-134-TEMP4-RTD-51	0.665	2.771	-16.704	ESF-HD-137-TEMP5-RTD-34	0.826	11.881	12.189
ESF-HD-134-TEMP4-RTD-52	0.663	2.772	-17.020	ESF-HD-137-TEMP5-RTD-35	0.828	11.879	12.489
ESF-HD-134-TEMP4-RTD-53	0.662	2.773	-17.335	ESF-HD-137-TEMP5-RTD-36	0.829	11.878	12.788
ESF-HD-134-TEMP4-RTD-54	0.660	2.774	-17.651	ESF-HD-137-TEMP5-RTD-37	0.831	11.877	13.088
ESF-HD-134-TEMP4-RTD-55	0.659	2.775	-17.967	ESF-HD-137-TEMP5-RTD-38	0.832	11.876	13.387
ESF-HD-134-TEMP4-RTD-56	0.657	2.775	-18.282	ESF-HD-137-TEMP5-RTD-39	0.834	11.875	13.686
ESF-HD-134-TEMP4-RTD-57	0.656	2.776	-18.598	ESF-HD-137-TEMP5-RTD-40	0.835	11.874	13.986
ESF-HD-134-TEMP4-RTD-58	0.654	2.777	-18.914	ESF-HD-137-TEMP5-RTD-41	0.837	11.872	14.285
ESF-HD-134-TEMP4-RTD-59	0.653	2.778	-19.230	ESF-HD-137-TEMP5-RTD-42	0.838	11.871	14.584
ESF-HD-134-TEMP4-RTD-60	0.651	2.779	-19.545	ESF-HD-137-TEMP5-RTD-43	0.840	11.870	14.884
ESF-HD-134-TEMP4-RTD-61	0.650	2.779	-19.861	ESF-HD-137-TEMP5-RTD-44	0.842	11.869	15.183
ESF-HD-134-TEMP4-RTD-62	0.648	2.780	-20.177	ESF-HD-137-TEMP5-RTD-45	0.843	11.868	15.482
ESF-HD-134-TEMP4-RTD-63	0.647	2.781	-20.492	ESF-HD-137-TEMP5-RTD-46	0.845	11.867	15.782
ESF-HD-134-TEMP4-RTD-64	0.645	2.782	-20.808	ESF-HD-137-TEMP5-RTD-47	0.846	11.865	16.081
ESF-HD-134-TEMP4-RTD-65	0.644	2.782	-21.124	ESF-HD-137-TEMP5-RTD-48	0.848	11.864	16.381
ESF-HD-134-TEMP4-RTD-66	0.642	2.783	-21.439	ESF-HD-137-TEMP5-RTD-49	0.849	11.863	16.680
ESF-HD-134-TEMP4-RTD-67	0.641	2.784	-21.755	ESF-HD-137-TEMP5-RTD-50	0.851	11.862	16.979
ESF-HD-137-TEMP5-RTD-1	0.774	11.919	2.310	ESF-HD-137-TEMP5-RTD-51	0.853	11.861	17.279
ESF-HD-137-TEMP5-RTD-2	0.776	11.918	2.610	ESF-HD-137-TEMP5-RTD-52	0.854	11.859	17.578
ESF-HD-137-TEMP5-RTD-3	0.777	11.917	2.909	ESF-HD-137-TEMP5-RTD-53	0.856	11.858	17.877
ESF-HD-137-TEMP5-RTD-4	0.779	11.916	3.208	ESF-HD-137-TEMP5-RTD-54	0.857	11.857	18.177
ESF-HD-137-TEMP5-RTD-5	0.781	11.914	3.508	ESF-HD-137-TEMP5-RTD-55	0.859	11.856	18.476
ESF-HD-137-TEMP5-RTD-6	0.782	11.913	3.807	ESF-HD-137-TEMP5-RTD-56	0.860	11.855	18.775
ESF-HD-137-TEMP5-RTD-7	0.784	11.912	4.107	ESF-HD-137-TEMP5-RTD-57	0.862	11.854	19.075
ESF-HD-137-TEMP5-RTD-8	0.785	11.911	4.406	ESF-HD-137-TEMP5-RTD-58	0.864	11.852	19.374
ESF-HD-137-TEMP5-RTD-9	0.787	11.910	4.705	ESF-HD-137-TEMP5-RTD-59	0.865	11.851	19.674
ESF-HD-137-TEMP5-RTD-10	0.788	11.909	5.005	ESF-HD-137-TEMP5-RTD-60	0.867	11.850	19.973
ESF-HD-137-TEMP5-RTD-11	0.790	11.907	5.304	ESF-HD-137-TEMP5-RTD-61	0.868	11.849	20.272
ESF-HD-137-TEMP5-RTD-12	0.792	11.906	5.603	ESF-HD-137-TEMP5-RTD-62	0.870	11.848	20.572

Table C-2. Gage Locations for the DST Temperature Gages (continued)

Gage ID	x	y	z	Gage ID	x	y	z
ESF-HD-137-TEMP5-RTD-63	0.871	11.847	20.871	ESF-HD-138-TEMP6-RTD-46	-11.276	11.638	11.245
ESF-HD-137-TEMP5-RTD-64	0.873	11.845	21.170	ESF-HD-138-TEMP6-RTD-47	-11.488	11.633	11.457
ESF-HD-137-TEMP5-RTD-65	0.874	11.844	21.470	ESF-HD-138-TEMP6-RTD-48	-11.700	11.627	11.670
ESF-HD-137-TEMP5-RTD-66	0.876	11.843	21.769	ESF-HD-138-TEMP6-RTD-49	-11.913	11.622	11.882
ESF-HD-137-TEMP5-RTD-67	0.878	11.842	22.068	ESF-HD-138-TEMP6-RTD-50	-12.125	11.616	12.094
ESF-HD-138-TEMP6-RTD-1	-1.721	11.887	1.697	ESF-HD-138-TEMP6-RTD-51	-12.337	11.610	12.306
ESF-HD-138-TEMP6-RTD-2	-1.933	11.881	1.909	ESF-HD-138-TEMP6-RTD-52	-12.550	11.605	12.518
ESF-HD-138-TEMP6-RTD-3	-2.145	11.876	2.121	ESF-HD-138-TEMP6-RTD-53	-12.762	11.599	12.731
ESF-HD-138-TEMP6-RTD-4	-2.358	11.870	2.333	ESF-HD-138-TEMP6-RTD-54	-12.974	11.594	12.943
ESF-HD-138-TEMP6-RTD-5	-2.570	11.865	2.545	ESF-HD-138-TEMP6-RTD-55	-13.187	11.588	13.155
ESF-HD-138-TEMP6-RTD-6	-2.782	11.859	2.757	ESF-HD-138-TEMP6-RTD-56	-13.399	11.583	13.367
ESF-HD-138-TEMP6-RTD-7	-2.995	11.854	2.970	ESF-HD-138-TEMP6-RTD-57	-13.611	11.577	13.579
ESF-HD-138-TEMP6-RTD-8	-3.207	11.848	3.182	ESF-HD-138-TEMP6-RTD-58	-13.824	11.572	13.792
ESF-HD-138-TEMP6-RTD-9	-3.419	11.843	3.394	ESF-HD-138-TEMP6-RTD-59	-14.036	11.566	14.004
ESF-HD-138-TEMP6-RTD-10	-3.632	11.837	3.606	ESF-HD-138-TEMP6-RTD-60	-14.248	11.561	14.216
ESF-HD-138-TEMP6-RTD-11	-3.844	11.832	3.818	ESF-HD-138-TEMP6-RTD-61	-14.461	11.555	14.428
ESF-HD-138-TEMP6-RTD-12	-4.056	11.826	4.031	ESF-HD-138-TEMP6-RTD-62	-14.673	11.550	14.640
ESF-HD-138-TEMP6-RTD-13	-4.269	11.821	4.243	ESF-HD-138-TEMP6-RTD-63	-14.885	11.544	14.853
ESF-HD-138-TEMP6-RTD-14	-4.481	11.815	4.455	ESF-HD-138-TEMP6-RTD-64	-15.098	11.539	15.065
ESF-HD-138-TEMP6-RTD-15	-4.693	11.809	4.667	ESF-HD-138-TEMP6-RTD-65	-15.310	11.533	15.277
ESF-HD-138-TEMP6-RTD-16	-4.906	11.804	4.879	ESF-HD-138-TEMP6-RTD-66	-15.522	11.528	15.489
ESF-HD-138-TEMP6-RTD-17	-5.118	11.798	5.092	ESF-HD-138-TEMP6-RTD-67	-15.735	11.522	15.701
ESF-HD-138-TEMP6-RTD-18	-5.330	11.793	5.304	ESF-HD-139-TEMP7-RTD-1	-2.309	11.890	-0.019
ESF-HD-138-TEMP6-RTD-19	-5.543	11.787	5.516	ESF-HD-139-TEMP7-RTD-2	-2.609	11.891	-0.016
ESF-HD-138-TEMP6-RTD-20	-5.755	11.782	5.728	ESF-HD-139-TEMP7-RTD-3	-2.909	11.892	-0.014
ESF-HD-138-TEMP6-RTD-21	-5.967	11.776	5.940	ESF-HD-139-TEMP7-RTD-4	-3.208	11.893	-0.011
ESF-HD-138-TEMP6-RTD-22	-6.180	11.771	6.153	ESF-HD-139-TEMP7-RTD-5	-3.508	11.894	-0.009
ESF-HD-138-TEMP6-RTD-23	-6.392	11.765	6.365	ESF-HD-139-TEMP7-RTD-6	-3.808	11.895	-0.007
ESF-HD-138-TEMP6-RTD-24	-6.604	11.760	6.577	ESF-HD-139-TEMP7-RTD-7	-4.107	11.896	-0.004
ESF-HD-138-TEMP6-RTD-25	-6.817	11.754	6.789	ESF-HD-139-TEMP7-RTD-8	-4.407	11.896	-0.002
ESF-HD-138-TEMP6-RTD-26	-7.029	11.749	7.001	ESF-HD-139-TEMP7-RTD-9	-4.707	11.897	0.001
ESF-HD-138-TEMP6-RTD-27	-7.241	11.743	7.214	ESF-HD-139-TEMP7-RTD-10	-5.006	11.898	0.003
ESF-HD-138-TEMP6-RTD-28	-7.454	11.738	7.426	ESF-HD-139-TEMP7-RTD-11	-5.306	11.899	0.006
ESF-HD-138-TEMP6-RTD-29	-7.666	11.732	7.638	ESF-HD-139-TEMP7-RTD-12	-5.606	11.900	0.008
ESF-HD-138-TEMP6-RTD-30	-7.878	11.727	7.850	ESF-HD-139-TEMP7-RTD-13	-5.905	11.901	0.011
ESF-HD-138-TEMP6-RTD-31	-8.091	11.721	8.062	ESF-HD-139-TEMP7-RTD-14	-6.205	11.902	0.013
ESF-HD-138-TEMP6-RTD-32	-8.303	11.715	8.275	ESF-HD-139-TEMP7-RTD-15	-6.505	11.903	0.016
ESF-HD-138-TEMP6-RTD-33	-8.515	11.710	8.487	ESF-HD-139-TEMP7-RTD-16	-6.804	11.904	0.018
ESF-HD-138-TEMP6-RTD-34	-8.728	11.704	8.699	ESF-HD-139-TEMP7-RTD-17	-7.104	11.905	0.021
ESF-HD-138-TEMP6-RTD-35	-8.940	11.699	8.911	ESF-HD-139-TEMP7-RTD-18	-7.404	11.906	0.023
ESF-HD-138-TEMP6-RTD-36	-9.152	11.693	9.123	ESF-HD-139-TEMP7-RTD-19	-7.703	11.907	0.026
ESF-HD-138-TEMP6-RTD-37	-9.365	11.688	9.335	ESF-HD-139-TEMP7-RTD-20	-8.003	11.908	0.028
ESF-HD-138-TEMP6-RTD-38	-9.577	11.682	9.548	ESF-HD-139-TEMP7-RTD-21	-8.303	11.909	0.031
ESF-HD-138-TEMP6-RTD-39	-9.789	11.677	9.760	ESF-HD-139-TEMP7-RTD-22	-8.602	11.909	0.033
ESF-HD-138-TEMP6-RTD-40	-10.002	11.671	9.972	ESF-HD-139-TEMP7-RTD-23	-8.902	11.910	0.036
ESF-HD-138-TEMP6-RTD-41	-10.214	11.666	10.184	ESF-HD-139-TEMP7-RTD-24	-9.202	11.911	0.038
ESF-HD-138-TEMP6-RTD-42	-10.426	11.660	10.396	ESF-HD-139-TEMP7-RTD-25	-9.502	11.912	0.041
ESF-HD-138-TEMP6-RTD-43	-10.639	11.655	10.609	ESF-HD-139-TEMP7-RTD-26	-9.801	11.913	0.043
ESF-HD-138-TEMP6-RTD-44	-10.851	11.649	10.821	ESF-HD-139-TEMP7-RTD-27	-10.101	11.914	0.046
ESF-HD-138-TEMP6-RTD-45	-11.063	11.644	11.033	ESF-HD-139-TEMP7-RTD-28	-10.401	11.915	0.048

Table C-2. Gage Locations for the DST Temperature Gages (continued)

Gage ID	x	y	z	Gage ID	x	y	z
ESF-HD-139-TEMP7-RTD-29	-10.700	11.916	0.051	ESF-HD-140-TEMP8-RTD-12	-4.794	11.885	-4.036
ESF-HD-139-TEMP7-RTD-30	-11.000	11.917	0.053	ESF-HD-140-TEMP8-RTD-13	-5.024	11.884	-4.230
ESF-HD-139-TEMP7-RTD-31	-11.300	11.918	0.056	ESF-HD-140-TEMP8-RTD-14	-5.254	11.882	-4.425
ESF-HD-139-TEMP7-RTD-32	-11.599	11.919	0.058	ESF-HD-140-TEMP8-RTD-15	-5.484	11.880	-4.619
ESF-HD-139-TEMP7-RTD-33	-11.899	11.920	0.061	ESF-HD-140-TEMP8-RTD-16	-5.714	11.879	-4.814
ESF-HD-139-TEMP7-RTD-34	-12.199	11.921	0.063	ESF-HD-140-TEMP8-RTD-17	-5.945	11.877	-5.009
ESF-HD-139-TEMP7-RTD-35	-12.498	11.922	0.065	ESF-HD-140-TEMP8-RTD-18	-6.175	11.875	-5.203
ESF-HD-139-TEMP7-RTD-36	-12.798	11.922	0.068	ESF-HD-140-TEMP8-RTD-19	-6.405	11.873	-5.398
ESF-HD-139-TEMP7-RTD-37	-13.098	11.923	0.070	ESF-HD-140-TEMP8-RTD-20	-6.635	11.872	-5.592
ESF-HD-139-TEMP7-RTD-38	-13.397	11.924	0.073	ESF-HD-140-TEMP8-RTD-21	-6.865	11.870	-5.787
ESF-HD-139-TEMP7-RTD-39	-13.697	11.925	0.075	ESF-HD-140-TEMP8-RTD-22	-7.096	11.868	-5.981
ESF-HD-139-TEMP7-RTD-40	-13.997	11.926	0.078	ESF-HD-140-TEMP8-RTD-23	-7.326	11.867	-6.176
ESF-HD-139-TEMP7-RTD-41	-14.296	11.927	0.080	ESF-HD-140-TEMP8-RTD-24	-7.556	11.865	-6.370
ESF-HD-139-TEMP7-RTD-42	-14.596	11.928	0.083	ESF-HD-140-TEMP8-RTD-25	-7.786	11.863	-6.565
ESF-HD-139-TEMP7-RTD-43	-14.896	11.929	0.085	ESF-HD-140-TEMP8-RTD-26	-8.016	11.861	-6.759
ESF-HD-139-TEMP7-RTD-44	-15.195	11.930	0.088	ESF-HD-140-TEMP8-RTD-27	-8.247	11.860	-6.954
ESF-HD-139-TEMP7-RTD-45	-15.495	11.931	0.090	ESF-HD-140-TEMP8-RTD-28	-8.477	11.858	-7.148
ESF-HD-139-TEMP7-RTD-46	-15.795	11.932	0.093	ESF-HD-140-TEMP8-RTD-29	-8.707	11.856	-7.343
ESF-HD-139-TEMP7-RTD-47	-16.094	11.933	0.095	ESF-HD-140-TEMP8-RTD-30	-8.937	11.854	-7.538
ESF-HD-139-TEMP7-RTD-48	-16.394	11.934	0.098	ESF-HD-140-TEMP8-RTD-31	-9.167	11.853	-7.732
ESF-HD-139-TEMP7-RTD-49	-16.694	11.935	0.100	ESF-HD-140-TEMP8-RTD-32	-9.397	11.851	-7.927
ESF-HD-139-TEMP7-RTD-50	-16.993	11.936	0.103	ESF-HD-140-TEMP8-RTD-33	-9.628	11.849	-8.121
ESF-HD-139-TEMP7-RTD-51	-17.293	11.936	0.105	ESF-HD-140-TEMP8-RTD-34	-9.858	11.848	-8.316
ESF-HD-139-TEMP7-RTD-52	-17.593	11.937	0.108	ESF-HD-140-TEMP8-RTD-35	-10.088	11.846	-8.510
ESF-HD-139-TEMP7-RTD-53	-17.892	11.938	0.110	ESF-HD-140-TEMP8-RTD-36	-10.318	11.844	-8.705
ESF-HD-139-TEMP7-RTD-54	-18.192	11.939	0.113	ESF-HD-140-TEMP8-RTD-37	-10.548	11.842	-8.899
ESF-HD-139-TEMP7-RTD-55	-18.492	11.940	0.115	ESF-HD-140-TEMP8-RTD-38	-10.779	11.841	-9.094
ESF-HD-139-TEMP7-RTD-56	-18.792	11.941	0.118	ESF-HD-140-TEMP8-RTD-39	-11.009	11.839	-9.288
ESF-HD-139-TEMP7-RTD-57	-19.091	11.942	0.120	ESF-HD-140-TEMP8-RTD-40	-11.239	11.837	-9.483
ESF-HD-139-TEMP7-RTD-58	-19.391	11.943	0.123	ESF-HD-140-TEMP8-RTD-41	-11.469	11.836	-9.678
ESF-HD-139-TEMP7-RTD-59	-19.691	11.944	0.125	ESF-HD-140-TEMP8-RTD-42	-11.699	11.834	-9.872
ESF-HD-139-TEMP7-RTD-60	-19.990	11.945	0.128	ESF-HD-140-TEMP8-RTD-43	-11.929	11.832	-10.067
ESF-HD-139-TEMP7-RTD-61	-20.290	11.946	0.130	ESF-HD-140-TEMP8-RTD-44	-12.160	11.830	-10.261
ESF-HD-139-TEMP7-RTD-62	-20.590	11.947	0.133	ESF-HD-140-TEMP8-RTD-45	-12.390	11.829	-10.456
ESF-HD-139-TEMP7-RTD-63	-20.889	11.948	0.135	ESF-HD-140-TEMP8-RTD-46	-12.620	11.827	-10.650
ESF-HD-139-TEMP7-RTD-64	-21.189	11.949	0.137	ESF-HD-140-TEMP8-RTD-47	-12.850	11.825	-10.845
ESF-HD-139-TEMP7-RTD-65	-21.489	11.949	0.140	ESF-HD-140-TEMP8-RTD-48	-13.080	11.823	-11.039
ESF-HD-139-TEMP7-RTD-66	-21.788	11.950	0.142	ESF-HD-140-TEMP8-RTD-49	-13.311	11.822	-11.234
ESF-HD-139-TEMP7-RTD-67	-22.088	11.951	0.145	ESF-HD-140-TEMP8-RTD-50	-13.541	11.820	-11.428
ESF-HD-140-TEMP8-RTD-1	-2.262	11.904	-1.896	ESF-HD-140-TEMP8-RTD-51	-13.771	11.818	-11.623
ESF-HD-140-TEMP8-RTD-2	-2.492	11.903	-2.090	ESF-HD-140-TEMP8-RTD-52	-14.001	11.817	-11.818
ESF-HD-140-TEMP8-RTD-3	-2.722	11.901	-2.285	ESF-HD-140-TEMP8-RTD-53	-14.231	11.815	-12.012
ESF-HD-140-TEMP8-RTD-4	-2.952	11.899	-2.479	ESF-HD-140-TEMP8-RTD-54	-14.462	11.813	-12.207
ESF-HD-140-TEMP8-RTD-5	-3.182	11.897	-2.674	ESF-HD-140-TEMP8-RTD-55	-14.692	11.811	-12.401
ESF-HD-140-TEMP8-RTD-6	-3.413	11.896	-2.869	ESF-HD-140-TEMP8-RTD-56	-14.922	11.810	-12.596
ESF-HD-140-TEMP8-RTD-7	-3.643	11.894	-3.063	ESF-HD-140-TEMP8-RTD-57	-15.152	11.808	-12.790
ESF-HD-140-TEMP8-RTD-8	-3.873	11.892	-3.258	ESF-HD-140-TEMP8-RTD-58	-15.382	11.806	-12.985
ESF-HD-140-TEMP8-RTD-9	-4.103	11.891	-3.452	ESF-HD-140-TEMP8-RTD-59	-15.612	11.805	-13.179
ESF-HD-140-TEMP8-RTD-10	-4.333	11.889	-3.647	ESF-HD-140-TEMP8-RTD-60	-15.843	11.803	-13.374
ESF-HD-140-TEMP8-RTD-11	-4.564	11.887	-3.841	ESF-HD-140-TEMP8-RTD-61	-16.073	11.801	-13.568

Table C-2. Gage Locations for the DST Temperature Gages (continued)

Gage ID	x	y	z	Gage ID	x	y	z
ESF-HD-140-TEMP8-RTD-62	-16.303	11.799	-13.763	ESF-HD-141-TEMP9-RTD-45	0.630	11.991	-16.407
ESF-HD-140-TEMP8-RTD-63	-16.533	11.798	-13.958	ESF-HD-141-TEMP9-RTD-46	0.627	11.993	-16.709
ESF-HD-140-TEMP8-RTD-64	-16.763	11.796	-14.152	ESF-HD-141-TEMP9-RTD-47	0.624	11.995	-17.010
ESF-HD-140-TEMP8-RTD-65	-16.994	11.794	-14.347	ESF-HD-141-TEMP9-RTD-48	0.621	11.997	-17.311
ESF-HD-140-TEMP8-RTD-66	-17.224	11.793	-14.541	ESF-HD-141-TEMP9-RTD-49	0.619	11.999	-17.613
ESF-HD-140-TEMP8-RTD-67	-17.454	11.791	-14.736	ESF-HD-141-TEMP9-RTD-50	0.616	12.001	-17.914
ESF-HD-141-TEMP9-RTD-1	0.750	11.903	-3.144	ESF-HD-141-TEMP9-RTD-51	0.613	12.003	-18.216
ESF-HD-141-TEMP9-RTD-2	0.747	11.905	-3.445	ESF-HD-141-TEMP9-RTD-52	0.610	12.005	-18.517
ESF-HD-141-TEMP9-RTD-3	0.745	11.907	-3.747	ESF-HD-141-TEMP9-RTD-53	0.608	12.007	-18.819
ESF-HD-141-TEMP9-RTD-4	0.742	11.909	-4.048	ESF-HD-141-TEMP9-RTD-54	0.605	12.009	-19.120
ESF-HD-141-TEMP9-RTD-5	0.739	11.911	-4.350	ESF-HD-141-TEMP9-RTD-55	0.602	12.011	-19.422
ESF-HD-141-TEMP9-RTD-6	0.736	11.913	-4.651	ESF-HD-141-TEMP9-RTD-56	0.599	12.013	-19.723
ESF-HD-141-TEMP9-RTD-7	0.734	11.915	-4.952	ESF-HD-141-TEMP9-RTD-57	0.597	12.015	-20.024
ESF-HD-141-TEMP9-RTD-8	0.731	11.917	-5.254	ESF-HD-141-TEMP9-RTD-58	0.594	12.017	-20.326
ESF-HD-141-TEMP9-RTD-9	0.728	11.919	-5.555	ESF-HD-141-TEMP9-RTD-59	0.591	12.019	-20.627
ESF-HD-141-TEMP9-RTD-10	0.725	11.921	-5.857	ESF-HD-141-TEMP9-RTD-60	0.589	12.021	-20.929
ESF-HD-141-TEMP9-RTD-11	0.723	11.923	-6.158	ESF-HD-141-TEMP9-RTD-61	0.586	12.023	-21.230
ESF-HD-141-TEMP9-RTD-12	0.720	11.925	-6.460	ESF-HD-141-TEMP9-RTD-62	0.583	12.024	-21.532
ESF-HD-141-TEMP9-RTD-13	0.717	11.927	-6.761	ESF-HD-141-TEMP9-RTD-63	0.580	12.026	-21.833
ESF-HD-141-TEMP9-RTD-14	0.714	11.929	-7.063	ESF-HD-141-TEMP9-RTD-64	0.578	12.028	-22.135
ESF-HD-141-TEMP9-RTD-15	0.712	11.931	-7.364	ESF-HD-141-TEMP9-RTD-65	0.575	12.030	-22.436
ESF-HD-141-TEMP9-RTD-16	0.709	11.933	-7.665	ESF-HD-141-TEMP9-RTD-66	0.572	12.032	-22.737
ESF-HD-141-TEMP9-RTD-17	0.706	11.935	-7.967	ESF-HD-141-TEMP9-RTD-67	0.569	12.034	-23.039
ESF-HD-141-TEMP9-RTD-18	0.703	11.937	-8.268	ESF-HD-142-TEMP10-RTD-1	1.435	11.911	-1.459
ESF-HD-141-TEMP9-RTD-19	0.701	11.939	-8.570	ESF-HD-142-TEMP10-RTD-2	1.650	11.911	-1.672
ESF-HD-141-TEMP9-RTD-20	0.698	11.941	-8.871	ESF-HD-142-TEMP10-RTD-3	1.865	11.910	-1.885
ESF-HD-141-TEMP9-RTD-21	0.695	11.943	-9.173	ESF-HD-142-TEMP10-RTD-4	2.080	11.910	-2.099
ESF-HD-141-TEMP9-RTD-22	0.693	11.945	-9.474	ESF-HD-142-TEMP10-RTD-5	2.295	11.910	-2.312
ESF-HD-141-TEMP9-RTD-23	0.690	11.947	-9.775	ESF-HD-142-TEMP10-RTD-6	2.510	11.909	-2.525
ESF-HD-141-TEMP9-RTD-24	0.687	11.949	-10.077	ESF-HD-142-TEMP10-RTD-7	2.725	11.909	-2.739
ESF-HD-141-TEMP9-RTD-25	0.684	11.951	-10.378	ESF-HD-142-TEMP10-RTD-8	2.940	11.908	-2.952
ESF-HD-141-TEMP9-RTD-26	0.682	11.953	-10.680	ESF-HD-142-TEMP10-RTD-9	3.155	11.908	-3.165
ESF-HD-141-TEMP9-RTD-27	0.679	11.955	-10.981	ESF-HD-142-TEMP10-RTD-10	3.370	11.907	-3.379
ESF-HD-141-TEMP9-RTD-28	0.676	11.957	-11.283	ESF-HD-142-TEMP10-RTD-11	3.585	11.907	-3.592
ESF-HD-141-TEMP9-RTD-29	0.673	11.959	-11.584	ESF-HD-142-TEMP10-RTD-12	3.800	11.907	-3.805
ESF-HD-141-TEMP9-RTD-30	0.671	11.961	-11.886	ESF-HD-142-TEMP10-RTD-13	4.015	11.906	-4.018
ESF-HD-141-TEMP9-RTD-31	0.668	11.963	-12.187	ESF-HD-142-TEMP10-RTD-14	4.230	11.906	-4.232
ESF-HD-141-TEMP9-RTD-32	0.665	11.965	-12.488	ESF-HD-142-TEMP10-RTD-15	4.445	11.905	-4.445
ESF-HD-141-TEMP9-RTD-33	0.662	11.967	-12.790	ESF-HD-142-TEMP10-RTD-16	4.661	11.905	-4.658
ESF-HD-141-TEMP9-RTD-34	0.660	11.969	-13.091	ESF-HD-142-TEMP10-RTD-17	4.876	11.904	-4.872
ESF-HD-141-TEMP9-RTD-35	0.657	11.971	-13.393	ESF-HD-142-TEMP10-RTD-18	5.091	11.904	-5.085
ESF-HD-141-TEMP9-RTD-36	0.654	11.973	-13.694	ESF-HD-142-TEMP10-RTD-19	5.306	11.903	-5.298
ESF-HD-141-TEMP9-RTD-37	0.651	11.975	-13.996	ESF-HD-142-TEMP10-RTD-20	5.521	11.903	-5.511
ESF-HD-141-TEMP9-RTD-38	0.649	11.977	-14.297	ESF-HD-142-TEMP10-RTD-21	5.736	11.903	-5.725
ESF-HD-141-TEMP9-RTD-39	0.646	11.979	-14.599	ESF-HD-142-TEMP10-RTD-22	5.951	11.902	-5.938
ESF-HD-141-TEMP9-RTD-40	0.643	11.981	-14.900	ESF-HD-142-TEMP10-RTD-23	6.166	11.902	-6.151
ESF-HD-141-TEMP9-RTD-41	0.641	11.983	-15.201	ESF-HD-142-TEMP10-RTD-24	6.381	11.901	-6.365
ESF-HD-141-TEMP9-RTD-42	0.638	11.985	-15.503	ESF-HD-142-TEMP10-RTD-25	6.596	11.901	-6.578
ESF-HD-141-TEMP9-RTD-43	0.635	11.987	-15.804	ESF-HD-142-TEMP10-RTD-26	6.811	11.900	-6.791
ESF-HD-141-TEMP9-RTD-44	0.632	11.989	-16.106	ESF-HD-142-TEMP10-RTD-27	7.026	11.900	-7.004

Table C-2. Gage Locations for the DST Temperature Gages (continued)

Gage ID	x	y	z	Gage ID	x	y	z
ESF-HD-142-TEMP10-RTD-28	7.241	11.899	-7.218	ESF-HD-143-TEMP11-RTD-11	5.377	11.893	-0.004
ESF-HD-142-TEMP10-RTD-29	7.456	11.899	-7.431	ESF-HD-143-TEMP11-RTD-12	5.677	11.894	-0.004
ESF-HD-142-TEMP10-RTD-30	7.671	11.899	-7.644	ESF-HD-143-TEMP11-RTD-13	5.976	11.894	-0.003
ESF-HD-142-TEMP10-RTD-31	7.886	11.898	-7.858	ESF-HD-143-TEMP11-RTD-14	6.275	11.895	-0.003
ESF-HD-142-TEMP10-RTD-32	8.101	11.898	-8.071	ESF-HD-143-TEMP11-RTD-15	6.574	11.895	-0.002
ESF-HD-142-TEMP10-RTD-33	8.316	11.897	-8.284	ESF-HD-143-TEMP11-RTD-16	6.873	11.896	-0.002
ESF-HD-142-TEMP10-RTD-34	8.531	11.897	-8.498	ESF-HD-143-TEMP11-RTD-17	7.172	11.896	-0.001
ESF-HD-142-TEMP10-RTD-35	8.746	11.896	-8.711	ESF-HD-143-TEMP11-RTD-18	7.471	11.896	-0.001
ESF-HD-142-TEMP10-RTD-36	8.961	11.896	-8.924	ESF-HD-143-TEMP11-RTD-19	7.771	11.897	0.000
ESF-HD-142-TEMP10-RTD-37	9.176	11.896	-9.137	ESF-HD-143-TEMP11-RTD-20	8.070	11.897	0.000
ESF-HD-142-TEMP10-RTD-38	9.391	11.895	-9.351	ESF-HD-143-TEMP11-RTD-21	8.369	11.898	0.000
ESF-HD-142-TEMP10-RTD-39	9.606	11.895	-9.564	ESF-HD-143-TEMP11-RTD-22	8.668	11.898	0.001
ESF-HD-142-TEMP10-RTD-40	9.821	11.894	-9.777	ESF-HD-143-TEMP11-RTD-23	8.967	11.899	0.001
ESF-HD-142-TEMP10-RTD-41	10.036	11.894	-9.991	ESF-HD-143-TEMP11-RTD-24	9.266	11.899	0.002
ESF-HD-142-TEMP10-RTD-42	10.251	11.893	-10.204	ESF-HD-143-TEMP11-RTD-25	9.566	11.899	0.002
ESF-HD-142-TEMP10-RTD-43	10.466	11.893	-10.417	ESF-HD-143-TEMP11-RTD-26	9.865	11.900	0.003
ESF-HD-142-TEMP10-RTD-44	10.681	11.892	-10.630	ESF-HD-143-TEMP11-RTD-27	10.164	11.900	0.003
ESF-HD-142-TEMP10-RTD-45	10.896	11.892	-10.844	ESF-HD-143-TEMP11-RTD-28	10.463	11.901	0.004
ESF-HD-142-TEMP10-RTD-46	11.111	11.892	-11.057	ESF-HD-143-TEMP11-RTD-29	10.762	11.901	0.004
ESF-HD-142-TEMP10-RTD-47	11.326	11.891	-11.270	ESF-HD-143-TEMP11-RTD-30	11.061	11.902	0.005
ESF-HD-142-TEMP10-RTD-48	11.541	11.891	-11.484	ESF-HD-143-TEMP11-RTD-31	11.361	11.902	0.005
ESF-HD-142-TEMP10-RTD-49	11.756	11.890	-11.697	ESF-HD-143-TEMP11-RTD-32	11.660	11.902	0.005
ESF-HD-142-TEMP10-RTD-50	11.971	11.890	-11.910	ESF-HD-143-TEMP11-RTD-33	11.959	11.903	0.006
ESF-HD-142-TEMP10-RTD-51	12.186	11.889	-12.124	ESF-HD-143-TEMP11-RTD-34	12.258	11.903	0.006
ESF-HD-142-TEMP10-RTD-52	12.401	11.889	-12.337	ESF-HD-143-TEMP11-RTD-35	12.557	11.904	0.007
ESF-HD-142-TEMP10-RTD-53	12.616	11.889	-12.550	ESF-HD-143-TEMP11-RTD-36	12.856	11.904	0.007
ESF-HD-142-TEMP10-RTD-54	12.831	11.888	-12.763	ESF-HD-143-TEMP11-RTD-37	13.156	11.905	0.008
ESF-HD-142-TEMP10-RTD-55	13.046	11.888	-12.977	ESF-HD-143-TEMP11-RTD-38	13.455	11.905	0.008
ESF-HD-142-TEMP10-RTD-56	13.261	11.887	-13.190	ESF-HD-143-TEMP11-RTD-39	13.754	11.905	0.009
ESF-HD-142-TEMP10-RTD-57	13.476	11.887	-13.403	ESF-HD-143-TEMP11-RTD-40	14.053	11.906	0.009
ESF-HD-142-TEMP10-RTD-58	13.691	11.886	-13.617	ESF-HD-143-TEMP11-RTD-41	14.352	11.906	0.010
ESF-HD-142-TEMP10-RTD-59	13.906	11.886	-13.830	ESF-HD-143-TEMP11-RTD-42	14.651	11.907	0.010
ESF-HD-142-TEMP10-RTD-60	14.121	11.885	-14.043	ESF-HD-143-TEMP11-RTD-43	14.951	11.907	0.011
ESF-HD-142-TEMP10-RTD-61	14.336	11.885	-14.256	ESF-HD-143-TEMP11-RTD-44	15.250	11.908	0.011
ESF-HD-142-TEMP10-RTD-62	14.551	11.885	-14.470	ESF-HD-143-TEMP11-RTD-45	15.549	11.908	0.011
ESF-HD-142-TEMP10-RTD-63	14.766	11.884	-14.683	ESF-HD-143-TEMP11-RTD-46	15.848	11.908	0.012
ESF-HD-142-TEMP10-RTD-64	14.981	11.884	-14.896	ESF-HD-143-TEMP11-RTD-47	16.147	11.909	0.012
ESF-HD-142-TEMP10-RTD-65	15.196	11.883	-15.110	ESF-HD-143-TEMP11-RTD-48	16.446	11.909	0.013
ESF-HD-142-TEMP10-RTD-66	15.411	11.883	-15.323	ESF-HD-143-TEMP11-RTD-49	16.746	11.910	0.013
ESF-HD-142-TEMP10-RTD-67	15.626	11.882	-15.536	ESF-HD-143-TEMP11-RTD-50	17.045	11.910	0.014
ESF-HD-143-TEMP11-RTD-1	2.386	11.889	-0.009	ESF-HD-143-TEMP11-RTD-51	17.344	11.911	0.014
ESF-HD-143-TEMP11-RTD-2	2.685	11.890	-0.008	ESF-HD-143-TEMP11-RTD-52	17.643	11.911	0.015
ESF-HD-143-TEMP11-RTD-3	2.984	11.890	-0.008	ESF-HD-143-TEMP11-RTD-53	17.942	11.911	0.015
ESF-HD-143-TEMP11-RTD-4	3.283	11.890	-0.007	ESF-HD-143-TEMP11-RTD-54	18.241	11.912	0.016
ESF-HD-143-TEMP11-RTD-5	3.582	11.891	-0.007	ESF-HD-143-TEMP11-RTD-55	18.541	11.912	0.016
ESF-HD-143-TEMP11-RTD-6	3.882	11.891	-0.006	ESF-HD-143-TEMP11-RTD-56	18.840	11.913	0.017
ESF-HD-143-TEMP11-RTD-7	4.181	11.892	-0.006	ESF-HD-143-TEMP11-RTD-57	19.139	11.913	0.017
ESF-HD-143-TEMP11-RTD-8	4.480	11.892	-0.006	ESF-HD-143-TEMP11-RTD-58	19.438	11.914	0.017
ESF-HD-143-TEMP11-RTD-9	4.779	11.893	-0.005	ESF-HD-143-TEMP11-RTD-59	19.737	11.914	0.018
ESF-HD-143-TEMP11-RTD-10	5.078	11.893	-0.005	ESF-HD-143-TEMP11-RTD-60	20.036	11.914	0.018

Table C-2. Gage Locations for the DST Temperature Gages (continued)

Gage ID	x	y	z	Gage ID	x	y	z
ESF-HD-143-TEMP11-RTD-61	20.336	11.915	0.019	ESF-HD-144-TEMP12-RTD-44	11.181	12.009	11.144
ESF-HD-143-TEMP11-RTD-62	20.635	11.915	0.019	ESF-HD-144-TEMP12-RTD-45	11.393	12.011	11.355
ESF-HD-143-TEMP11-RTD-63	20.934	11.916	0.020	ESF-HD-144-TEMP12-RTD-46	11.605	12.014	11.567
ESF-HD-143-TEMP11-RTD-64	21.233	11.916	0.020	ESF-HD-144-TEMP12-RTD-47	11.817	12.016	11.779
ESF-HD-143-TEMP11-RTD-65	21.532	11.917	0.021	ESF-HD-144-TEMP12-RTD-48	12.029	12.018	11.991
ESF-HD-143-TEMP11-RTD-66	21.831	11.917	0.021	ESF-HD-144-TEMP12-RTD-49	12.241	12.020	12.202
ESF-HD-143-TEMP11-RTD-67	22.131	11.917	0.022	ESF-HD-144-TEMP12-RTD-50	12.453	12.022	12.414
ESF-HD-144-TEMP12-RTD-1	2.066	11.916	2.039	ESF-HD-144-TEMP12-RTD-51	12.665	12.024	12.626
ESF-HD-144-TEMP12-RTD-2	2.278	11.918	2.251	ESF-HD-144-TEMP12-RTD-52	12.877	12.027	12.838
ESF-HD-144-TEMP12-RTD-3	2.490	11.920	2.462	ESF-HD-144-TEMP12-RTD-53	13.089	12.029	13.049
ESF-HD-144-TEMP12-RTD-4	2.702	11.922	2.674	ESF-HD-144-TEMP12-RTD-54	13.301	12.031	13.261
ESF-HD-144-TEMP12-RTD-5	2.914	11.924	2.886	ESF-HD-144-TEMP12-RTD-55	13.513	12.033	13.473
ESF-HD-144-TEMP12-RTD-6	3.126	11.927	3.098	ESF-HD-144-TEMP12-RTD-56	13.724	12.035	13.685
ESF-HD-144-TEMP12-RTD-7	3.338	11.929	3.309	ESF-HD-144-TEMP12-RTD-57	13.936	12.037	13.896
ESF-HD-144-TEMP12-RTD-8	3.550	11.931	3.521	ESF-HD-144-TEMP12-RTD-58	14.148	12.040	14.108
ESF-HD-144-TEMP12-RTD-9	3.761	11.933	3.733	ESF-HD-144-TEMP12-RTD-59	14.360	12.042	14.320
ESF-HD-144-TEMP12-RTD-10	3.973	11.935	3.945	ESF-HD-144-TEMP12-RTD-60	14.572	12.044	14.532
ESF-HD-144-TEMP12-RTD-11	4.185	11.937	4.156	ESF-HD-144-TEMP12-RTD-61	14.784	12.046	14.743
ESF-HD-144-TEMP12-RTD-12	4.397	11.940	4.368	ESF-HD-144-TEMP12-RTD-62	14.996	12.048	14.955
ESF-HD-144-TEMP12-RTD-13	4.609	11.942	4.580	ESF-HD-144-TEMP12-RTD-63	15.208	12.050	15.167
ESF-HD-144-TEMP12-RTD-14	4.821	11.944	4.791	ESF-HD-144-TEMP12-RTD-64	15.420	12.053	15.378
ESF-HD-144-TEMP12-RTD-15	5.033	11.946	5.003	ESF-HD-144-TEMP12-RTD-65	15.632	12.055	15.590
ESF-HD-144-TEMP12-RTD-16	5.245	11.948	5.215	ESF-HD-144-TEMP12-RTD-66	15.844	12.057	15.802
ESF-HD-144-TEMP12-RTD-17	5.457	11.950	5.427	ESF-HD-144-TEMP12-RTD-67	16.056	12.059	16.014
ESF-HD-144-TEMP12-RTD-18	5.669	11.953	5.638	ESF-HD-158-TEMP13-RTD-1	0.762	22.856	2.311
ESF-HD-144-TEMP12-RTD-19	5.881	11.955	5.850	ESF-HD-158-TEMP13-RTD-2	0.756	22.864	2.611
ESF-HD-144-TEMP12-RTD-20	6.093	11.957	6.062	ESF-HD-158-TEMP13-RTD-3	0.751	22.873	2.910
ESF-HD-144-TEMP12-RTD-21	6.305	11.959	6.274	ESF-HD-158-TEMP13-RTD-4	0.746	22.882	3.210
ESF-HD-144-TEMP12-RTD-22	6.517	11.961	6.485	ESF-HD-158-TEMP13-RTD-5	0.741	22.890	3.509
ESF-HD-144-TEMP12-RTD-23	6.729	11.964	6.697	ESF-HD-158-TEMP13-RTD-6	0.736	22.899	3.809
ESF-HD-144-TEMP12-RTD-24	6.941	11.966	6.909	ESF-HD-158-TEMP13-RTD-7	0.731	22.908	4.108
ESF-HD-144-TEMP12-RTD-25	7.153	11.968	7.121	ESF-HD-158-TEMP13-RTD-8	0.726	22.916	4.408
ESF-HD-144-TEMP12-RTD-26	7.365	11.970	7.332	ESF-HD-158-TEMP13-RTD-9	0.720	22.925	4.707
ESF-HD-144-TEMP12-RTD-27	7.577	11.972	7.544	ESF-HD-158-TEMP13-RTD-10	0.715	22.934	5.007
ESF-HD-144-TEMP12-RTD-28	7.789	11.974	7.756	ESF-HD-158-TEMP13-RTD-11	0.710	22.942	5.306
ESF-HD-144-TEMP12-RTD-29	8.001	11.977	7.968	ESF-HD-158-TEMP13-RTD-12	0.705	22.951	5.606
ESF-HD-144-TEMP12-RTD-30	8.213	11.979	8.179	ESF-HD-158-TEMP13-RTD-13	0.700	22.960	5.905
ESF-HD-144-TEMP12-RTD-31	8.425	11.981	8.391	ESF-HD-158-TEMP13-RTD-14	0.695	22.968	6.205
ESF-HD-144-TEMP12-RTD-32	8.637	11.983	8.603	ESF-HD-158-TEMP13-RTD-15	0.689	22.977	6.505
ESF-HD-144-TEMP12-RTD-33	8.849	11.985	8.815	ESF-HD-158-TEMP13-RTD-16	0.684	22.986	6.804
ESF-HD-144-TEMP12-RTD-34	9.061	11.987	9.026	ESF-HD-158-TEMP13-RTD-17	0.679	22.994	7.104
ESF-HD-144-TEMP12-RTD-35	9.273	11.990	9.238	ESF-HD-158-TEMP13-RTD-18	0.674	23.003	7.403
ESF-HD-144-TEMP12-RTD-36	9.485	11.992	9.450	ESF-HD-158-TEMP13-RTD-19	0.669	23.012	7.703
ESF-HD-144-TEMP12-RTD-37	9.697	11.994	9.662	ESF-HD-158-TEMP13-RTD-20	0.664	23.020	8.002
ESF-HD-144-TEMP12-RTD-38	9.909	11.996	9.873	ESF-HD-158-TEMP13-RTD-21	0.658	23.029	8.302
ESF-HD-144-TEMP12-RTD-39	10.121	11.998	10.085	ESF-HD-158-TEMP13-RTD-22	0.653	23.038	8.601
ESF-HD-144-TEMP12-RTD-40	10.333	12.000	10.297	ESF-HD-158-TEMP13-RTD-23	0.648	23.046	8.901
ESF-HD-144-TEMP12-RTD-41	10.545	12.003	10.508	ESF-HD-158-TEMP13-RTD-24	0.643	23.055	9.200
ESF-HD-144-TEMP12-RTD-42	10.757	12.005	10.720	ESF-HD-158-TEMP13-RTD-25	0.638	23.064	9.500
ESF-HD-144-TEMP12-RTD-43	10.969	12.007	10.932	ESF-HD-158-TEMP13-RTD-26	0.633	23.072	9.799

Table C-2. Gage Locations for the DST Temperature Gages (continued)

Gage ID	x	y	z	Gage ID	x	y	z
ESF-HD-158-TEMP13-RTD-27	0.628	23.081	10.099	ESF-HD-159-TEMP14-RTD-10	-3.644	22.884	3.646
ESF-HD-158-TEMP13-RTD-28	0.622	23.090	10.398	ESF-HD-159-TEMP14-RTD-11	-3.858	22.885	3.863
ESF-HD-158-TEMP13-RTD-29	0.617	23.099	10.698	ESF-HD-159-TEMP14-RTD-12	-4.073	22.886	4.080
ESF-HD-158-TEMP13-RTD-30	0.612	23.107	10.997	ESF-HD-159-TEMP14-RTD-13	-4.287	22.887	4.297
ESF-HD-158-TEMP13-RTD-31	0.607	23.116	11.297	ESF-HD-159-TEMP14-RTD-14	-4.502	22.888	4.514
ESF-HD-158-TEMP13-RTD-32	0.602	23.125	11.596	ESF-HD-159-TEMP14-RTD-15	-4.716	22.888	4.731
ESF-HD-158-TEMP13-RTD-33	0.597	23.133	11.896	ESF-HD-159-TEMP14-RTD-16	-4.931	22.889	4.948
ESF-HD-158-TEMP13-RTD-34	0.591	23.142	12.196	ESF-HD-159-TEMP14-RTD-17	-5.145	22.890	5.165
ESF-HD-158-TEMP13-RTD-35	0.586	23.151	12.495	ESF-HD-159-TEMP14-RTD-18	-5.360	22.891	5.382
ESF-HD-158-TEMP13-RTD-36	0.581	23.159	12.795	ESF-HD-159-TEMP14-RTD-19	-5.574	22.892	5.600
ESF-HD-158-TEMP13-RTD-37	0.576	23.168	13.094	ESF-HD-159-TEMP14-RTD-20	-5.789	22.893	5.817
ESF-HD-158-TEMP13-RTD-38	0.571	23.177	13.394	ESF-HD-159-TEMP14-RTD-21	-6.003	22.893	6.034
ESF-HD-158-TEMP13-RTD-39	0.566	23.185	13.693	ESF-HD-159-TEMP14-RTD-22	-6.218	22.894	6.251
ESF-HD-158-TEMP13-RTD-40	0.560	23.194	13.993	ESF-HD-159-TEMP14-RTD-23	-6.433	22.895	6.468
ESF-HD-158-TEMP13-RTD-41	0.555	23.203	14.292	ESF-HD-159-TEMP14-RTD-24	-6.647	22.896	6.685
ESF-HD-158-TEMP13-RTD-42	0.550	23.211	14.592	ESF-HD-159-TEMP14-RTD-25	-6.862	22.897	6.902
ESF-HD-158-TEMP13-RTD-43	0.545	23.220	14.891	ESF-HD-159-TEMP14-RTD-26	-7.076	22.898	7.119
ESF-HD-158-TEMP13-RTD-44	0.540	23.229	15.191	ESF-HD-159-TEMP14-RTD-27	-7.291	22.899	7.336
ESF-HD-158-TEMP13-RTD-45	0.535	23.237	15.490	ESF-HD-159-TEMP14-RTD-28	-7.505	22.899	7.553
ESF-HD-158-TEMP13-RTD-46	0.529	23.246	15.790	ESF-HD-159-TEMP14-RTD-29	-7.720	22.900	7.770
ESF-HD-158-TEMP13-RTD-47	0.524	23.255	16.089	ESF-HD-159-TEMP14-RTD-30	-7.934	22.901	7.988
ESF-HD-158-TEMP13-RTD-48	0.519	23.263	16.389	ESF-HD-159-TEMP14-RTD-31	-8.149	22.902	8.205
ESF-HD-158-TEMP13-RTD-49	0.514	23.272	16.688	ESF-HD-159-TEMP14-RTD-32	-8.363	22.903	8.422
ESF-HD-158-TEMP13-RTD-50	0.509	23.281	16.988	ESF-HD-159-TEMP14-RTD-33	-8.578	22.904	8.639
ESF-HD-158-TEMP13-RTD-51	0.504	23.289	17.287	ESF-HD-159-TEMP14-RTD-34	-8.792	22.905	8.856
ESF-HD-158-TEMP13-RTD-52	0.499	23.298	17.587	ESF-HD-159-TEMP14-RTD-35	-9.007	22.905	9.073
ESF-HD-158-TEMP13-RTD-53	0.493	23.307	17.887	ESF-HD-159-TEMP14-RTD-36	-9.221	22.906	9.290
ESF-HD-158-TEMP13-RTD-54	0.488	23.315	18.186	ESF-HD-159-TEMP14-RTD-37	-9.436	22.907	9.507
ESF-HD-158-TEMP13-RTD-55	0.483	23.324	18.486	ESF-HD-159-TEMP14-RTD-38	-9.650	22.908	9.724
ESF-HD-158-TEMP13-RTD-56	0.478	23.333	18.785	ESF-HD-159-TEMP14-RTD-39	-9.865	22.909	9.941
ESF-HD-158-TEMP13-RTD-57	0.473	23.341	19.085	ESF-HD-159-TEMP14-RTD-40	-10.079	22.910	10.158
ESF-HD-158-TEMP13-RTD-58	0.468	23.350	19.384	ESF-HD-159-TEMP14-RTD-41	-10.294	22.911	10.376
ESF-HD-158-TEMP13-RTD-59	0.462	23.359	19.684	ESF-HD-159-TEMP14-RTD-42	-10.508	22.911	10.593
ESF-HD-158-TEMP13-RTD-60	0.457	23.367	19.983	ESF-HD-159-TEMP14-RTD-43	-10.723	22.912	10.810
ESF-HD-158-TEMP13-RTD-61	0.452	23.376	20.283	ESF-HD-159-TEMP14-RTD-44	-10.937	22.913	11.027
ESF-HD-158-TEMP13-RTD-62	0.447	23.385	20.582	ESF-HD-159-TEMP14-RTD-45	-11.152	22.914	11.244
ESF-HD-158-TEMP13-RTD-63	0.442	23.393	20.882	ESF-HD-159-TEMP14-RTD-46	-11.366	22.915	11.461
ESF-HD-158-TEMP13-RTD-64	0.437	23.402	21.181	ESF-HD-159-TEMP14-RTD-47	-11.581	22.916	11.678
ESF-HD-158-TEMP13-RTD-65	0.431	23.411	21.481	ESF-HD-159-TEMP14-RTD-48	-11.795	22.916	11.895
ESF-HD-158-TEMP13-RTD-66	0.426	23.419	21.780	ESF-HD-159-TEMP14-RTD-49	-12.010	22.917	12.112
ESF-HD-158-TEMP13-RTD-67	0.421	23.428	22.080	ESF-HD-159-TEMP14-RTD-50	-12.224	22.918	12.329
ESF-HD-159-TEMP14-RTD-1	-1.713	22.876	1.692	ESF-HD-159-TEMP14-RTD-51	-12.439	22.919	12.546
ESF-HD-159-TEMP14-RTD-2	-1.928	22.877	1.909	ESF-HD-159-TEMP14-RTD-52	-12.653	22.920	12.763
ESF-HD-159-TEMP14-RTD-3	-2.142	22.878	2.126	ESF-HD-159-TEMP14-RTD-53	-12.868	22.921	12.981
ESF-HD-159-TEMP14-RTD-4	-2.357	22.879	2.343	ESF-HD-159-TEMP14-RTD-54	-13.082	22.922	13.198
ESF-HD-159-TEMP14-RTD-5	-2.571	22.880	2.560	ESF-HD-159-TEMP14-RTD-55	-13.297	22.922	13.415
ESF-HD-159-TEMP14-RTD-6	-2.786	22.881	2.777	ESF-HD-159-TEMP14-RTD-56	-13.511	22.923	13.632
ESF-HD-159-TEMP14-RTD-7	-3.000	22.882	2.994	ESF-HD-159-TEMP14-RTD-57	-13.726	22.924	13.849
ESF-HD-159-TEMP14-RTD-8	-3.215	22.882	3.212	ESF-HD-159-TEMP14-RTD-58	-13.940	22.925	14.066
ESF-HD-159-TEMP14-RTD-9	-3.429	22.883	3.429	ESF-HD-159-TEMP14-RTD-59	-14.155	22.926	14.283

Table C-2. Gage Locations for the DST Temperature Gages (continued)

Gage ID	x	y	z	Gage ID	x	y	z
ESF-HD-159-TEMP14-RTD-60	-14.369	22.927	14.500	ESF-HD-160-TEMP15-RTD-43	-14.867	22.923	0.064
ESF-HD-159-TEMP14-RTD-61	-14.584	22.928	14.717	ESF-HD-160-TEMP15-RTD-44	-15.169	22.925	0.066
ESF-HD-159-TEMP14-RTD-62	-14.798	22.928	14.934	ESF-HD-160-TEMP15-RTD-45	-15.470	22.926	0.068
ESF-HD-159-TEMP14-RTD-63	-15.013	22.929	15.151	ESF-HD-160-TEMP15-RTD-46	-15.771	22.927	0.069
ESF-HD-159-TEMP14-RTD-64	-15.228	22.930	15.369	ESF-HD-160-TEMP15-RTD-47	-16.072	22.928	0.071
ESF-HD-159-TEMP14-RTD-65	-15.442	22.931	15.586	ESF-HD-160-TEMP15-RTD-48	-16.373	22.930	0.073
ESF-HD-159-TEMP14-RTD-66	-15.657	22.932	15.803	ESF-HD-160-TEMP15-RTD-49	-16.674	22.931	0.074
ESF-HD-159-TEMP14-RTD-67	-15.871	22.933	16.020	ESF-HD-160-TEMP15-RTD-50	-16.975	22.932	0.076
ESF-HD-160-TEMP15-RTD-1	-2.222	22.870	-0.006	ESF-HD-160-TEMP15-RTD-51	-17.276	22.933	0.078
ESF-HD-160-TEMP15-RTD-2	-2.523	22.871	-0.004	ESF-HD-160-TEMP15-RTD-52	-17.577	22.935	0.079
ESF-HD-160-TEMP15-RTD-3	-2.824	22.872	-0.002	ESF-HD-160-TEMP15-RTD-53	-17.878	22.936	0.081
ESF-HD-160-TEMP15-RTD-4	-3.125	22.874	-0.001	ESF-HD-160-TEMP15-RTD-54	-18.179	22.937	0.083
ESF-HD-160-TEMP15-RTD-5	-3.426	22.875	0.001	ESF-HD-160-TEMP15-RTD-55	-18.480	22.939	0.084
ESF-HD-160-TEMP15-RTD-6	-3.727	22.876	0.003	ESF-HD-160-TEMP15-RTD-56	-18.782	22.940	0.086
ESF-HD-160-TEMP15-RTD-7	-4.028	22.877	0.004	ESF-HD-160-TEMP15-RTD-57	-19.083	22.941	0.088
ESF-HD-160-TEMP15-RTD-8	-4.330	22.879	0.006	ESF-HD-160-TEMP15-RTD-58	-19.384	22.942	0.089
ESF-HD-160-TEMP15-RTD-9	-4.631	22.880	0.008	ESF-HD-160-TEMP15-RTD-59	-19.685	22.944	0.091
ESF-HD-160-TEMP15-RTD-10	-4.932	22.881	0.009	ESF-HD-160-TEMP15-RTD-60	-19.986	22.945	0.092
ESF-HD-160-TEMP15-RTD-11	-5.233	22.883	0.011	ESF-HD-160-TEMP15-RTD-61	-20.287	22.946	0.094
ESF-HD-160-TEMP15-RTD-12	-5.534	22.884	0.013	ESF-HD-160-TEMP15-RTD-62	-20.588	22.947	0.096
ESF-HD-160-TEMP15-RTD-13	-5.835	22.885	0.014	ESF-HD-160-TEMP15-RTD-63	-20.889	22.949	0.097
ESF-HD-160-TEMP15-RTD-14	-6.136	22.886	0.016	ESF-HD-160-TEMP15-RTD-64	-21.190	22.950	0.099
ESF-HD-160-TEMP15-RTD-15	-6.437	22.888	0.018	ESF-HD-160-TEMP15-RTD-65	-21.491	22.951	0.101
ESF-HD-160-TEMP15-RTD-16	-6.738	22.889	0.019	ESF-HD-160-TEMP15-RTD-66	-21.792	22.953	0.102
ESF-HD-160-TEMP15-RTD-17	-7.039	22.890	0.021	ESF-HD-160-TEMP15-RTD-67	-22.093	22.954	0.104
ESF-HD-160-TEMP15-RTD-18	-7.340	22.891	0.023	ESF-HD-161-TEMP16-RTD-1	-1.274	22.875	-1.276
ESF-HD-160-TEMP15-RTD-19	-7.641	22.893	0.024	ESF-HD-161-TEMP16-RTD-2	-1.492	22.880	-1.492
ESF-HD-160-TEMP15-RTD-20	-7.943	22.894	0.026	ESF-HD-161-TEMP16-RTD-3	-1.711	22.885	-1.708
ESF-HD-160-TEMP15-RTD-21	-8.244	22.895	0.028	ESF-HD-161-TEMP16-RTD-4	-1.929	22.891	-1.924
ESF-HD-160-TEMP15-RTD-22	-8.545	22.897	0.029	ESF-HD-161-TEMP16-RTD-5	-2.148	22.896	-2.140
ESF-HD-160-TEMP15-RTD-23	-8.846	22.898	0.031	ESF-HD-161-TEMP16-RTD-6	-2.366	22.902	-2.356
ESF-HD-160-TEMP15-RTD-24	-9.147	22.899	0.033	ESF-HD-161-TEMP16-RTD-7	-2.585	22.907	-2.572
ESF-HD-160-TEMP15-RTD-25	-9.448	22.900	0.034	ESF-HD-161-TEMP16-RTD-8	-2.803	22.913	-2.788
ESF-HD-160-TEMP15-RTD-26	-9.749	22.902	0.036	ESF-HD-161-TEMP16-RTD-9	-3.022	22.918	-3.004
ESF-HD-160-TEMP15-RTD-27	-10.050	22.903	0.038	ESF-HD-161-TEMP16-RTD-10	-3.241	22.923	-3.221
ESF-HD-160-TEMP15-RTD-28	-10.351	22.904	0.039	ESF-HD-161-TEMP16-RTD-11	-3.459	22.929	-3.437
ESF-HD-160-TEMP15-RTD-29	-10.652	22.905	0.041	ESF-HD-161-TEMP16-RTD-12	-3.678	22.934	-3.653
ESF-HD-160-TEMP15-RTD-30	-10.953	22.907	0.043	ESF-HD-161-TEMP16-RTD-13	-3.896	22.940	-3.869
ESF-HD-160-TEMP15-RTD-31	-11.254	22.908	0.044	ESF-HD-161-TEMP16-RTD-14	-4.115	22.945	-4.085
ESF-HD-160-TEMP15-RTD-32	-11.556	22.909	0.046	ESF-HD-161-TEMP16-RTD-15	-4.333	22.950	-4.301
ESF-HD-160-TEMP15-RTD-33	-11.857	22.911	0.048	ESF-HD-161-TEMP16-RTD-16	-4.552	22.956	-4.517
ESF-HD-160-TEMP15-RTD-34	-12.158	22.912	0.049	ESF-HD-161-TEMP16-RTD-17	-4.770	22.961	-4.733
ESF-HD-160-TEMP15-RTD-35	-12.459	22.913	0.051	ESF-HD-161-TEMP16-RTD-18	-4.989	22.967	-4.949
ESF-HD-160-TEMP15-RTD-36	-12.760	22.914	0.053	ESF-HD-161-TEMP16-RTD-19	-5.208	22.972	-5.165
ESF-HD-160-TEMP15-RTD-37	-13.061	22.916	0.054	ESF-HD-161-TEMP16-RTD-20	-5.426	22.978	-5.381
ESF-HD-160-TEMP15-RTD-38	-13.362	22.917	0.056	ESF-HD-161-TEMP16-RTD-21	-5.645	22.983	-5.598
ESF-HD-160-TEMP15-RTD-39	-13.663	22.918	0.058	ESF-HD-161-TEMP16-RTD-22	-5.863	22.988	-5.814
ESF-HD-160-TEMP15-RTD-40	-13.964	22.919	0.059	ESF-HD-161-TEMP16-RTD-23	-6.082	22.994	-6.030
ESF-HD-160-TEMP15-RTD-41	-14.265	22.921	0.061	ESF-HD-161-TEMP16-RTD-24	-6.300	22.999	-6.246
ESF-HD-160-TEMP15-RTD-42	-14.566	22.922	0.063	ESF-HD-161-TEMP16-RTD-25	-6.519	23.005	-6.462

Table C-2. Gage Locations for the DST Temperature Gages (continued)

Gage ID	x	y	z	Gage ID	x	y	z
ESF-HD-161-TEMP16-RTD-26	-6.737	23.010	-6.678	ESF-HD-162-TEMP17-RTD-9	0.775	22.865	-3.763
ESF-HD-161-TEMP16-RTD-27	-6.956	23.015	-6.894	ESF-HD-162-TEMP17-RTD-10	0.776	22.867	-4.062
ESF-HD-161-TEMP16-RTD-28	-7.175	23.021	-7.110	ESF-HD-162-TEMP17-RTD-11	0.777	22.870	-4.361
ESF-HD-161-TEMP16-RTD-29	-7.393	23.026	-7.326	ESF-HD-162-TEMP17-RTD-12	0.778	22.872	-4.660
ESF-HD-161-TEMP16-RTD-30	-7.612	23.032	-7.542	ESF-HD-162-TEMP17-RTD-13	0.779	22.874	-4.959
ESF-HD-161-TEMP16-RTD-31	-7.830	23.037	-7.758	ESF-HD-162-TEMP17-RTD-14	0.779	22.876	-5.258
ESF-HD-161-TEMP16-RTD-32	-8.049	23.043	-7.974	ESF-HD-162-TEMP17-RTD-15	0.780	22.878	-5.557
ESF-HD-161-TEMP16-RTD-33	-8.267	23.048	-8.191	ESF-HD-162-TEMP17-RTD-16	0.781	22.881	-5.856
ESF-HD-161-TEMP16-RTD-34	-8.486	23.053	-8.407	ESF-HD-162-TEMP17-RTD-17	0.782	22.883	-6.156
ESF-HD-161-TEMP16-RTD-35	-8.704	23.059	-8.623	ESF-HD-162-TEMP17-RTD-18	0.783	22.885	-6.455
ESF-HD-161-TEMP16-RTD-36	-8.923	23.064	-8.839	ESF-HD-162-TEMP17-RTD-19	0.784	22.887	-6.754
ESF-HD-161-TEMP16-RTD-37	-9.142	23.070	-9.055	ESF-HD-162-TEMP17-RTD-20	0.784	22.889	-7.053
ESF-HD-161-TEMP16-RTD-38	-9.360	23.075	-9.271	ESF-HD-162-TEMP17-RTD-21	0.785	22.891	-7.352
ESF-HD-161-TEMP16-RTD-39	-9.579	23.080	-9.487	ESF-HD-162-TEMP17-RTD-22	0.786	22.894	-7.651
ESF-HD-161-TEMP16-RTD-40	-9.797	23.086	-9.703	ESF-HD-162-TEMP17-RTD-23	0.787	22.896	-7.950
ESF-HD-161-TEMP16-RTD-41	-10.016	23.091	-9.919	ESF-HD-162-TEMP17-RTD-24	0.788	22.898	-8.249
ESF-HD-161-TEMP16-RTD-42	-10.234	23.097	-10.135	ESF-HD-162-TEMP17-RTD-25	0.789	22.900	-8.549
ESF-HD-161-TEMP16-RTD-43	-10.453	23.102	-10.351	ESF-HD-162-TEMP17-RTD-26	0.789	22.902	-8.848
ESF-HD-161-TEMP16-RTD-44	-10.671	23.108	-10.568	ESF-HD-162-TEMP17-RTD-27	0.790	22.905	-9.147
ESF-HD-161-TEMP16-RTD-45	-10.890	23.113	-10.784	ESF-HD-162-TEMP17-RTD-28	0.791	22.907	-9.446
ESF-HD-161-TEMP16-RTD-46	-11.108	23.118	-11.000	ESF-HD-162-TEMP17-RTD-29	0.792	22.909	-9.745
ESF-HD-161-TEMP16-RTD-47	-11.327	23.124	-11.216	ESF-HD-162-TEMP17-RTD-30	0.793	22.911	-10.044
ESF-HD-161-TEMP16-RTD-48	-11.546	23.129	-11.432	ESF-HD-162-TEMP17-RTD-31	0.794	22.913	-10.343
ESF-HD-161-TEMP16-RTD-49	-11.764	23.135	-11.648	ESF-HD-162-TEMP17-RTD-32	0.794	22.915	-10.642
ESF-HD-161-TEMP16-RTD-50	-11.983	23.140	-11.864	ESF-HD-162-TEMP17-RTD-33	0.795	22.918	-10.941
ESF-HD-161-TEMP16-RTD-51	-12.201	23.145	-12.080	ESF-HD-162-TEMP17-RTD-34	0.796	22.920	-11.241
ESF-HD-161-TEMP16-RTD-52	-12.420	23.151	-12.296	ESF-HD-162-TEMP17-RTD-35	0.797	22.922	-11.540
ESF-HD-161-TEMP16-RTD-53	-12.638	23.156	-12.512	ESF-HD-162-TEMP17-RTD-36	0.798	22.924	-11.839
ESF-HD-161-TEMP16-RTD-54	-12.857	23.162	-12.728	ESF-HD-162-TEMP17-RTD-37	0.799	22.926	-12.138
ESF-HD-161-TEMP16-RTD-55	-13.075	23.167	-12.944	ESF-HD-162-TEMP17-RTD-38	0.799	22.929	-12.437
ESF-HD-161-TEMP16-RTD-56	-13.294	23.173	-13.161	ESF-HD-162-TEMP17-RTD-39	0.800	22.931	-12.736
ESF-HD-161-TEMP16-RTD-57	-13.513	23.178	-13.377	ESF-HD-162-TEMP17-RTD-40	0.801	22.933	-13.035
ESF-HD-161-TEMP16-RTD-58	-13.731	23.183	-13.593	ESF-HD-162-TEMP17-RTD-41	0.802	22.935	-13.334
ESF-HD-161-TEMP16-RTD-59	-13.950	23.189	-13.809	ESF-HD-162-TEMP17-RTD-42	0.803	22.937	-13.634
ESF-HD-161-TEMP16-RTD-60	-14.168	23.194	-14.025	ESF-HD-162-TEMP17-RTD-43	0.804	22.940	-13.933
ESF-HD-161-TEMP16-RTD-61	-14.387	23.200	-14.241	ESF-HD-162-TEMP17-RTD-44	0.804	22.942	-14.232
ESF-HD-161-TEMP16-RTD-62	-14.605	23.205	-14.457	ESF-HD-162-TEMP17-RTD-45	0.805	22.944	-14.531
ESF-HD-161-TEMP16-RTD-63	-14.824	23.210	-14.673	ESF-HD-162-TEMP17-RTD-46	0.806	22.946	-14.830
ESF-HD-161-TEMP16-RTD-64	-15.042	23.216	-14.889	ESF-HD-162-TEMP17-RTD-47	0.807	22.948	-15.129
ESF-HD-161-TEMP16-RTD-65	-15.261	23.221	-15.105	ESF-HD-162-TEMP17-RTD-48	0.808	22.950	-15.428
ESF-HD-161-TEMP16-RTD-66	-15.480	23.227	-15.321	ESF-HD-162-TEMP17-RTD-49	0.809	22.953	-15.727
ESF-HD-161-TEMP16-RTD-67	-15.698	23.232	-15.538	ESF-HD-162-TEMP17-RTD-50	0.809	22.955	-16.026
ESF-HD-162-TEMP17-RTD-1	0.769	22.848	-1.370	ESF-HD-162-TEMP17-RTD-51	0.810	22.957	-16.326
ESF-HD-162-TEMP17-RTD-2	0.769	22.850	-1.669	ESF-HD-162-TEMP17-RTD-52	0.811	22.959	-16.625
ESF-HD-162-TEMP17-RTD-3	0.770	22.852	-1.968	ESF-HD-162-TEMP17-RTD-53	0.812	22.961	-16.924
ESF-HD-162-TEMP17-RTD-4	0.771	22.854	-2.267	ESF-HD-162-TEMP17-RTD-54	0.813	22.964	-17.223
ESF-HD-162-TEMP17-RTD-5	0.772	22.857	-2.566	ESF-HD-162-TEMP17-RTD-55	0.814	22.966	-17.522
ESF-HD-162-TEMP17-RTD-6	0.773	22.859	-2.865	ESF-HD-162-TEMP17-RTD-56	0.814	22.968	-17.821
ESF-HD-162-TEMP17-RTD-7	0.774	22.861	-3.164	ESF-HD-162-TEMP17-RTD-57	0.815	22.970	-18.120
ESF-HD-162-TEMP17-RTD-8	0.774	22.863	-3.464	ESF-HD-162-TEMP17-RTD-58	0.816	22.972	-18.419

Table C-2. Gage Locations for the DST Temperature Gages (continued)

Gage ID	x	y	z	Gage ID	x	y	z
ESF-HD-162-TEMP17-RTD-59	0.817	22.974	-18.719	ESF-HD-163-TEMP18-RTD-42	10.200	22.634	-10.317
ESF-HD-162-TEMP17-RTD-60	0.818	22.977	-19.018	ESF-HD-163-TEMP18-RTD-43	10.411	22.629	-10.530
ESF-HD-162-TEMP17-RTD-61	0.819	22.979	-19.317	ESF-HD-163-TEMP18-RTD-44	10.623	22.625	-10.743
ESF-HD-162-TEMP17-RTD-62	0.819	22.981	-19.616	ESF-HD-163-TEMP18-RTD-45	10.835	22.620	-10.955
ESF-HD-162-TEMP17-RTD-63	0.820	22.983	-19.915	ESF-HD-163-TEMP18-RTD-46	11.047	22.615	-11.168
ESF-HD-162-TEMP17-RTD-64	0.821	22.985	-20.214	ESF-HD-163-TEMP18-RTD-47	11.259	22.611	-11.381
ESF-HD-162-TEMP17-RTD-65	0.822	22.988	-20.513	ESF-HD-163-TEMP18-RTD-48	11.470	22.606	-11.593
ESF-HD-162-TEMP17-RTD-66	0.823	22.990	-20.812	ESF-HD-163-TEMP18-RTD-49	11.682	22.601	-11.806
ESF-HD-162-TEMP17-RTD-67	0.824	22.992	-21.112	ESF-HD-163-TEMP18-RTD-50	11.894	22.596	-12.019
ESF-HD-163-TEMP18-RTD-1	1.515	22.828	-1.597	ESF-HD-163-TEMP18-RTD-51	12.106	22.592	-12.231
ESF-HD-163-TEMP18-RTD-2	1.727	22.823	-1.810	ESF-HD-163-TEMP18-RTD-52	12.318	22.587	-12.444
ESF-HD-163-TEMP18-RTD-3	1.939	22.818	-2.022	ESF-HD-163-TEMP18-RTD-53	12.529	22.582	-12.657
ESF-HD-163-TEMP18-RTD-4	2.151	22.813	-2.235	ESF-HD-163-TEMP18-RTD-54	12.741	22.578	-12.869
ESF-HD-163-TEMP18-RTD-5	2.363	22.809	-2.448	ESF-HD-163-TEMP18-RTD-55	12.953	22.573	-13.082
ESF-HD-163-TEMP18-RTD-6	2.575	22.804	-2.660	ESF-HD-163-TEMP18-RTD-56	13.165	22.568	-13.295
ESF-HD-163-TEMP18-RTD-7	2.786	22.799	-2.873	ESF-HD-163-TEMP18-RTD-57	13.377	22.563	-13.508
ESF-HD-163-TEMP18-RTD-8	2.998	22.795	-3.086	ESF-HD-163-TEMP18-RTD-58	13.588	22.559	-13.720
ESF-HD-163-TEMP18-RTD-9	3.210	22.790	-3.298	ESF-HD-163-TEMP18-RTD-59	13.800	22.554	-13.933
ESF-HD-163-TEMP18-RTD-10	3.422	22.785	-3.511	ESF-HD-163-TEMP18-RTD-60	14.012	22.549	-14.146
ESF-HD-163-TEMP18-RTD-11	3.634	22.780	-3.724	ESF-HD-163-TEMP18-RTD-61	14.224	22.545	-14.358
ESF-HD-163-TEMP18-RTD-12	3.845	22.776	-3.937	ESF-HD-163-TEMP18-RTD-62	14.436	22.540	-14.571
ESF-HD-163-TEMP18-RTD-13	4.057	22.771	-4.149	ESF-HD-163-TEMP18-RTD-63	14.647	22.535	-14.784
ESF-HD-163-TEMP18-RTD-14	4.269	22.766	-4.362	ESF-HD-163-TEMP18-RTD-64	14.859	22.530	-14.996
ESF-HD-163-TEMP18-RTD-15	4.481	22.762	-4.575	ESF-HD-163-TEMP18-RTD-65	15.071	22.526	-15.209
ESF-HD-163-TEMP18-RTD-16	4.693	22.757	-4.787	ESF-HD-163-TEMP18-RTD-66	15.283	22.521	-15.422
ESF-HD-163-TEMP18-RTD-17	4.904	22.752	-5.000	ESF-HD-163-TEMP18-RTD-67	15.495	22.516	-15.634
ESF-HD-163-TEMP18-RTD-18	5.116	22.747	-5.213	ESF-HD-164-TEMP19-RTD-1	1.913	22.716	0.008
ESF-HD-163-TEMP18-RTD-19	5.328	22.743	-5.425	ESF-HD-164-TEMP19-RTD-2	2.222	22.719	0.012
ESF-HD-163-TEMP18-RTD-20	5.540	22.738	-5.638	ESF-HD-164-TEMP19-RTD-3	2.531	22.721	0.016
ESF-HD-163-TEMP18-RTD-21	5.752	22.733	-5.851	ESF-HD-164-TEMP19-RTD-4	2.840	22.723	0.021
ESF-HD-163-TEMP18-RTD-22	5.963	22.729	-6.063	ESF-HD-164-TEMP19-RTD-5	3.148	22.726	0.025
ESF-HD-163-TEMP18-RTD-23	6.175	22.724	-6.276	ESF-HD-164-TEMP19-RTD-6	3.457	22.728	0.029
ESF-HD-163-TEMP18-RTD-24	6.387	22.719	-6.489	ESF-HD-164-TEMP19-RTD-7	3.766	22.730	0.034
ESF-HD-163-TEMP18-RTD-25	6.599	22.714	-6.702	ESF-HD-164-TEMP19-RTD-8	4.074	22.732	0.038
ESF-HD-163-TEMP18-RTD-26	6.811	22.710	-6.914	ESF-HD-164-TEMP19-RTD-9	4.383	22.735	0.042
ESF-HD-163-TEMP18-RTD-27	7.022	22.705	-7.127	ESF-HD-164-TEMP19-RTD-10	4.692	22.737	0.047
ESF-HD-163-TEMP18-RTD-28	7.234	22.700	-7.340	ESF-HD-164-TEMP19-RTD-11	5.000	22.739	0.051
ESF-HD-163-TEMP18-RTD-29	7.446	22.695	-7.552	ESF-HD-164-TEMP19-RTD-12	5.309	22.741	0.056
ESF-HD-163-TEMP18-RTD-30	7.658	22.691	-7.765	ESF-HD-164-TEMP19-RTD-13	5.618	22.744	0.060
ESF-HD-163-TEMP18-RTD-31	7.870	22.686	-7.978	ESF-HD-164-TEMP19-RTD-14	5.926	22.746	0.064
ESF-HD-163-TEMP18-RTD-32	8.081	22.681	-8.190	ESF-HD-164-TEMP19-RTD-15	6.235	22.748	0.069
ESF-HD-163-TEMP18-RTD-33	8.293	22.677	-8.403	ESF-HD-164-TEMP19-RTD-16	6.544	22.751	0.073
ESF-HD-163-TEMP18-RTD-34	8.505	22.672	-8.616	ESF-HD-164-TEMP19-RTD-17	6.852	22.753	0.077
ESF-HD-163-TEMP18-RTD-35	8.717	22.667	-8.828	ESF-HD-164-TEMP19-RTD-18	7.161	22.755	0.082
ESF-HD-163-TEMP18-RTD-36	8.929	22.662	-9.041	ESF-HD-164-TEMP19-RTD-19	7.470	22.757	0.086
ESF-HD-163-TEMP18-RTD-37	9.141	22.658	-9.254	ESF-HD-164-TEMP19-RTD-20	7.778	22.760	0.090
ESF-HD-163-TEMP18-RTD-38	9.352	22.653	-9.466	ESF-HD-164-TEMP19-RTD-21	8.087	22.762	0.095
ESF-HD-163-TEMP18-RTD-39	9.564	22.648	-9.679	ESF-HD-164-TEMP19-RTD-22	8.396	22.764	0.099
ESF-HD-163-TEMP18-RTD-40	9.776	22.644	-9.892	ESF-HD-164-TEMP19-RTD-23	8.704	22.767	0.103
ESF-HD-163-TEMP18-RTD-41	9.988	22.639	-10.105	ESF-HD-164-TEMP19-RTD-24	9.013	22.769	0.108

Table C-2. Gage Locations for the DST Temperature Gages (continued)

Gage ID	x	y	z	Gage ID	x	y	z
ESF-HD-164-TEMP19-RTD-25	9.322	22.771	0.112	ESF-HD-165-TEMP20-RTD-8	3.171	22.836	3.191
ESF-HD-164-TEMP19-RTD-26	9.630	22.773	0.116	ESF-HD-165-TEMP20-RTD-9	3.384	22.835	3.404
ESF-HD-164-TEMP19-RTD-27	9.939	22.776	0.121	ESF-HD-165-TEMP20-RTD-10	3.597	22.834	3.616
ESF-HD-164-TEMP19-RTD-28	10.248	22.778	0.125	ESF-HD-165-TEMP20-RTD-11	3.810	22.832	3.829
ESF-HD-164-TEMP19-RTD-29	10.557	22.780	0.129	ESF-HD-165-TEMP20-RTD-12	4.023	22.831	4.042
ESF-HD-164-TEMP19-RTD-30	10.865	22.782	0.134	ESF-HD-165-TEMP20-RTD-13	4.235	22.830	4.254
ESF-HD-164-TEMP19-RTD-31	11.174	22.785	0.138	ESF-HD-165-TEMP20-RTD-14	4.448	22.828	4.467
ESF-HD-164-TEMP19-RTD-32	11.483	22.787	0.143	ESF-HD-165-TEMP20-RTD-15	4.661	22.827	4.680
ESF-HD-164-TEMP19-RTD-33	11.791	22.789	0.147	ESF-HD-165-TEMP20-RTD-16	4.874	22.826	4.893
ESF-HD-164-TEMP19-RTD-34	12.100	22.792	0.151	ESF-HD-165-TEMP20-RTD-17	5.086	22.824	5.105
ESF-HD-164-TEMP19-RTD-35	12.409	22.794	0.156	ESF-HD-165-TEMP20-RTD-18	5.299	22.823	5.318
ESF-HD-164-TEMP19-RTD-36	12.717	22.796	0.160	ESF-HD-165-TEMP20-RTD-19	5.512	22.821	5.531
ESF-HD-164-TEMP19-RTD-37	13.026	22.798	0.164	ESF-HD-165-TEMP20-RTD-20	5.725	22.820	5.743
ESF-HD-164-TEMP19-RTD-38	13.335	22.801	0.169	ESF-HD-165-TEMP20-RTD-21	5.938	22.819	5.956
ESF-HD-164-TEMP19-RTD-39	13.643	22.803	0.173	ESF-HD-165-TEMP20-RTD-22	6.150	22.817	6.169
ESF-HD-164-TEMP19-RTD-40	13.952	22.805	0.177	ESF-HD-165-TEMP20-RTD-23	6.363	22.816	6.382
ESF-HD-164-TEMP19-RTD-41	14.261	22.807	0.182	ESF-HD-165-TEMP20-RTD-24	6.576	22.815	6.594
ESF-HD-164-TEMP19-RTD-42	14.569	22.810	0.186	ESF-HD-165-TEMP20-RTD-25	6.789	22.813	6.807
ESF-HD-164-TEMP19-RTD-43	14.878	22.812	0.190	ESF-HD-165-TEMP20-RTD-26	7.001	22.812	7.020
ESF-HD-164-TEMP19-RTD-44	15.187	22.814	0.195	ESF-HD-165-TEMP20-RTD-27	7.214	22.811	7.233
ESF-HD-164-TEMP19-RTD-45	15.495	22.817	0.199	ESF-HD-165-TEMP20-RTD-28	7.427	22.809	7.445
ESF-HD-164-TEMP19-RTD-46	15.804	22.819	0.203	ESF-HD-165-TEMP20-RTD-29	7.640	22.808	7.658
ESF-HD-164-TEMP19-RTD-47	16.113	22.821	0.208	ESF-HD-165-TEMP20-RTD-30	7.852	22.806	7.871
ESF-HD-164-TEMP19-RTD-48	16.421	22.823	0.212	ESF-HD-165-TEMP20-RTD-31	8.065	22.805	8.083
ESF-HD-164-TEMP19-RTD-49	16.730	22.826	0.217	ESF-HD-165-TEMP20-RTD-32	8.278	22.804	8.296
ESF-HD-164-TEMP19-RTD-50	17.039	22.828	0.221	ESF-HD-165-TEMP20-RTD-33	8.491	22.802	8.509
ESF-HD-164-TEMP19-RTD-51	17.347	22.830	0.225	ESF-HD-165-TEMP20-RTD-34	8.704	22.801	8.722
ESF-HD-164-TEMP19-RTD-52	17.656	22.833	0.230	ESF-HD-165-TEMP20-RTD-35	8.916	22.800	8.934
ESF-HD-164-TEMP19-RTD-53	17.965	22.835	0.234	ESF-HD-165-TEMP20-RTD-36	9.129	22.798	9.147
ESF-HD-164-TEMP19-RTD-54	18.273	22.837	0.238	ESF-HD-165-TEMP20-RTD-37	9.342	22.797	9.360
ESF-HD-164-TEMP19-RTD-55	18.582	22.839	0.243	ESF-HD-165-TEMP20-RTD-38	9.555	22.796	9.572
ESF-HD-164-TEMP19-RTD-56	18.891	22.842	0.247	ESF-HD-165-TEMP20-RTD-39	9.767	22.794	9.785
ESF-HD-164-TEMP19-RTD-57	19.200	22.844	0.251	ESF-HD-165-TEMP20-RTD-40	9.980	22.793	9.998
ESF-HD-164-TEMP19-RTD-58	19.508	22.846	0.256	ESF-HD-165-TEMP20-RTD-41	10.193	22.792	10.211
ESF-HD-164-TEMP19-RTD-59	19.817	22.848	0.260	ESF-HD-165-TEMP20-RTD-42	10.406	22.790	10.423
ESF-HD-164-TEMP19-RTD-60	20.126	22.851	0.264	ESF-HD-165-TEMP20-RTD-43	10.618	22.789	10.636
ESF-HD-164-TEMP19-RTD-61	20.434	22.853	0.269	ESF-HD-165-TEMP20-RTD-44	10.831	22.787	10.849
ESF-HD-164-TEMP19-RTD-62	20.743	22.855	0.273	ESF-HD-165-TEMP20-RTD-45	11.044	22.786	11.062
ESF-HD-164-TEMP19-RTD-63	21.052	22.858	0.277	ESF-HD-165-TEMP20-RTD-46	11.257	22.785	11.274
ESF-HD-164-TEMP19-RTD-64	21.360	22.860	0.282	ESF-HD-165-TEMP20-RTD-47	11.470	22.783	11.487
ESF-HD-164-TEMP19-RTD-65	21.669	22.862	0.286	ESF-HD-165-TEMP20-RTD-48	11.682	22.782	11.700
ESF-HD-164-TEMP19-RTD-66	21.978	22.864	0.290	ESF-HD-165-TEMP20-RTD-49	11.895	22.781	11.912
ESF-HD-164-TEMP19-RTD-67	22.286	22.867	0.295	ESF-HD-165-TEMP20-RTD-50	12.108	22.779	12.125
ESF-HD-165-TEMP20-RTD-1	1.682	22.846	1.702	ESF-HD-165-TEMP20-RTD-51	12.321	22.778	12.338
ESF-HD-165-TEMP20-RTD-2	1.895	22.845	1.914	ESF-HD-165-TEMP20-RTD-52	12.533	22.777	12.551
ESF-HD-165-TEMP20-RTD-3	2.108	22.843	2.127	ESF-HD-165-TEMP20-RTD-53	12.746	22.775	12.763
ESF-HD-165-TEMP20-RTD-4	2.320	22.842	2.340	ESF-HD-165-TEMP20-RTD-54	12.959	22.774	12.976
ESF-HD-165-TEMP20-RTD-5	2.533	22.840	2.553	ESF-HD-165-TEMP20-RTD-55	13.172	22.773	13.189
ESF-HD-165-TEMP20-RTD-6	2.746	22.839	2.765	ESF-HD-165-TEMP20-RTD-56	13.385	22.771	13.401
ESF-HD-165-TEMP20-RTD-7	2.959	22.838	2.978	ESF-HD-165-TEMP20-RTD-57	13.597	22.770	13.614

Table C-2. Gage Locations for the DST Temperature Gages (continued)

Gage ID	x	y	z	Gage ID	x	y	z
ESF-HD-165-TEMP20-RTD-58	13.810	22.768	13.827	ESF-HD-168-TEMP21-RTD-41	-0.237	31.968	15.166
ESF-HD-165-TEMP20-RTD-59	14.023	22.767	14.040	ESF-HD-168-TEMP21-RTD-42	-0.241	31.969	15.466
ESF-HD-165-TEMP20-RTD-60	14.236	22.766	14.252	ESF-HD-168-TEMP21-RTD-43	-0.245	31.969	15.766
ESF-HD-165-TEMP20-RTD-61	14.448	22.764	14.465	ESF-HD-168-TEMP21-RTD-44	-0.249	31.970	16.066
ESF-HD-165-TEMP20-RTD-62	14.661	22.763	14.678	ESF-HD-168-TEMP21-RTD-45	-0.253	31.970	16.366
ESF-HD-165-TEMP20-RTD-63	14.874	22.762	14.891	ESF-HD-168-TEMP21-RTD-46	-0.257	31.970	16.666
ESF-HD-165-TEMP20-RTD-64	15.087	22.760	15.103	ESF-HD-168-TEMP21-RTD-47	-0.261	31.971	16.966
ESF-HD-165-TEMP20-RTD-65	15.299	22.759	15.316	ESF-HD-168-TEMP21-RTD-48	-0.265	31.971	17.266
ESF-HD-165-TEMP20-RTD-66	15.512	22.758	15.529	ESF-HD-168-TEMP21-RTD-49	-0.269	31.971	17.567
ESF-HD-165-TEMP20-RTD-67	15.725	22.756	15.741	ESF-HD-168-TEMP21-RTD-50	-0.273	31.972	17.867
ESF-HD-168-TEMP21-RTD-1	-0.080	31.953	3.162	ESF-HD-168-TEMP21-RTD-51	-0.277	31.972	18.167
ESF-HD-168-TEMP21-RTD-2	-0.084	31.954	3.463	ESF-HD-168-TEMP21-RTD-52	-0.281	31.973	18.467
ESF-HD-168-TEMP21-RTD-3	-0.088	31.954	3.763	ESF-HD-168-TEMP21-RTD-53	-0.284	31.973	18.767
ESF-HD-168-TEMP21-RTD-4	-0.092	31.954	4.063	ESF-HD-168-TEMP21-RTD-54	-0.288	31.973	19.067
ESF-HD-168-TEMP21-RTD-5	-0.096	31.955	4.363	ESF-HD-168-TEMP21-RTD-55	-0.292	31.974	19.367
ESF-HD-168-TEMP21-RTD-6	-0.100	31.955	4.663	ESF-HD-168-TEMP21-RTD-56	-0.296	31.974	19.667
ESF-HD-168-TEMP21-RTD-7	-0.104	31.956	4.963	ESF-HD-168-TEMP21-RTD-57	-0.300	31.974	19.967
ESF-HD-168-TEMP21-RTD-8	-0.108	31.956	5.263	ESF-HD-168-TEMP21-RTD-58	-0.304	31.975	20.267
ESF-HD-168-TEMP21-RTD-9	-0.112	31.956	5.563	ESF-HD-168-TEMP21-RTD-59	-0.308	31.975	20.567
ESF-HD-168-TEMP21-RTD-10	-0.116	31.957	5.863	ESF-HD-168-TEMP21-RTD-60	-0.312	31.976	20.867
ESF-HD-168-TEMP21-RTD-11	-0.120	31.957	6.163	ESF-HD-168-TEMP21-RTD-61	-0.316	31.976	21.168
ESF-HD-168-TEMP21-RTD-12	-0.124	31.957	6.463	ESF-HD-168-TEMP21-RTD-62	-0.320	31.976	21.468
ESF-HD-168-TEMP21-RTD-13	-0.127	31.958	6.763	ESF-HD-168-TEMP21-RTD-63	-0.324	31.977	21.768
ESF-HD-168-TEMP21-RTD-14	-0.131	31.958	7.064	ESF-HD-168-TEMP21-RTD-64	-0.328	31.977	22.068
ESF-HD-168-TEMP21-RTD-15	-0.135	31.959	7.364	ESF-HD-168-TEMP21-RTD-65	-0.332	31.977	22.368
ESF-HD-168-TEMP21-RTD-16	-0.139	31.959	7.664	ESF-HD-168-TEMP21-RTD-66	-0.336	31.978	22.668
ESF-HD-168-TEMP21-RTD-17	-0.143	31.959	7.964	ESF-HD-168-TEMP21-RTD-67	-0.339	31.978	22.968
ESF-HD-168-TEMP21-RTD-18	-0.147	31.960	8.264	ESF-HD-169-TEMP22-RTD-1	0.001	32.015	-2.014
ESF-HD-168-TEMP21-RTD-19	-0.151	31.960	8.564	ESF-HD-169-TEMP22-RTD-2	0.005	32.021	-2.317
ESF-HD-168-TEMP21-RTD-20	-0.155	31.960	8.864	ESF-HD-169-TEMP22-RTD-3	0.009	32.027	-2.621
ESF-HD-168-TEMP21-RTD-21	-0.159	31.961	9.164	ESF-HD-169-TEMP22-RTD-4	0.013	32.033	-2.924
ESF-HD-168-TEMP21-RTD-22	-0.163	31.961	9.464	ESF-HD-169-TEMP22-RTD-5	0.016	32.040	-3.227
ESF-HD-168-TEMP21-RTD-23	-0.167	31.962	9.764	ESF-HD-169-TEMP22-RTD-6	0.020	32.046	-3.531
ESF-HD-168-TEMP21-RTD-24	-0.171	31.962	10.064	ESF-HD-169-TEMP22-RTD-7	0.024	32.052	-3.834
ESF-HD-168-TEMP21-RTD-25	-0.175	31.962	10.364	ESF-HD-169-TEMP22-RTD-8	0.028	32.058	-4.137
ESF-HD-168-TEMP21-RTD-26	-0.178	31.963	10.665	ESF-HD-169-TEMP22-RTD-9	0.031	32.064	-4.441
ESF-HD-168-TEMP21-RTD-27	-0.182	31.963	10.965	ESF-HD-169-TEMP22-RTD-10	0.035	32.070	-4.744
ESF-HD-168-TEMP21-RTD-28	-0.186	31.964	11.265	ESF-HD-169-TEMP22-RTD-11	0.039	32.076	-5.047
ESF-HD-168-TEMP21-RTD-29	-0.190	31.964	11.565	ESF-HD-169-TEMP22-RTD-12	0.043	32.082	-5.351
ESF-HD-168-TEMP21-RTD-30	-0.194	31.964	11.865	ESF-HD-169-TEMP22-RTD-13	0.046	32.088	-5.654
ESF-HD-168-TEMP21-RTD-31	-0.198	31.965	12.165	ESF-HD-169-TEMP22-RTD-14	0.050	32.094	-5.957
ESF-HD-168-TEMP21-RTD-32	-0.202	31.965	12.465	ESF-HD-169-TEMP22-RTD-15	0.054	32.101	-6.261
ESF-HD-168-TEMP21-RTD-33	-0.206	31.965	12.765	ESF-HD-169-TEMP22-RTD-16	0.058	32.107	-6.564
ESF-HD-168-TEMP21-RTD-34	-0.210	31.966	13.065	ESF-HD-169-TEMP22-RTD-17	0.061	32.113	-6.867
ESF-HD-168-TEMP21-RTD-35	-0.214	31.966	13.365	ESF-HD-169-TEMP22-RTD-18	0.065	32.119	-7.171
ESF-HD-168-TEMP21-RTD-36	-0.218	31.967	13.665	ESF-HD-169-TEMP22-RTD-19	0.069	32.125	-7.474
ESF-HD-168-TEMP21-RTD-37	-0.222	31.967	13.966	ESF-HD-169-TEMP22-RTD-20	0.073	32.131	-7.777
ESF-HD-168-TEMP21-RTD-38	-0.226	31.967	14.266	ESF-HD-169-TEMP22-RTD-21	0.076	32.137	-8.081
ESF-HD-168-TEMP21-RTD-39	-0.230	31.968	14.566	ESF-HD-169-TEMP22-RTD-22	0.080	32.143	-8.384
ESF-HD-168-TEMP21-RTD-40	-0.233	31.968	14.866	ESF-HD-169-TEMP22-RTD-23	0.084	32.149	-8.687

Table C-2. Gage Locations for the DST Temperature Gages (continued)

Gage ID	x	y	z	Gage ID	x	y	z
ESF-HD-169-TEMP22-RTD-24	0.087	32.155	-8.991	ESF-HD-170-TEMP23-RTD-7	0.751	39.289	4.313
ESF-HD-169-TEMP22-RTD-25	0.091	32.162	-9.294	ESF-HD-170-TEMP23-RTD-8	0.751	39.286	4.609
ESF-HD-169-TEMP22-RTD-26	0.095	32.168	-9.597	ESF-HD-170-TEMP23-RTD-9	0.750	39.283	4.905
ESF-HD-169-TEMP22-RTD-27	0.099	32.174	-9.901	ESF-HD-170-TEMP23-RTD-10	0.750	39.281	5.201
ESF-HD-169-TEMP22-RTD-28	0.102	32.180	-10.204	ESF-HD-170-TEMP23-RTD-11	0.750	39.278	5.497
ESF-HD-169-TEMP22-RTD-29	0.106	32.186	-10.507	ESF-HD-170-TEMP23-RTD-12	0.750	39.275	5.792
ESF-HD-169-TEMP22-RTD-30	0.110	32.192	-10.811	ESF-HD-170-TEMP23-RTD-13	0.750	39.272	6.088
ESF-HD-169-TEMP22-RTD-31	0.114	32.198	-11.114	ESF-HD-170-TEMP23-RTD-14	0.750	39.269	6.384
ESF-HD-169-TEMP22-RTD-32	0.117	32.204	-11.417	ESF-HD-170-TEMP23-RTD-15	0.750	39.267	6.680
ESF-HD-169-TEMP22-RTD-33	0.121	32.210	-11.721	ESF-HD-170-TEMP23-RTD-16	0.750	39.264	6.976
ESF-HD-169-TEMP22-RTD-34	0.125	32.216	-12.024	ESF-HD-170-TEMP23-RTD-17	0.750	39.261	7.272
ESF-HD-169-TEMP22-RTD-35	0.129	32.223	-12.327	ESF-HD-170-TEMP23-RTD-18	0.750	39.258	7.568
ESF-HD-169-TEMP22-RTD-36	0.132	32.229	-12.631	ESF-HD-170-TEMP23-RTD-19	0.750	39.255	7.863
ESF-HD-169-TEMP22-RTD-37	0.136	32.235	-12.934	ESF-HD-170-TEMP23-RTD-20	0.750	39.252	8.159
ESF-HD-169-TEMP22-RTD-38	0.140	32.241	-13.237	ESF-HD-170-TEMP23-RTD-21	0.750	39.250	8.455
ESF-HD-169-TEMP22-RTD-39	0.144	32.247	-13.541	ESF-HD-170-TEMP23-RTD-22	0.749	39.247	8.751
ESF-HD-169-TEMP22-RTD-40	0.147	32.253	-13.844	ESF-HD-170-TEMP23-RTD-23	0.749	39.244	9.047
ESF-HD-169-TEMP22-RTD-41	0.151	32.259	-14.147	ESF-HD-170-TEMP23-RTD-24	0.749	39.241	9.343
ESF-HD-169-TEMP22-RTD-42	0.155	32.265	-14.451	ESF-HD-170-TEMP23-RTD-25	0.749	39.238	9.639
ESF-HD-169-TEMP22-RTD-43	0.159	32.271	-14.754	ESF-HD-170-TEMP23-RTD-26	0.749	39.235	9.935
ESF-HD-169-TEMP22-RTD-44	0.162	32.277	-15.058	ESF-HD-170-TEMP23-RTD-27	0.749	39.233	10.230
ESF-HD-169-TEMP22-RTD-45	0.166	32.284	-15.361	ESF-HD-170-TEMP23-RTD-28	0.749	39.230	10.526
ESF-HD-169-TEMP22-RTD-46	0.170	32.290	-15.664	ESF-HD-170-TEMP23-RTD-29	0.749	39.227	10.822
ESF-HD-169-TEMP22-RTD-47	0.174	32.296	-15.968	ESF-HD-170-TEMP23-RTD-30	0.749	39.224	11.118
ESF-HD-169-TEMP22-RTD-48	0.177	32.302	-16.271	ESF-HD-170-TEMP23-RTD-31	0.749	39.221	11.414
ESF-HD-169-TEMP22-RTD-49	0.181	32.308	-16.574	ESF-HD-170-TEMP23-RTD-32	0.749	39.219	11.710
ESF-HD-169-TEMP22-RTD-50	0.185	32.314	-16.878	ESF-HD-170-TEMP23-RTD-33	0.749	39.216	12.006
ESF-HD-169-TEMP22-RTD-51	0.189	32.320	-17.181	ESF-HD-170-TEMP23-RTD-34	0.749	39.213	12.302
ESF-HD-169-TEMP22-RTD-52	0.192	32.326	-17.484	ESF-HD-170-TEMP23-RTD-35	0.748	39.210	12.597
ESF-HD-169-TEMP22-RTD-53	0.196	32.332	-17.788	ESF-HD-170-TEMP23-RTD-36	0.748	39.207	12.893
ESF-HD-169-TEMP22-RTD-54	0.200	32.338	-18.091	ESF-HD-170-TEMP23-RTD-37	0.748	39.204	13.189
ESF-HD-169-TEMP22-RTD-55	0.203	32.345	-18.394	ESF-HD-170-TEMP23-RTD-38	0.748	39.202	13.485
ESF-HD-169-TEMP22-RTD-56	0.207	32.351	-18.698	ESF-HD-170-TEMP23-RTD-39	0.748	39.199	13.781
ESF-HD-169-TEMP22-RTD-57	0.211	32.357	-19.001	ESF-HD-170-TEMP23-RTD-40	0.748	39.196	14.077
ESF-HD-169-TEMP22-RTD-58	0.215	32.363	-19.304	ESF-HD-170-TEMP23-RTD-41	0.748	39.193	14.373
ESF-HD-169-TEMP22-RTD-59	0.218	32.369	-19.608	ESF-HD-170-TEMP23-RTD-42	0.748	39.190	14.669
ESF-HD-169-TEMP22-RTD-60	0.222	32.375	-19.911	ESF-HD-170-TEMP23-RTD-43	0.748	39.188	14.964
ESF-HD-169-TEMP22-RTD-61	0.226	32.381	-20.214	ESF-HD-170-TEMP23-RTD-44	0.748	39.185	15.260
ESF-HD-169-TEMP22-RTD-62	0.230	32.387	-20.518	ESF-HD-170-TEMP23-RTD-45	0.748	39.182	15.556
ESF-HD-169-TEMP22-RTD-63	0.233	32.393	-20.821	ESF-HD-170-TEMP23-RTD-46	0.748	39.179	15.852
ESF-HD-169-TEMP22-RTD-64	0.237	32.399	-21.124	ESF-HD-170-TEMP23-RTD-47	0.748	39.176	16.148
ESF-HD-169-TEMP22-RTD-65	0.241	32.406	-21.428	ESF-HD-170-TEMP23-RTD-48	0.747	39.173	16.444
ESF-HD-169-TEMP22-RTD-66	0.245	32.412	-21.731	ESF-HD-170-TEMP23-RTD-49	0.747	39.171	16.740
ESF-HD-169-TEMP22-RTD-67	0.248	32.418	-22.034	ESF-HD-170-TEMP23-RTD-50	0.747	39.168	17.036
ESF-HD-170-TEMP23-RTD-1	0.751	39.306	2.538	ESF-HD-170-TEMP23-RTD-51	0.747	39.165	17.331
ESF-HD-170-TEMP23-RTD-2	0.751	39.303	2.834	ESF-HD-170-TEMP23-RTD-52	0.747	39.162	17.627
ESF-HD-170-TEMP23-RTD-3	0.751	39.300	3.130	ESF-HD-170-TEMP23-RTD-53	0.747	39.159	17.923
ESF-HD-170-TEMP23-RTD-4	0.751	39.298	3.425	ESF-HD-170-TEMP23-RTD-54	0.747	39.157	18.219
ESF-HD-170-TEMP23-RTD-5	0.751	39.295	3.721	ESF-HD-170-TEMP23-RTD-55	0.747	39.154	18.515
ESF-HD-170-TEMP23-RTD-6	0.751	39.292	4.017	ESF-HD-170-TEMP23-RTD-56	0.747	39.151	18.811

Table C-2. Gage Locations for the DST Temperature Gages (continued)

Gage ID	x	y	z	Gage ID	x	y	z
ESF-HD-170-TEMP23-RTD-57	0.747	39.148	19.107	ESF-HD-171-TEMP24-RTD-40	-10.000	39.301	10.043
ESF-HD-170-TEMP23-RTD-58	0.747	39.145	19.403	ESF-HD-171-TEMP24-RTD-41	-10.207	39.300	10.252
ESF-HD-170-TEMP23-RTD-59	0.747	39.142	19.698	ESF-HD-171-TEMP24-RTD-42	-10.414	39.300	10.461
ESF-HD-170-TEMP23-RTD-60	0.747	39.140	19.994	ESF-HD-171-TEMP24-RTD-43	-10.621	39.300	10.670
ESF-HD-170-TEMP23-RTD-61	0.746	39.137	20.290	ESF-HD-171-TEMP24-RTD-44	-10.828	39.299	10.879
ESF-HD-170-TEMP23-RTD-62	0.746	39.134	20.586	ESF-HD-171-TEMP24-RTD-45	-11.036	39.299	11.088
ESF-HD-170-TEMP23-RTD-63	0.746	39.131	20.882	ESF-HD-171-TEMP24-RTD-46	-11.243	39.299	11.297
ESF-HD-170-TEMP23-RTD-64	0.746	39.128	21.178	ESF-HD-171-TEMP24-RTD-47	-11.450	39.298	11.506
ESF-HD-170-TEMP23-RTD-65	0.746	39.125	21.474	ESF-HD-171-TEMP24-RTD-48	-11.657	39.298	11.715
ESF-HD-170-TEMP23-RTD-66	0.746	39.123	21.769	ESF-HD-171-TEMP24-RTD-49	-11.864	39.298	11.925
ESF-HD-170-TEMP23-RTD-67	0.746	39.120	22.065	ESF-HD-171-TEMP24-RTD-50	-12.071	39.297	12.134
ESF-HD-171-TEMP24-RTD-1	-1.922	39.313	1.887	ESF-HD-171-TEMP24-RTD-51	-12.278	39.297	12.343
ESF-HD-171-TEMP24-RTD-2	-2.129	39.312	2.096	ESF-HD-171-TEMP24-RTD-52	-12.486	39.297	12.552
ESF-HD-171-TEMP24-RTD-3	-2.336	39.312	2.305	ESF-HD-171-TEMP24-RTD-53	-12.693	39.297	12.761
ESF-HD-171-TEMP24-RTD-4	-2.543	39.312	2.514	ESF-HD-171-TEMP24-RTD-54	-12.900	39.296	12.970
ESF-HD-171-TEMP24-RTD-5	-2.750	39.311	2.724	ESF-HD-171-TEMP24-RTD-55	-13.107	39.296	13.179
ESF-HD-171-TEMP24-RTD-6	-2.957	39.311	2.933	ESF-HD-171-TEMP24-RTD-56	-13.314	39.296	13.388
ESF-HD-171-TEMP24-RTD-7	-3.165	39.311	3.142	ESF-HD-171-TEMP24-RTD-57	-13.521	39.295	13.598
ESF-HD-171-TEMP24-RTD-8	-3.372	39.310	3.351	ESF-HD-171-TEMP24-RTD-58	-13.728	39.295	13.807
ESF-HD-171-TEMP24-RTD-9	-3.579	39.310	3.560	ESF-HD-171-TEMP24-RTD-59	-13.935	39.295	14.016
ESF-HD-171-TEMP24-RTD-10	-3.786	39.310	3.769	ESF-HD-171-TEMP24-RTD-60	-14.143	39.294	14.225
ESF-HD-171-TEMP24-RTD-11	-3.993	39.310	3.978	ESF-HD-171-TEMP24-RTD-61	-14.350	39.294	14.434
ESF-HD-171-TEMP24-RTD-12	-4.200	39.309	4.187	ESF-HD-171-TEMP24-RTD-62	-14.557	39.294	14.643
ESF-HD-171-TEMP24-RTD-13	-4.407	39.309	4.396	ESF-HD-171-TEMP24-RTD-63	-14.764	39.293	14.852
ESF-HD-171-TEMP24-RTD-14	-4.615	39.309	4.606	ESF-HD-171-TEMP24-RTD-64	-14.971	39.293	15.061
ESF-HD-171-TEMP24-RTD-15	-4.822	39.308	4.815	ESF-HD-171-TEMP24-RTD-65	-15.178	39.293	15.270
ESF-HD-171-TEMP24-RTD-16	-5.029	39.308	5.024	ESF-HD-171-TEMP24-RTD-66	-15.385	39.293	15.480
ESF-HD-171-TEMP24-RTD-17	-5.236	39.308	5.233	ESF-HD-171-TEMP24-RTD-67	-15.592	39.292	15.689
ESF-HD-171-TEMP24-RTD-18	-5.443	39.307	5.442	ESF-HD-172-TEMP25-RTD-1	-1.652	39.283	-1.822
ESF-HD-171-TEMP24-RTD-19	-5.650	39.307	5.651	ESF-HD-172-TEMP25-RTD-2	-1.864	39.277	-2.034
ESF-HD-171-TEMP24-RTD-20	-5.857	39.307	5.860	ESF-HD-172-TEMP25-RTD-3	-2.076	39.271	-2.247
ESF-HD-171-TEMP24-RTD-21	-6.064	39.306	6.069	ESF-HD-172-TEMP25-RTD-4	-2.288	39.265	-2.459
ESF-HD-171-TEMP24-RTD-22	-6.272	39.306	6.278	ESF-HD-172-TEMP25-RTD-5	-2.501	39.259	-2.671
ESF-HD-171-TEMP24-RTD-23	-6.479	39.306	6.488	ESF-HD-172-TEMP25-RTD-6	-2.713	39.252	-2.884
ESF-HD-171-TEMP24-RTD-24	-6.686	39.306	6.697	ESF-HD-172-TEMP25-RTD-7	-2.925	39.246	-3.096
ESF-HD-171-TEMP24-RTD-25	-6.893	39.305	6.906	ESF-HD-172-TEMP25-RTD-8	-3.137	39.240	-3.309
ESF-HD-171-TEMP24-RTD-26	-7.100	39.305	7.115	ESF-HD-172-TEMP25-RTD-9	-3.350	39.234	-3.521
ESF-HD-171-TEMP24-RTD-27	-7.307	39.305	7.324	ESF-HD-172-TEMP25-RTD-10	-3.562	39.228	-3.733
ESF-HD-171-TEMP24-RTD-28	-7.514	39.304	7.533	ESF-HD-172-TEMP25-RTD-11	-3.774	39.221	-3.946
ESF-HD-171-TEMP24-RTD-29	-7.722	39.304	7.742	ESF-HD-172-TEMP25-RTD-12	-3.986	39.215	-4.158
ESF-HD-171-TEMP24-RTD-30	-7.929	39.304	7.951	ESF-HD-172-TEMP25-RTD-13	-4.199	39.209	-4.370
ESF-HD-171-TEMP24-RTD-31	-8.136	39.303	8.161	ESF-HD-172-TEMP25-RTD-14	-4.411	39.203	-4.583
ESF-HD-171-TEMP24-RTD-32	-8.343	39.303	8.370	ESF-HD-172-TEMP25-RTD-15	-4.623	39.197	-4.795
ESF-HD-171-TEMP24-RTD-33	-8.550	39.303	8.579	ESF-HD-172-TEMP25-RTD-16	-4.835	39.191	-5.008
ESF-HD-171-TEMP24-RTD-34	-8.757	39.302	8.788	ESF-HD-172-TEMP25-RTD-17	-5.048	39.184	-5.220
ESF-HD-171-TEMP24-RTD-35	-8.964	39.302	8.997	ESF-HD-172-TEMP25-RTD-18	-5.260	39.178	-5.432
ESF-HD-171-TEMP24-RTD-36	-9.171	39.302	9.206	ESF-HD-172-TEMP25-RTD-19	-5.472	39.172	-5.645
ESF-HD-171-TEMP24-RTD-37	-9.379	39.301	9.415	ESF-HD-172-TEMP25-RTD-20	-5.684	39.166	-5.857
ESF-HD-171-TEMP24-RTD-38	-9.586	39.301	9.624	ESF-HD-172-TEMP25-RTD-21	-5.897	39.160	-6.069
ESF-HD-171-TEMP24-RTD-39	-9.793	39.301	9.833	ESF-HD-172-TEMP25-RTD-22	-6.109	39.153	-6.282

Table C-2. Gage Locations for the DST Temperature Gages (continued)

Gage ID	x	y	z	Gage ID	x	y	z
ESF-HD-172-TEMP25-RTD-23	-6.321	39.147	-6.494	ESF-HD-173-TEMP26-RTD-6	0.755	39.307	-3.233
ESF-HD-172-TEMP25-RTD-24	-6.533	39.141	-6.707	ESF-HD-173-TEMP26-RTD-7	0.754	39.304	-3.535
ESF-HD-172-TEMP25-RTD-25	-6.746	39.135	-6.919	ESF-HD-173-TEMP26-RTD-8	0.753	39.301	-3.836
ESF-HD-172-TEMP25-RTD-26	-6.958	39.129	-7.131	ESF-HD-173-TEMP26-RTD-9	0.753	39.298	-4.138
ESF-HD-172-TEMP25-RTD-27	-7.170	39.123	-7.344	ESF-HD-173-TEMP26-RTD-10	0.752	39.294	-4.440
ESF-HD-172-TEMP25-RTD-28	-7.382	39.116	-7.556	ESF-HD-173-TEMP26-RTD-11	0.752	39.291	-4.742
ESF-HD-172-TEMP25-RTD-29	-7.595	39.110	-7.768	ESF-HD-173-TEMP26-RTD-12	0.751	39.288	-5.044
ESF-HD-172-TEMP25-RTD-30	-7.807	39.104	-7.981	ESF-HD-173-TEMP26-RTD-13	0.750	39.285	-5.346
ESF-HD-172-TEMP25-RTD-31	-8.019	39.098	-8.193	ESF-HD-173-TEMP26-RTD-14	0.750	39.282	-5.648
ESF-HD-172-TEMP25-RTD-32	-8.231	39.092	-8.406	ESF-HD-173-TEMP26-RTD-15	0.749	39.279	-5.949
ESF-HD-172-TEMP25-RTD-33	-8.443	39.085	-8.618	ESF-HD-173-TEMP26-RTD-16	0.749	39.276	-6.251
ESF-HD-172-TEMP25-RTD-34	-8.656	39.079	-8.830	ESF-HD-173-TEMP26-RTD-17	0.748	39.273	-6.553
ESF-HD-172-TEMP25-RTD-35	-8.868	39.073	-9.043	ESF-HD-173-TEMP26-RTD-18	0.747	39.270	-6.855
ESF-HD-172-TEMP25-RTD-36	-9.080	39.067	-9.255	ESF-HD-173-TEMP26-RTD-19	0.747	39.266	-7.157
ESF-HD-172-TEMP25-RTD-37	-9.292	39.061	-9.467	ESF-HD-173-TEMP26-RTD-20	0.746	39.263	-7.459
ESF-HD-172-TEMP25-RTD-38	-9.505	39.055	-9.680	ESF-HD-173-TEMP26-RTD-21	0.746	39.260	-7.761
ESF-HD-172-TEMP25-RTD-39	-9.717	39.048	-9.892	ESF-HD-173-TEMP26-RTD-22	0.745	39.257	-8.062
ESF-HD-172-TEMP25-RTD-40	-9.929	39.042	-10.105	ESF-HD-173-TEMP26-RTD-23	0.744	39.254	-8.364
ESF-HD-172-TEMP25-RTD-41	-10.141	39.036	-10.317	ESF-HD-173-TEMP26-RTD-24	0.744	39.251	-8.666
ESF-HD-172-TEMP25-RTD-42	-10.354	39.030	-10.529	ESF-HD-173-TEMP26-RTD-25	0.743	39.248	-8.968
ESF-HD-172-TEMP25-RTD-43	-10.566	39.024	-10.742	ESF-HD-173-TEMP26-RTD-26	0.742	39.245	-9.270
ESF-HD-172-TEMP25-RTD-44	-10.778	39.017	-10.954	ESF-HD-173-TEMP26-RTD-27	0.742	39.241	-9.572
ESF-HD-172-TEMP25-RTD-45	-10.990	39.011	-11.166	ESF-HD-173-TEMP26-RTD-28	0.741	39.238	-9.874
ESF-HD-172-TEMP25-RTD-46	-11.203	39.005	-11.379	ESF-HD-173-TEMP26-RTD-29	0.741	39.235	-10.175
ESF-HD-172-TEMP25-RTD-47	-11.415	38.999	-11.591	ESF-HD-173-TEMP26-RTD-30	0.740	39.232	-10.477
ESF-HD-172-TEMP25-RTD-48	-11.627	38.993	-11.804	ESF-HD-173-TEMP26-RTD-31	0.739	39.229	-10.779
ESF-HD-172-TEMP25-RTD-49	-11.839	38.987	-12.016	ESF-HD-173-TEMP26-RTD-32	0.739	39.226	-11.081
ESF-HD-172-TEMP25-RTD-50	-12.052	38.980	-12.228	ESF-HD-173-TEMP26-RTD-33	0.738	39.223	-11.383
ESF-HD-172-TEMP25-RTD-51	-12.264	38.974	-12.441	ESF-HD-173-TEMP26-RTD-34	0.738	39.220	-11.685
ESF-HD-172-TEMP25-RTD-52	-12.476	38.968	-12.653	ESF-HD-173-TEMP26-RTD-35	0.737	39.217	-11.987
ESF-HD-172-TEMP25-RTD-53	-12.688	38.962	-12.865	ESF-HD-173-TEMP26-RTD-36	0.736	39.213	-12.289
ESF-HD-172-TEMP25-RTD-54	-12.901	38.956	-13.078	ESF-HD-173-TEMP26-RTD-37	0.736	39.210	-12.590
ESF-HD-172-TEMP25-RTD-55	-13.113	38.949	-13.290	ESF-HD-173-TEMP26-RTD-38	0.735	39.207	-12.892
ESF-HD-172-TEMP25-RTD-56	-13.325	38.943	-13.503	ESF-HD-173-TEMP26-RTD-39	0.735	39.204	-13.194
ESF-HD-172-TEMP25-RTD-57	-13.537	38.937	-13.715	ESF-HD-173-TEMP26-RTD-40	0.734	39.201	-13.496
ESF-HD-172-TEMP25-RTD-58	-13.750	38.931	-13.927	ESF-HD-173-TEMP26-RTD-41	0.733	39.198	-13.798
ESF-HD-172-TEMP25-RTD-59	-13.962	38.925	-14.140	ESF-HD-173-TEMP26-RTD-42	0.733	39.195	-14.100
ESF-HD-172-TEMP25-RTD-60	-14.174	38.919	-14.352	ESF-HD-173-TEMP26-RTD-43	0.732	39.192	-14.402
ESF-HD-172-TEMP25-RTD-61	-14.386	38.912	-14.564	ESF-HD-173-TEMP26-RTD-44	0.731	39.189	-14.703
ESF-HD-172-TEMP25-RTD-62	-14.599	38.906	-14.777	ESF-HD-173-TEMP26-RTD-45	0.731	39.185	-15.005
ESF-HD-172-TEMP25-RTD-63	-14.811	38.900	-14.989	ESF-HD-173-TEMP26-RTD-46	0.730	39.182	-15.307
ESF-HD-172-TEMP25-RTD-64	-15.023	38.894	-15.202	ESF-HD-173-TEMP26-RTD-47	0.730	39.179	-15.609
ESF-HD-172-TEMP25-RTD-65	-15.235	38.888	-15.414	ESF-HD-173-TEMP26-RTD-48	0.729	39.176	-15.911
ESF-HD-172-TEMP25-RTD-66	-15.447	38.881	-15.626	ESF-HD-173-TEMP26-RTD-49	0.728	39.173	-16.213
ESF-HD-172-TEMP25-RTD-67	-15.660	38.875	-15.839	ESF-HD-173-TEMP26-RTD-50	0.728	39.170	-16.515
ESF-HD-173-TEMP26-RTD-1	0.758	39.323	-1.723	ESF-HD-173-TEMP26-RTD-51	0.727	39.167	-16.816
ESF-HD-173-TEMP26-RTD-2	0.757	39.319	-2.025	ESF-HD-173-TEMP26-RTD-52	0.727	39.164	-17.118
ESF-HD-173-TEMP26-RTD-3	0.756	39.316	-2.327	ESF-HD-173-TEMP26-RTD-53	0.726	39.160	-17.420
ESF-HD-173-TEMP26-RTD-4	0.756	39.313	-2.629	ESF-HD-173-TEMP26-RTD-54	0.725	39.157	-17.722
ESF-HD-173-TEMP26-RTD-5	0.755	39.310	-2.931	ESF-HD-173-TEMP26-RTD-55	0.725	39.154	-18.024

Table C-2. Gage Locations for the DST Temperature Gages (continued)

Gage ID	x	y	z	Gage ID	x	y	z
ESF-HD-173-TEMP26-RTD-56	0.724	39.151	-18.326	ESF-HD-174-TEMP27-RTD-39	10.057	39.098	-9.504
ESF-HD-173-TEMP26-RTD-57	0.724	39.148	-18.628	ESF-HD-174-TEMP27-RTD-40	10.282	39.093	-9.714
ESF-HD-173-TEMP26-RTD-58	0.723	39.145	-18.929	ESF-HD-174-TEMP27-RTD-41	10.506	39.087	-9.924
ESF-HD-173-TEMP26-RTD-59	0.722	39.142	-19.231	ESF-HD-174-TEMP27-RTD-42	10.731	39.082	-10.134
ESF-HD-173-TEMP26-RTD-60	0.722	39.139	-19.533	ESF-HD-174-TEMP27-RTD-43	10.955	39.076	-10.344
ESF-HD-173-TEMP26-RTD-61	0.721	39.136	-19.835	ESF-HD-174-TEMP27-RTD-44	11.180	39.071	-10.554
ESF-HD-173-TEMP26-RTD-62	0.721	39.132	-20.137	ESF-HD-174-TEMP27-RTD-45	11.404	39.065	-10.763
ESF-HD-173-TEMP26-RTD-63	0.720	39.129	-20.439	ESF-HD-174-TEMP27-RTD-46	11.629	39.060	-10.973
ESF-HD-173-TEMP26-RTD-64	0.719	39.126	-20.741	ESF-HD-174-TEMP27-RTD-47	11.853	39.054	-11.183
ESF-HD-173-TEMP26-RTD-65	0.719	39.123	-21.042	ESF-HD-174-TEMP27-RTD-48	12.078	39.049	-11.393
ESF-HD-173-TEMP26-RTD-66	0.718	39.120	-21.344	ESF-HD-174-TEMP27-RTD-49	12.302	39.043	-11.603
ESF-HD-173-TEMP26-RTD-67	0.717	39.117	-21.646	ESF-HD-174-TEMP27-RTD-50	12.527	39.038	-11.813
ESF-HD-174-TEMP27-RTD-1	1.524	39.308	-1.530	ESF-HD-174-TEMP27-RTD-51	12.752	39.032	-12.022
ESF-HD-174-TEMP27-RTD-2	1.749	39.302	-1.740	ESF-HD-174-TEMP27-RTD-52	12.976	39.027	-12.232
ESF-HD-174-TEMP27-RTD-3	1.973	39.297	-1.950	ESF-HD-174-TEMP27-RTD-53	13.201	39.021	-12.442
ESF-HD-174-TEMP27-RTD-4	2.198	39.291	-2.160	ESF-HD-174-TEMP27-RTD-54	13.425	39.016	-12.652
ESF-HD-174-TEMP27-RTD-5	2.422	39.286	-2.370	ESF-HD-174-TEMP27-RTD-55	13.650	39.010	-12.862
ESF-HD-174-TEMP27-RTD-6	2.647	39.280	-2.580	ESF-HD-174-TEMP27-RTD-56	13.874	39.005	-13.072
ESF-HD-174-TEMP27-RTD-7	2.871	39.275	-2.789	ESF-HD-174-TEMP27-RTD-57	14.099	38.999	-13.282
ESF-HD-174-TEMP27-RTD-8	3.096	39.269	-2.999	ESF-HD-174-TEMP27-RTD-58	14.323	38.994	-13.491
ESF-HD-174-TEMP27-RTD-9	3.320	39.264	-3.209	ESF-HD-174-TEMP27-RTD-59	14.548	38.988	-13.701
ESF-HD-174-TEMP27-RTD-10	3.545	39.258	-3.419	ESF-HD-174-TEMP27-RTD-60	14.773	38.983	-13.911
ESF-HD-174-TEMP27-RTD-11	3.770	39.253	-3.629	ESF-HD-174-TEMP27-RTD-61	14.997	38.977	-14.121
ESF-HD-174-TEMP27-RTD-12	3.994	39.247	-3.839	ESF-HD-174-TEMP27-RTD-62	15.222	38.972	-14.331
ESF-HD-174-TEMP27-RTD-13	4.219	39.242	-4.048	ESF-HD-174-TEMP27-RTD-63	15.446	38.966	-14.541
ESF-HD-174-TEMP27-RTD-14	4.443	39.236	-4.258	ESF-HD-174-TEMP27-RTD-64	15.671	38.961	-14.750
ESF-HD-174-TEMP27-RTD-15	4.668	39.231	-4.468	ESF-HD-174-TEMP27-RTD-65	15.895	38.955	-14.960
ESF-HD-174-TEMP27-RTD-16	4.892	39.225	-4.678	ESF-HD-174-TEMP27-RTD-66	16.120	38.950	-15.170
ESF-HD-174-TEMP27-RTD-17	5.117	39.220	-4.888	ESF-HD-174-TEMP27-RTD-67	16.344	38.944	-15.380
ESF-HD-174-TEMP27-RTD-18	5.341	39.214	-5.098	ESF-HD-175-TEMP28-RTD-1	1.936	39.319	1.900
ESF-HD-174-TEMP27-RTD-19	5.566	39.208	-5.307	ESF-HD-175-TEMP28-RTD-2	2.146	39.317	2.116
ESF-HD-174-TEMP27-RTD-20	5.790	39.203	-5.517	ESF-HD-175-TEMP28-RTD-3	2.355	39.315	2.331
ESF-HD-174-TEMP27-RTD-21	6.015	39.197	-5.727	ESF-HD-175-TEMP28-RTD-4	2.565	39.313	2.547
ESF-HD-174-TEMP27-RTD-22	6.240	39.192	-5.937	ESF-HD-175-TEMP28-RTD-5	2.774	39.311	2.762
ESF-HD-174-TEMP27-RTD-23	6.464	39.186	-6.147	ESF-HD-175-TEMP28-RTD-6	2.984	39.308	2.978
ESF-HD-174-TEMP27-RTD-24	6.689	39.181	-6.357	ESF-HD-175-TEMP28-RTD-7	3.193	39.306	3.193
ESF-HD-174-TEMP27-RTD-25	6.913	39.175	-6.567	ESF-HD-175-TEMP28-RTD-8	3.403	39.304	3.409
ESF-HD-174-TEMP27-RTD-26	7.138	39.170	-6.776	ESF-HD-175-TEMP28-RTD-9	3.612	39.302	3.624
ESF-HD-174-TEMP27-RTD-27	7.362	39.164	-6.986	ESF-HD-175-TEMP28-RTD-10	3.822	39.300	3.840
ESF-HD-174-TEMP27-RTD-28	7.587	39.159	-7.196	ESF-HD-175-TEMP28-RTD-11	4.031	39.298	4.055
ESF-HD-174-TEMP27-RTD-29	7.811	39.153	-7.406	ESF-HD-175-TEMP28-RTD-12	4.241	39.296	4.271
ESF-HD-174-TEMP27-RTD-30	8.036	39.148	-7.616	ESF-HD-175-TEMP28-RTD-13	4.450	39.294	4.486
ESF-HD-174-TEMP27-RTD-31	8.261	39.142	-7.826	ESF-HD-175-TEMP28-RTD-14	4.660	39.291	4.702
ESF-HD-174-TEMP27-RTD-32	8.485	39.137	-8.035	ESF-HD-175-TEMP28-RTD-15	4.870	39.289	4.917
ESF-HD-174-TEMP27-RTD-33	8.710	39.131	-8.245	ESF-HD-175-TEMP28-RTD-16	5.079	39.287	5.133
ESF-HD-174-TEMP27-RTD-34	8.934	39.126	-8.455	ESF-HD-175-TEMP28-RTD-17	5.289	39.285	5.348
ESF-HD-174-TEMP27-RTD-35	9.159	39.120	-8.665	ESF-HD-175-TEMP28-RTD-18	5.498	39.283	5.564
ESF-HD-174-TEMP27-RTD-36	9.383	39.115	-8.875	ESF-HD-175-TEMP28-RTD-19	5.708	39.281	5.779
ESF-HD-174-TEMP27-RTD-37	9.608	39.109	-9.085	ESF-HD-175-TEMP28-RTD-20	5.917	39.279	5.995
ESF-HD-174-TEMP27-RTD-38	9.832	39.104	-9.295	ESF-HD-175-TEMP28-RTD-21	6.127	39.276	6.210

Table C-2. Gage Locations for the DST Temperature Gages (concluded)

Gage ID	x	y	z	Gage ID	x	y	z
ESF-HD-175-TEMP28-RTD-22	6.336	39.274	6.426	ESF-HD-175-TEMP28-RTD-45	11.156	39.225	11.382
ESF-HD-175-TEMP28-RTD-23	6.546	39.272	6.641	ESF-HD-175-TEMP28-RTD-46	11.365	39.223	11.598
ESF-HD-175-TEMP28-RTD-24	6.755	39.270	6.857	ESF-HD-175-TEMP28-RTD-47	11.575	39.221	11.813
ESF-HD-175-TEMP28-RTD-25	6.965	39.268	7.072	ESF-HD-175-TEMP28-RTD-48	11.785	39.219	12.029
ESF-HD-175-TEMP28-RTD-26	7.175	39.266	7.288	ESF-HD-175-TEMP28-RTD-49	11.994	39.217	12.244
ESF-HD-175-TEMP28-RTD-27	7.384	39.264	7.503	ESF-HD-175-TEMP28-RTD-50	12.204	39.215	12.460
ESF-HD-175-TEMP28-RTD-28	7.594	39.262	7.719	ESF-HD-175-TEMP28-RTD-51	12.413	39.213	12.675
ESF-HD-175-TEMP28-RTD-29	7.803	39.259	7.934	ESF-HD-175-TEMP28-RTD-52	12.623	39.210	12.891
ESF-HD-175-TEMP28-RTD-30	8.013	39.257	8.150	ESF-HD-175-TEMP28-RTD-53	12.832	39.208	13.106
ESF-HD-175-TEMP28-RTD-31	8.222	39.255	8.365	ESF-HD-175-TEMP28-RTD-54	13.042	39.206	13.322
ESF-HD-175-TEMP28-RTD-32	8.432	39.253	8.581	ESF-HD-175-TEMP28-RTD-55	13.251	39.204	13.537
ESF-HD-175-TEMP28-RTD-33	8.641	39.251	8.796	ESF-HD-175-TEMP28-RTD-56	13.461	39.202	13.753
ESF-HD-175-TEMP28-RTD-34	8.851	39.249	9.012	ESF-HD-175-TEMP28-RTD-57	13.670	39.200	13.968
ESF-HD-175-TEMP28-RTD-35	9.060	39.247	9.227	ESF-HD-175-TEMP28-RTD-58	13.880	39.198	14.184
ESF-HD-175-TEMP28-RTD-36	9.270	39.245	9.443	ESF-HD-175-TEMP28-RTD-59	14.089	39.195	14.399
ESF-HD-175-TEMP28-RTD-37	9.480	39.242	9.658	ESF-HD-175-TEMP28-RTD-60	14.299	39.193	14.615
ESF-HD-175-TEMP28-RTD-38	9.689	39.240	9.874	ESF-HD-175-TEMP28-RTD-61	14.509	39.191	14.830
ESF-HD-175-TEMP28-RTD-39	9.899	39.238	10.089	ESF-HD-175-TEMP28-RTD-62	14.718	39.189	15.046
ESF-HD-175-TEMP28-RTD-40	10.108	39.236	10.305	ESF-HD-175-TEMP28-RTD-63	14.928	39.187	15.261
ESF-HD-175-TEMP28-RTD-41	10.318	39.234	10.520	ESF-HD-175-TEMP28-RTD-64	15.137	39.185	15.477
ESF-HD-175-TEMP28-RTD-42	10.527	39.232	10.736	ESF-HD-175-TEMP28-RTD-65	15.347	39.183	15.692
ESF-HD-175-TEMP28-RTD-43	10.737	39.230	10.951	ESF-HD-175-TEMP28-RTD-66	15.556	39.181	15.908
ESF-HD-175-TEMP28-RTD-44	10.946	39.227	11.167	ESF-HD-175-TEMP28-RTD-67	15.766	39.178	16.123

Plate Loading Test Thermocouples
(distance from collar; not x,y,z coordinates)

Hot side (Borehole 188)			Ambient side (Borehole 187)			
HD-PL MPBX-1-TC-1		0.0	HD-PL MPBX-2-TC-1		0.0	
HD-PL MPBX-1-TC-2		0.65	HD-PL MPBX-2-TC-2		0.63	
HD-PL MPBX-1-TC-3		0.73	HD-PL MPBX-2-TC-3		0.85	
HD-PL MPBX-1-TC-4		2.70	HD-PL MPBX-2-TC-4		2.20	

Table C-3. Multiple Point Borehole Extensometers

Gage ID	x	y	z	Gage ID	x	y	z
Lateral MPBX Anchor Stations				ESF-HD-157-MPBX10-ANC-1	0.000	21.034	-3.684
ESF-HD-81-MPBX1-ANC-1	6.959	-3.630	3.441	ESF-HD-157-MPBX10-ANC-2	0.003	21.033	-4.674
ESF-HD-81-MPBX1-ANC-2	6.925	3.870	3.418	ESF-HD-157-MPBX10-ANC-3	0.007	21.030	-6.674
ESF-HD-81-MPBX1-ANC-3	6.878	13.870	3.389	ESF-HD-157-MPBX10-ANC-4	0.029	21.015	-16.924
ESF-HD-81-MPBX1-ANC-4	6.869	15.870	3.383	ESF-HD-178-MPBX11-ANC-1	1.813	41.136	3.163
ESF-HD-81-MPBX1-ANC-5	6.814	27.869	3.347	ESF-HD-178-MPBX11-ANC-2	2.310	41.133	4.043
ESF-HD-81-MPBX1-ANC-6	6.786	33.869	3.329	ESF-HD-178-MPBX11-ANC-3	3.412	41.128	5.993
ESF-HD-82-MPBX2-ANC-1	-7.185	0.241	3.373	ESF-HD-178-MPBX11-ANC-4	8.581	41.104	15.144
ESF-HD-82-MPBX2-ANC-2	-7.283	7.240	3.324	ESF-HD-179-MPBX12-ANC-1	-1.832	41.138	3.183
ESF-HD-82-MPBX2-ANC-3	-7.381	14.239	3.275	ESF-HD-179-MPBX12-ANC-2	-2.326	41.133	4.053
ESF-HD-82-MPBX2-ANC-4	-7.479	21.238	3.226	ESF-HD-179-MPBX12-ANC-3	-3.308	41.123	5.784
ESF-HD-82-MPBX2-ANC-5	-7.577	28.237	3.177	ESF-HD-179-MPBX12-ANC-4	-8.758	41.067	15.385
ESF-HD-82-MPBX2-ANC-6	-7.669	34.836	3.131	ESF-HD-180-MPBX13-ANC-1	0.020	41.129	3.897
Heated Drift MPBX Anchor Stations				ESF-HD-180-MPBX13-ANC-2	0.025	41.127	4.637
ESF-HD-147-MPBX3-ANC-1	1.827	13.702	3.169	ESF-HD-180-MPBX13-ANC-3	0.040	41.119	6.657
ESF-HD-147-MPBX3-ANC-2	2.321	13.699	4.039	ESF-HD-180-MPBX13-ANC-4	0.119	41.080	17.377
ESF-HD-147-MPBX3-ANC-3	3.309	13.691	5.778	ESF-HD-181-MPBX14-ANC-1	0.040	41.196	-3.458
ESF-HD-147-MPBX3-ANC-4	8.595	13.654	15.081	ESF-HD-181-MPBX14-ANC-2	0.044	41.197	-4.708
ESF-HD-148-MPBX4-ANC-1	-1.945	13.723	3.337	ESF-HD-181-MPBX14-ANC-3	0.050	41.199	-6.718
ESF-HD-148-MPBX4-ANC-2	-2.425	13.722	4.157	ESF-HD-181-MPBX14-ANC-4	0.081	41.210	-17.458
ESF-HD-148-MPBX4-ANC-3	-3.434	13.718	5.883	Cross Drift MPBX-LVDT Locations			
ESF-HD-148-MPBX4-ANC-4	-8.758	13.700	14.991	ESF-HD-CDEX-MPBX1	0.425	42.357	2.010
ESF-HD-149-MPBX5-ANC-1	-0.033	13.691	3.524	ESF-HD-CDEX-MPBX2	2.047	42.269	-0.016
ESF-HD-149-MPBX5-ANC-2	-0.037	13.685	4.524	Access Observation Drift MPBX Anchor Stations			
ESF-HD-149-MPBX5-ANC-3	-0.047	13.673	6.564	ESF-SDM-42-MPBX1-ANC-1	-4.763	13.694	-0.136
ESF-HD-149-MPBX5-ANC-4	-0.096	13.609	17.434	ESF-SDM-42-MPBX1-ANC-2	-6.726	13.704	0.245
ESF-HD-150-MPBX6-ANC-1	0.024	13.708	-3.739	ESF-SDM-42-MPBX1-ANC-3	-7.708	13.709	0.436
ESF-HD-150-MPBX6-ANC-2	0.032	13.715	-4.739	ESF-SDM-42-MPBX1-ANC-4	-9.671	13.719	0.817
ESF-HD-150-MPBX6-ANC-3	0.049	13.729	-6.739	ESF-SDM-42-MPBX1-ANC-5	-11.635	13.729	1.199
ESF-HD-150-MPBX6-ANC-4	0.138	13.802	-17.238	ESF-SDM-42-MPBX1-ANC-6	-13.598	13.739	1.580
ESF-HD-154-MPBX7-ANC-1	1.842	21.019	3.135	ESF-SDM-43-MPBX2-ANC-1	-4.577	20.757	0.567
ESF-HD-154-MPBX7-ANC-2	2.348	21.019	3.997	ESF-SDM-43-MPBX2-ANC-2	-5.561	20.769	0.748
ESF-HD-154-MPBX7-ANC-3	3.336	21.018	5.678	ESF-SDM-43-MPBX2-ANC-3	-7.528	20.794	1.108
ESF-HD-154-MPBX7-ANC-4	8.804	21.011	14.992	ESF-SDM-43-MPBX2-ANC-4	-9.495	20.818	1.468
ESF-HD-155-MPBX8-ANC-1	-1.867	21.000	3.199	ESF-SDM-43-MPBX2-ANC-5	-11.462	20.843	1.829
ESF-HD-155-MPBX8-ANC-2	-2.372	20.994	4.051	ESF-SDM-43-MPBX2-ANC-6	-13.429	20.867	2.189
ESF-HD-155-MPBX8-ANC-3	-3.381	20.983	5.755	ESF-SDM-44-MPBX3-ANC-1	-5.085	32.186	-0.057
ESF-HD-155-MPBX8-ANC-4	-8.757	20.922	14.832	ESF-SDM-44-MPBX3-ANC-2	-6.063	32.181	0.151
ESF-HD-156-MPBX9-ANC-1	-0.010	20.997	3.604	ESF-SDM-44-MPBX3-ANC-3	-8.019	32.173	0.567
ESF-HD-156-MPBX9-ANC-2	-0.007	20.993	4.604	ESF-SDM-44-MPBX3-ANC-4	-9.976	32.164	0.982
ESF-HD-156-MPBX9-ANC-3	-0.002	20.985	6.604	ESF-SDM-44-MPBX3-ANC-5	-11.932	32.156	1.398
ESF-HD-156-MPBX9-ANC-4	0.028	20.944	17.354	ESF-SDM-44-MPBX3-ANC-6	-13.888	32.147	1.813
Plate Loading Test MPBX Anchors (distance from collar; not x,y,z coordinates)							
Hot side (Borehole 188)				Ambient side (Borehole 187)			
HD-PL MPBX-1-ANC-1		0.86		HD-PL MPBX-2-ANC-1		0.87	
HD-PL MPBX-1-ANC-2		1.54		HD-PL MPBX-2-ANC-2		1.31	
HD-PL MPBX-1-ANC-3		3.21		HD-PL MPBX-2-ANC-3		2.70	

Table C-4. Strain Data Obtained from the DST, Corrected for Thermal Expansion of Strain Gages (Extension Positive)

Gage ID	As-Built Locations (m)			Days after startup													
	x	y	z	0	7	14	21	28	35	42	49	56	63	70	77	84	97
Concrete Surface Strain Gauge Rosettes																	
ESF-HD-RSG-1-AXL	0.407	36.875	2.530	-361.9	-257.5	-214.5	-168.6	-129.5	-111.2	-91.52	-76.3	-55.39	-47.84	-33.85	-22.07	-20.55	-15.3
ESF-HD-RSG-1-CIR	0.407	36.875	2.530	-82.89	45.79	24.952	16.151	-17.61	-35.71	-64.65	-97.96	-119.5	-130.2	-155.6	-174.2	-193.9	-191.7
ESF-HD-RSG-1-DIA	0.407	36.875	2.530	1408.4	-967.8	-1004	-1021	-1037	-1039	-1050	-1068	-1077	-1106	-1113	-1132	-1151	-1158
ESF-HD-RSG-2-AXL	2.345	36.947	1.155	-29.42	116.59	157.69	182.52	208.71	217.24	235.04	248.05	260.46	278.82	276.83	295.01	304.77	304.85
ESF-HD-RSG-2-CIR	2.345	36.947	1.155	1130.5	761.76	1475.5	1198.7	1998.6	1955.1	1841.7	2040.5	2217.3	2128.9	1877	1654.5	1429.9	1527.4
ESF-HD-RSG-2-DIA	2.345	36.947	1.155	-62.71	28.616	63.655	97.604	123.81	156.64	180.52	187.45	202.9	221.27	240.53	243.54	256.34	265.52
ESF-HD-RSG-3-AXL	2.353	37.166	-0.714	-1777	-2122	-2158	-2164	-2162	-2130	-2104	-2093	-2072	-2069	-2038	-2029	-2017	-2009
ESF-HD-RSG-3-CIR	2.353	37.166	-0.714	-75.11	-2262	-2301	-2255	-2214	-2149	-2011	-1782	-1473	-1153	452.4	2237.3	3643.8	5093.3
ESF-HD-RSG-3-DIA	2.353	37.166	-0.714	-52.66	12.809	58.237	97.865	135.35	197.94	242.05	277.48	316.41	336.99	365.55	379.53	397.45	405.54
ESF-HD-RSG-4-AXL	-2.314	36.971	-0.979	-86.86	36.641	76.975	115.46	152.3	190.04	209.03	243.84	270.25	291.67	312.72	331.65	347.17	360.93
ESF-HD-RSG-4-CIR	-2.314	36.971	-0.979	-83.66	79.343	122.71	173.34	222.33	266.14	306.38	329.03	346.33	343.46	364.5	368.25	383.77	391.45
ESF-HD-RSG-4-DIA	-2.314	36.971	-0.979	-48.21	-9.792	6.2342	2.221	26.936	52.536	86.714	97.269	123.67	129.91	138.83	151.67	164.18	181
ESF-HD-RSG-5-AXL	-2.417	36.886	1.048	89.45	74.441	102.38	133.88	148.42	165.54	174.16	175.36	175.29	181.95	182.03	190.5	193.74	196.28
ESF-HD-RSG-6-AXL	0.438	41.578	2.553	-75.82	111.03	155.51	197.35	233.67	264.93	306.13	322.7	344.37	374.2	392.1	408.38	426.15	434.88
ESF-HD-RSG-6-CIR	0.438	41.578	2.553	-76.98	58.219	44.981	16.996	-7.374	-21.64	-47.21	-85.21	-106	-103.5	-115.9	-123.9	-136.5	-136.8
ESF-HD-RSG-7-AXL	2.373	41.700	1.128	-41.59	9.4504	32.43	64.828	95.732	131.38	169.82	190.22	223.91	257.5	270.72	295.96	315.69	321.9
ESF-HD-RSG-7-CIR	2.373	41.700	1.128	-69.16	91.26	132.45	167.88	195.74	228.35	248.56	253.77	277.32	287.65	303.9	310.92	321.55	330.8
ESF-HD-RSG-7-DIA	2.373	41.700	1.128	-29.45	118.81	156.96	189.35	214.16	234.62	260.9	275.22	292.7	306.06	304.1	317.2	333.89	340.1
ESF-HD-RSG-8-AXL	2.303	41.778	-0.858	-7306	-8358	-8376	-8402	-8388	-8358	-8294	-8240	-8152	-8134	-7778	-7623	-7388	-6980
ESF-HD-RSG-8-CIR	2.303	41.778	-0.858	-469.5	77.795	385.53	609.75	827.78	920.6	1066.7	1412.4	3509.1	20344	9E+08	1E+09	9E+08	9E+08
ESF-HD-RSG-8-DIA	2.303	41.778	-0.858	-41.32	68.559	117.96	153.71	186.25	233.49	270.12	302.45	336.99	354.39	390.98	413.99	436.78	440.58
ESF-HD-RSG-9-AXL	-2.333	41.595	-1.041	-94.01	321.56	339.4	348.44	348.88	365.54	416.47	440.34	470.72	492.89	504.84	520.14	524.26	525.44
ESF-HD-RSG-9-DIA	-2.333	41.595	-1.041	-74.73	389.46	419.45	446.69	474.44	512.35	557.2	599.26	614.46	645.76	642.5	663.91	686.22	681.29
ESF-HD-RSG-10-AXL	-2.358	41.544	1.209	-67.21	75.058	105.31	130.46	165.42	184.78	205.07	234.11	247.99	263.69	279.17	297.96	308.39	316.71
ESF-HD-RSG-10-CIR	-2.358	41.544	1.209	-96.87	36.293	87.823	116.01	163.1	206.75	227.05	256.06	291.2	319.06	343.64	368.52	381.97	396.33
ESF-HD-RSG-11-AXL	0.080	44.534	2.755	-53.42	182.14	232.51	278.62	297.95	313.87	324.98	329.73	350.37	358.09	347.91	362.82	376.58	371.58
ESF-HD-RSG-11-CIR	0.080	44.534	2.755	-52.44	85.898	51.235	21.431	-7.812	-40.44	-65.72	-85.23	-110.1	-123.6	-154.9	-158.2	-165.6	-176.7
ESF-HD-RSG-11-DIA	0.080	44.534	2.755	-89.04	341.02	430.9	449.64	450.7	445.33	429.09	394.32	372.46	343.74	336.59	330.26	319.73	317.74
ESF-HD-RSG-12-AXL	2.396	44.566	1.095	-71.34	93.273	140.57	178.18	211.24	240.15	264.6	286.04	309.02	325.69	339.16	342.14	359.06	364.52
ESF-HD-RSG-12-DIA	2.396	44.566	1.095	-5.324	13.437	33.389	40.654	52.479	78.364	90.682	100.02	113.89	124.48	125.84	131.84	127.53	133.03
ESF-HD-RSG-13-AXL	2.326	44.645	-0.950	-100.3	80.354	146.45	178.51	203.7	235.91	270.54	281.42	303.78	315.58	338.35	344.42	361.47	371.04
ESF-HD-RSG-13-CIR	2.326	44.645	-0.950	-64.54	158.66	242.98	320.62	367.07	429.66	479.47	514.67	546.12	570.05	592.82	611.01	628.06	634.6
ESF-HD-RSG-13-DIA	2.326	44.645	-0.950	-101.1	49.231	136.59	199.04	251.57	298.97	339.67	365.76	388.1	421.21	431.77	443.9	467.02	470.54
ESF-HD-RSG-14-AXL	-2.305	44.484	-1.048	54.492	176.32	217.21	250.65	284.01	322.07	356.69	409.15	466.74	498.48	487	516.7	548.77	542.44
ESF-HD-RSG-14-CIR	-2.305	44.484	-1.048	-3579	-31396	-5E+05											
ESF-HD-RSG-14-DIA	-2.305	44.484	-1.048	-66.89	103.58	147.52	174.89	214.33	246.32	293.09	324.28	357.57	392.36	414.29	444	469.99	472.77
ESF-HD-RSG-15-AXL	-2.357	44.484	1.149	8.3235	116.95	145.63	171.9	199.39	207.7	221.02	242.04	264.21	292.54	274.54	291.82	309.34	299.53
ESF-HD-RSG-15-CIR	-2.357	44.484	1.149	-42.95	93.037	152.11	184.45	205.85	232.39	254.81	263.67	273.7	292.93	296.18	292.21	303.66	309.02
ESF-HD-RSG-15-DIA	-2.357	44.484	1.149	1E+06	1E+06	1E+06	1E+06	1E+06	1E+06	1E+06	1E+06	1E+06	1E+06	1E+06	1E+06	1E+06	1E+06
Evaluation Gages																	
ESF-HD-RSG-16-EVL1	2.000	39.700	-1.280	-197.9	44.978	73.161	84.579	77.177	88.784	81.003	81.146	76.576	83.954	60.214	63.347	65.556	64.664
ESF-HD-RSG-16-EVL2	2.000	39.700	-1.280	-158.6	99.499	118.56	133.01	128.64	134.17	144.6	150.81	152.3	153.6	132.89	136.02	147.32	137.33
ESF-HD-RSG-17-EVL1	2.000	39.700	-1.280	-185.6	121.06	182.65	212.27	195.74	195.18	175.25	163.23	152.59	156.93	142.28	175.76	202.24	183.13
ESF-HD-RSG-17-EVL2	2.000	39.700	-1.280	-41.765	84.857	149.41	220.01	277.13	359.04	429.71	516.12	590.72	680.85	759.05	831.4	897.89	912.97
ESF-HD-RSG-18-EVL1	2.000	39.700	-1.280	-167	142.68	195.16	218.7	214.31	204.65	199.89	190.89	201.5	248.34	215.47	251.99	293.64	274.51
ESF-HD-RSG-18-EVL2	2.000	39.700	-1.280	-50.99	-62.62	-61.9	-52.14	-55.86	-53.03	-43.21	-48.1	-46.52	-50.72	-48.64	-40.21	-40.72	-34.8

Table C-4. Strain Data Obtained from the DST, Corrected for Thermal Expansion of Strain Gages (Extension Positive) (concluded)

Gage ID	As-Built Locations (m)			Days after startup															
	x	y	z	91	98	105	112	119	126	133	140	147	154	161	168	175	179		
Concrete Surface Strain Gauge Rosettes																			
ESF-HD-RSG-1-AXL	0.407	36.875	2.530	-2.453	-4.817	11.954	40.833	33.647	44.731	59.386	63.48	63.489	75.408	77.527	97.386	97.354	102.33		
ESF-HD-RSG-1-CIR	0.407	36.875	2.530	-203.1	-208.4	-206.8	-211.3	-212.4	-207.4	-210.9	-203.8	-194.7	-185.8	-180.6	-157.7	-142.6	-134.6		
ESF-HD-RSG-1-DIA	0.407	36.875	2.530	-1163	-1175	-1167	-1178	-1185	-1180	-1174	-1176	-1173	-1176	-1165	-1151	-1136	-1134		
ESF-HD-RSG-2-AXL	2.345	36.947	1.155	324.99	330	347.96	384.95	382.4	393.02	409.97	421.63	420.61	436.01	439.74	467.56	478.96	482.62		
ESF-HD-RSG-2-CIR	2.345	36.947	1.155	3202.6	2140.1	148.34	164.09	-138.7	99.365	-193.1	929.42	342.42	75.677	-311.6	46.545	-302.8	167.76		
ESF-HD-RSG-2-DIA	2.345	36.947	1.155	267.45	278.53	281.32	303.14	309.69	320.31	325.12	333.75	335.77	342.06	354.9	367.55	381.98	391.71		
ESF-HD-RSG-3-AXL	2.353	37.166	-0.714	-203	-1994	-1996	-1968	-1963	-1946	-1936	-1924	-1926	-1916	-1913	-1896	-1884	-1885		
ESF-HD-RSG-3-CIR	2.353	37.166	-0.714	4051.7	52832	3E+08	34650	40389											
ESF-HD-RSG-3-DIA	2.353	37.166	-0.714	417.14	436	445.71	468.19	475.68	495.46	508.99	521.16	525.33	532.04	541.25	552.09	570.06	574.65		
ESF-HD-RSG-4-AXL	-2.314	36.971	-0.979	368.63	373.65	390.48	417.67	428.17	444.54	450.38	465.41	461.36	467.01	468.19	497.04	490.77	494.67		
ESF-HD-RSG-4-CIR	-2.314	36.971	-0.979	399.16	404.17	430.11	457.3	464.76	490.24	496.09	498.97	491.87	491.45	477.45	485.05	475.76	476.61		
ESF-HD-RSG-4-DIA	-2.314	36.971	-0.979	185.66	202.84	234.83	252.92	272.53	279.8	303.84	315.83	333.06	329.6	336.89	347.48	353.36	351.18		
ESF-HD-RSG-5-AXL	-2.417	36.886	1.048	208.23	204.19	207.64	221.39	218.18	222.76	224.32	221.83	226.98	235.35	244.16	267.98	271.57	269.28		
ESF-HD-RSG-6-AXL	0.438	41.578	2.553	445.26	446.93	470.84	493.77	498.26	517.59	524.23	541.67	543.87	544.3	549.38	565.52	576.9	572.89		
ESF-HD-RSG-6-CIR	0.438	41.578	2.553	-138.5	-121.6	-97.76	-83.93	-82.45	-84.36	-77.72	-66.34	-67.13	-66.67	-64.55	-54.55	-37.11	-31.99		
ESF-HD-RSG-7-AXL	2.373	41.700	1.128	334.72	357.23	380.03	412	409.32	421.37	423.17	479	485.55	486.69	490.17	492.18	503.55	501.49		
ESF-HD-RSG-7-CIR	2.373	41.700	1.128	340.58	338.81	358.57	378.39	375.72	372.6	365.28	363.44	363.93	368.12	374.64	382.7	384.97	388.99		
ESF-HD-RSG-7-DIA	2.373	41.700	1.128	349.88	348.11	358.76	393.76	394.12	375.83	389.76	381.85	394.47	383.48	399.1	416.28	424.62	410.42		
ESF-HD-RSG-8-AXL	2.303	41.778	-0.858	-7223	-5805	-4617	-5994	-5338	-1877	-2526	-2562	-5260	-5305	-6144	-6581	-6629	-6566		
ESF-HD-RSG-8-CIR	2.303	41.778	-0.858	5E+08	9E+08	1E+09	9E+08	9E+08	1E+09	1E+09	1E+09	1E+09	1E+09	37387	40713	3080.4	954.62	325.46	280.66
ESF-HD-RSG-8-DIA	2.303	41.778	-0.858	473.52	474.07	497.82	537.12	572.49	579.71	591.65	589.21	578.24	581.03	587.26	590.01	601.58	602.29		
ESF-HD-RSG-9-AXL	-2.333	41.595	-1.041	546.04	550.56	576.9	600.7	611.26	600.03	627.07	643.42	632.28	643.37	654.45	673.16	662.2	674.29		
ESF-HD-RSG-9-DIA	-2.333	41.595	-1.041	704.94	697.3	711.51	762.63	782.3	774.1	792.05	802.32	779	793.12	779.88	798.64	796.78	796.73		
ESF-HD-RSG-10-AXL	-2.358	41.544	1.209	326.91	320.78	343.11	357.91	357.04	349.32	356.79	368.26	376.55	381.85	385.14	406.35	405.51	409.82		
ESF-HD-RSG-10-CIR	-2.358	41.544	1.209	412.62	427.72	444	486.12	509.53	535.21	542.69	551.11	541.16	549.49	546.68	558.82	564.04	571.39		
ESF-HD-RSG-11-AXL	0.080	44.534	2.755	392.51	388.06	399.63	423.92	414.75	403.2	436.57	434.31	450.57	465.42	485.15	498.12	509.95	491.18		
ESF-HD-RSG-11-CIR	0.080	44.534	2.755	-177	-196.6	-197.1	-194	-203.2	-214.7	-199.5	-204.8	-200.7	-198	-187.3	-165.2	-165.5	-157		
ESF-HD-RSG-11-DIA	0.080	44.534	2.755	335.65	316.01	318.49	345.82	336.66	325.11	352.42	359.26	369.43	384.28	391.84	413.96	419.72	425.23		
ESF-HD-RSG-12-AXL	2.396	44.566	1.095	379.58	372.44	373.28	382.89	384.64	389.29	401.6	402.69	405.35	417.25	437.51	458.22	468.91	478.47		
ESF-HD-RSG-12-DIA	2.396	44.566	1.095	151.11	150.07	166.07	184.8	195.66	188.18	209.57	219.77	231.56	231.33	248.59	269.25	289.04	292.54		
ESF-HD-RSG-13-AXL	2.326	44.645	-0.950	375.88	389.63	402.01	416	419.7	429.16	439.99	438.1	441.55	443.57	449.18	469.87	471.47	485.3		
ESF-HD-RSG-13-CIR	2.326	44.645	-0.950	657.66	665.33	680.73	706.87	701.45	704.83	706.54	704.63	686.83	682.78	676.24	693.87	692.44	694.12		
ESF-HD-RSG-13-DIA	2.326	44.645	-0.950	493.59	492.17	507.57	530.67	540.43	543.82	530.35	516.3	501.56	488.4	487.96	490.4	482.9	493.69		
ESF-HD-RSG-14-AXL	-2.305	44.484	-1.048	607.66	582.41	604.4	686.36	692.54	683.62	718.59	745.2	742.43	757.24	769.43	795.87	782.06	780.77		
ESF-HD-RSG-14-CIR	-2.305	44.484	-1.048	-5E+05	-5E+05	-5E+05	-5E+05	-5E+05	-5E+05	-5E+05	-5E+05	-5E+05	-5E+05	-5E+05	-5E+05	-5E+05	-5E+05		
ESF-HD-RSG-14-DIA	-2.305	44.484	-1.048	486.35	506.67	528.66	565.05	574.27	589.65	600.33	614.78	615.95	614.68	617.76	610.81	621.29	626.08		
ESF-HD-RSG-15-AXL	-2.357	44.484	1.149	336.08	318.76	341.38	393.23	388.24	370.03	404.47	413.85	429.52	431.48	446.53	474.14	468.69	466.19		
ESF-HD-RSG-15-CIR	-2.357	44.484	1.149	312.17	316.09	323.55	332.9	327.92	321.85	322.91	317.12	326.7	322.6	337.64	347.05	353.74	354.28		
ESF-HD-RSG-15-DIA	-2.357	44.484	1.149	1E+06	1E+06	1E+06	1E+06	1E+06	1E+06	1E+06	1E+06	1E+06	1E+06	1E+06	1E+06	1E+06	1E+06		
Evaluation Gages																			
ESF-HD-RSG-16-EVL1	2.000	39.700	-1.280	105.72	83.902	102.86	174.72	184.86	177.97	211.89	238.96	246.66	273.53	298.45	336.34	348.3	352.7		
ESF-HD-RSG-16-EVL2	2.000	39.700	-1.280	169.28	153.53	172.48	238.28	230.22	223.32	257.25	272.18	279.88	303.72	316.51	342.26	348.14	343.45		
ESF-HD-RSG-17-EVL1	2.000	39.700	-1.280	224.19	202.36	221.31	290.15	288.16	287.32	312.16	327.09	331.74	349.51	365.32	388.05	396.98	392.28		
ESF-HD-RSG-17-EVL2	2.000	39.700	-1.280	976.63	1022.1	1085.8	1149.5	1198.2	1246.9	1286.4	1335.2	1368.7	1408.4	1442	1484.7	1524.4	1536.7		
ESF-HD-RSG-18-EVL1	2.000	39.700	-1.280	352.01	321.05	361.26	457.43	476.68	463.7	521.93	555.08	562.75	586.59	623.63	679.78	676.56	684		
ESF-HD-RSG-18-EVL2	2.000	39.700	-1.280	-38.12	-38.4	-29.53	-20.62	-23.75	-17.73	-14.73	-11.71	-11.71	-8.638	-8.587	0.6233	3.7312	3.7999		

Page intentionally blank

Appendix D

Time History Plots of Failed and Suspect Gages from the DST

This appendix includes time history plots of failed and suspect temperature gages from the DST. A list of all failed and suspect thermal-mechanical gages identified to date and their mode of failure is included in Section 5.

Page intentionally blank

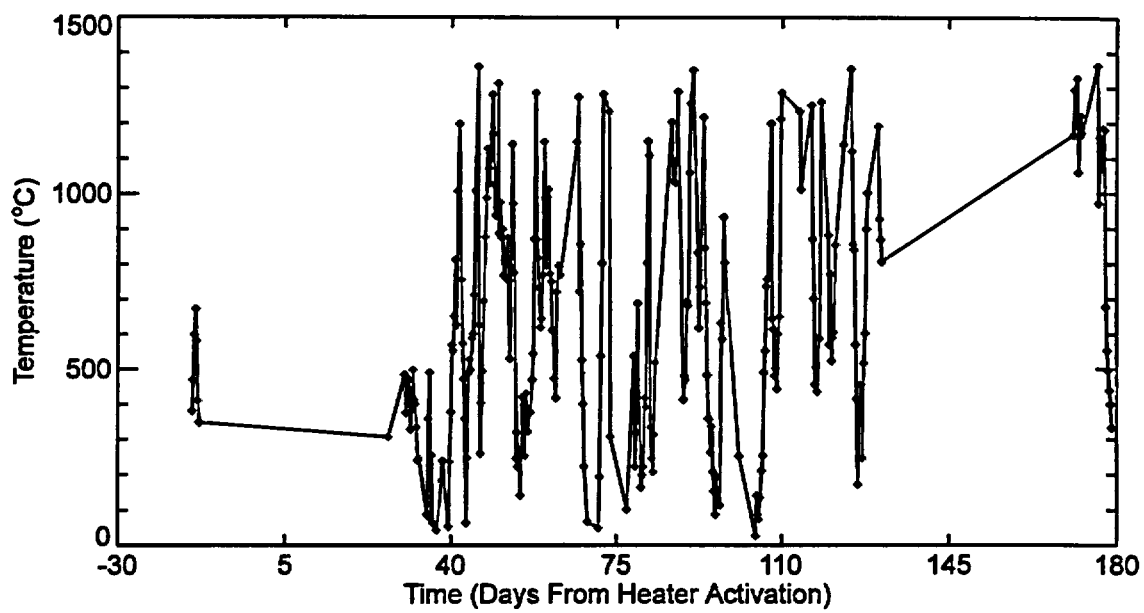


Figure D-1. Data from failed gage ESF-HD-83-WH1-TC-2.

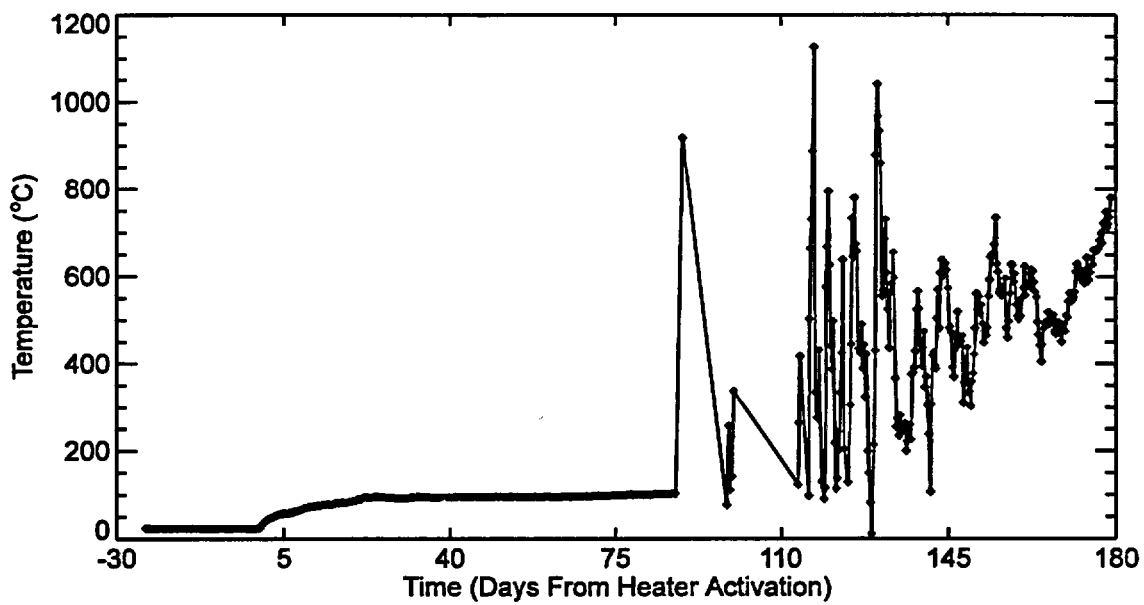


Figure D-2. Data from failed gage ESF-HD-84-WH2-TC-3.

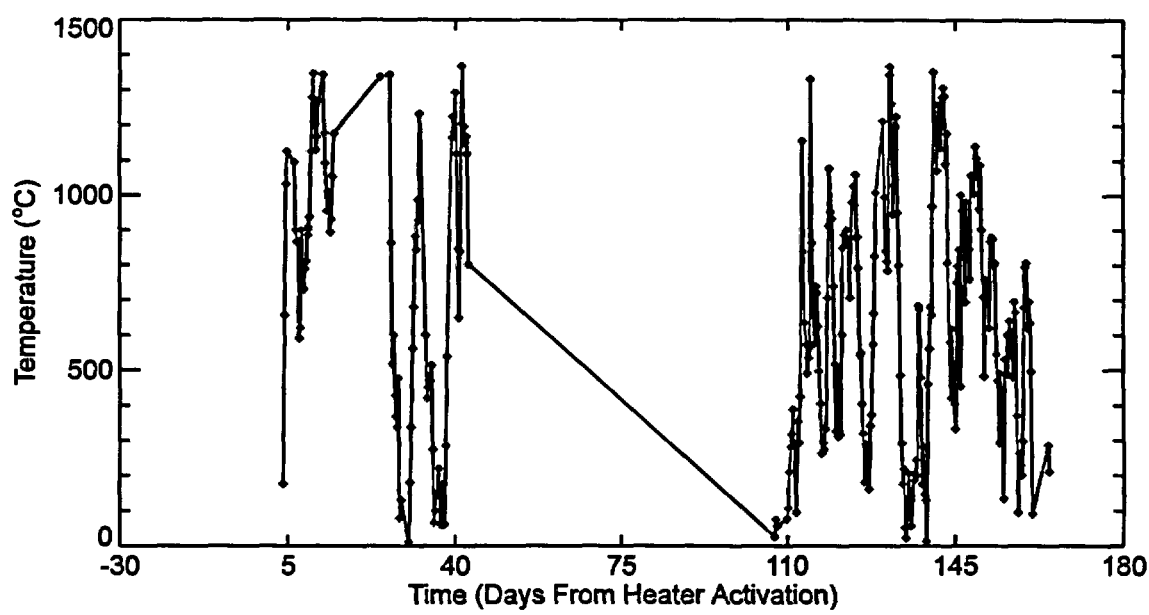


Figure D-3. Data from failed gage ESF-HD-86-WH4-TC-4.

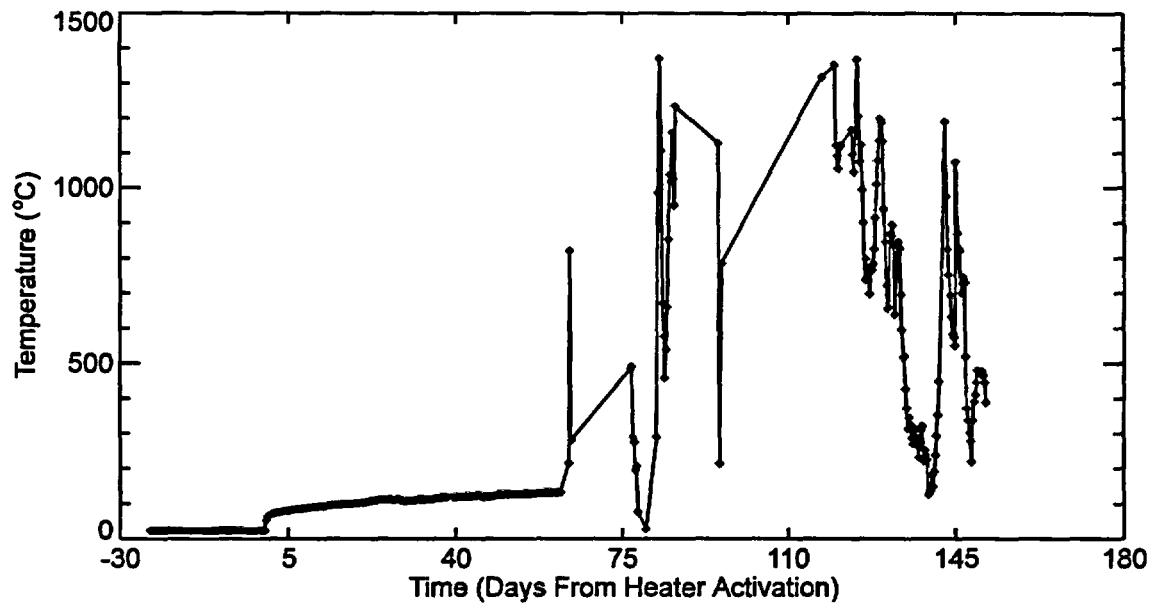


Figure D-4. Data from failed gage ESF-HD-87-WH5-TC-5.

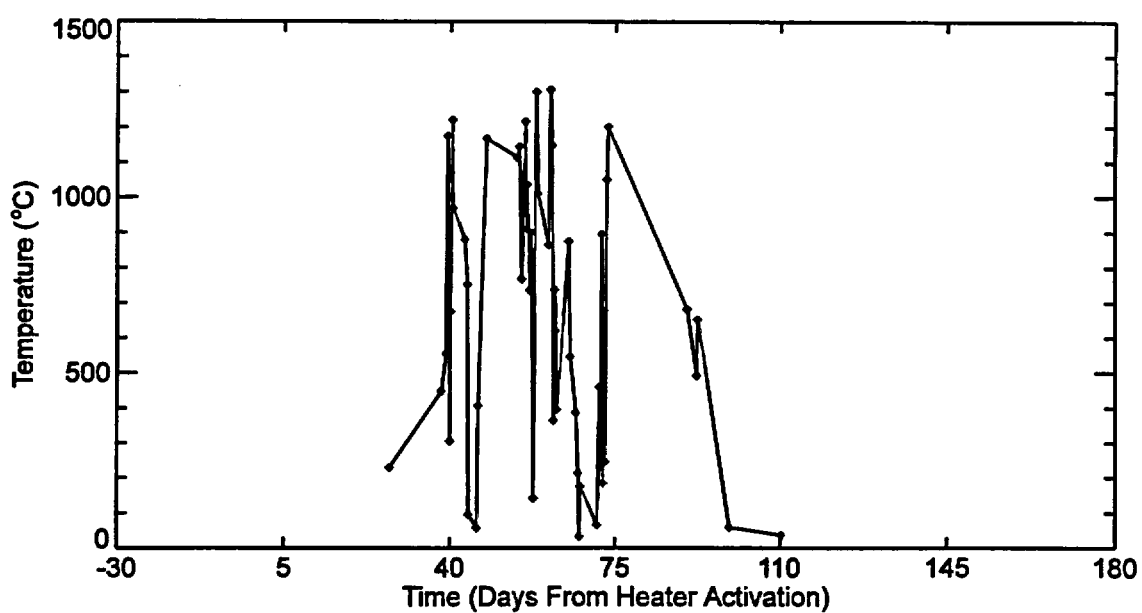


Figure D-5. Data from failed gage ESF-HD-97-WH15-TC-3.

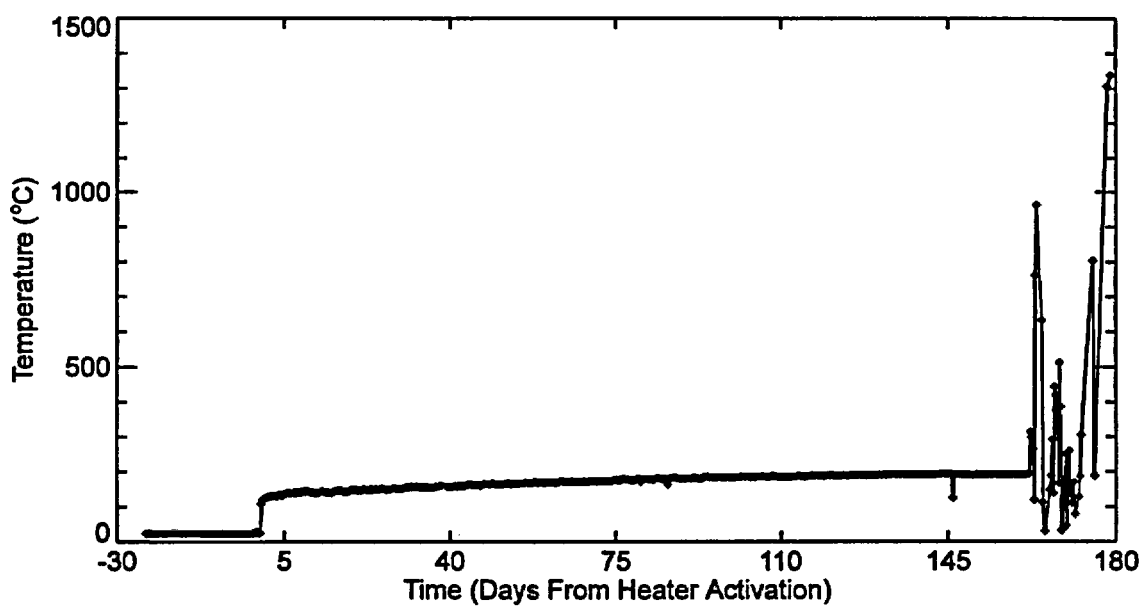


Figure D-6. Data from failed gage ESF-HD-103-WH21-TC-5.

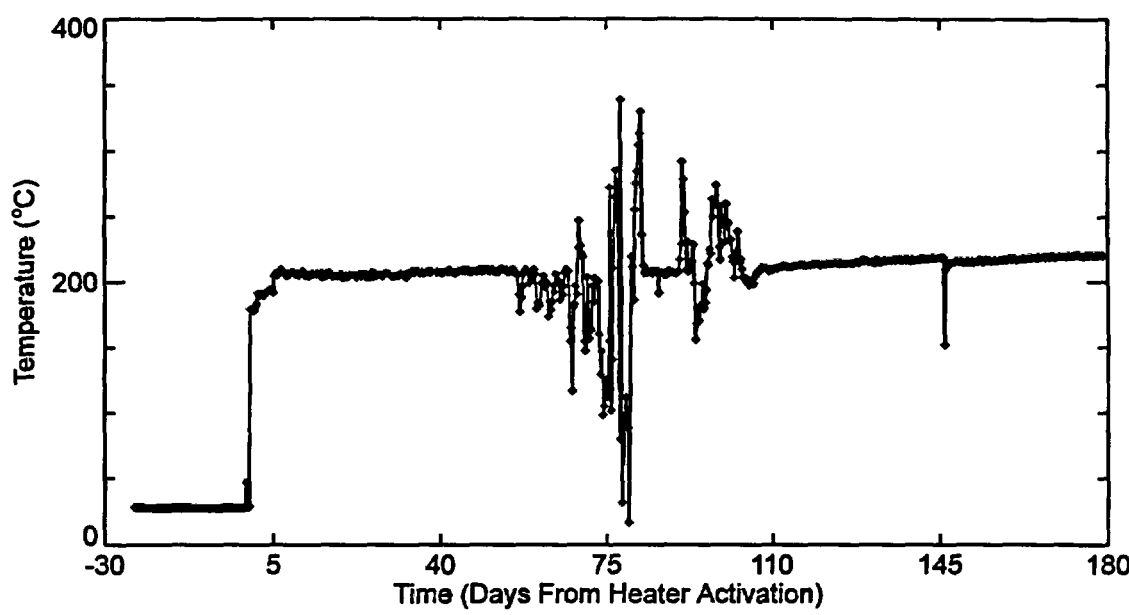


Figure D-7. Data from failed gage ESF-HD-104-WH22-TC-1.

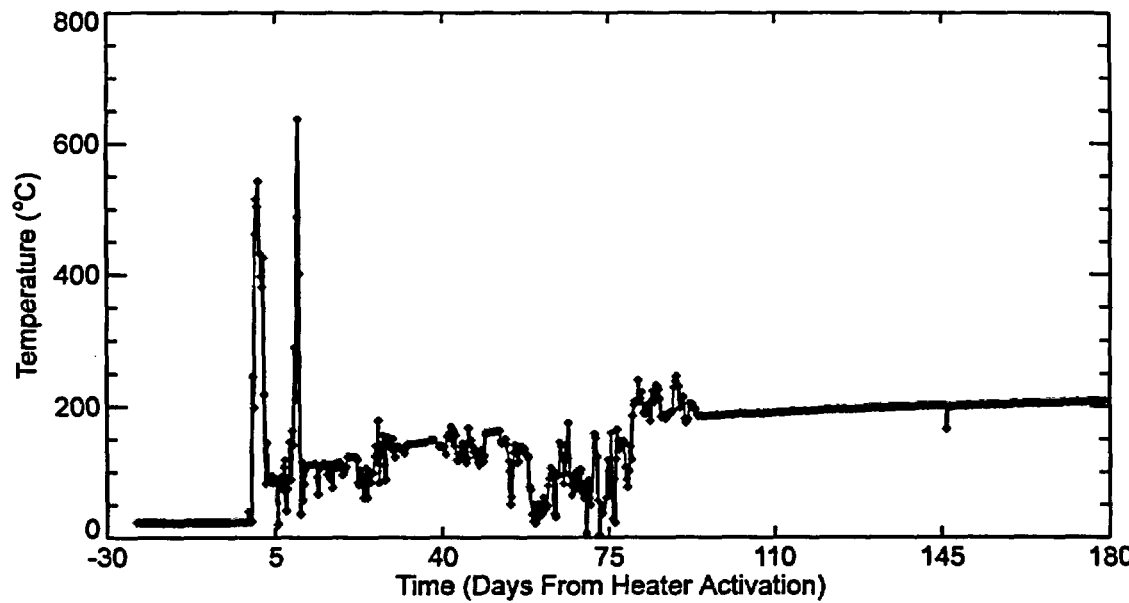


Figure D-8. Data from failed gage ESF-HD-104-WH22-TC-4.

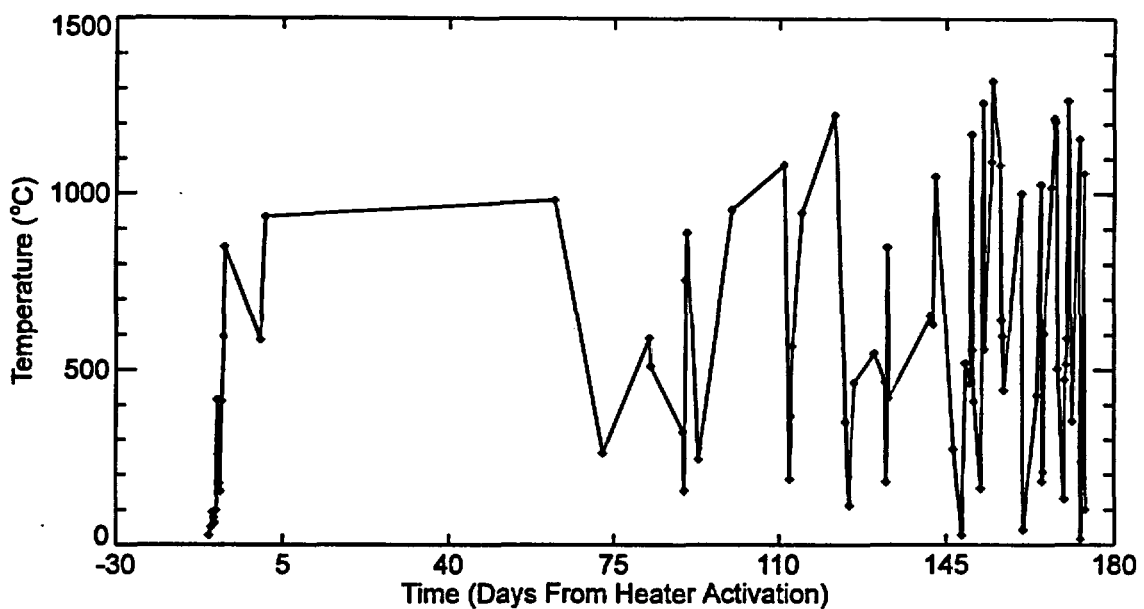


Figure D-9. Data from failed gage ESF-HD-108-WH26-TC-1.

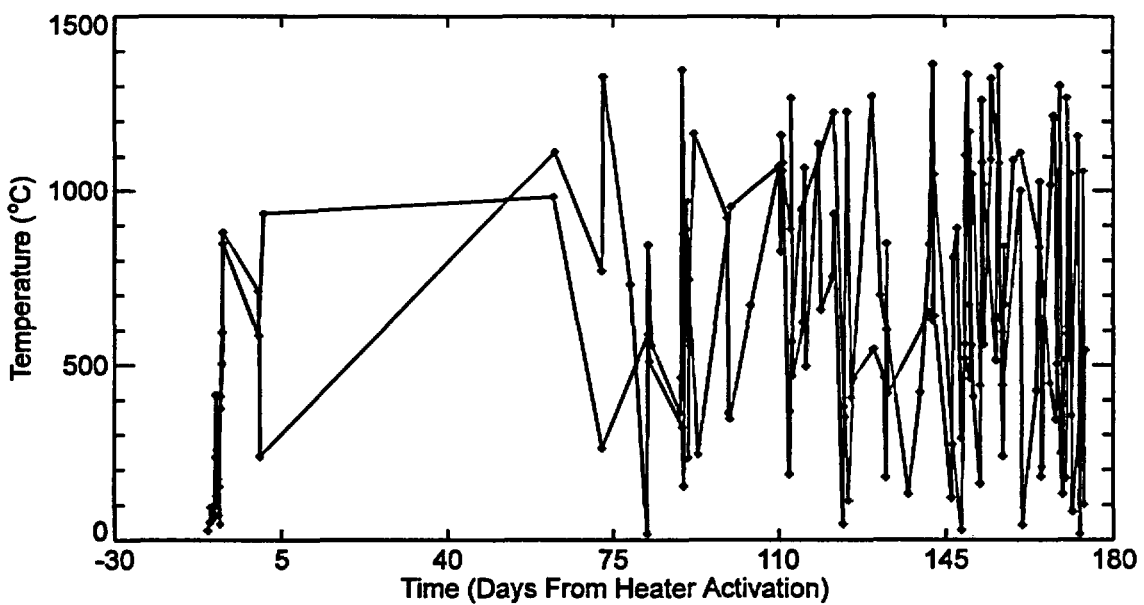


Figure D-10. Data from failed gage ESF-HD-108-WH26-TC-2.

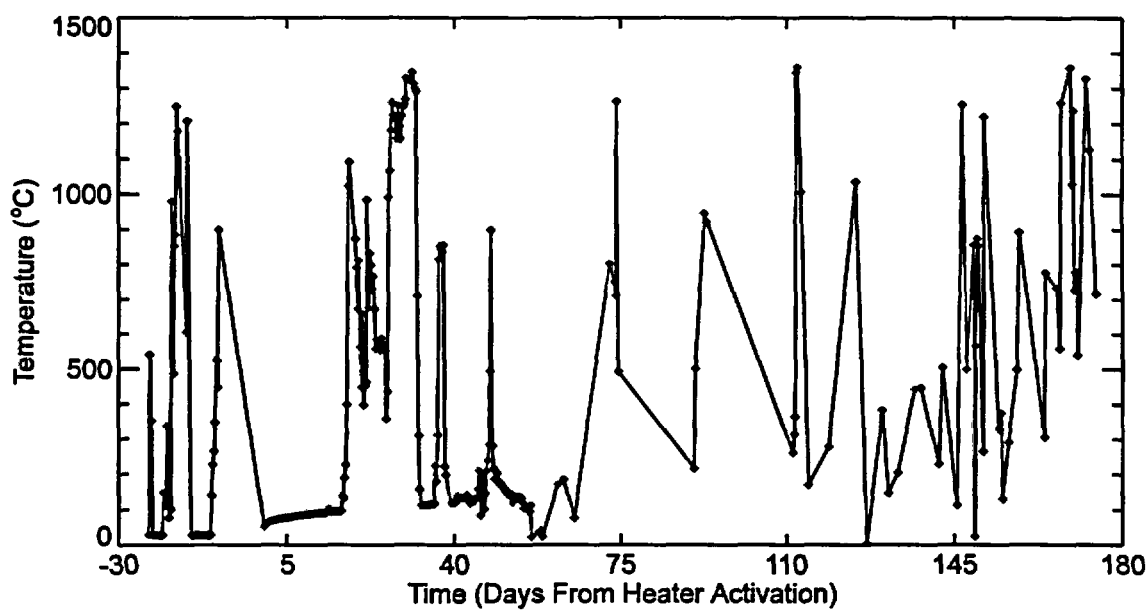


Figure D-11. Data from failed gage ESF-HD-111-WH29-TC-1.

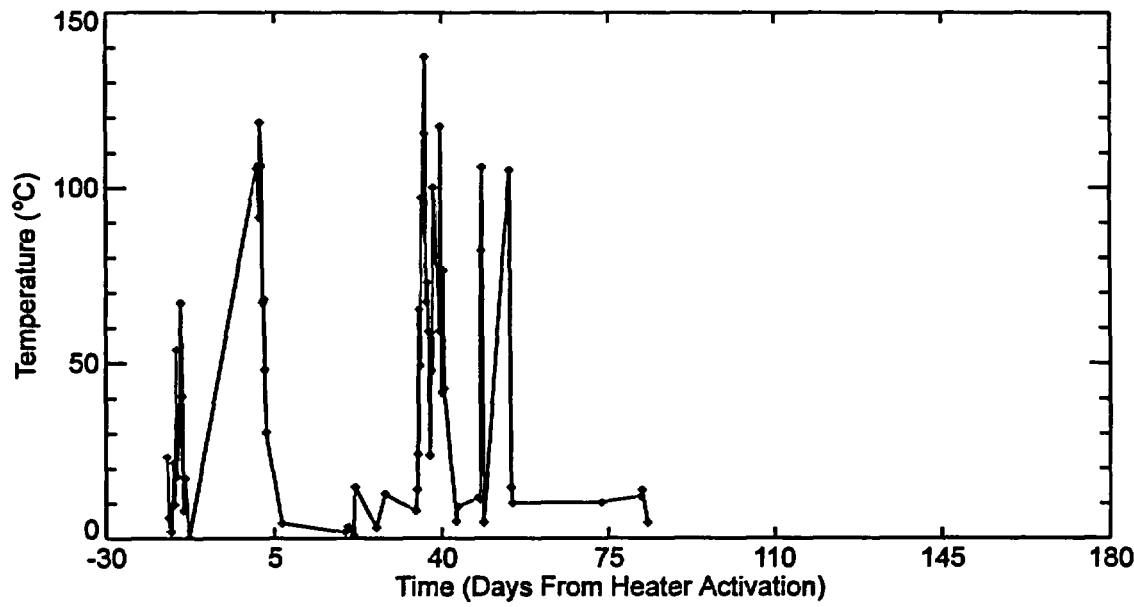


Figure D-12. Data from failed gage ESF-HD-130-WH48-TC-1.

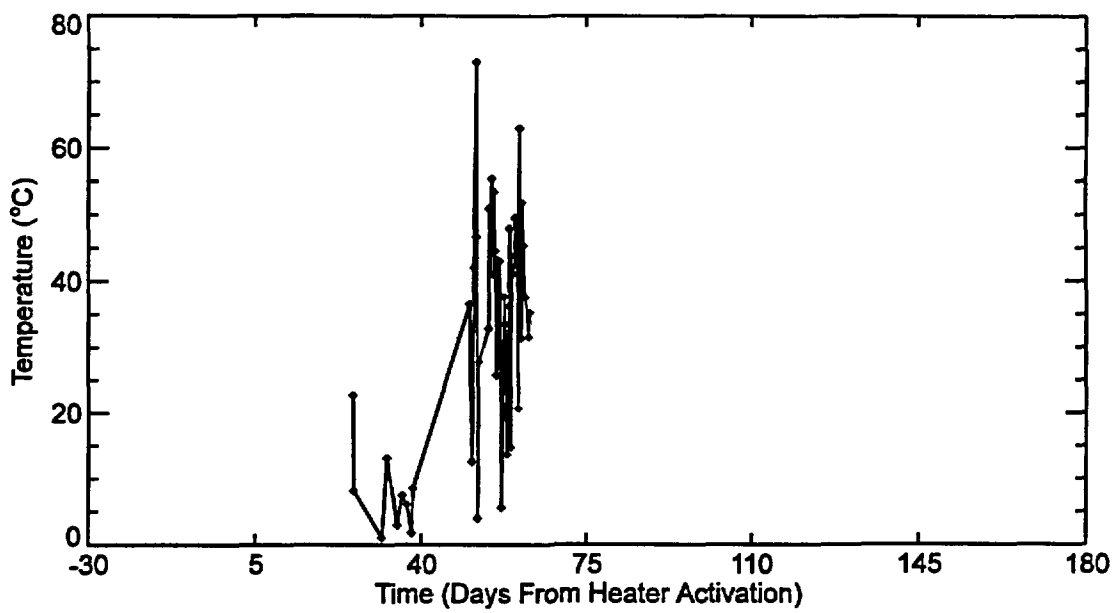


Figure D-13. Data from failed gage ESF-HD-132-WH50-TC-4.

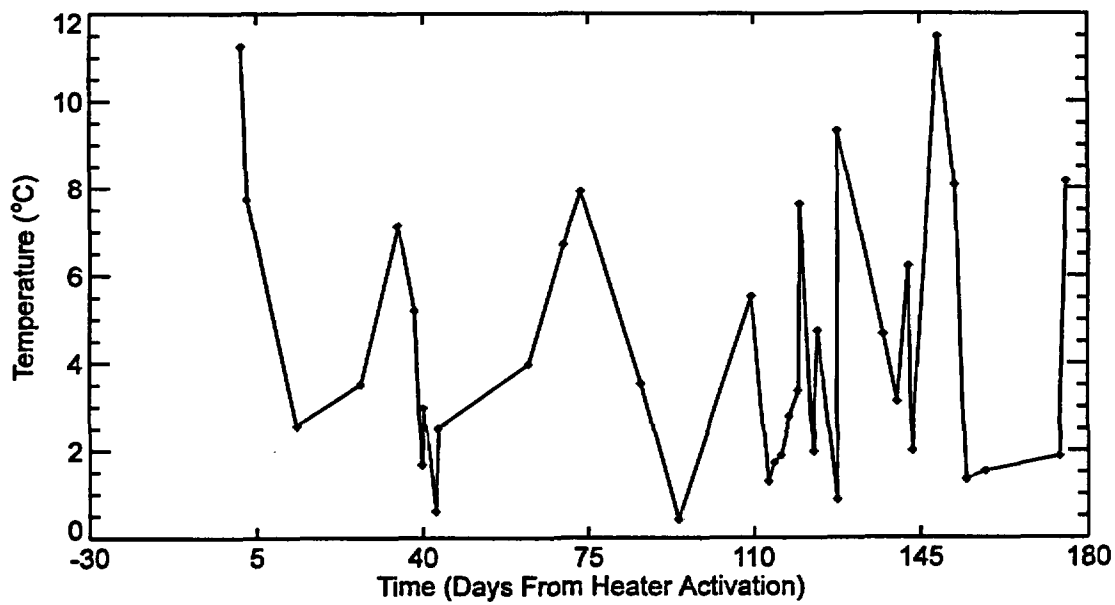


Figure D-14. Data from failed gage ESF-HD-CAN1-TC-2.

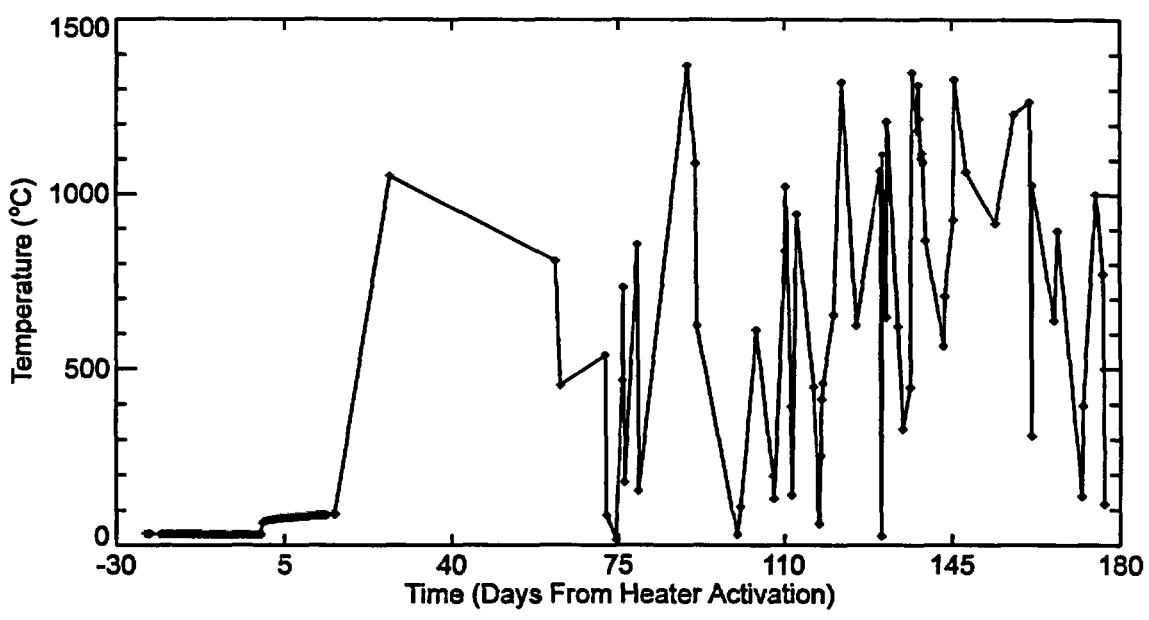


Figure D-15. Data from failed gage ESF-HD-CAN3-TC-5.

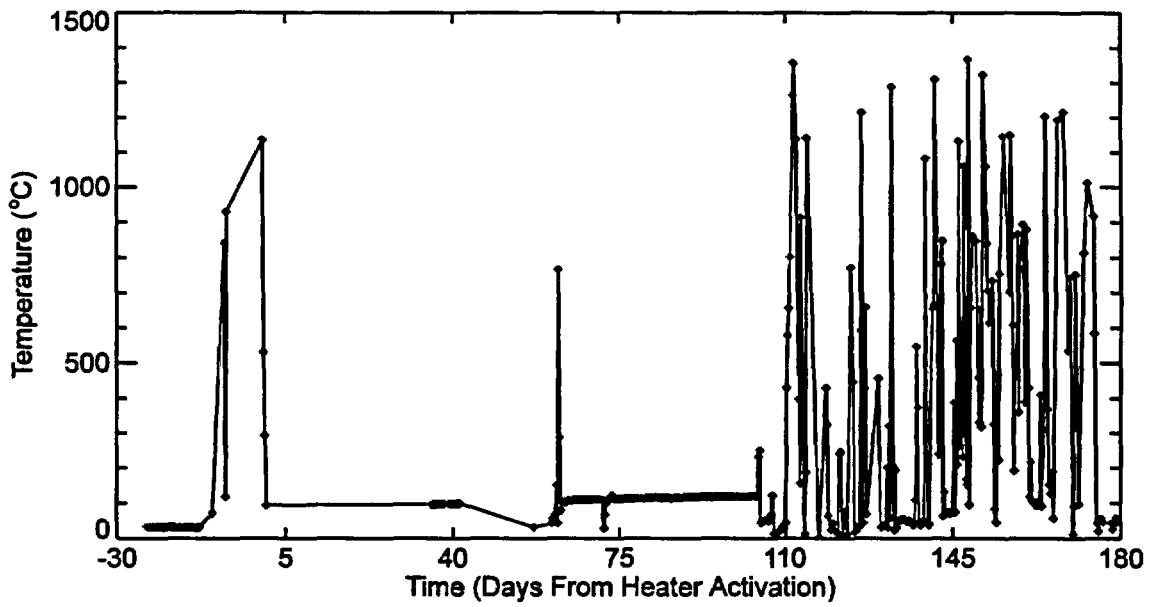


Figure D-16. Data from failed gage ESF-HD-CAN6-TC-8.

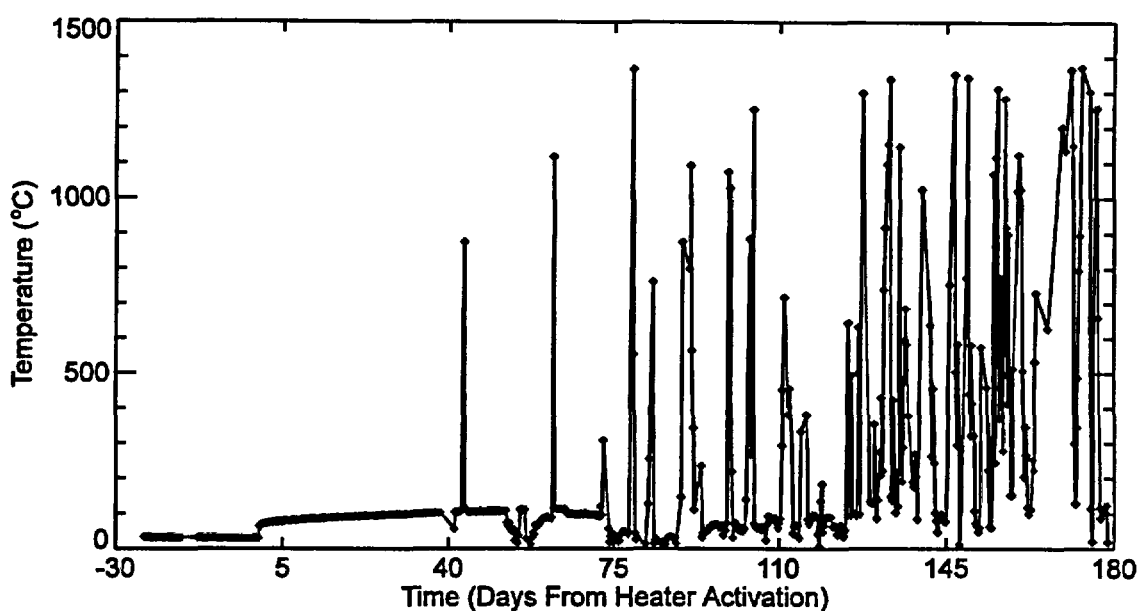


Figure D-17. Data from failed gage ESF-HD-CAN7-TC-1.

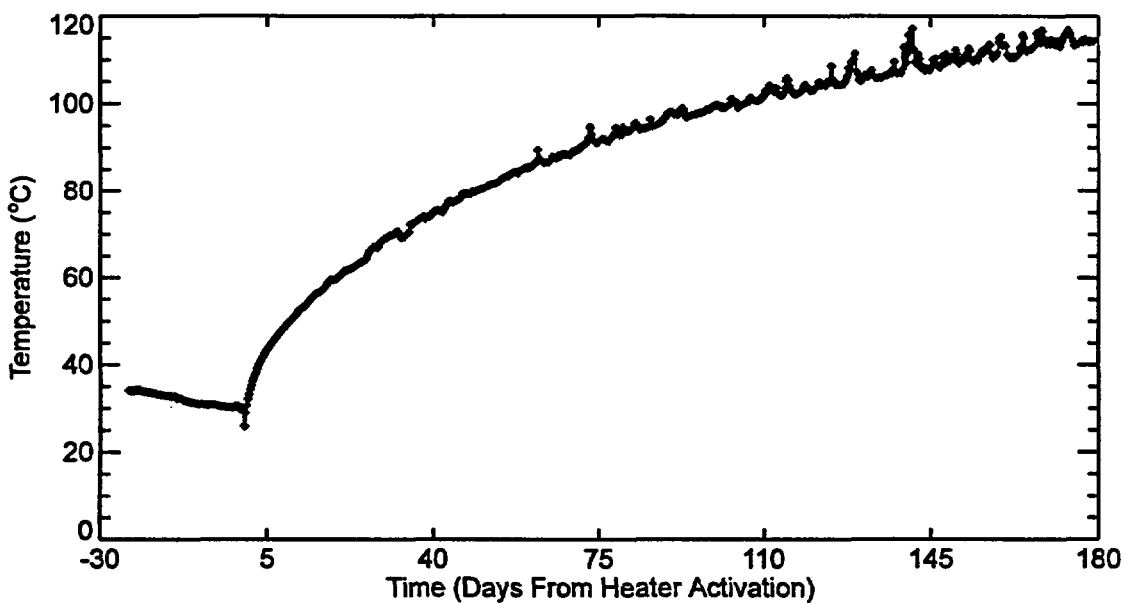


Figure D-18. Data from failed gage ESF-HD-CAN7-TC-2.

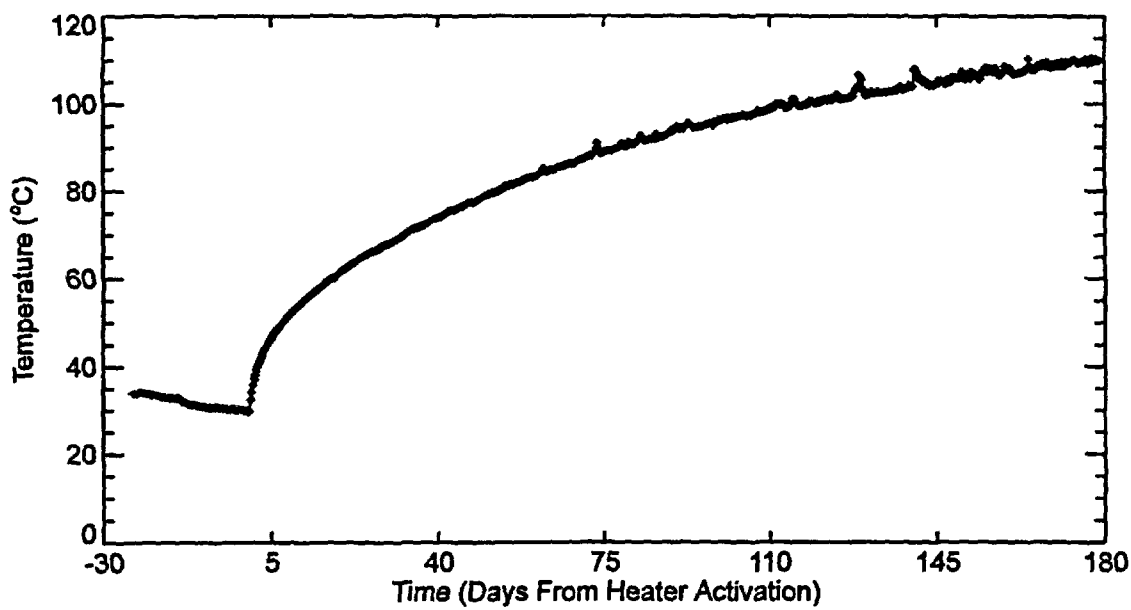


Figure D-19. Data from failed gage ESF-HD-CAN9-TC-7.

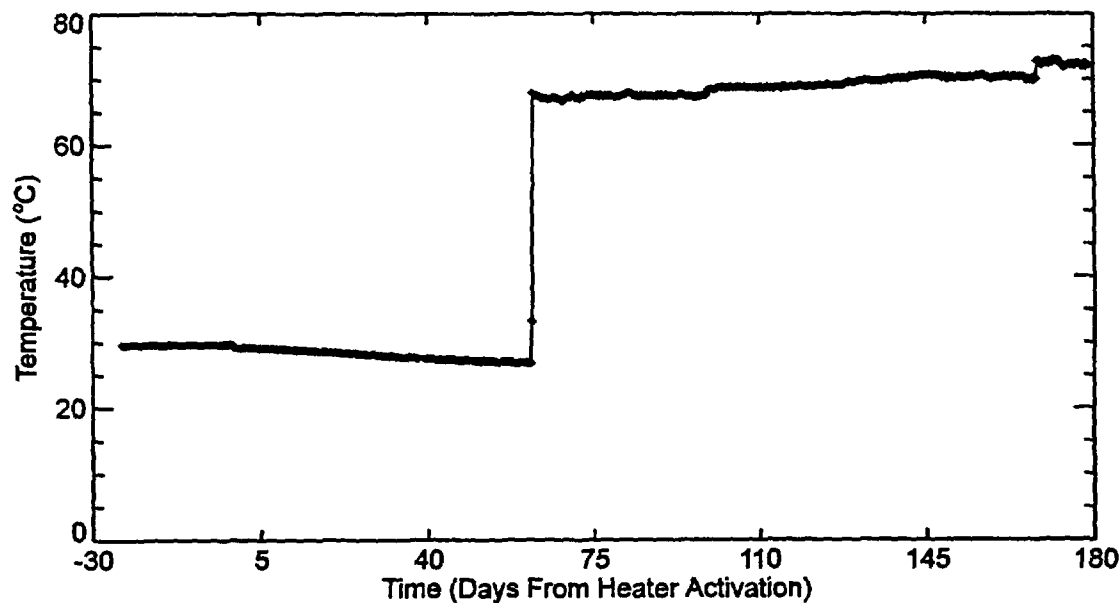


Figure D-20. Data from failed gage ESF-HD-79-TEMP1-RTD-10.

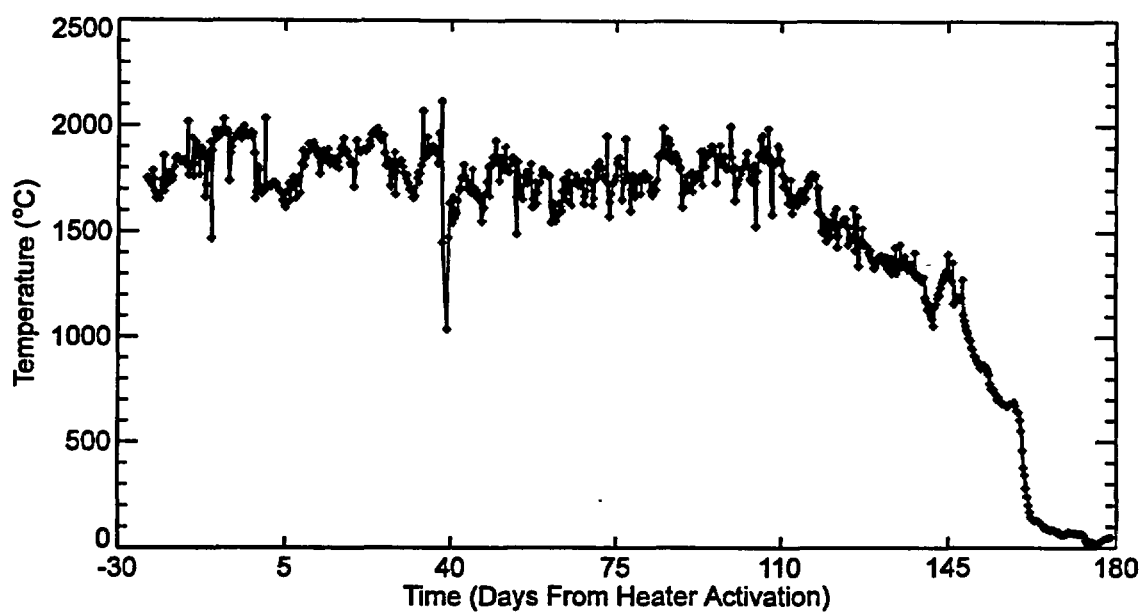


Figure D-21. Data from failed gage ESF-HD-80-TEMP2-RTD-46.

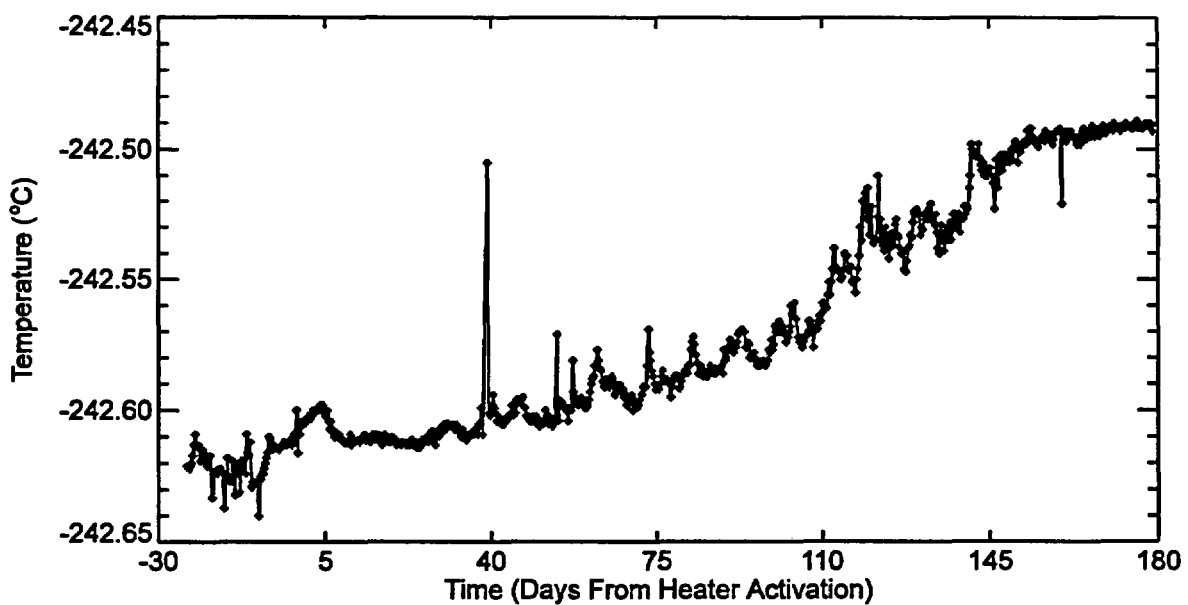


Figure D-22. Data from failed gage ESF-HD-133-TEMP3-RTD-64.

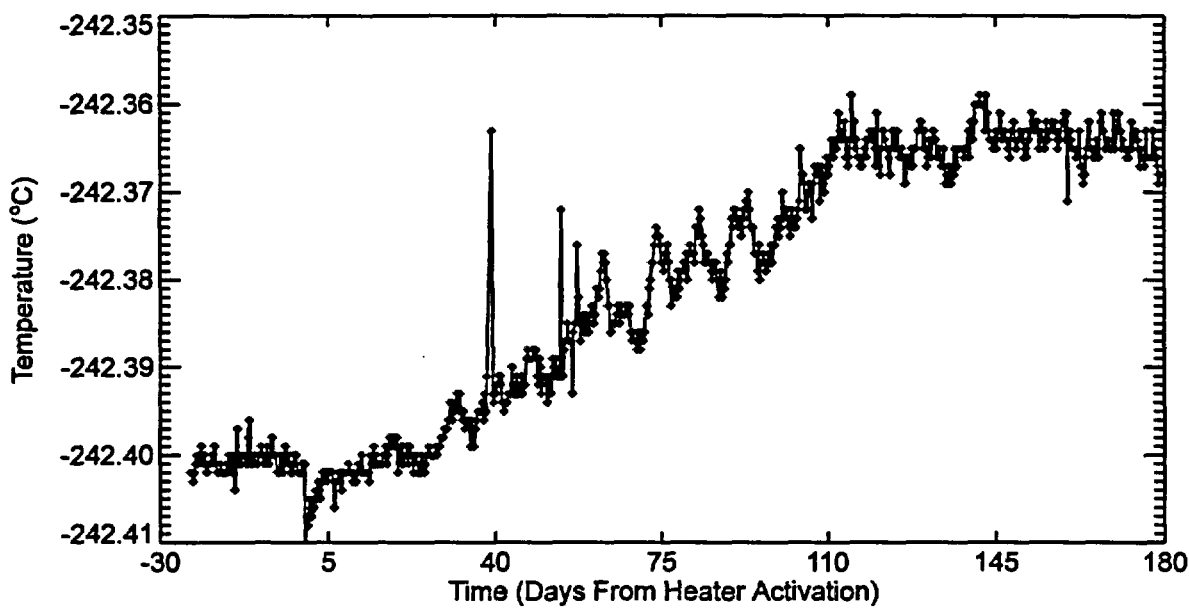


Figure D-23. Data from failed gage ESF-HD-138-TEMP6-RTD-32.

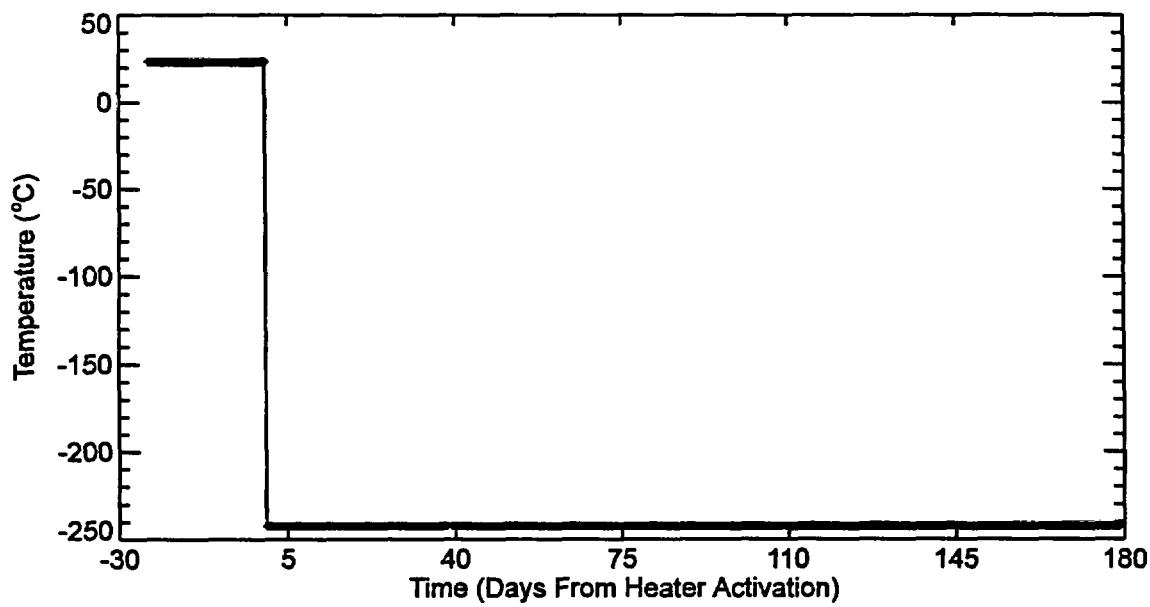


Figure D-24. Data from failed gage ESF-HD-138-TEMP6-RTD-40.

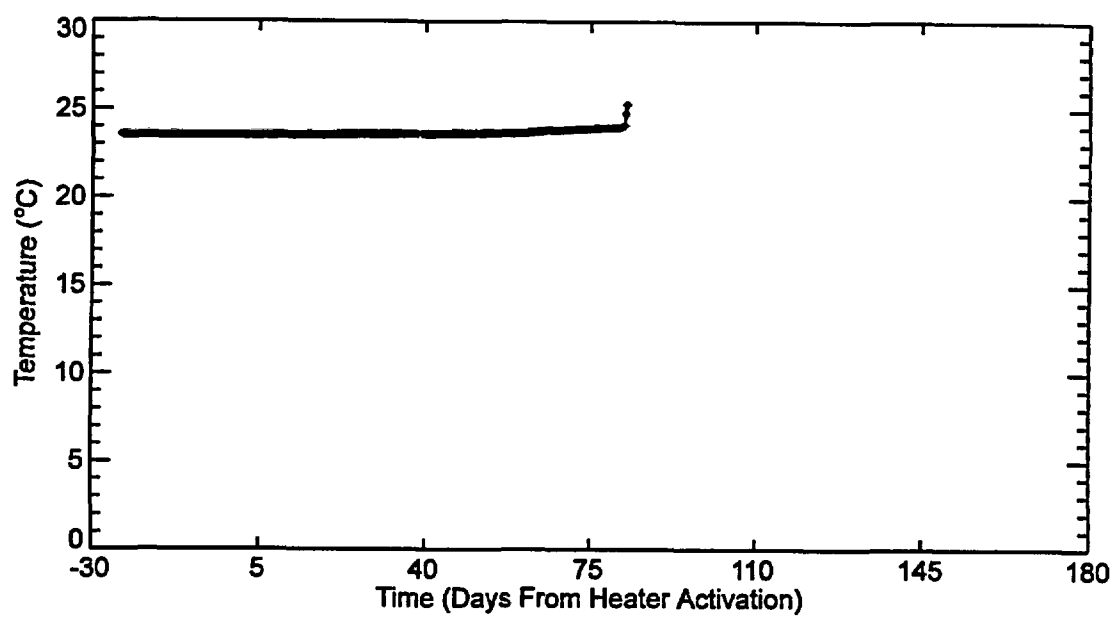


Figure D-25. Data from failed gage ESF-HD-138-TEMP6-RTD-47.

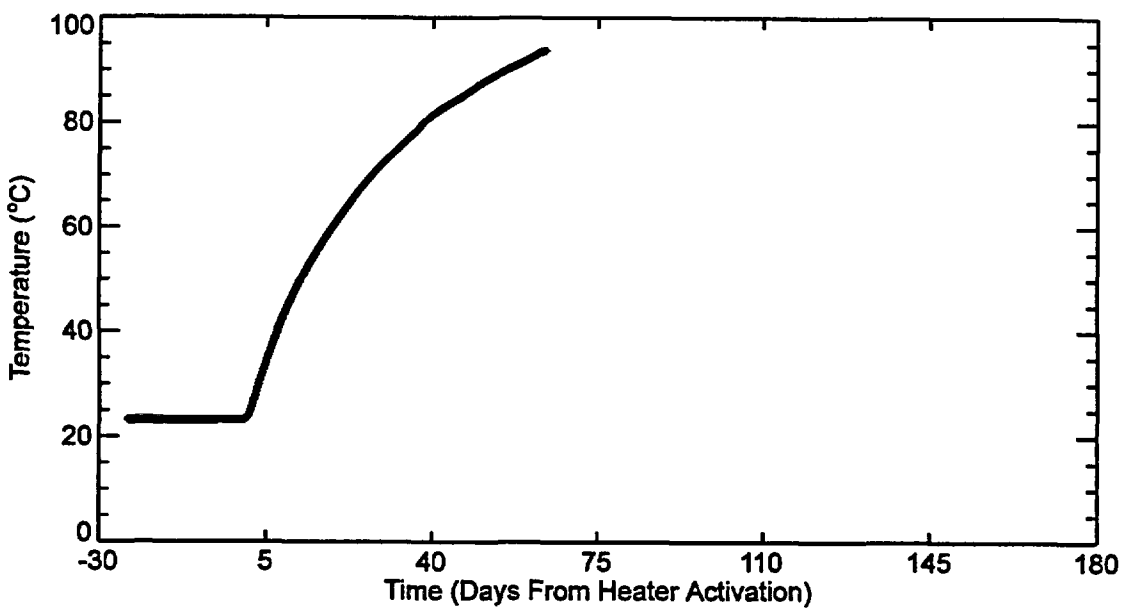


Figure D-26. Data from failed gage ESF-HD-139-TEMP7-RTD-31.

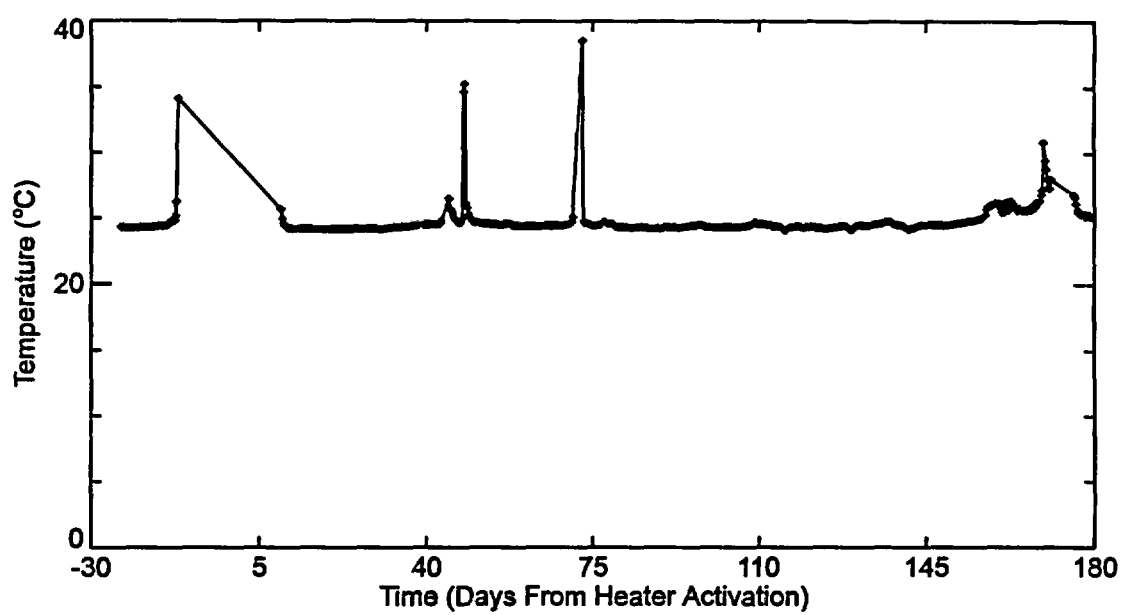


Figure D-27. Data from failed gage ESF-HD-141-TEMP9-RTD-36.

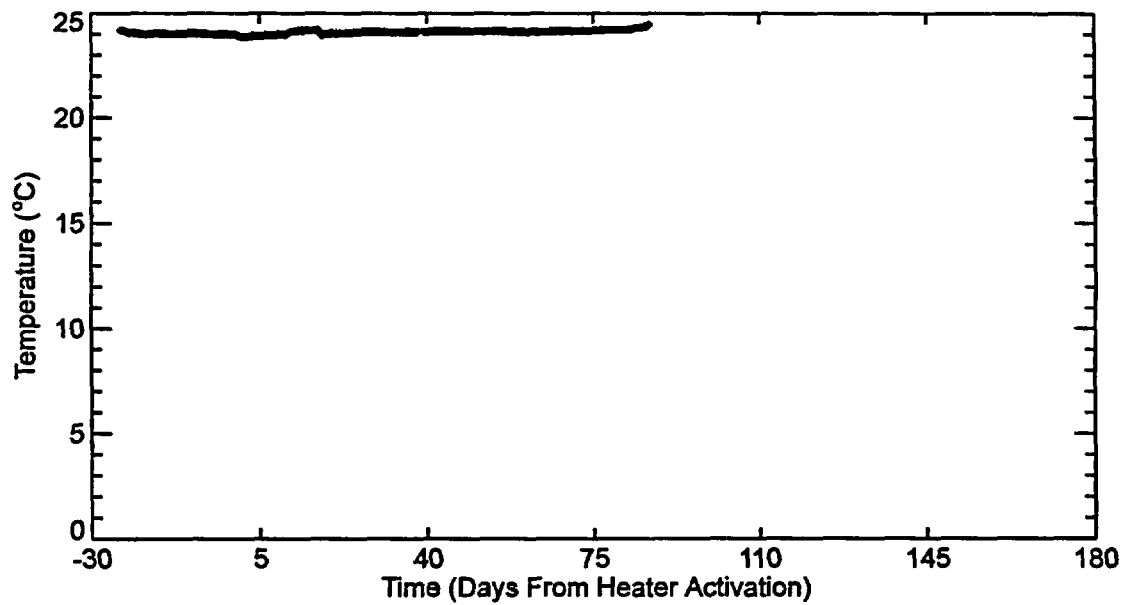


Figure D-28. Data from failed gage ESF-HD-141-TEMP9-RTD-40.

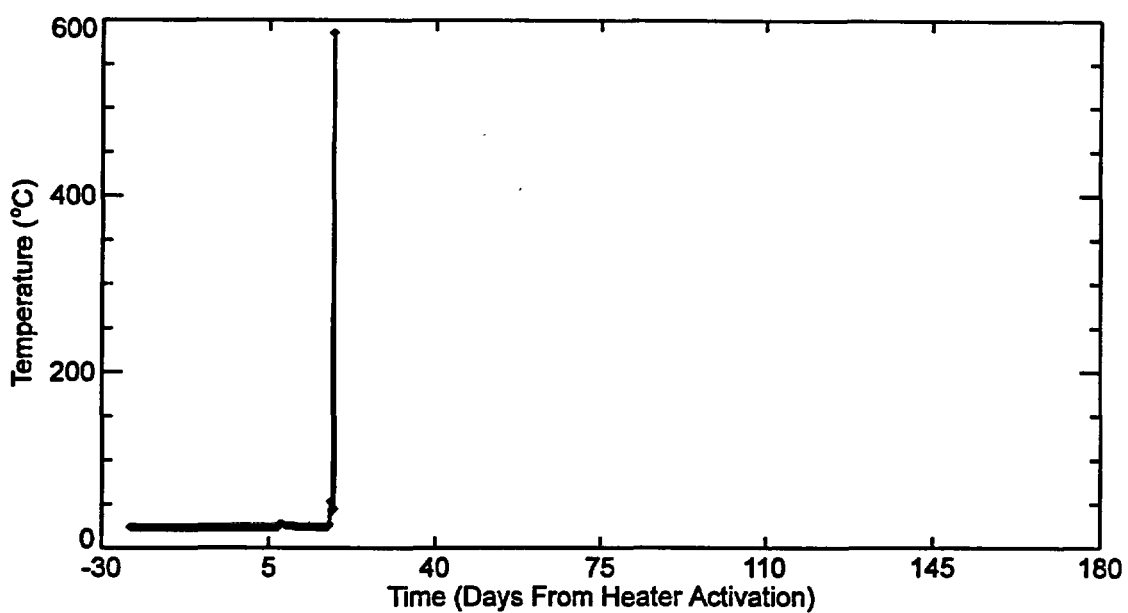


Figure D-29. Data from failed gage ESF-HD-141-TEMP9-RTD-41.

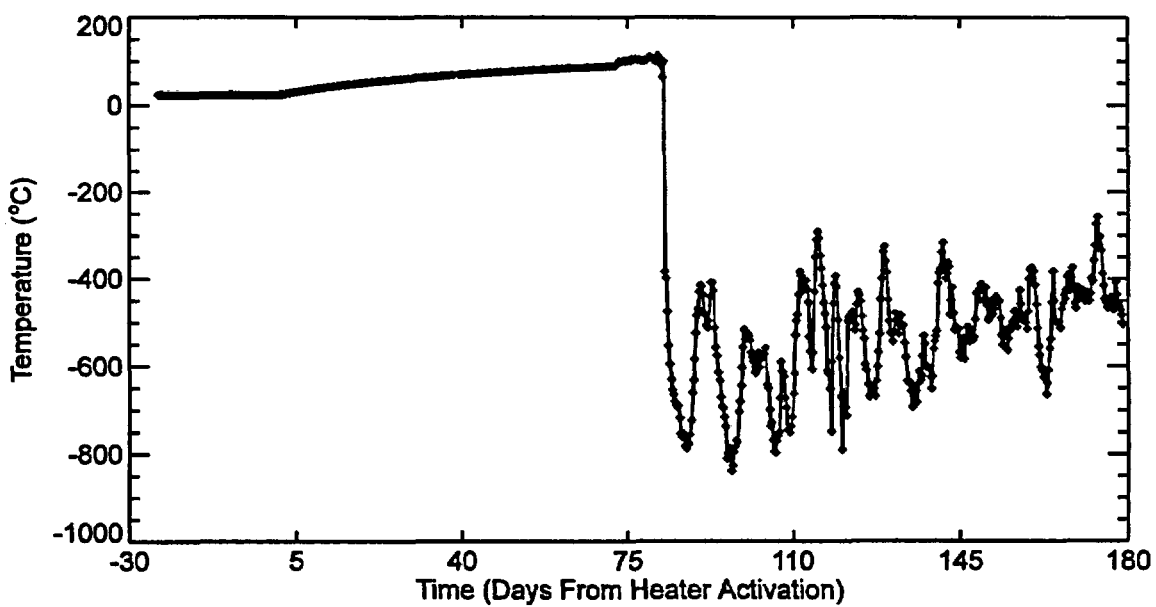


Figure D-30. Data from failed gage ESF-HD-143-TEMP11-RTD-24.

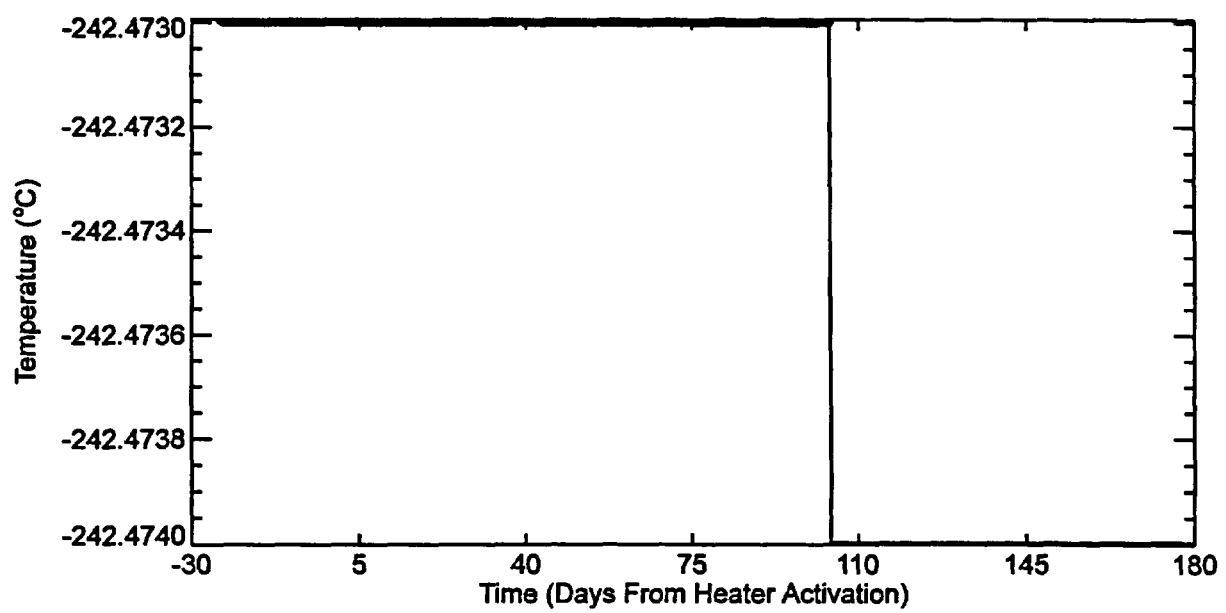


Figure D-31. Data from failed gage ESF-HD-143-TEMP11-RTD-40.

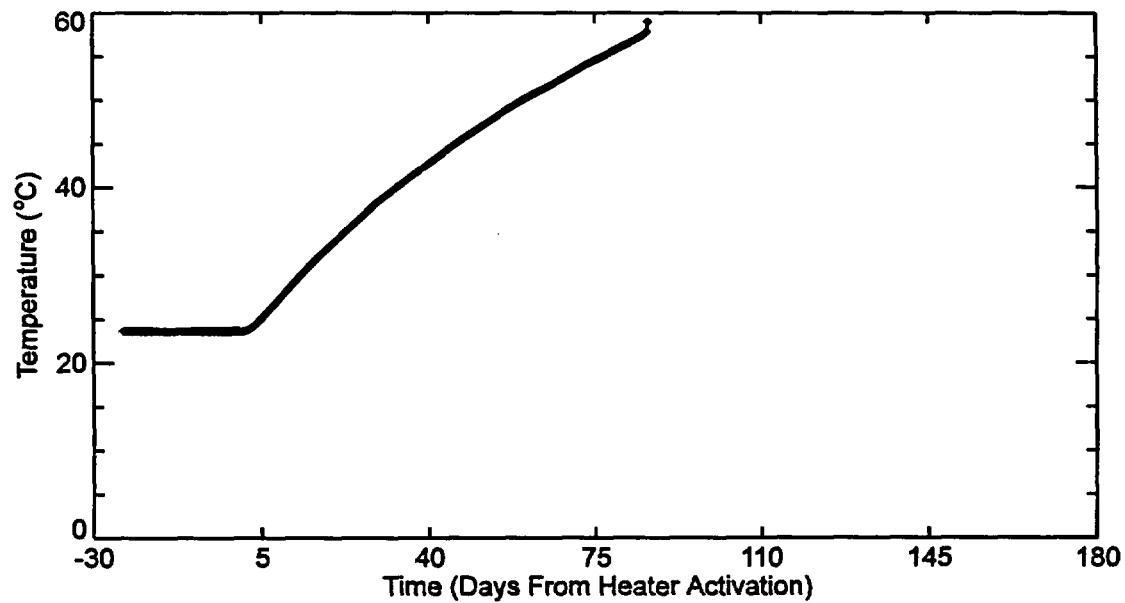


Figure D-32. Data from failed gage ESF-HD-143-TEMP11-RTD-42.

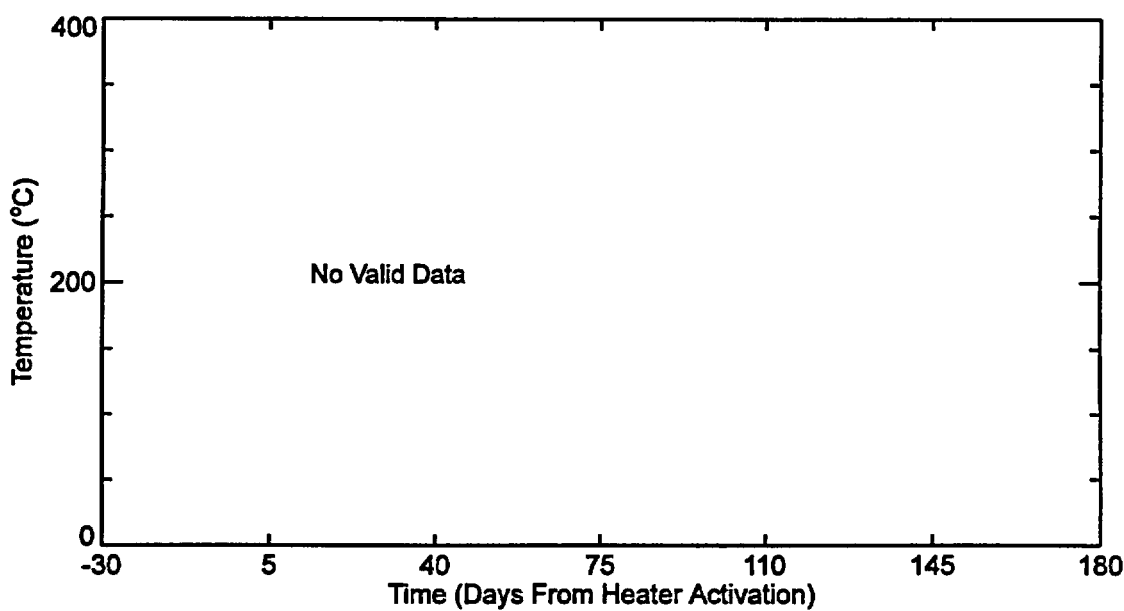


Figure D-33. Data from failed gage ESF-HD-143-TEMP11-RTD-67.

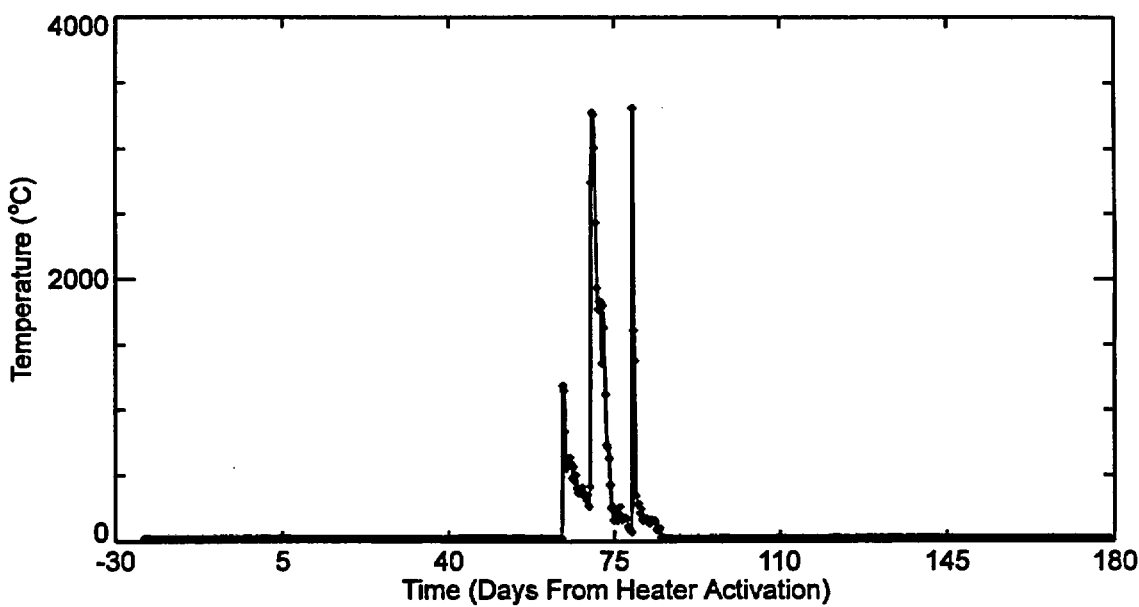


Figure D-34. Data from failed gage ESF-HD-144-TEMP12-RTD-33.

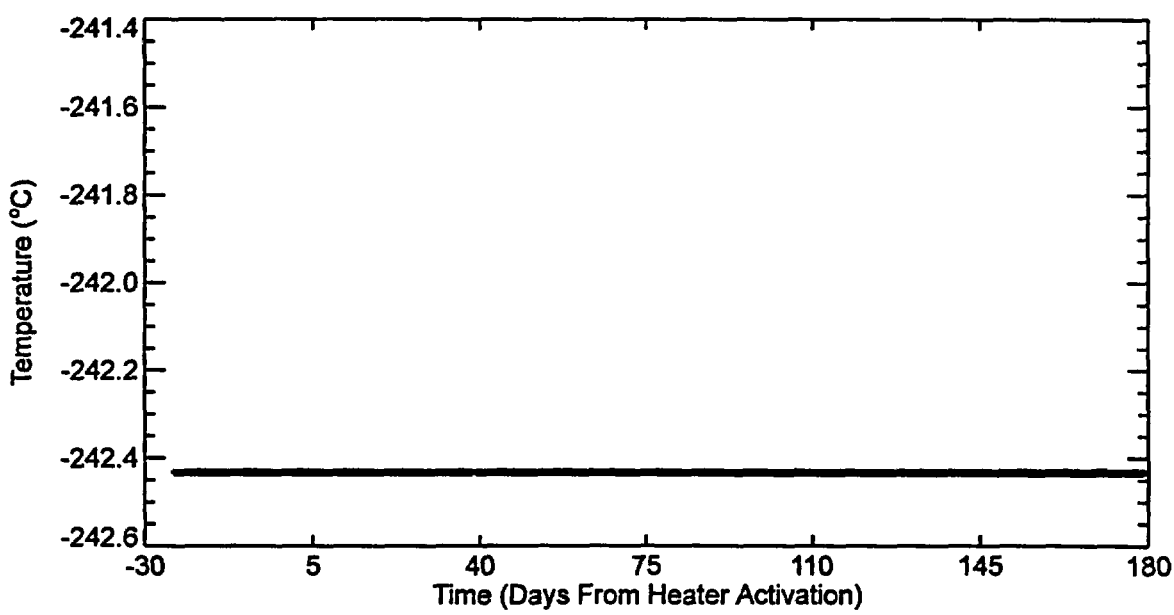


Figure D-35. Data from failed gage ESF-HD-158-TEMP13-RTD-7.

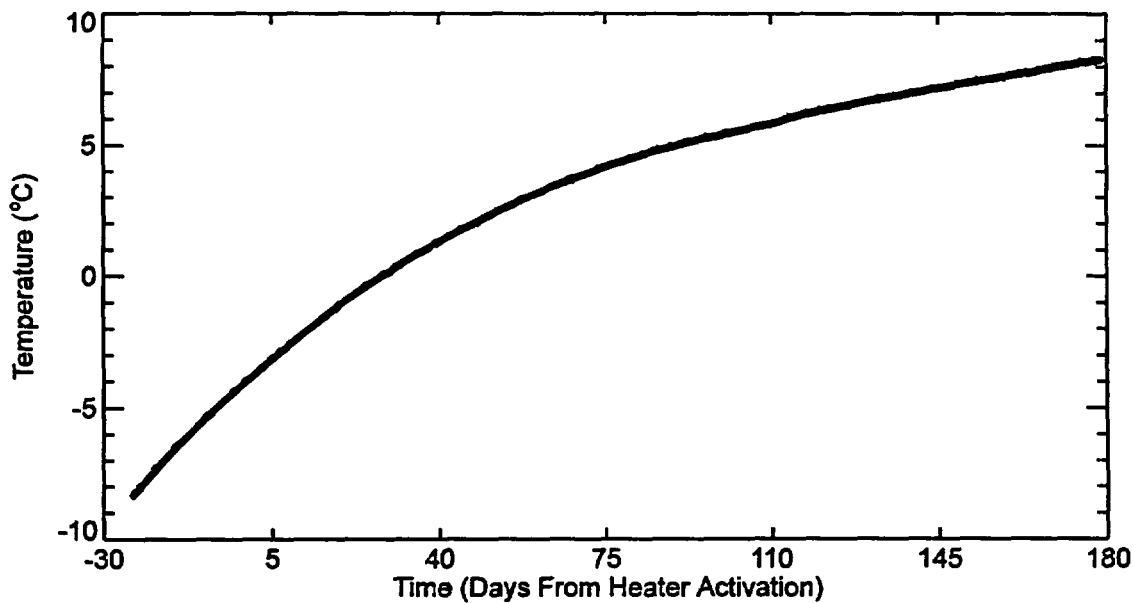


Figure D-36. Data from failed gage ESF-HD-161-TEMP16-RTD-64.

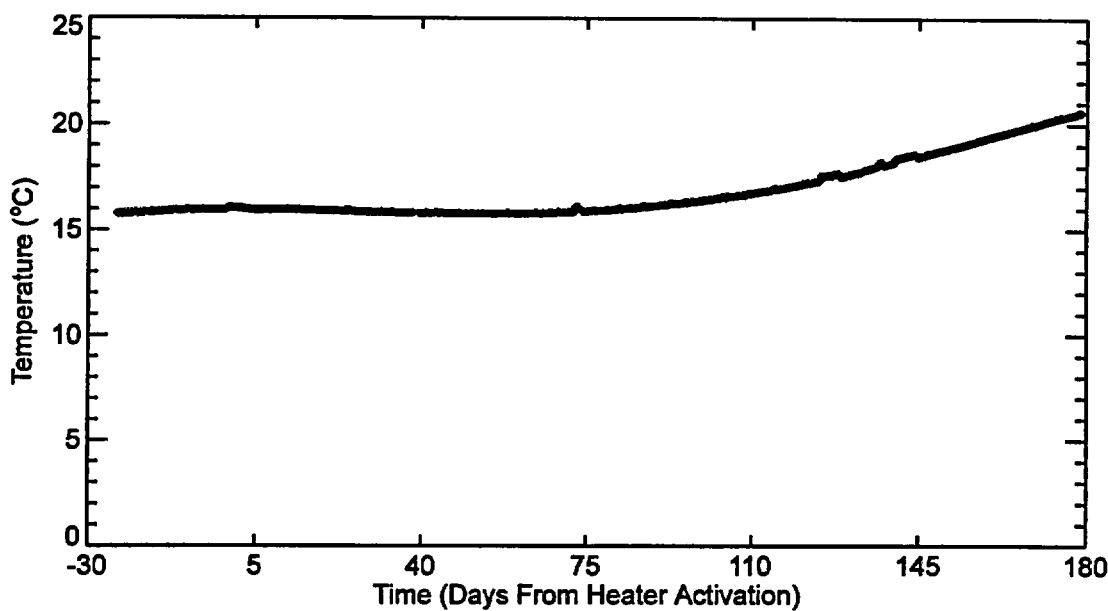


Figure D-37. Data from failed gage ESF-HD-168-TEMP21-RTD-28.

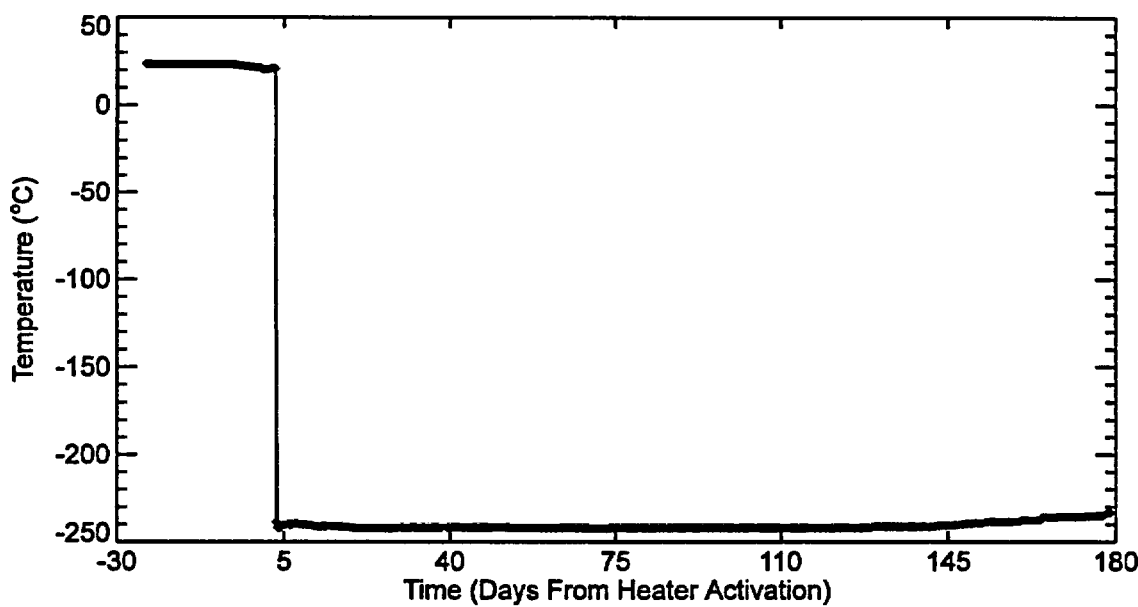


Figure D-38. Data from failed gage ESF-HD-168-TEMP21-RTD-31.

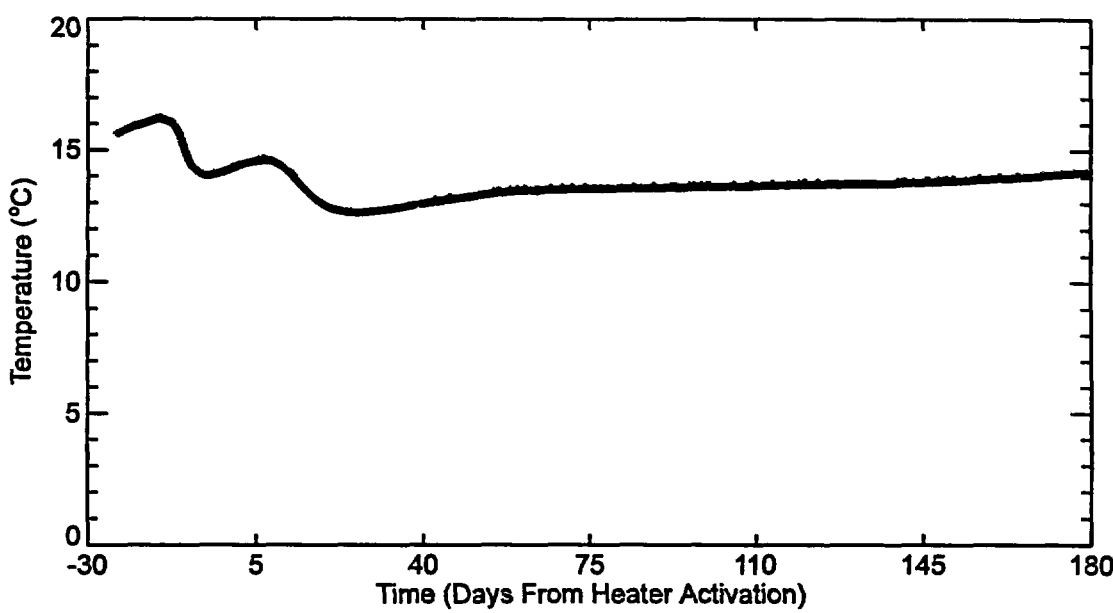


Figure D-39. Data from failed gage ESF-HD-168-TEMP21-RTD-40.

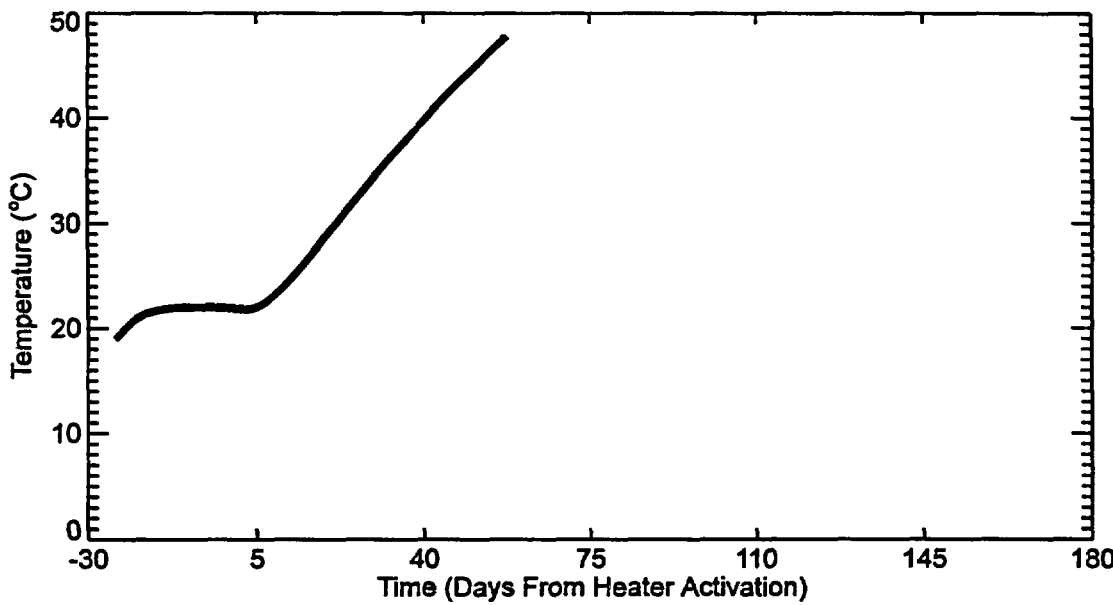


Figure D-40. Data from failed gage ESF-HD-169-TEMP22-RTD-5.

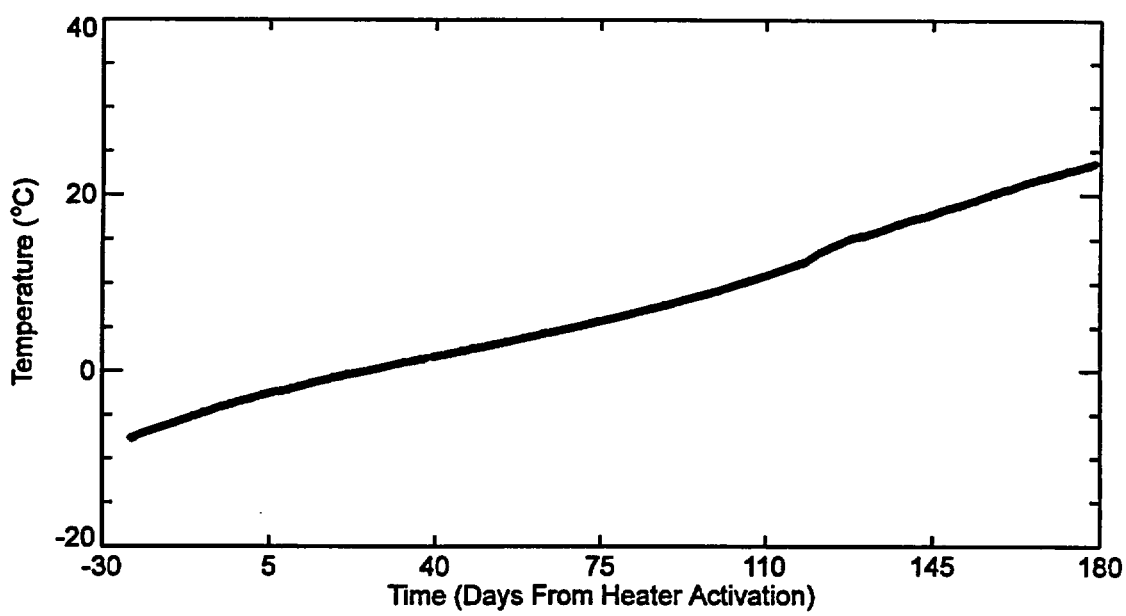


Figure D-41. Data from failed gage ESF-HD-169-TEMP22-RTD-22.

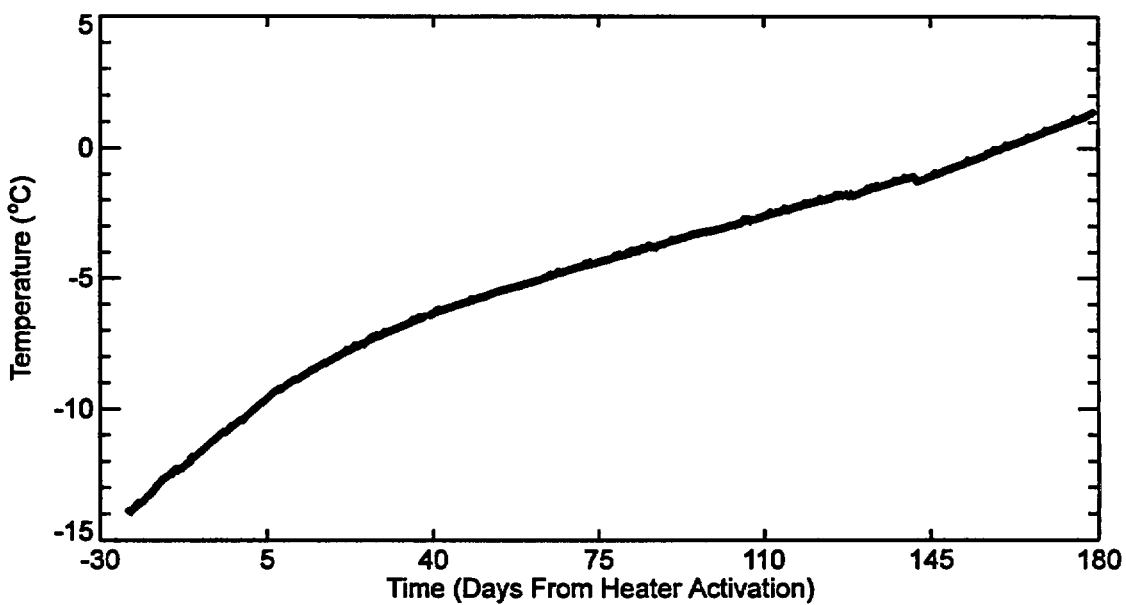


Figure D-42. Data from failed gage ESF-HD-169-TEMP23-RTD-29.

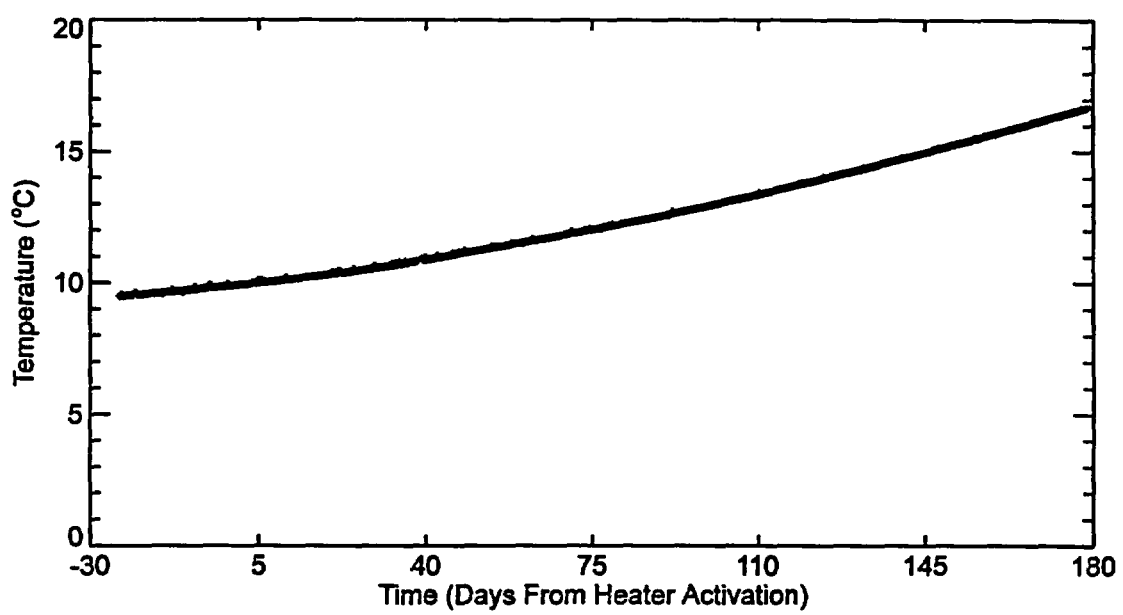


Figure D-43. Data from failed gage ESF-HD-169-TEMP22-RTD-38.

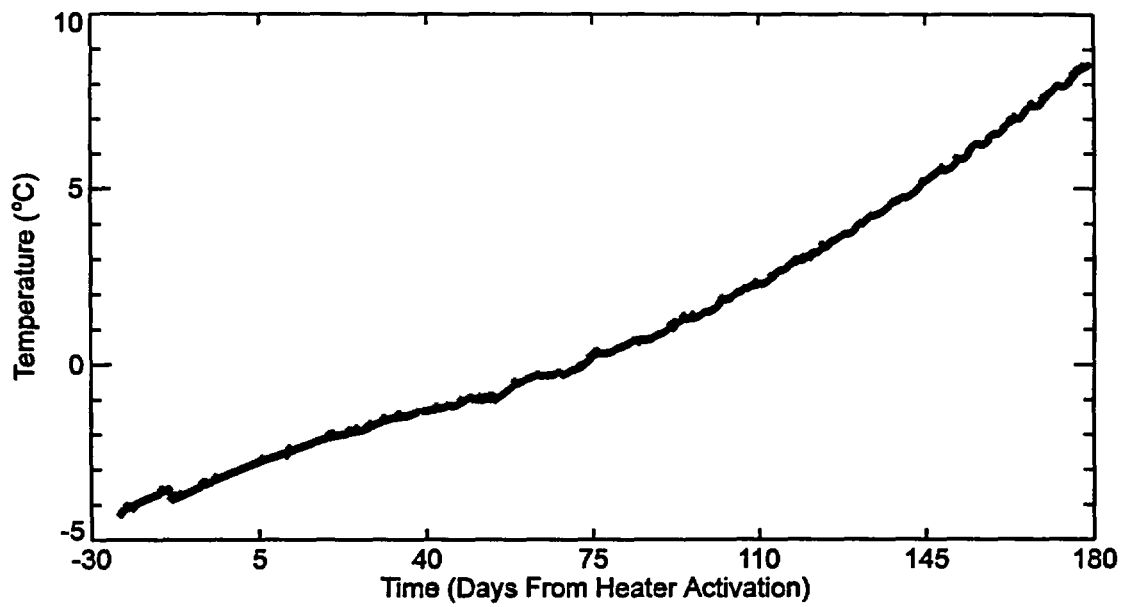


Figure D-44. Data from failed gage ESF-HD-170-TEMP23-RTD-28.

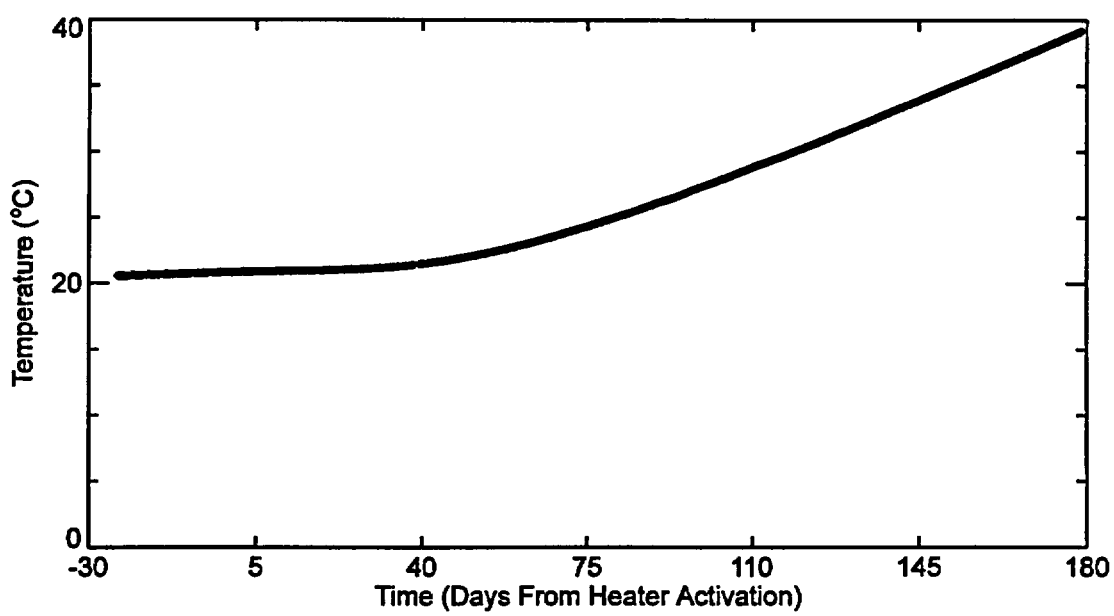


Figure D-45. Data from failed gage ESF-HD-171-TEMP24-RTD-22.

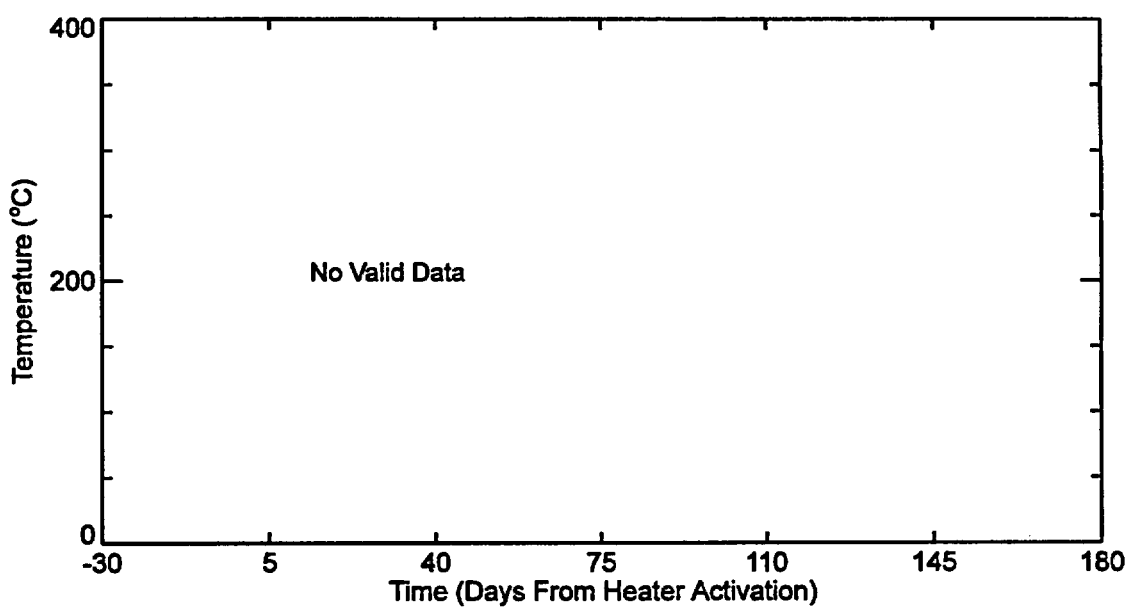


Figure D-46. Data from failed gage ESF-HD-171-TEMP24-RTD-53.

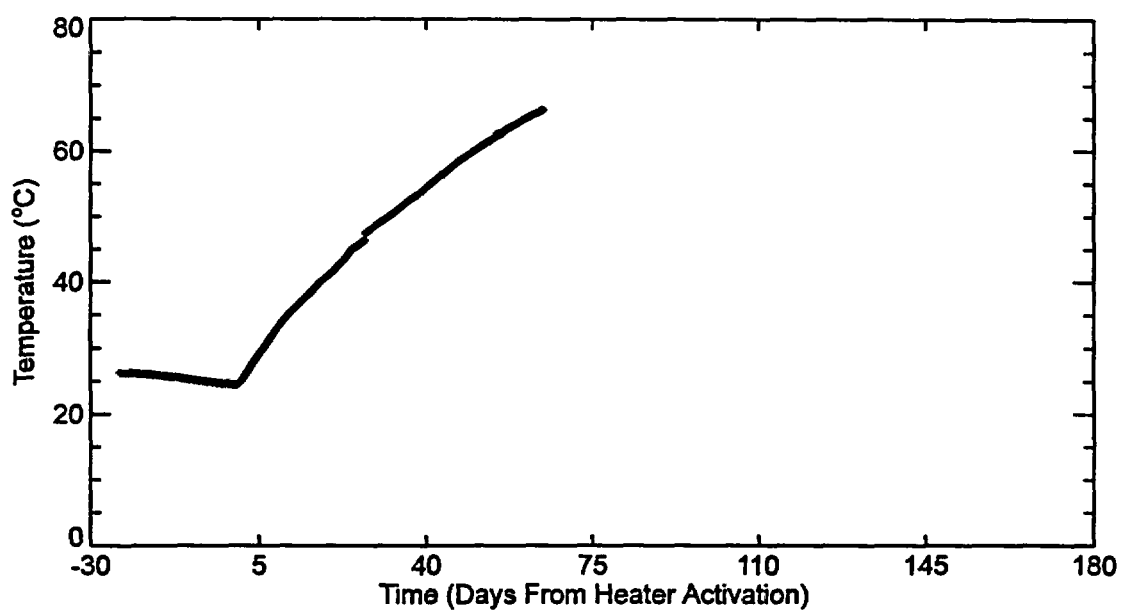


Figure D-47. Data from failed gage ESF-HD-172-TEMP25-RTD-2.

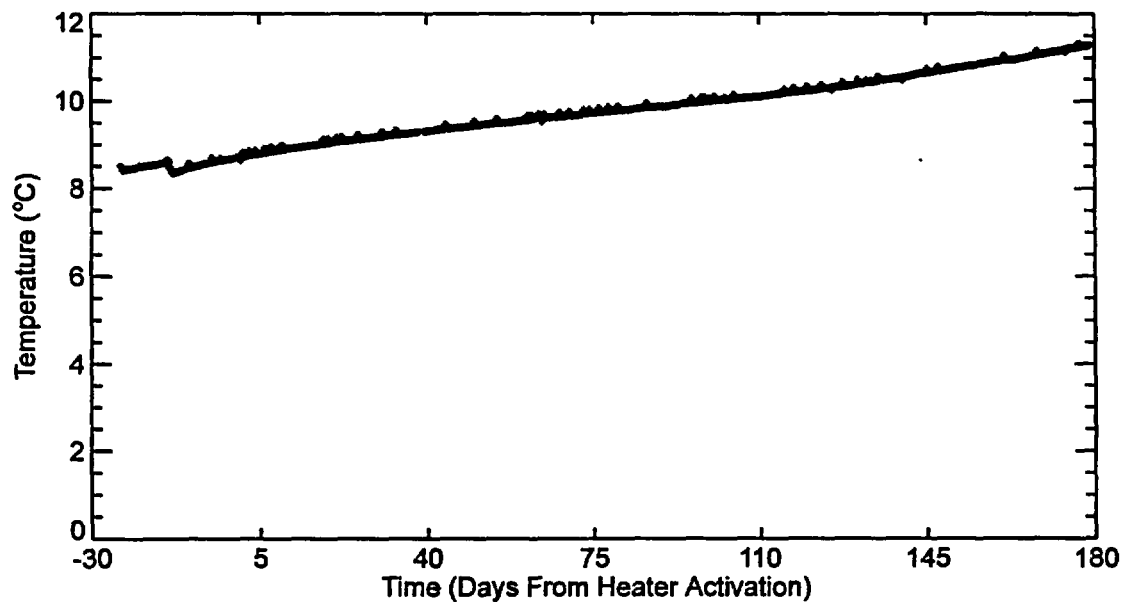


Figure D-48. Data from failed gage ESF-HD-173-TEMP26-RTD-42.

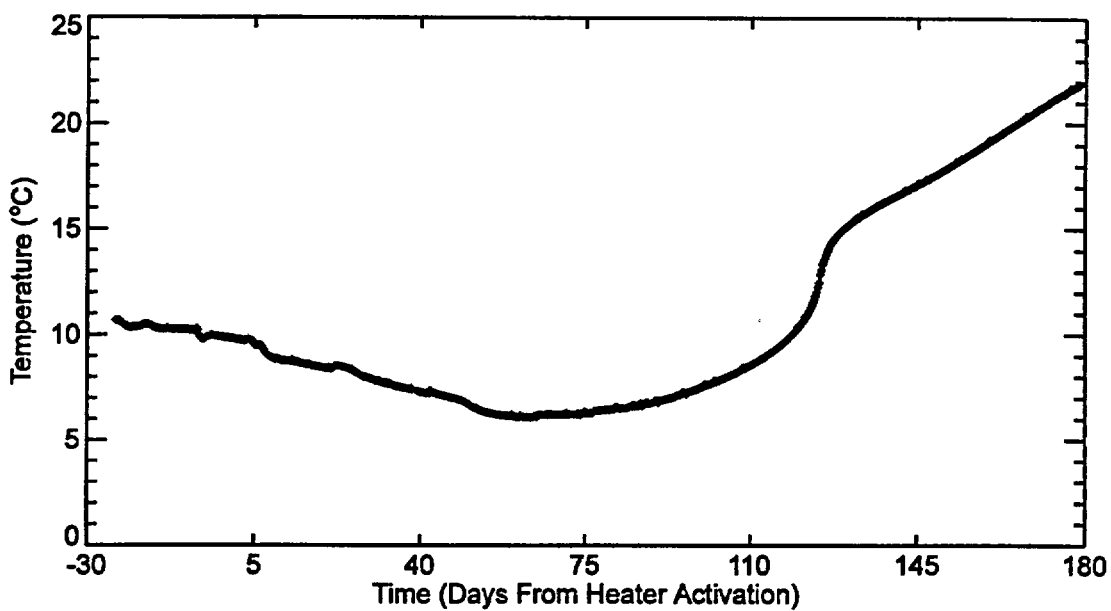


Figure D-49. Data from failed gage ESF-HD-175-TEMP28-RTD-31.

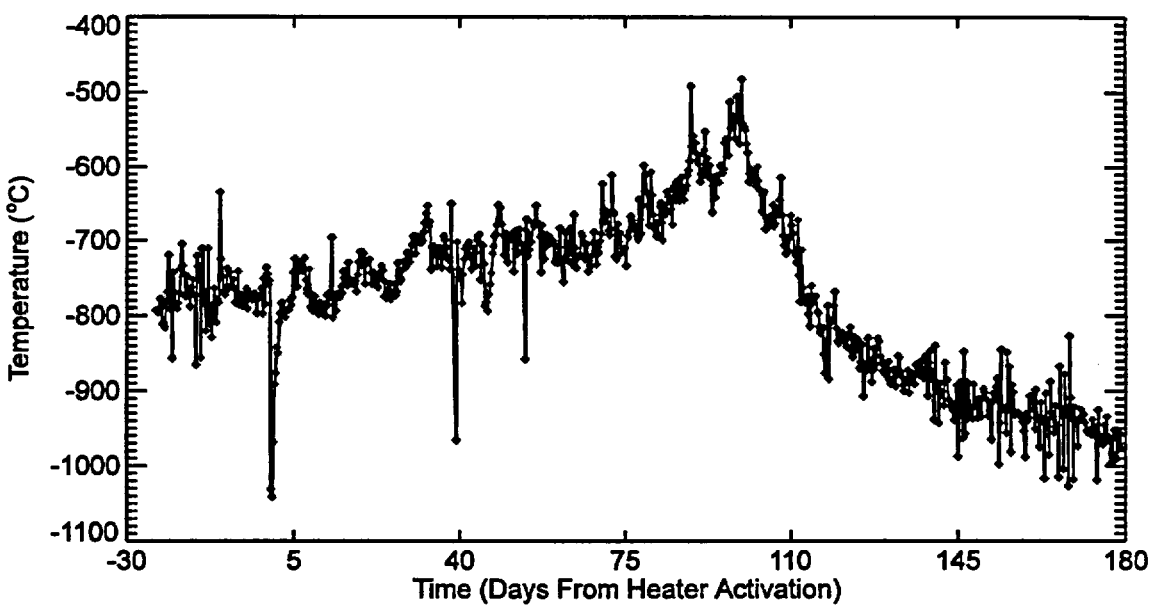


Figure D-50. Data from failed gage ESF-HD-175-TEMP28-RTD-34.

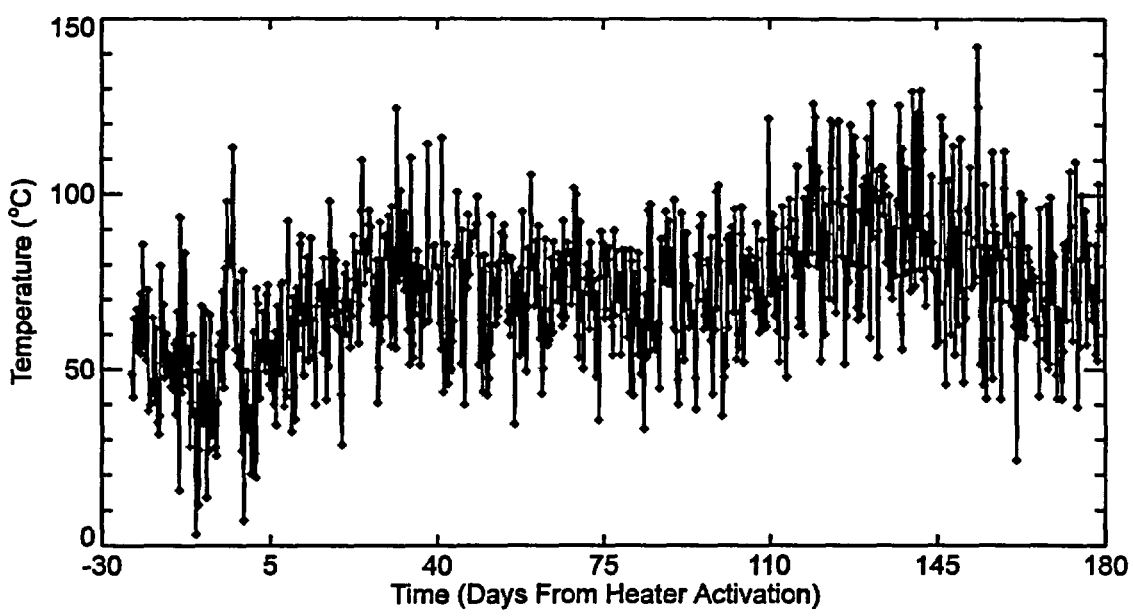


Figure D-51. Data from failed gage ESF-HD-82-MPBX2-TC-19.

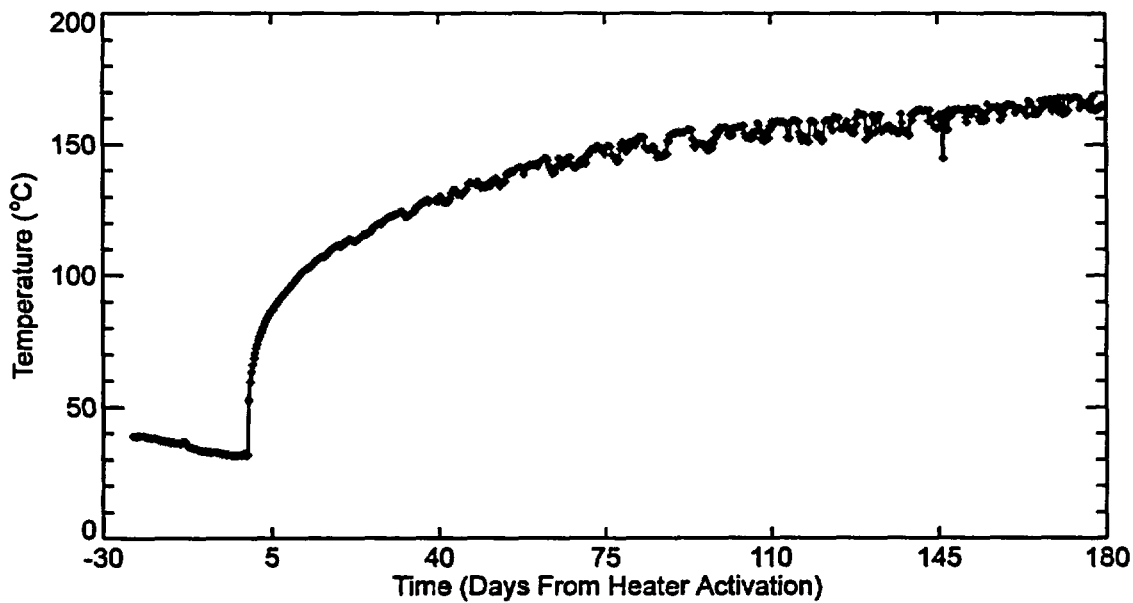


Figure D-52. Data from failed gage ESF-HD-148-MPBX4-TC-3.

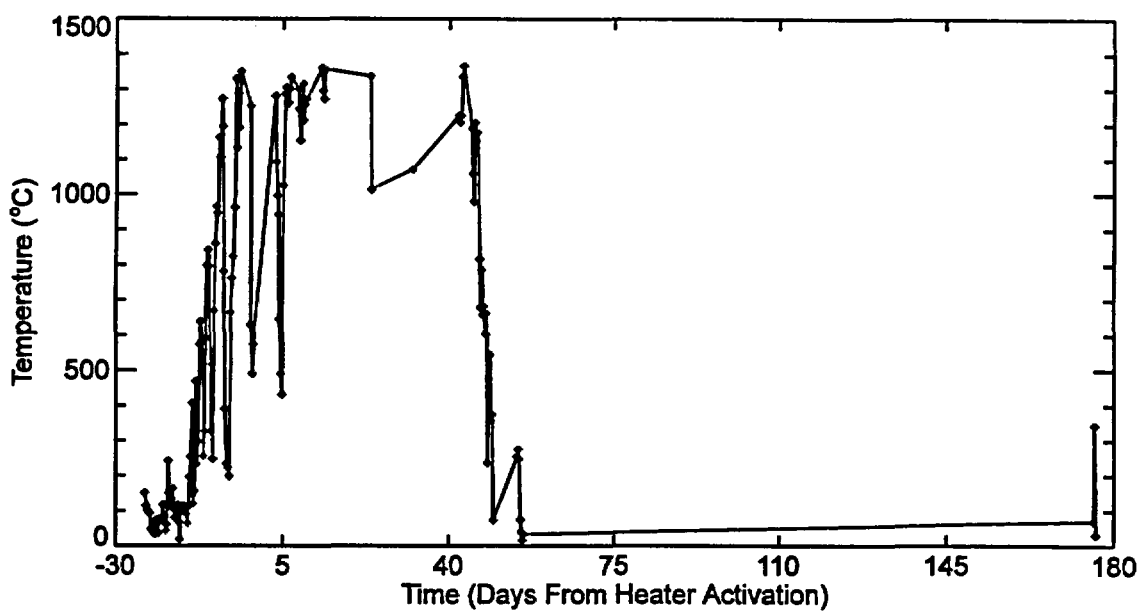


Figure D-53. Data from failed gage ESF-HD-148-MPBX4-TC-6.

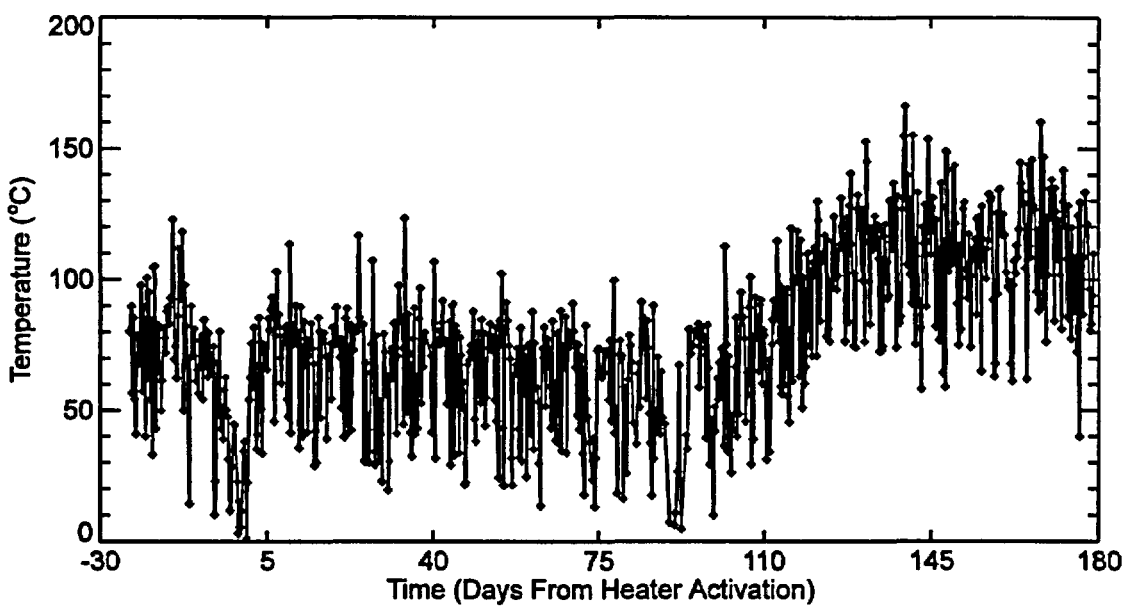


Figure D-54. Data from failed gage ESF-HD-150-MPBX6-TC-2.

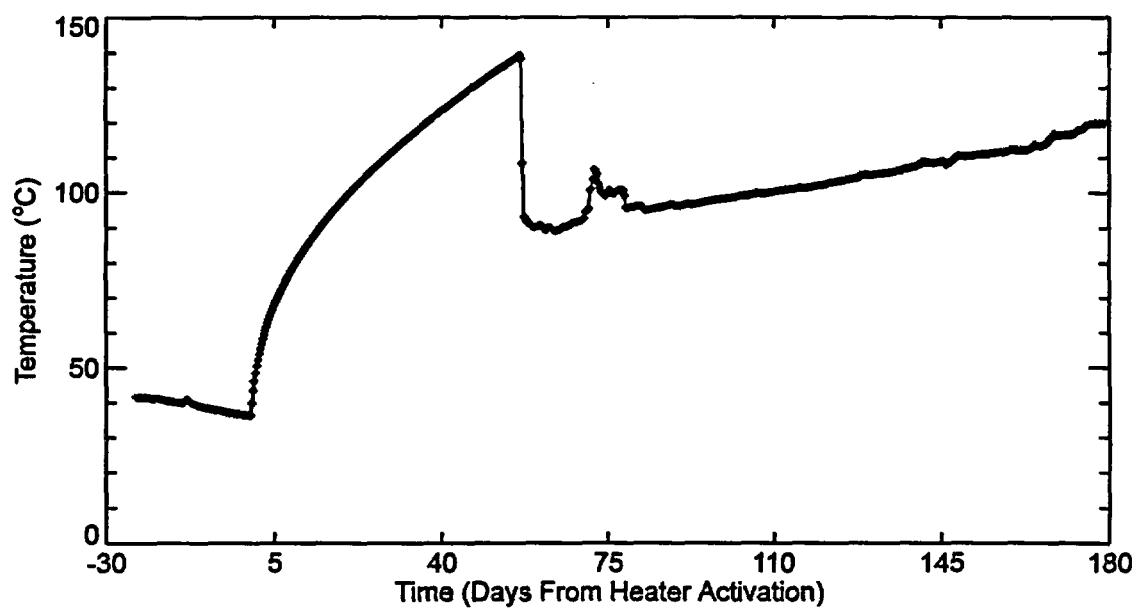


Figure D-55. Data from failed gage ESF-HD-150-MPBX6-TC-7.

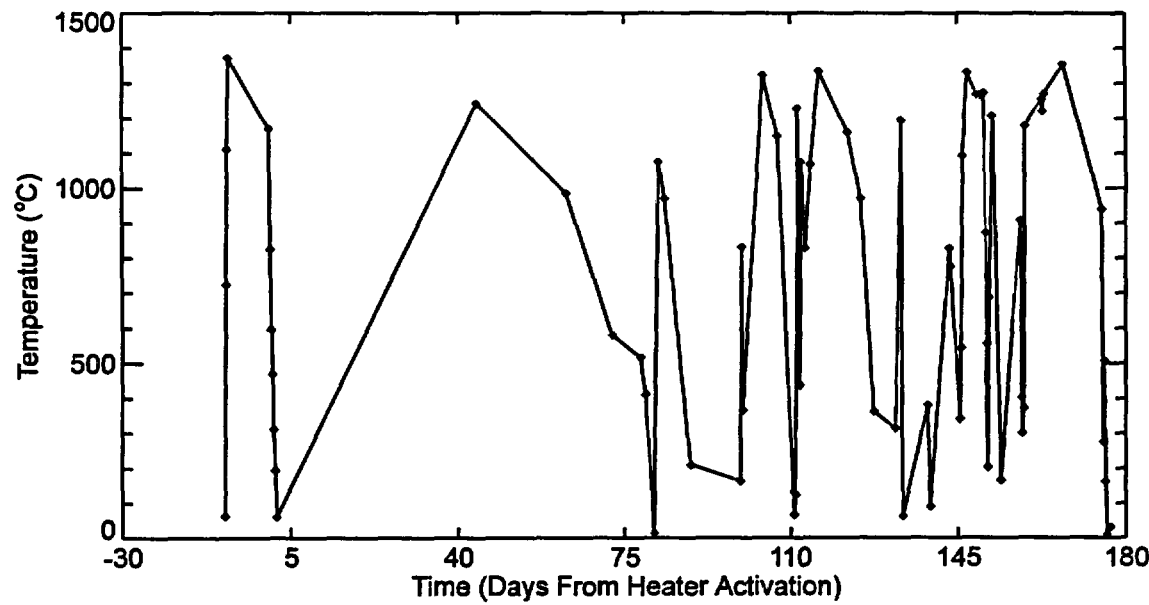


Figure D-56. Data from failed gage ESF-HD-155-MPBX8-TC-1.

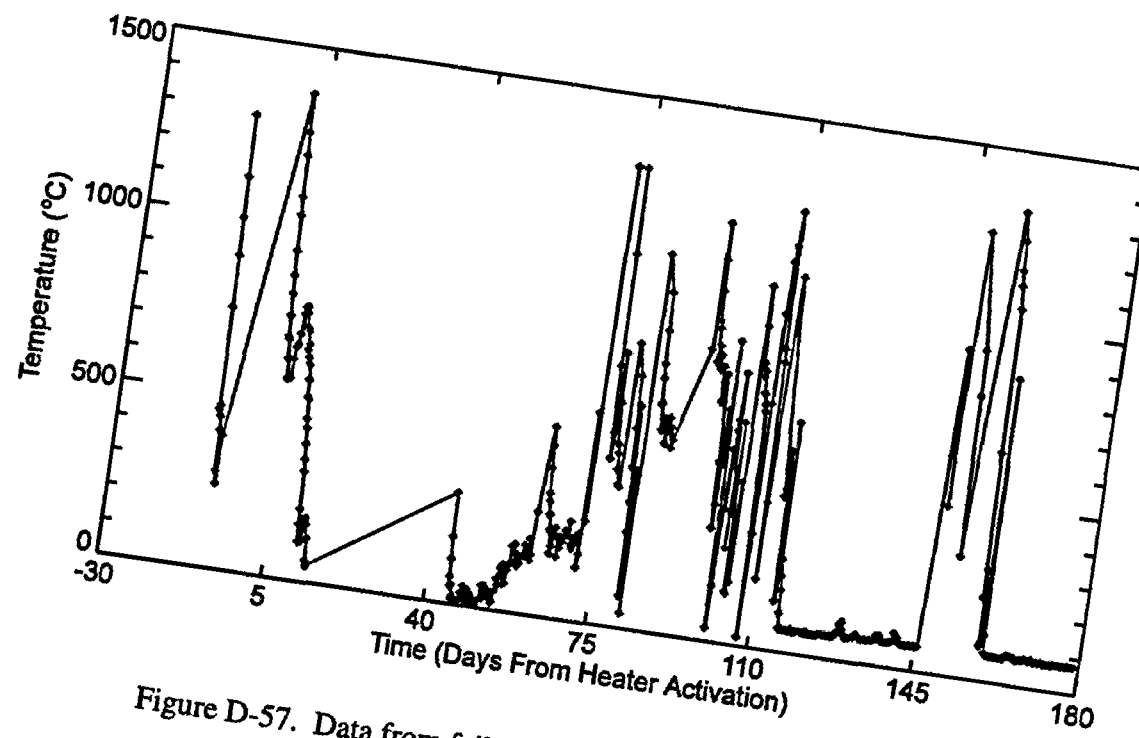


Figure D-57. Data from failed gage ESF-HD-155-MPBX8-TC-3.

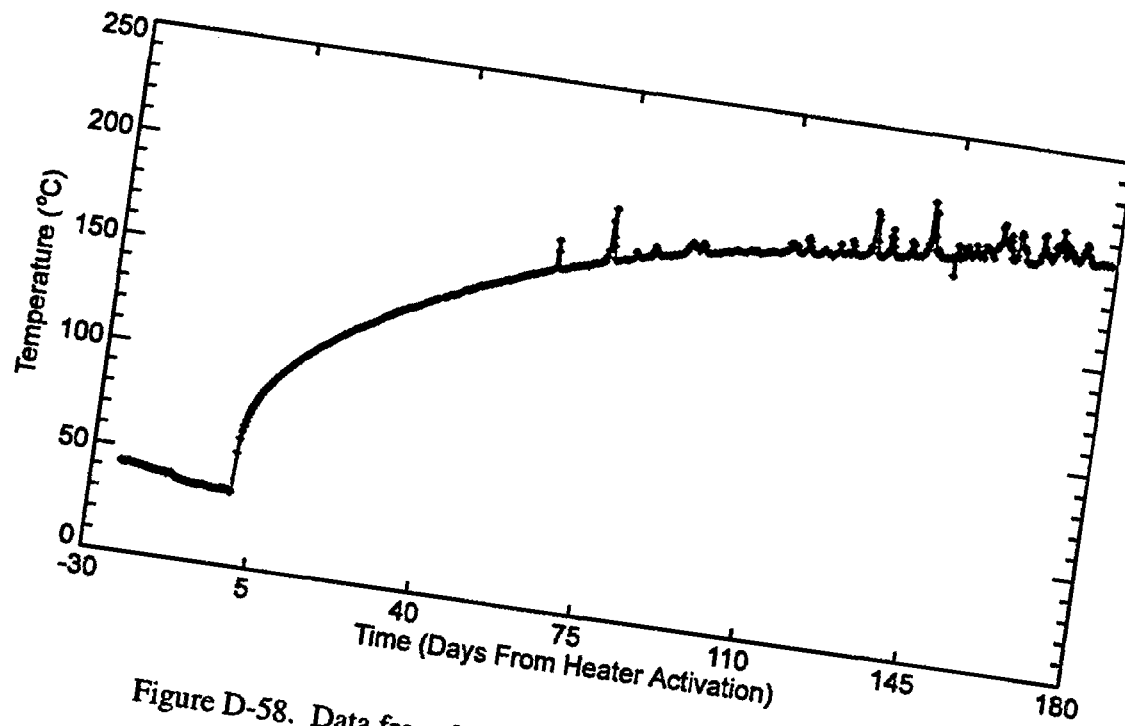


Figure D-58. Data from failed gage ESF-HD-155-MPBX8-TC-6.

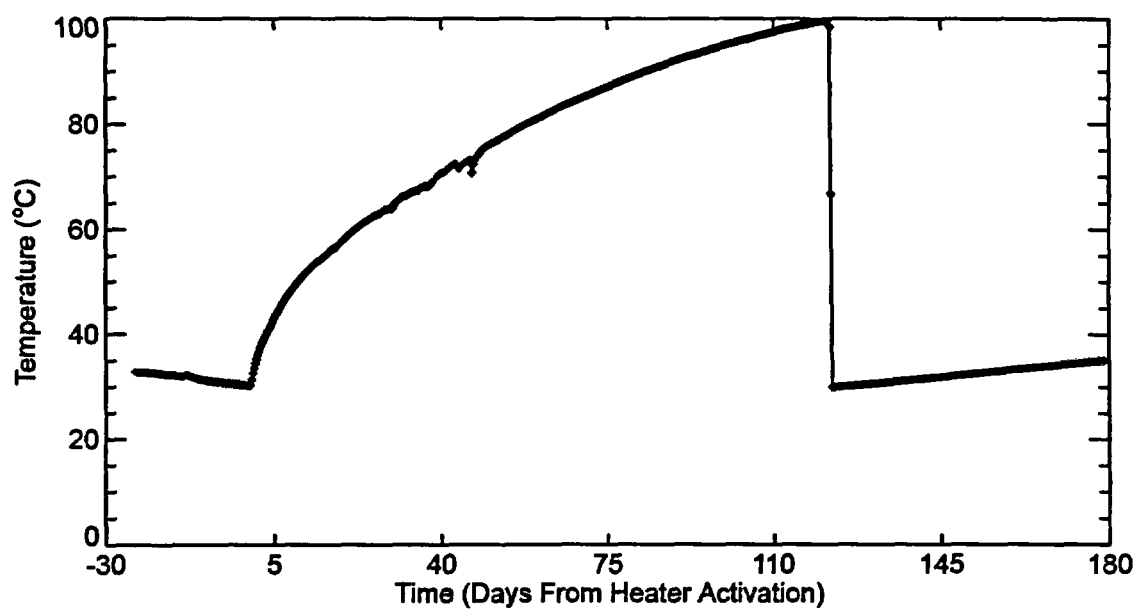


Figure D-59. Data from failed gage ESF-HD-157-MPBX10-TC-6.

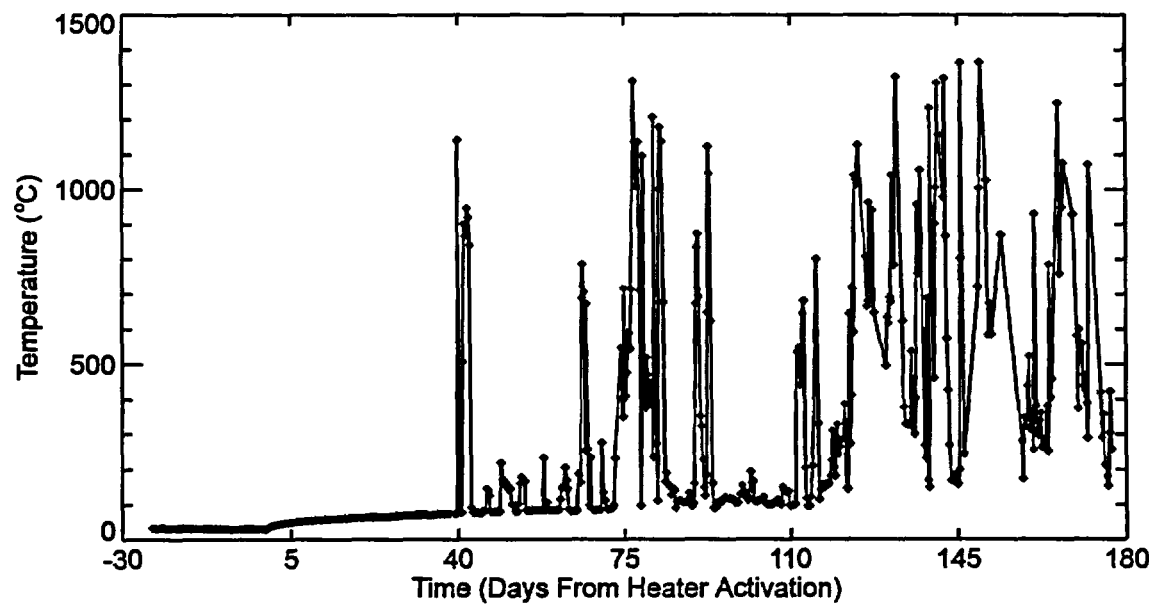


Figure D-60. Data from failed gage ESF-HD-178-MPBX11-TC-1.

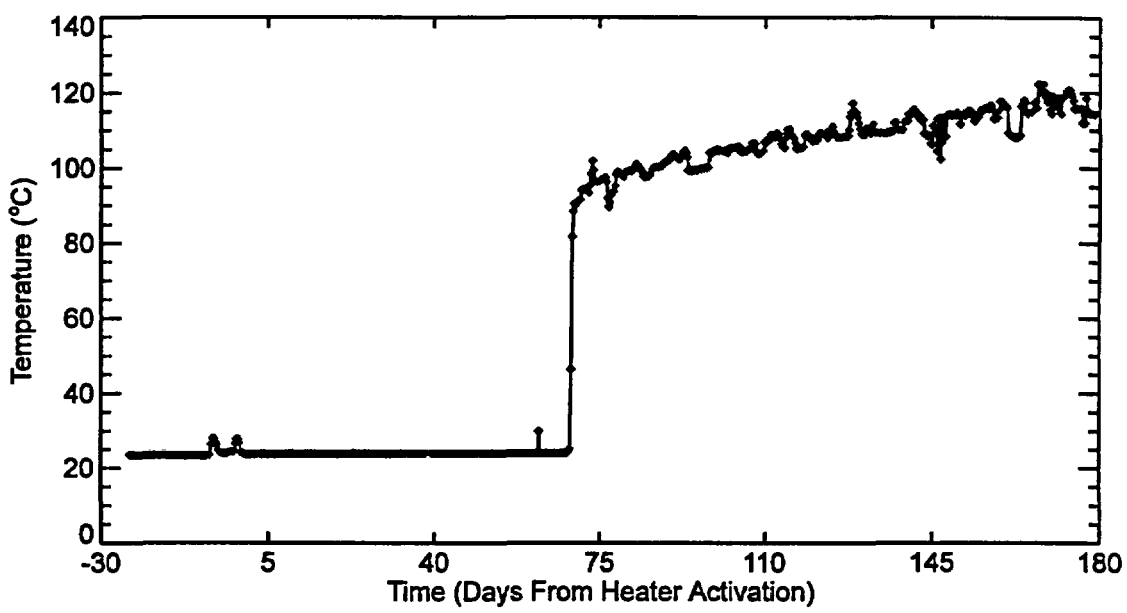


Figure D-61. Data from failed gage ESF-HD-178-MPBX11-TC-8.

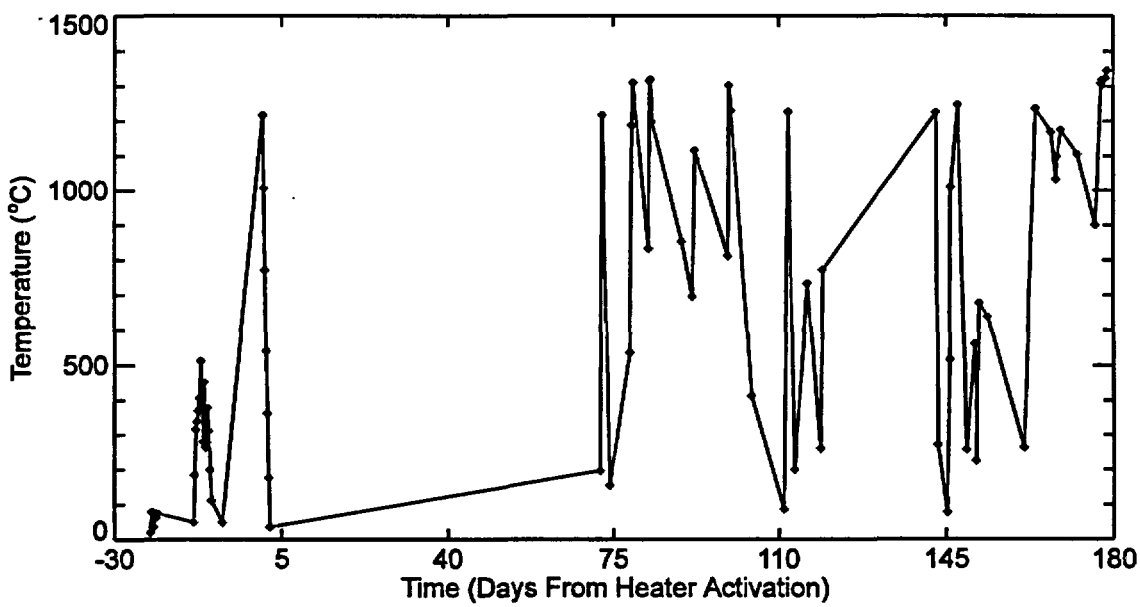


Figure D-62. Data from failed gage ESF-HD-179-MPBX12-TC-3.

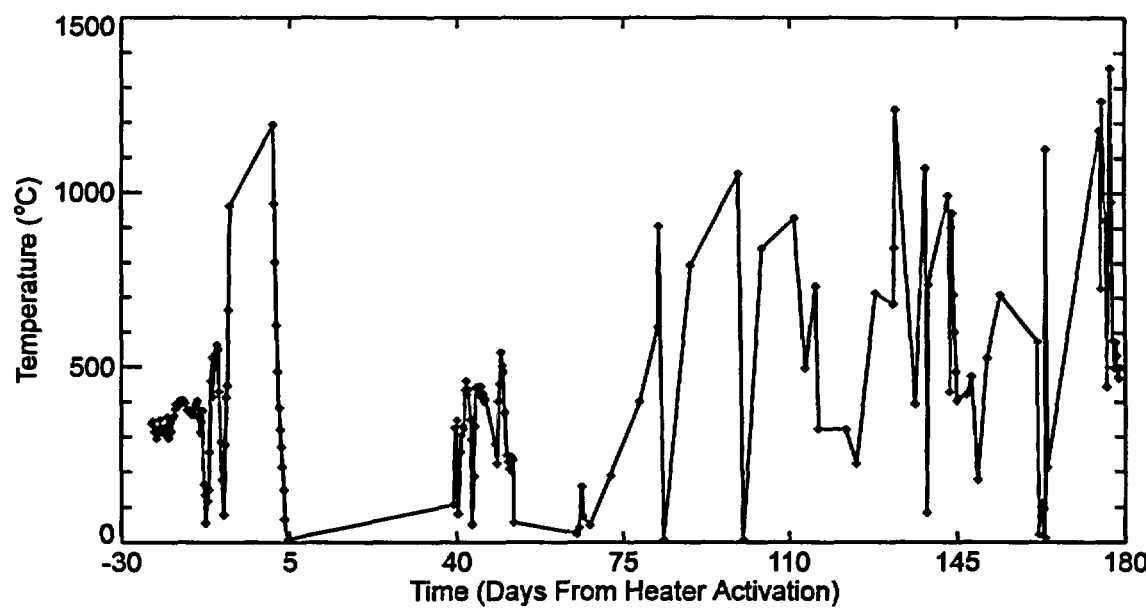


Figure D-63. Data from failed gage ESF-HD-179-MPBX12-TC-5.

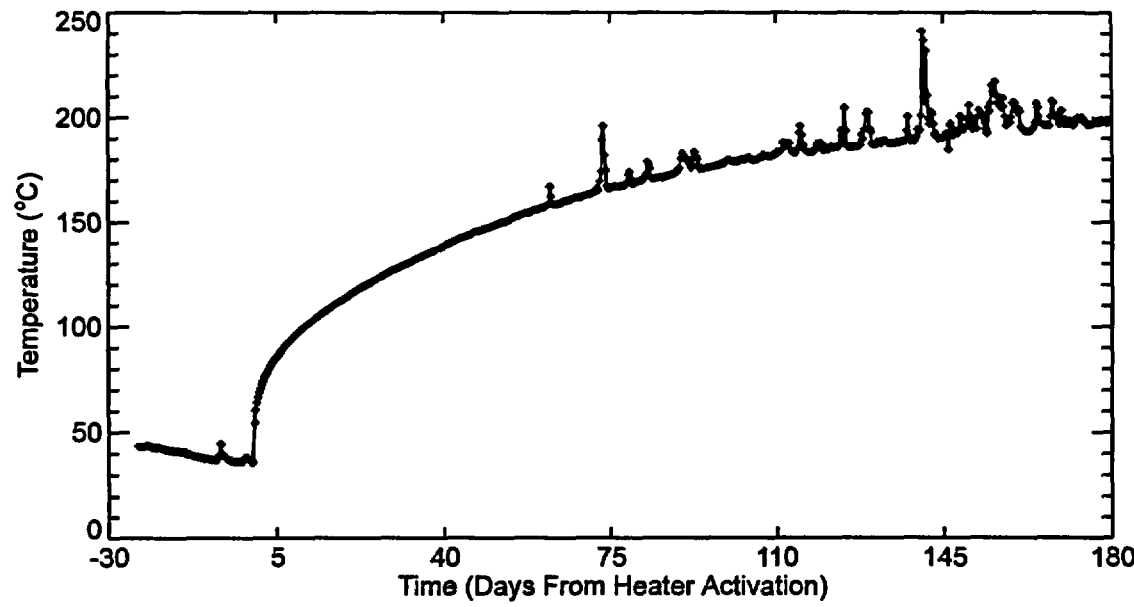


Figure D-64. Data from failed gage ESF-HD-179-MPBX12-TC-6.

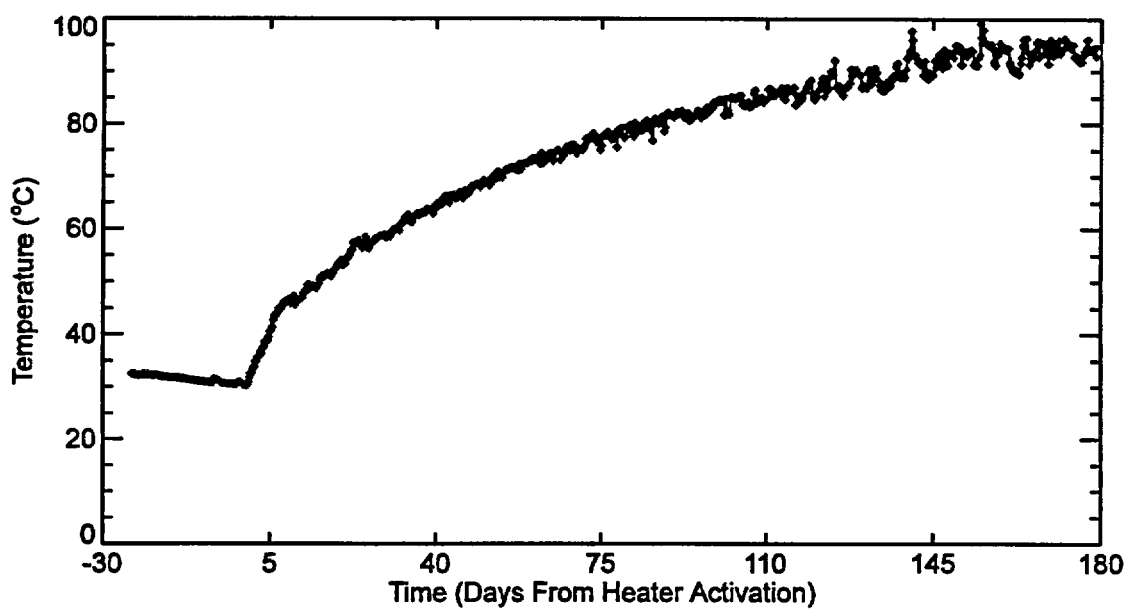


Figure D-65. Data from failed gage ESF-HD-180-MPBX13-TC-5.

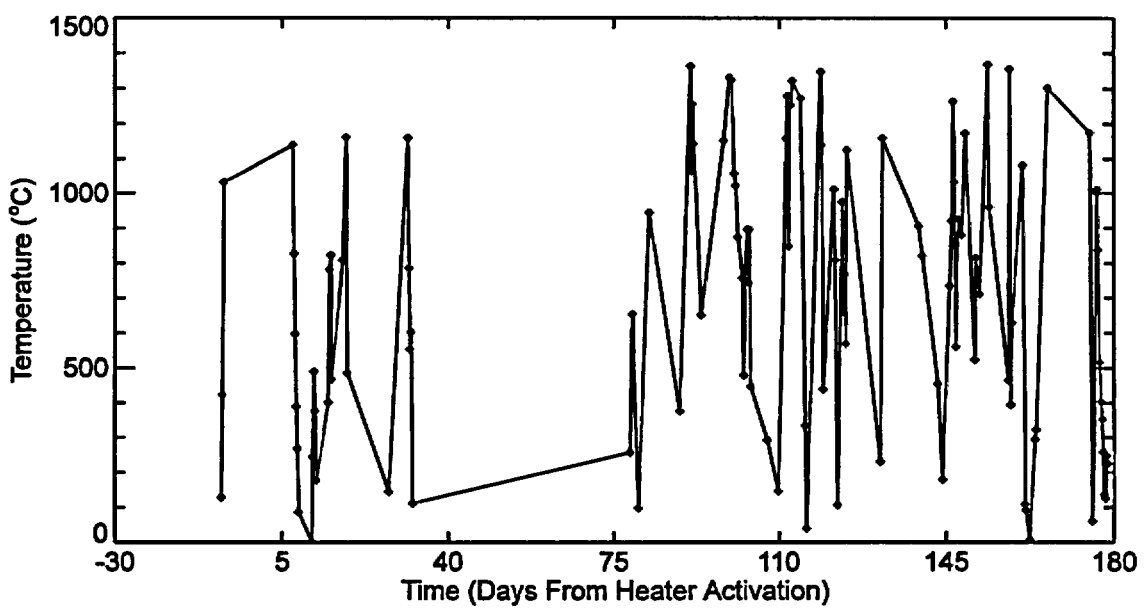


Figure D-66. Data from failed gage ESF-HD-181-MPBX14-TC-6.

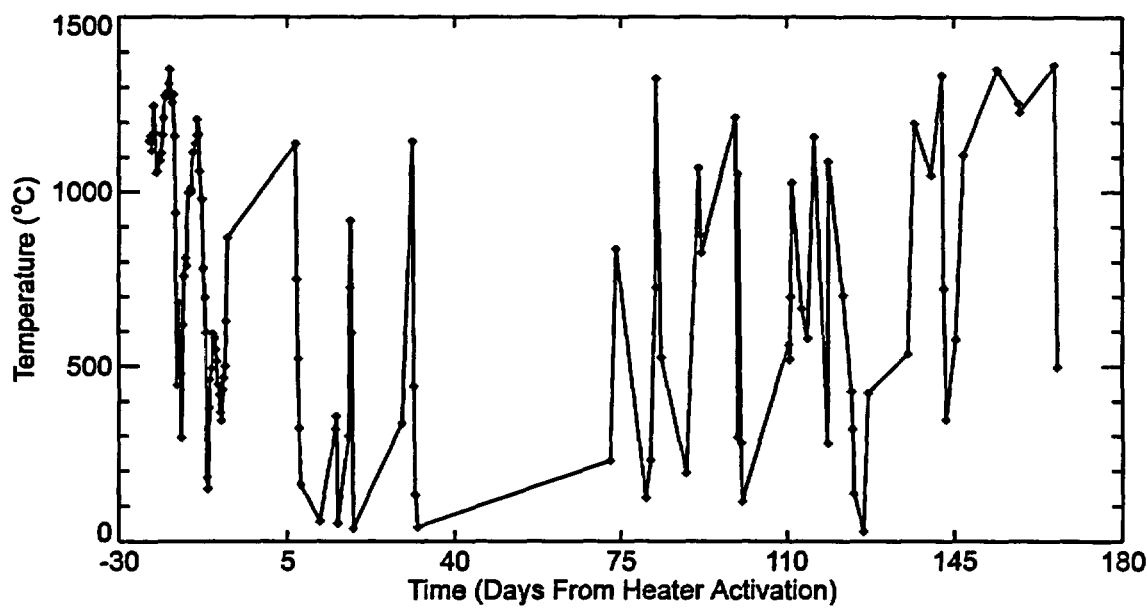


Figure D-67. Data from failed gage ESF-HD-181-MPBX14-TC-8.

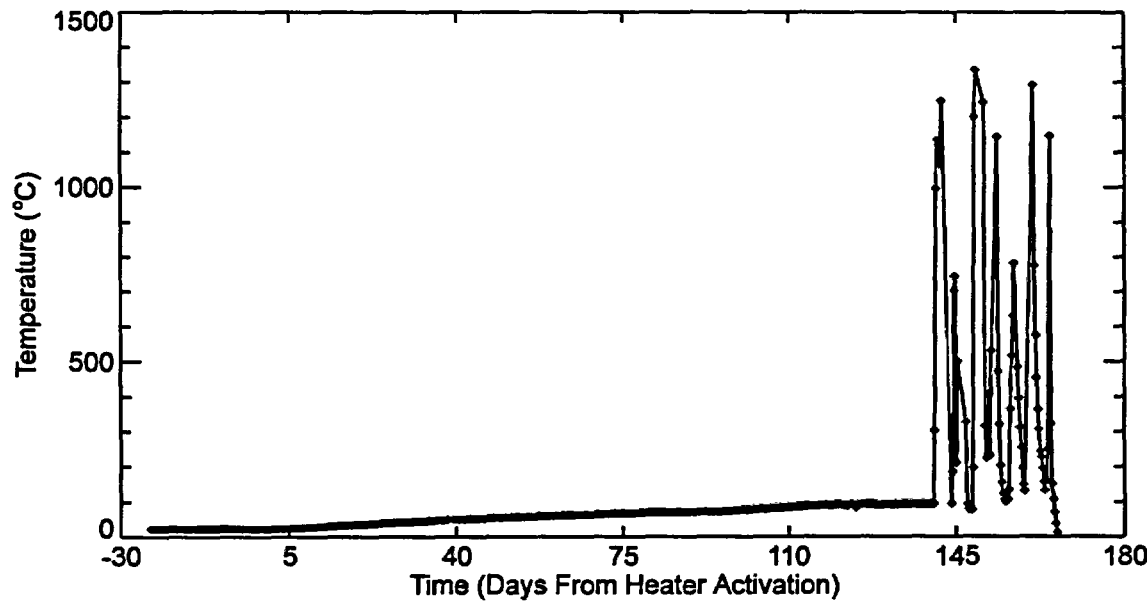


Figure D-68. Data from failed gage ESF-SDM-42-MPBX1-TC-5.

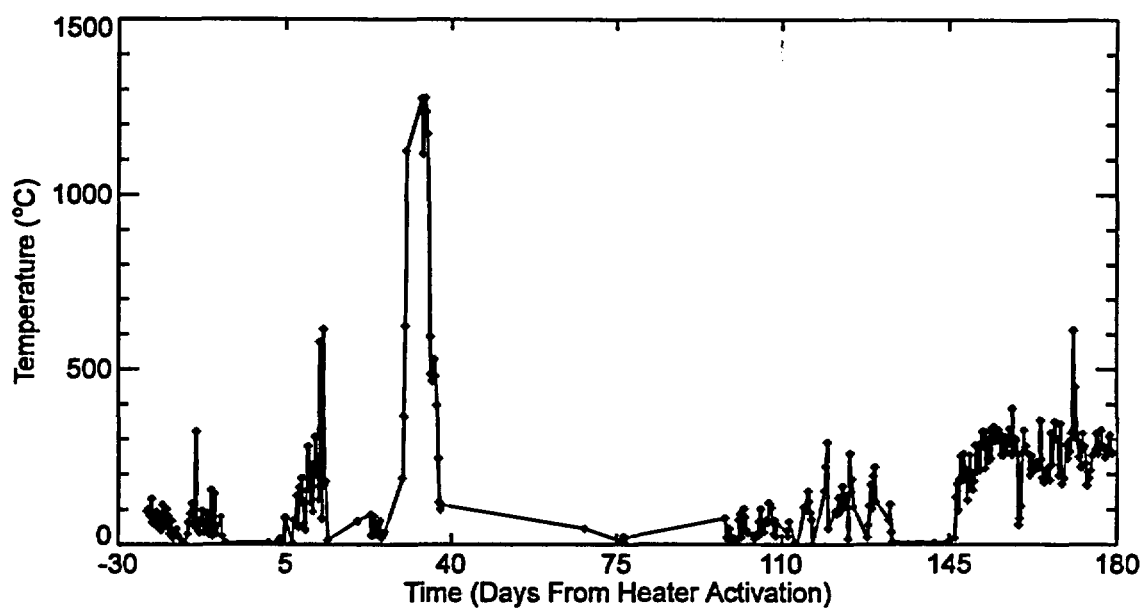


Figure D-69. Data from failed gage ESF-SDM-42-MPBX1-TC-8.

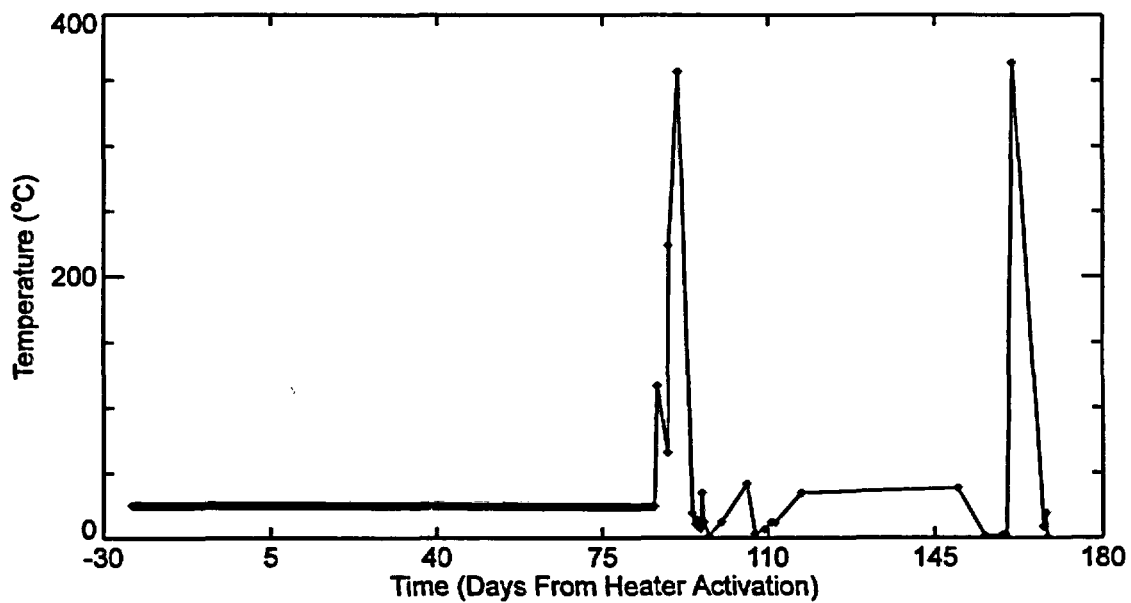


Figure D-70. Data from failed gage ESF-SDM-43-MPBX2-TC-1.

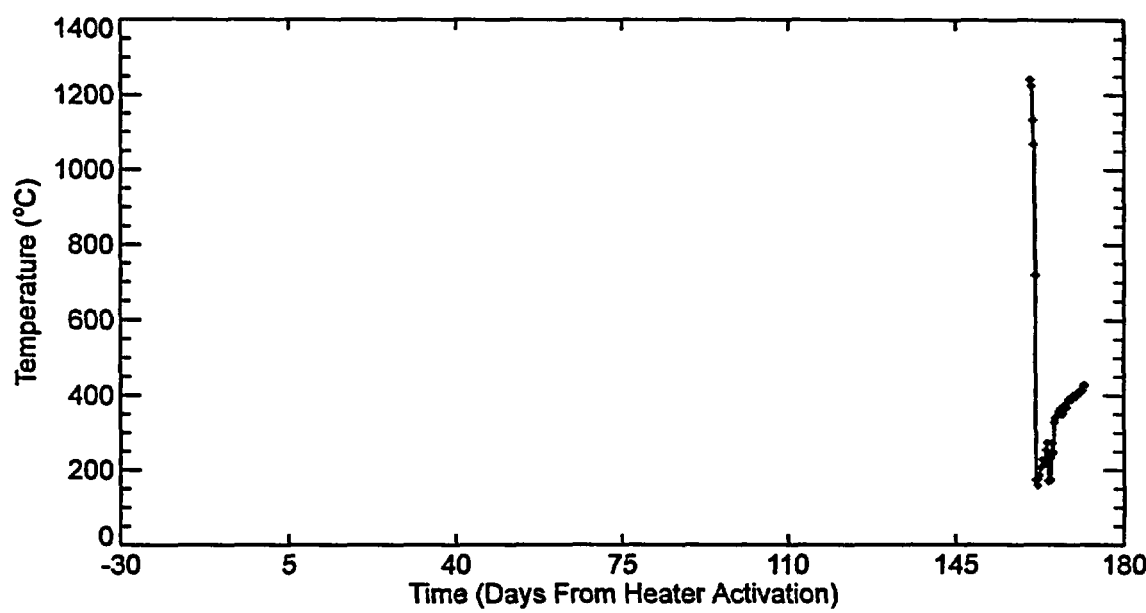


Figure D-71. Data from failed gage ESF-SDM-43-MPBX2-TC-4.

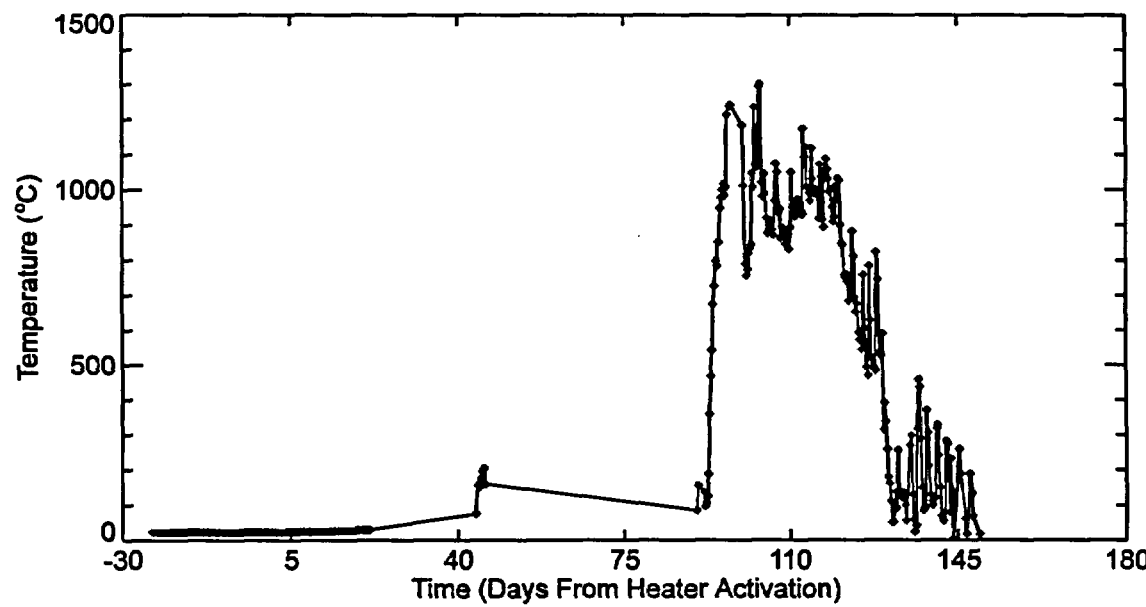


Figure D-72. Data from failed gage ESF-SDM-43-MPBX2-TC-5.

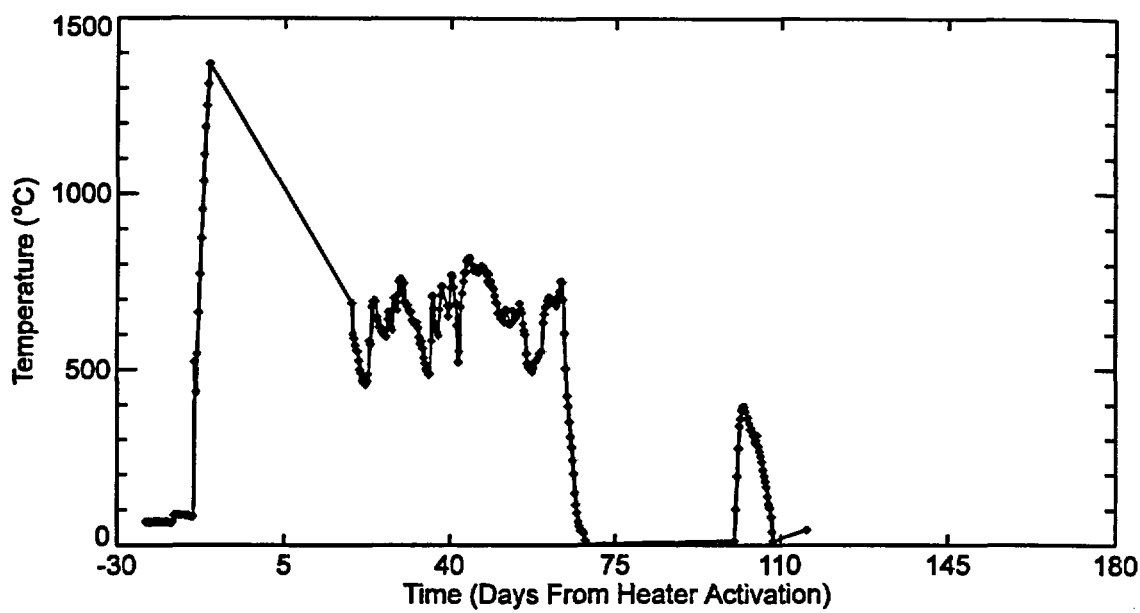


Figure D-73. Data from failed gage ESF-SDM-43-MPBX2-TC-14.

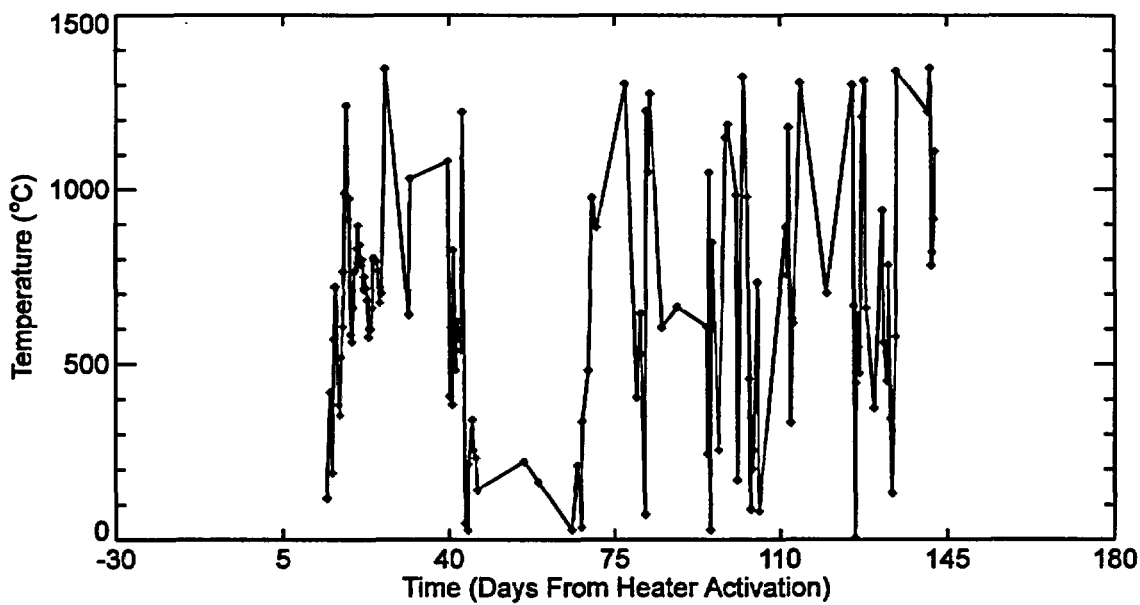


Figure D-74. Data from failed gage ESF-SDM-44-MPBX3-TC-9.

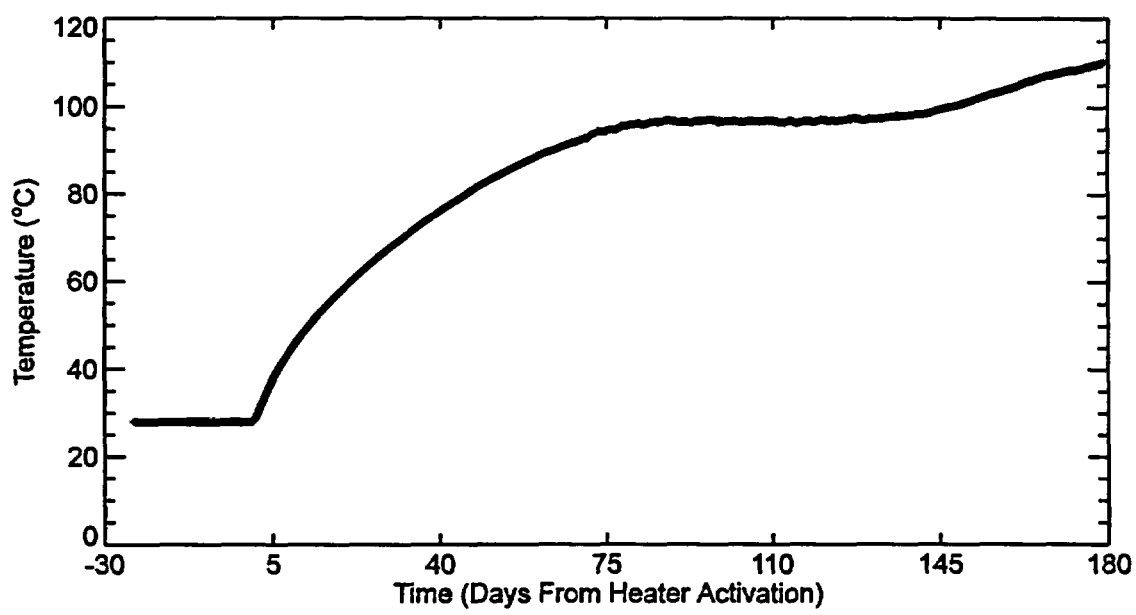


Figure D-75. Data from failed gage ESF-SDM-44-MPBX3-TC-13.

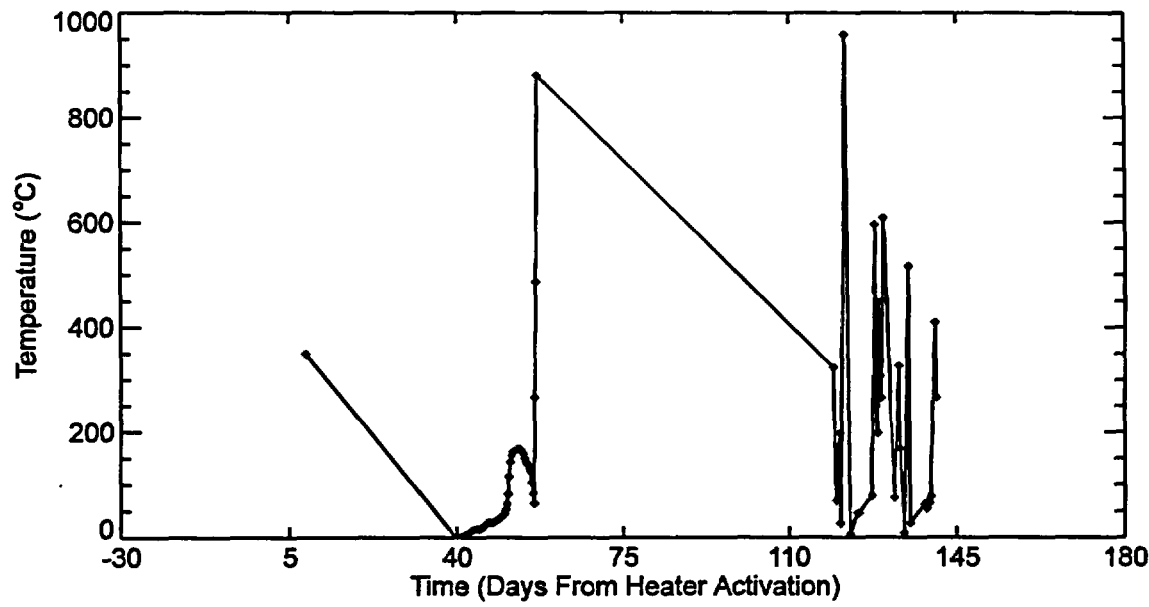


Figure D-76. Data from failed gage ESF-SDM-44-MPBX3-TC-14.

Appendix E

Interim Report on Creep Testing of Cast-In-Place Concrete

**Sandia National Laboratories
Albuquerque, NM 87185**

15 July 1998

**Technical Data Information Form 306911
Data Tracking Number SNL23030598001.002**

CONTENTS

1.0 Introduction	3
2.0 Specimen Acquisition	3
3.0 Experimental Procedure	4
3.1 Specimen Assembly.....	4
3.2 Pressure Vessel and Load Frame	5
3.3 Preliminary Tests	5
3.3.1 Tests of Strain Gage Epoxy.....	5
3.3.2 Temperature Distribution in Test Specimen	6
3.3.3 Trial Test.....	6
3.4 Constant Load (Creep) Test Procedure.....	7
3.5 Deviations of Test Procedure from ASTM C512-87.....	8
4.0 Test Results	9
4.1 Deformations during Heating and Stabilization	9
4.2 Elastic Moduli.....	14
4.3 Creep Strains.....	14
4.4 ASTM C512-87 Reporting Requirements.....	17
5.0 Discussion of Results	17
6.0 Summary and Conclusions	18
7.0 References	18

FIGURES

Figure 1. Strains versus time for specimen CIP5A	10
Figure 2. Strains versus time for specimen CIP16A	10
Figure 3. Strains versus time for specimen CIP20A	11
Figure 4. Strains versus temperature for specimen CIP5A	11
Figure 5. Strains versus temperature for specimen CIP16A	12
Figure 6. Strains versus temperature for specimen CIP20A	12
Figure 7. Creep strains versus time for CIP16A.....	15
Figure 8. Creep strains versus time for CIP19A.....	15
Figure 9. Creep strains calculated from external LVDTs versus time for CIP16A.....	16
Figure 10. Creep strains calculated from external LVDTs versus time for CIP16A.....	16

TABLES

Table 1. List of Milestone SP2540M4 and SP2932M4 Criteria	3
Table 2. Specimen Identification Numbers and Test Dates	4
Table 3. Test Matrix.....	7
Table 4. Preliminary Values Coefficients of Thermal Expansion.....	13
Table 5. Elastic Properties of CIP Concrete	14

1.0 Introduction

This report contains the interim results of a suite of laboratory tests (in progress) designed to assist in the characterization of materials used in the Drift Scale Test (DST) in the Thermal Testing Facility of the Exploratory Studies Facility (ESF) at Yucca Mountain, Nevada. A cast-in-place (CIP) concrete liner was emplaced in the Heated Drift before initiation of heating. As the drift is heated, the temperature of the concrete liner will increase. If the liner were unconstrained, then it would thermally expand. Because the liner is constrained by the surrounding rock, the thermal loading will generate stresses in the concrete. These stresses, however, will be partially relieved by creep of the concrete. This testing program was designed to assess the magnitude of the projected creep strains and the impact of these strains on the thermally-induced stresses. Eighteen test specimens were cast into specimen molds during emplacement of the CIP concrete liner used in the DST. The CIP specimens were allowed to cure below ground under the same conditions as the CIP liner. Ten of these specimens were used to determine unconfined compressive strength and static elastic moduli (Brodsky, 1998), and eight specimens were retained for determination of creep properties. Creep test data collected through 22 June 1998 are reported here.

This work was performed by Sandia National Laboratories (SNL) under Yucca Mountain Project WBS number 1.2.3.14.2. This document is being submitted to the technical information database under Technical Data Information Form (TDIF) 306911. It is also being submitted to the M&O as Appendix E of deliverable SP2540M4/SP2932M4 TDIF 306910. The completion of this document satisfies CRWMS M&O Level 4 Milestone SP2540M4 and SP2932M4. The criteria for this milestone are given in Table 1.¹

Table 1. List of Milestone SP2540M4 and SP2932M4 Criteria

SNL will perform creep and thermal expansion tests at ambient and elevated temperatures on concrete cylinders from the CIP liner in the Drift Scale Test. A progress report on the test results will be included in the Second Quarter TDIF (SP2540M4) and Draft DST Progress Report #1 (SP2932M4).	
Criteria for Milestone SP2540M4 and SP2932M4	Location
Thermal Expansion Test Data	Section 4.1
Creep Test Data	Section 4.3

2.0 Specimen Acquisition

Specimens were manufactured by casting CIP concrete into specimen molds at the time the CIP liner was constructed in the Heated Drift. Two types of concrete specimens were cast that differed in the amount of steel fiber reinforcement included in each mix. The specimens with low steel fiber content were cast on 8 April 1997, and those with high steel fiber content were cast on 26 April 1997, as specified in Table 2. The CIP specimens were allowed to cure below ground under the same conditions as the CIP tunnel liner. Concrete specimens were shipped

¹ All references to figures, tables, and report sections give here pertain to this appendix and not the main body of TDIF 306910.

from the Yucca Mountain Project Sample Management Facility (SMF) to SNL in Albuquerque on 1 December 1997.

Eighteen specimens were cast, 9 with low steel fiber content and 9 with high steel fiber content. Five specimens of each type were tested in a previous study (Brodsy, 1998). Of those, two specimens of each type were tested to failure in unconfined compression to measure elastic moduli and fracture strength, and three specimens of each type were cycled between 0 and 40% of failure strength for measurements of elastic moduli. The remaining 8 specimens (4 of each type) are being used in this study.

Creep test specimens are right circular cylinders with nominal dimensions of 203 mm (8 in.) in length and 101.6 mm (4 in.) in diameter. These specimens were subcored from the cast specimens, which were 305 mm (12 in.) in length and 152 mm (6 in.) in diameter. Creep test specimens were subcored and ground dry.

Specimens were assigned identification numbers by the SMF. Modifications to the identification numbers were made in accord with SNL QA Implementation Procedure (QAIP) 20-3 entitled "Sample Control." The SMF specimen identification number is correlated with an abbreviated form the test specimen identification number in Table 2.

Table 2. Specimen Identification Numbers and Test Dates

SMF ^(a) Specimen Identification	Abbreviated Creep Test Specimen Identification	Concrete Type (Low or High Steel Fiber Content)	Date of Specimen Casting	Start Date for Laboratory Test	Specimen Age at Start of Test (Days)
SPC00525005	CIP5A	Low	4-8-97	5-7-98	395
SPC00525016	CIP16A	High	4-26-97	5-9-98	388
SPC00525019	CIP19A	High	4-26-97	5-29-98	398
SPC00525020	CIP20A	High	4-26-97	6-3-98	403

(a) SMF: Sample Management Facility

3.0 Experimental Procedure

3.1 Specimen Assembly

Four electrical resistance strain gages were bonded to each test specimen using a high temperature epoxy. Two strain gages, each 122 mm (4.8 in.) long, were oriented parallel to the specimen axis, centered at the specimen midheight, and applied 180° apart. The two circumferential gages, each 101.6 mm (4-in) in length, were mounted perpendicular to axis of the specimen midheight and on opposing sides. The surfaces underneath the strain gages were prepared by filling surface irregularities with high temperature epoxy mixed with grout. A special low viscosity epoxy was used that cures at room temperature but can be used at temperatures up to 260°C.

Specimens were placed between two endcaps and then placed in flexible Viton jackets to prevent the silicon oil confining fluid from penetrating the specimen. The upper endcap was vented to the atmosphere through a central 1.27 mm (0.050 in.) diameter hole. The upper endcap

contained channels that provided pathways for steam to reach the vent from the specimen/jacket interface. Copper foil strips were placed between the Viton jacket and the channel entryways so that they could not be sealed by the Viton.

3.2 Pressure Vessel and Load Frame

A triaxial test system was used comprising a pressure vessel and load frame. The specimen assembly was placed inside the pressure vessel, which was then filled with silicone oil. For tests requiring confining pressure, the silicone oil is pressurized. For these tests at ambient pressures, the silicone oil functioned as a heat transfer medium and facilitated transfer of heat to the specimen. An actuator provided hydraulic pressure to the loading column and axially loaded the specimen. Heaters were located in the upper section of the pressure vessel, the midsection, and inside the lower piston that enters the pressure vessel. These three heated zones were controlled independently. Temperatures were maintained to within $\pm 1^{\circ}\text{C}$ with set-point controllers that regulated power to the heaters. SNL's creep test systems are located in an interior room in which temperature is maintained constant to within $\pm 1^{\circ}\text{C}$.

Axial force was measured by a load cell in the loading column external to the pressure vessel. Specimen deformations were measured using strain gages as described in Section 3.1 and also using Linear Variable Differential Transformers (LVDTs) located below the pressure vessel. The LVDTs monitor displacement of the loading piston relative to the bottom of the pressure vessel and can be used to calculate axial specimen strains when the system is at constant pressure and temperature. Axial force, strains, LVDT displacements, and temperatures were measured at regular intervals by a computerized data acquisition system.

3.3 Preliminary Tests

Before tests were conducted on concrete test specimens, several tests were conducted to assess the effectiveness of the strain gage epoxy and to determine the best method of evenly heating the specimens in the test frames.

3.3.1 Tests of Strain Gage Epoxy

Strain gages were purchased from BLH Electronics. The epoxies sold by BLH and other strain gage manufacturers for strain gage use at 200°C all require curing at elevated temperature. This posed a dilemma because thermal expansion measurements were required during the first heating cycle. If the bonding agent required heat for curing, then an initial heating cycle would have to be conducted during which no useful data could be collected. Thermally cycling the concrete before applying axial load was also undesirable. A search was therefore conducted for alternative epoxies and Duralco 4461 epoxy was found and selected. This epoxy cures at room temperature and can be used to 260°C . It has low viscosity and is used in high temperature applications requiring thin bonds.

Several tests were conducted to test the effectiveness of Duralco 4461 epoxy. In the first test, six strain gages were applied to a cylindrical specimen with known elastic properties (titanium alloy Ti-6Al-4V). Two strain gages were bonded using BLH's EPY-500 epoxy for use up to 260°C . The epoxy was cured at elevated temperature as per the manufacturer's specifications and essentially served as the control adhesive. Two strain gages were then bonded using M-Bond

300 epoxy made by Micromeasurements Group. This epoxy cures at approximately room temperature and can be used for applications up to 150°C. This adhesive was difficult to use and did not stick reliably to the strain gages, causing failure of one of the two gages. The two remaining strain gages were applied using Duralco 4461 and cured at room temperature. The specimen was loaded in compression to determine elastic moduli at room temperature. It was then heated to 250°C. Elastic moduli were remeasured at approximately 250°C, at 150°C, and at room temperature as the specimen cooled. The strain gages bonded with Duralco 4461 epoxy provided moduli that were in accord with published values at all temperatures and performed at least as well as those bonded with EPY-500 epoxy.

The second epoxy test was conducted using a remnant of CIP concrete that had been removed from the end of a test specimen when it was machined down in size from 305 mm (12 in.) to 203 mm (8 in.) in length. Three strain gages were bonded to the concrete remnant using the same procedure as described above for the titanium specimen. The specimen was then heated to 200°C and the strain gage outputs were monitored for consistency for several days. Comparison of outputs and visual examination of the strain gages showed no evidence of detachment of the strain gage that had been bonded using Duralco 4461 epoxy.

3.3.2 Temperature Distribution in Test Specimen

A CIP concrete specimen that had been cycled to 40% of its unconfined compressive strength in a previous study (Brodsky, 1998) was used to determine the temperature setpoints required to evenly heat a test specimen. The concrete specimen was reduced in size to that used for creep tests. Three small-diameter (4–5 mm) holes were drilled from one side of the sample to its axis to accommodate thermocouples. The holes were located 12.7 mm from the top of the specimen, 12.7 mm from the bottom of the specimen, and at midheight. A fourth hole was drilled 12.7 mm into side of the specimen at midheight to measure temperature near the outer circumference. The pressure vessels were provided with three independently heated zones. The setpoints for each heater were determined such that temperature gradients within the specimen were minimized at each potential test temperature. This was repeated for each pressure vessel and test frame. The maximum temperature variations within the specimen (at an average specimen temperature of 200°C) were 1.5–3°C for the type of test frame used for CIP5A, CIP16A, and CIP20A, and 5–6°C for the type of test frame used for CIP19A. CIP19A is a room temperature test and so its temperature variations are expected to be well within 1°C. The setpoints determined during these temperature calibrations were used during testing; however, a measurement thermocouple was also placed alongside the test specimen as an additional check of specimen temperature.

3.3.3 Trial Test

The first test was conducted on specimen CIP5A. The specimen assembly was placed in a pressure vessel and heated to 200°C at a heating rate of 3°C/hour. This is well below the heating rate of 17°C/hour used by Oland et al. (1980) on larger test specimens and also lower than the 4°C/hour rate suggested by the M&O (1998) for assessment of concrete properties at elevated temperatures. During heating from approximately 100°C to 200°C, steam was not able to exit the vent in the upper platen as quickly as it was generated. The flexible Viton jacket apparently inflated, pushing a large volume of silicone oil out of the vessel. The jacket developed a leak and

silicone oil penetrated the test specimen. When the specimen jacket was removed the strain gages could be visually examined. Small gas or steam bubbles had apparently formed under one of the axial strain gages. This test experience was very valuable in that it led to modifications of the specimen assembly and test procedure. The modifications included the addition of channels in the upper platen to facilitate fluid and steam transfer to the vent, a reduction of the heating rate, and the addition of two constant temperature stabilization periods near boiling.

3.4 Constant Load (Creep) Test Procedure

In a constant load or creep test, a constant load is applied to a specimen under a set of controlled environmental conditions. The resulting time-dependent strains induced by the load application are measured. The procedure used here follows that given in ASTM C512-87, *Standard Test Method for Creep of Concrete in Compression* except as noted in this report (Section 3.5). The ASTM standard does not address elevated temperature tests.

The test matrix is given in Table 3. Each concrete type will be tested using at least two stress levels at a single temperature (200°C) and two temperatures at a single stress level (30% of short term strength). If time permits, multistage tests will be conducted to obtain data at additional conditions. As an example, if the strain rates on CIP19A become so low that further changes are not measurable, then the stress or temperature will be increased to obtain additional data.

Table 3. Test Matrix

Specimen ID	Concrete Type	Temperature	Creep Stress ^(a)	Status
CIP19A	High steel fiber content	20°C	30%	In Progress
CIP16A	High steel fiber content	200°C	30%	In Progress
CIP20A	High steel fiber content	200°C	50%	In Progress
CIP5A	Low steel fiber content	200°C	N/A ^(c)	Terminated
TBD ^(b)	Low steel fiber content	20°C	30%	Planned
TBD ^(b)	Low steel fiber content	200°C	30%	Planned
TBD ^(b)	Low steel fiber content	200°C	50%	Planned

(a) Stress values are given as a percentage of the room-temperature unconfined compressive strength determined in a previous study (Brodsky, 1998). No elevated temperature failure strength data were available. Strength values for the two levels of fiber reinforcement were not significantly different, so values were averaged to obtain a strength of 55.5 MPa. A 30% load is therefore 16.6 MPa and a 50% load corresponds to 27.7 MPa.

(b) TBD: To be Determined

(c) Not applicable. This test was terminated before load was applied.

Test specimens were assembled as described in Section 3.1 and placed in the pressure vessel. For tests conducted at 200°C , specimens were heated at approximately $3^{\circ}\text{C}/\text{hour}$ until a temperature of 98°C was reached. The heating rates for the individual heated zones varied so that they all reached target temperatures at nearly the same time. Temperature was maintained for approximately 1 to 1.5 days to allow the moisture in the specimen to slowly equilibrate at just above boiling ($95\text{--}96^{\circ}\text{C}$ at the altitude of the testing laboratory). The specimen was then heated at $1^{\circ}\text{C}/\text{hour}$ to 110°C ($3^{\circ}\text{C}/\text{hour}$ for CIP16A), and temperature was again maintained for approximately 1 to 1.5 days to allow equilibration. Temperature was then raised at $1^{\circ}\text{C}/\text{hour}$

until the specimen reached 200°C. Temperature was maintained until either the strain gages and LVDTs reached stable values or load application was required to maintain the testing schedule. Test CIP16A was held at 200°C for 22 days and CIP20A was held for 17 days. The strain gage outputs were still changing with time when the specimens were loaded. Specimens were quickly loaded to the creep stress. Stress and temperature were maintained while deformations, load, and temperature were measured at preset time intervals.

3.5 Deviations of Test Procedure from ASTM C512-87

ASTM C512-87, *Standard Test Method for Creep of Concrete in Compression*, was developed for unconfined testing of concrete specimens at room temperature. The procedure followed here deviated from the ASTM procedure as follows:

- Axial Load: The ASTM procedure states that creep is proportional to stress from 0 to 40% of the concrete compressive strength. It therefore recommends that creep stress not exceed the 40% value. However, Neville (1996) states that the upper limit of proportionality is generally between 40% and 60% of the compressive strength. Creep tests on concrete performed by Oland et al. (1980) were conducted at 20% or 50% of the 28-day unconfined compressive strength. Because these are the first tests of this type to be performed on this CIP concrete, the test matrix was designed to optimize the differences in creep rates occurring under different conditions to see if differences were measurable. A higher stress level also better simulates the expected service condition of the CIP liner. An upper stress of 50% was therefore used rather than the ASTM limit.
- Specimen Size: ASTM C512-87 test method states that specimens should be 150 ± 1.6 mm ($6 \pm 1/16$ in.) in diameter and at least 292 mm (11.5 in.) in length. Maximum aggregate size should be no greater than 50 mm (2 in.). Alternative specimen size requirements for triaxial tests are given in ASTM C192-90a, *Standard Practice for Making and Curing Concrete Test Specimens in the Laboratory*. This procedure is cited in ASTM C801-91, *Standard Test Method for Determining the Mechanical Properties of Concrete Under Triaxial Loads*. ASTM C192-90a gives a minimum specimen size of 50 mm (2-in) in diameter and 100 mm (4-in) in length, providing that the specimen diameter is at least three times the maximum aggregate size. In these tests it was necessary to reduce the specimens' size to approximately 100 mm (4 in.) in diameter and 200 mm (8 in.) in length so that they could be accommodated by the pressure vessels. The maximum aggregate size is approximately 19 mm (0.75 in.), but most of the aggregate is substantially smaller. The test specimens used here meet the aggregate size requirements of ASTM C512 and the size requirements of ASTM C192-90a and ASTM C801-91.
- Strain Gage Length: ASTM C512 requires strain gages to be at least three times the maximum aggregate size but less than the specimen length minus one specimen diameter. This would require the strain gages to be greater than 57 mm (2.25 in.) to meet the aggregate size requirement and less than 102 mm (4 in.) to meet the specimen dimension requirement. The axial strain gages are 122 mm (4.8 in.) and the circumferential gages are 102 mm (4 in.). The lateral strain gages are within specifications and the axial gages are very close to the required range. The slightly longer axial gages could be minimally affected by end constraints.

- Number of Specimens Tested: ASTM C512 calls for casting a minimum of six nominally identical specimens. Two are to be tested for strength, two for creep properties, and two would function as control specimens for measurement of further curing. Two nominally identical specimens were tested for strength properties at room temperature (Brodsky, 1998) between 1/30/98 and 2/10/98. At that time the specimens had been curing for approximately 280–310 days. Insufficient specimens were cast and insufficient machine time was available to measure deformations of control specimens under the same temperatures as the creep test specimens or to measure strength at elevated temperature.
- Casting and Curing: ASTM C512 provides a standard curing sequence; however, it states that other curing conditions may be substituted when information is required for specific applications. The curing process used for these specimens was not standard but instead was designed to best simulate the curing process to which the CIP tunnel liner was subjected.
- Age at Loading: According to ASTM C512 the compressive strength is to be determined immediately before loading the creep specimens. This was not feasible because of the small number of available test specimens. The compressive strengths were determined approximately 4–5 months before initiation of the creep tests; however, the specimens were 280–310 days old at the time the strength tests were performed. The curing process is most rapid in young concrete and asymptotically approaches full cure.
- Test Duration: ASTM C512 states that creep test durations should be one year. The Yucca Mountain Project schedule did not include such long-duration tests; however, the creep rate slows over time. Once the creep rate has slowed sufficiently that additional creep rate reductions are below the resolution of the instrumentation, or below the noise level associated with very small thermal fluctuations, then the test can be terminated with a minimal loss of useful data.

4.0 Test Results

4.1 Deformations during Heating and Stabilization

Strain versus time curves are shown for specimens CIP5A, CIP16A, and CIP20A in Figures 1, 2, and 3, respectively. Only the heating and thermal stabilization periods are shown. As noted in the text, a jacket leak was surmised for CIP5A and so the test was cooled and terminated. One axial gage failed on CIP20A at approximately one day test duration. Strain versus temperature curves are given in Figures 4, 5, and 6 for CIP5A, CIP16A, and CIP20A, respectively.

Between room temperature and 95°C the strain-versus-temperature curves are reasonably linear. Linear fits to the strain-versus-temperature data over this range provided coefficients of thermal expansion (CTEs) shown in Table 4. The coefficients are approximately 13–14 $\mu\epsilon/^\circ\text{C}$ (where $\mu\epsilon$ is microstrain) for axial expansion and 16–17 $\mu\epsilon/^\circ\text{C}$ for lateral expansion. A verification of the thermal corrections is currently being conducted for the different types of strain gages. It is currently not known if the difference between axial and lateral value CTEs results from an incorrect strain gage thermal correction or if it is real.

One potential source of anisotropy is the steel fibers. Visual observation of finished specimens does not provide sufficient information to assess the orientation or lengths of the fibers.

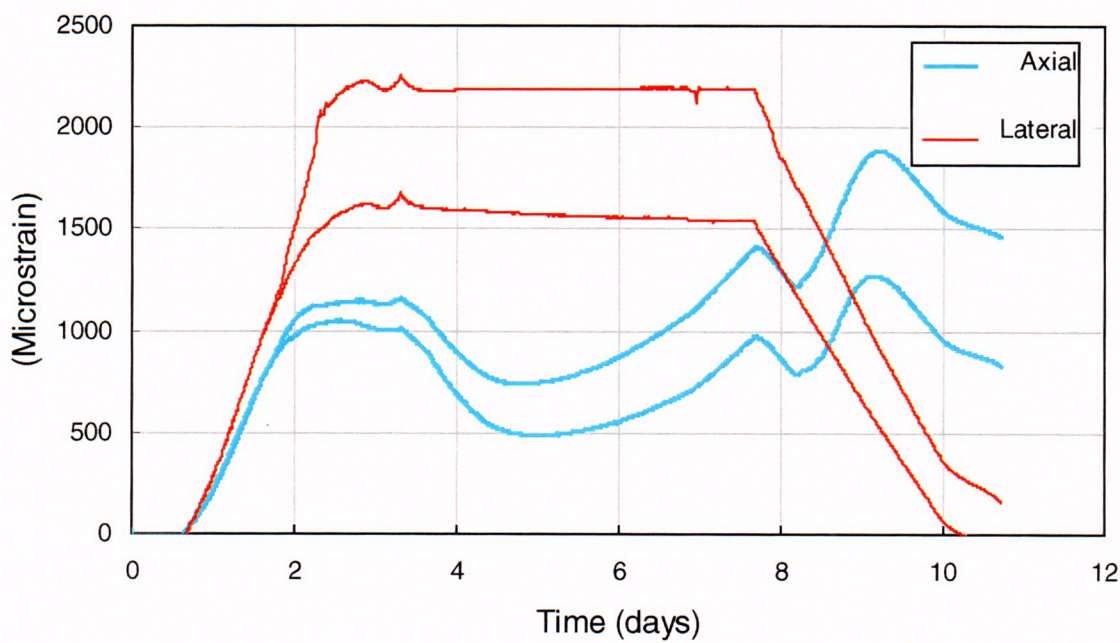


Figure 1. Strains versus time for specimen CIP5A during heating, stabilization at 200°C, and cooling. The specimen reached 100°C at 1.8 days, 200°C at 3.3 days, and began cooling at 7.7 days.

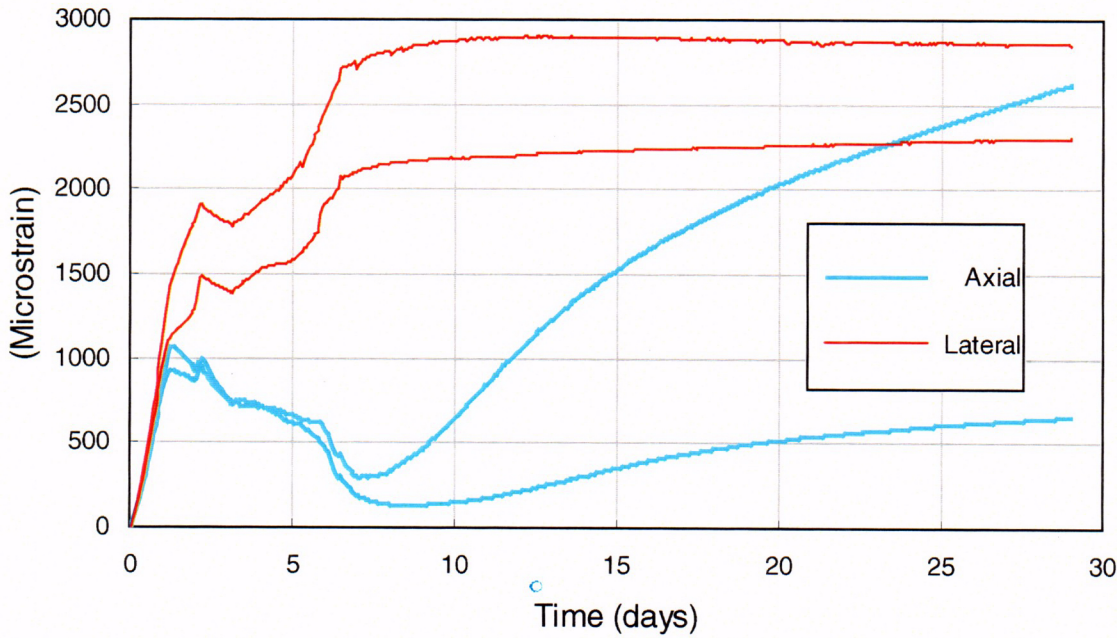


Figure 2. Strains versus time for specimen CIP16A during heating, stabilization at 200°C, and cooling. The specimen reached 98°C at 1.2 days, was heated from 98 to 110°C between 2.1 and 2.3 days, remained at 110°C until 3.1 days, and reached 200°C at 7.1 days.

C 82

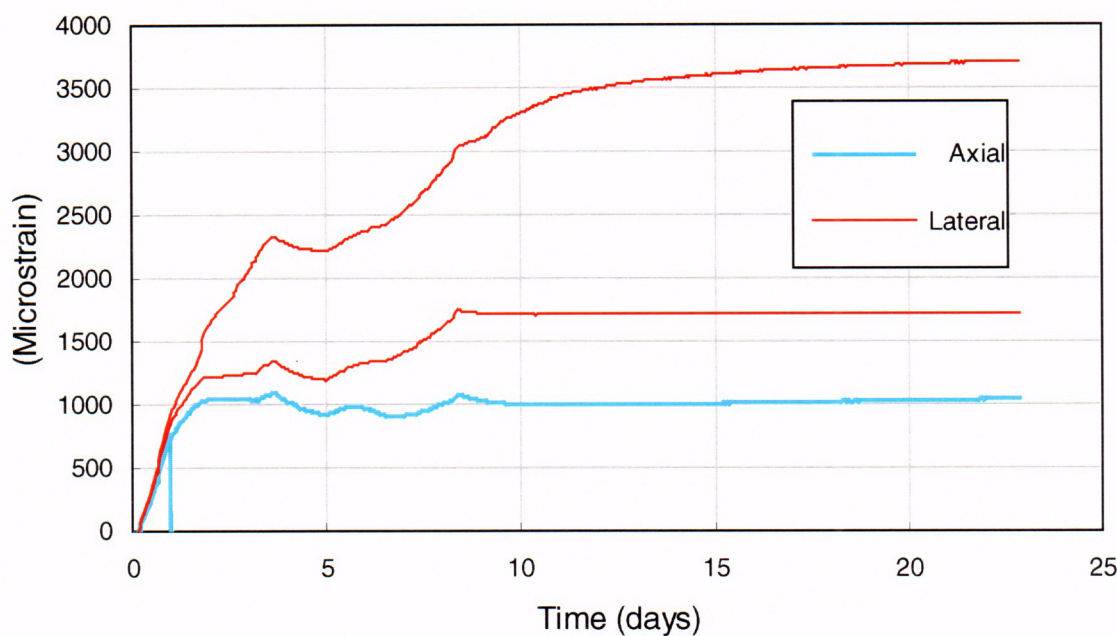


Figure 3. Strains versus time for specimen CIP20A during heating, stabilization at 200°C, and cooling. The specimen reached 98°C at 1.7 days, was heated from 98 to 110°C between 3.3 and 3.8 days, remained at 110°C until 5.0 days, and reached 200°C at 8.4 days. One axial gage failed at 1.0 days.

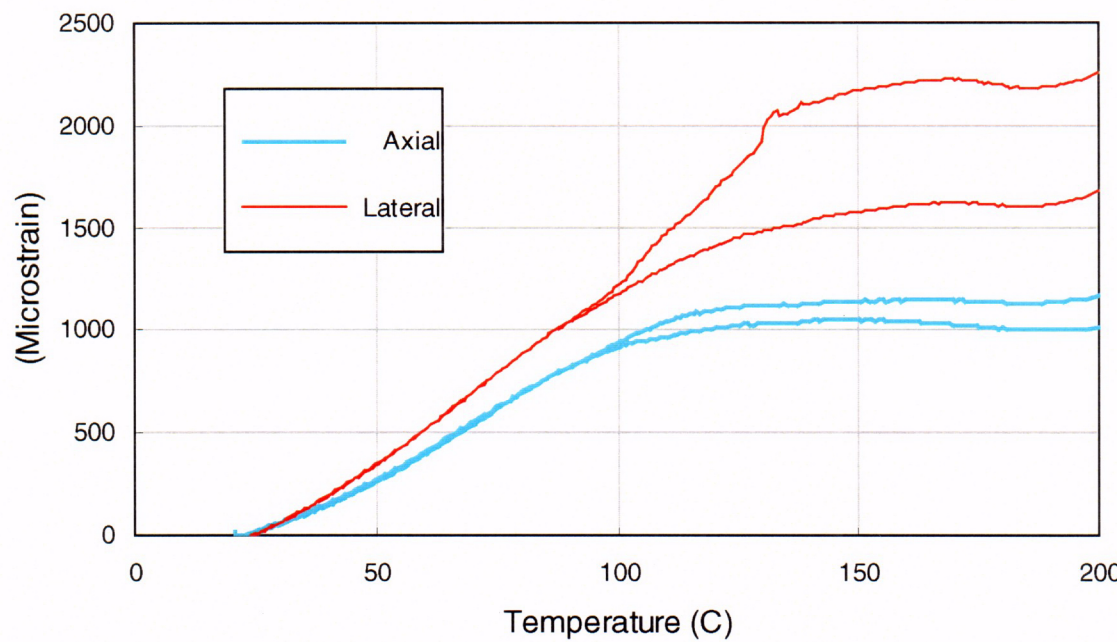


Figure 4. Strains versus temperature for specimen CIP5A during heating.

C 83

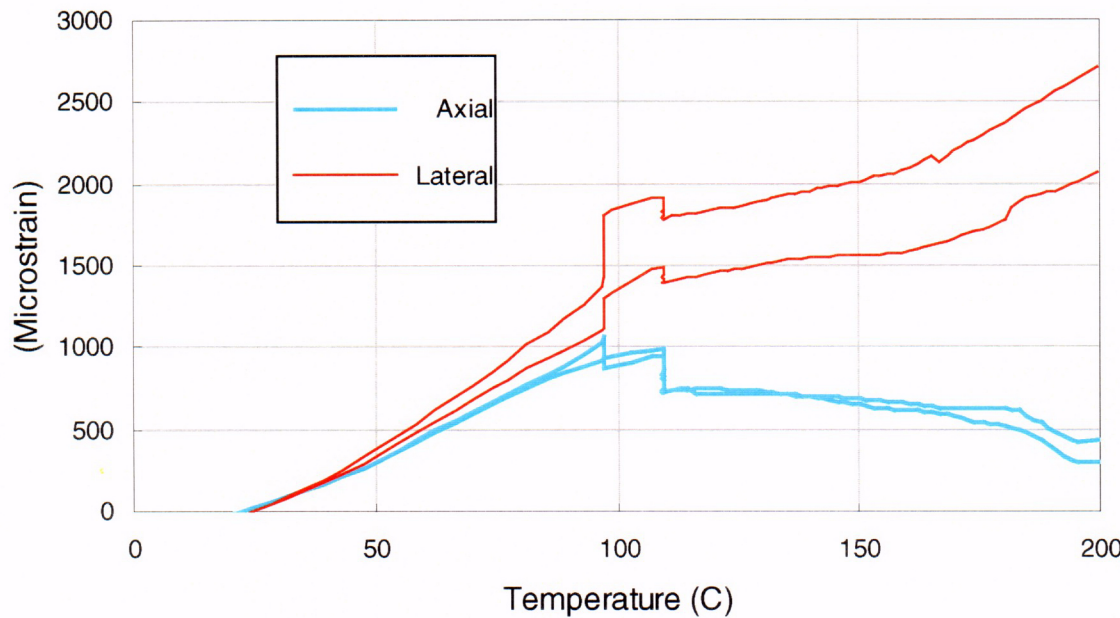


Figure 5. Strains versus temperature for specimen CIP16A during heating.

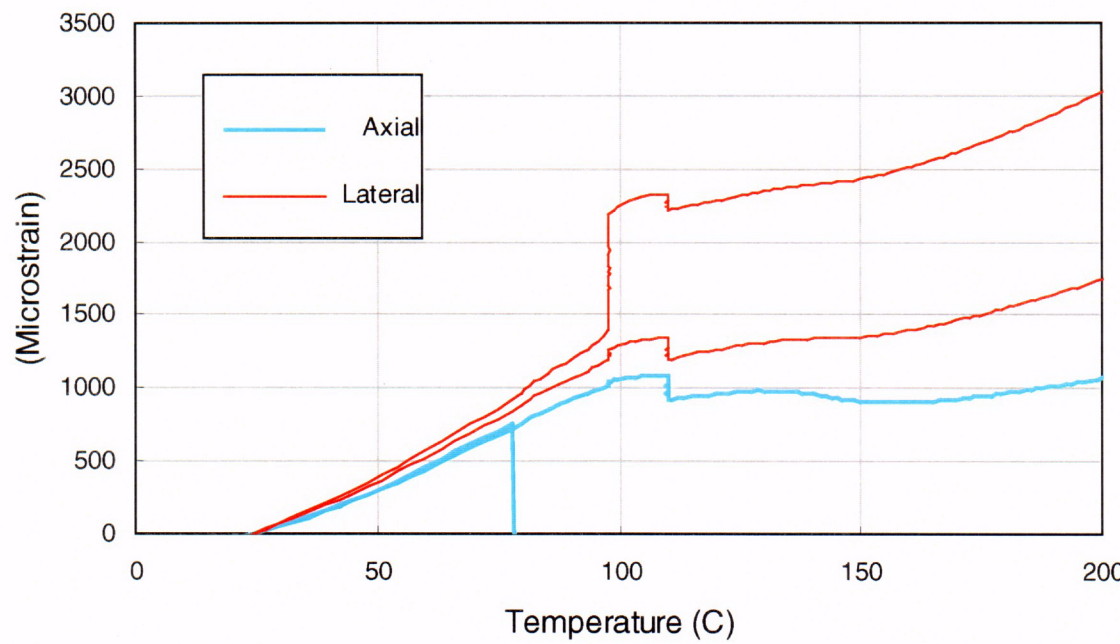


Figure 6. Strains versus temperature for specimen CIP20A during heating.

C 84

Limited observations of failed specimens tested previously show that the fibers are up to 100 mm long and are hooked or folded at one end. The fiber length is 0.67 of the diameter of the original specimen molds (150 mm). It is possible that the fibers became preferentially oriented during casting or rodding of the specimens.

Table 4. Preliminary Values Coefficients of Thermal Expansion

	CIP5A ($\mu\epsilon$)	CIP16A ($\mu\epsilon$)	CIP20A ($\mu\epsilon$)
Axial CTE ($\mu\epsilon/^\circ\text{C}$)	13	13	14
Lateral CTE ($\mu\epsilon/^\circ\text{C}$)	16	17	17

Specimens CIP16A and CIP20A were permitted to stabilize at 98°C. During this time, CIP16A showed shrinkage in the axial direction and expansion in the lateral direction. CIP20A showed small expansions for one axial and one lateral strain gage and larger expansion on the other lateral gage. It is inferred that some shrinkage is taking place in CIP16A associated with dehydration of the specimen. The mechanism for expansion at constant temperature is not known. The epoxy used to bond the strain gages will be further investigated to be sure that its behavior is stable.

As temperature is raised from 98 to 110°C both specimens show thermal expansion. During stabilization at 110°C both specimens also show consistent shrinkage. As specimens are heated from 110 to 200°C. CIP16A shows clear shrinkage in the axial direction yet expansion in the lateral direction. CIP20A shows essentially no net change in axial strain (i.e., thermal expansion and shrinkage rates are approximately equal) and some lateral expansion.

A collection tube was used to trap moisture that evolved from CIP20A as it heated from room temperature to 200°C. The objective of this addition to the testing program was to measure the total volume of liquid generated. Liquid volumes were not monitored at regular temperature intervals; however, some observations were made. Very little moisture condensed between room temperature and 98°C. Liquid generation accelerated as the specimen was heated to 110°C and liquid accumulation continued throughout heating up to 200°C. A total of approximately 130 ml were collected between room temperature and 200°C, and as much as another 10 ml evolved early in the stabilization phase at 200°C.

Perhaps the most puzzling behavior observed in the heating cycles is the response recorded at a constant temperature of 200°C. It was anticipated that some shrinkage might occur but that stable strain values would be achieved. Specimen CIP5A showed stable lateral strains, but showed axial shrinkage followed by axial expansion. At the time CIP5A was run, this behavior was attributed to a jacket leak. Test CIP16A was run subsequently and similar behavior was observed. The lateral strains showed some expansion but reached stable values within approximately 5 days. The axial strains, however, both showed initial shrinkage followed by expansion. Test CIP20A showed stable lateral strains or lateral expansion stabilizing within approximately 5 days, and again, axial shrinkage followed by a very small amount of axial expansion. The axial expansion in CIP20A is on the order of tens of microstrain over a time period of 17 days, whereas in CIP16A it is on the order of hundreds (on one axial gage) to over

2000 microstrain (on the other axial gage) over 22 days. Further tests will be conducted on the Duralco 4461 epoxy to be sure that this is not an effect of the strain gage bonding agent. There are insufficient LVDT data from CIP16A for comparison with the strain gages. LVDT data from CIP20A show small compressive strains during stabilization at 200°C.

4.2 Elastic Moduli

Elastic moduli (Young's modulus and Poisson's ratio) were calculated when axial loads were applied to specimens CIP19A and CIP16A. Shortly after load was applied to CIP16A a hydraulic valve malfunctioned. The specimen had to be unloaded for approximately 20 minutes while repairs were performed. For that specimen, elastic moduli were calculated for the initial loadup and also the unload and reload cycle associated with the valve repair. The data are shown in Table 5. This table also shows elastic moduli determined on this concrete during unconfined compression tests at room temperature (Brodsky, 1998). The moduli determined during the creep tests are very consistent with one another but are lower than the moduli determined during unconfined compression tests. The creep test moduli were determined between 50 $\mu\epsilon$ (axially) and 30% of unconfined compressive strength, whereas the other moduli were determined between 50 $\mu\epsilon$ (axially) and 40% of unconfined compressive strength. This difference should not cause the moduli measured during creep tests to be low.

Table 5. Elastic Properties of CIP Concrete^(a)

	Brodsky, 1998	CIP19A Loading	CIP16A Loading	CIP16A Unloading	CIP16A Reloading
Young's Modulus (GPa)	33.6 ± 1.7	26.6	25.8	28.8	30.9
Poisson's Ratio	0.25	0.31	0.35	0.27	0.27

(a) All specimens are from the CIP batch with higher steel fiber content.

4.3 Creep Strains

Creep strains versus time are given in Figures 7 and 8 for CIP16A and CIP19A, respectively. Both specimens are at the same axial load, but CIP16A is at 200°C whereas CIP19A is at 20°C. For CIP16A, lateral strain gages showed extension and both axial gages showed initial compression, as expected. The CIP16A axial strain gage that had shown an extensional strain rate at a constant temperature of 200°C appears to be well bonded to the concrete because both axial strain gages provided very comparable and reasonable Young's modulus values during loading. However, the strain gage then continued to extend during the creep portion of the test. The remaining axial strain gage began to extend after 2 days under load. CIP19A at room temperature shows very reasonable creep data. Lateral expansion and axial compression were measured, with strain rates decreasing as a function of time. As expected, comparison of Figures 7 and 8 shows that initial creep strains are higher at elevated temperature than at room temperature.

The displacements measured by the LVDTs were converted to specimen strain and are shown in Figures 9 and 10 for CIP16A and CIP19A, respectively. The LVDTs for CIP16A show larger axial strains than the bonded axial strain gages, whereas the LVDTs for CIP19A are very consistent with the axial strain data.

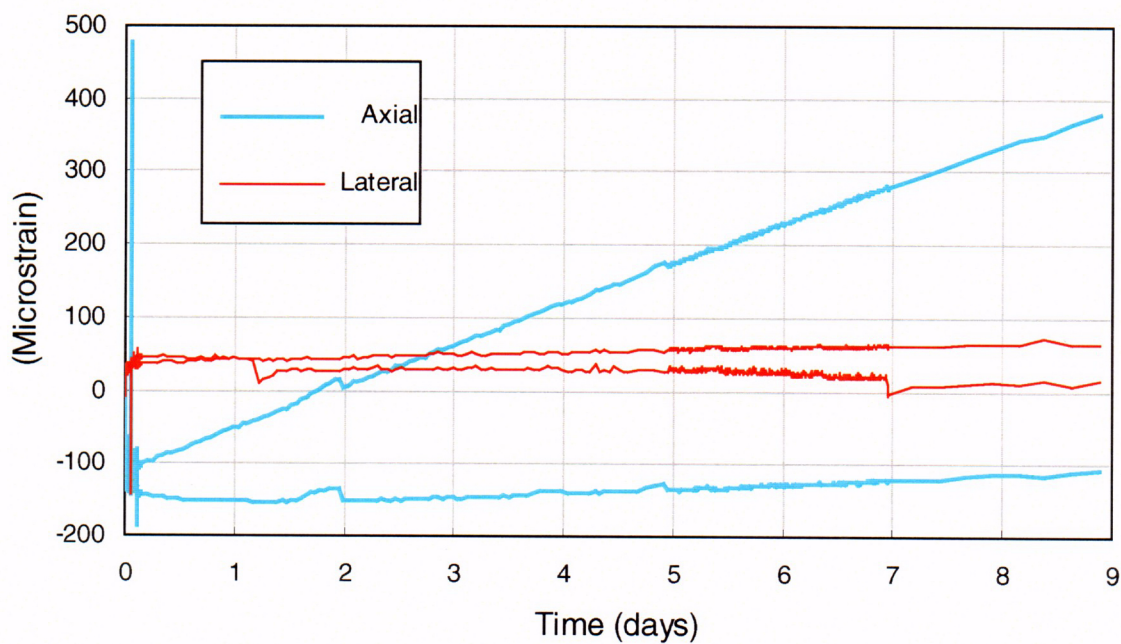


Figure 7. Creep strains versus time for CIP16A. Axial load is 16.6 MPa, temperature is 200°C.

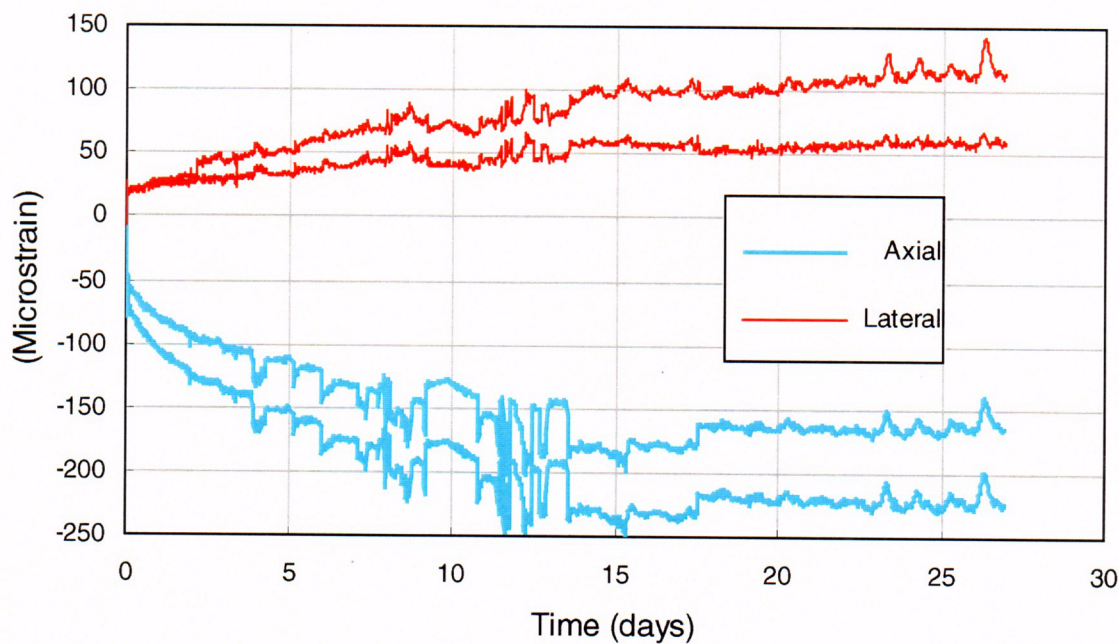


Figure 8. Creep strains versus time for CIP19A. Axial load is 16.6 MPa, temperature is 20°C.

C 85

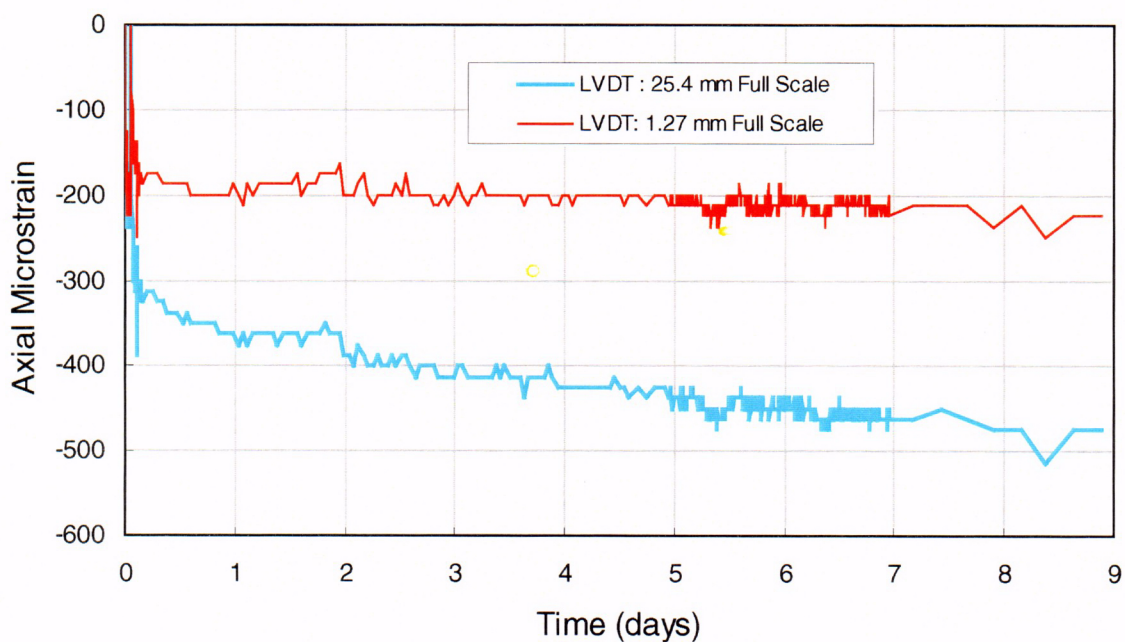


Figure 9. Creep strains calculated from external LVDTs versus time for CIP16A. Axial load is 16.6 MPa, temperature is 200°C.

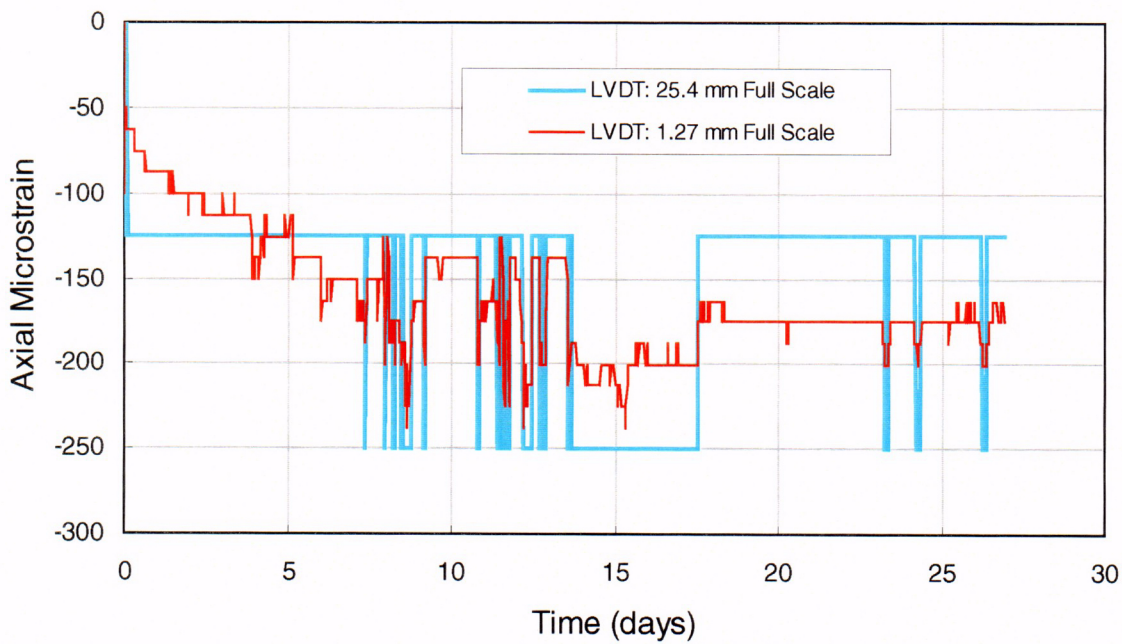


Figure 10. Creep strains calculated from external LVDTs versus time for CIP16A. Axial load is 16.6 MPa, temperature is 20°C.

① 86

4.4 ASTM C512-87 Reporting Requirements

ASTM C512-87, *Standard Test Method for Creep of Concrete in Compression*, includes reporting requirements. Some of these requirements pertain to the casting of the specimens, and these data should be in the possession of the M&O. Inquiries will be made to obtain this information for the final report. The reporting requirements are addressed as follows:

- Cement content, water-cement ratio, maximum aggregate size, slump, and air content: Outside of laboratory scope. These data should have been retained by the M&O during casting of the specimens and will be addressed in the final report. Maximum aggregate size is approximately 19 mm.
- Type and source of cement, aggregate, admixture, and mixing water (if other than fresh water is used): Outside of laboratory scope. These data should have been retained by the M&O during casting of the specimens and will be addressed in the final report.
- Position of cylinders when cast: Outside of laboratory scope. These data should have been retained by the M&O during casting of the specimens and will be addressed in the final report.
- Storage conditions prior to and subsequent to loading: Specimens were stored on site underground until shipment to SNL so that the samples would cure under the same conditions as the CIP tunnel liner. Once at SNL they were kept in a storage building where temperature did not drop below 10°C.
- Age at time of loading: See Table 2.
- Compressive strength at age of loading: Not directly measured. Two nominally identical high steel fiber content and two nominally identical low steel fiber content specimens were tested for strength properties (Brodsky, 1998) between 1/30/98 and 2/10/98. At that time the specimens had been curing for approximately 280–310 days.
- Type of strain measuring device: Electrical resistance strain gages were bonded to the specimens, and external LVDTs were also used to measure axial strain.
- Magnitude of any preload: Approximately 0.1– 0.2 MPa.
- Intensity of applied load: See Table 3.
- Initial elastic strain: See Table 5.
- Creep strain per pound per square inch (or kilopascal) at designated ages up to one year: This will be addressed in final report when the full creep curves are presented.
- Creep rate, if determined: This will be addressed in final report when the full creep curves are presented.

5.0 Discussion of Results

The results accumulated to date are insufficient to draw conclusions about the magnitudes of CIP concrete creep rates or their dependence on temperature and stress difference. These issues will be addressed in the final report.

One unexpected observation was that the strain gages all show evidence of expansion under constant conditions at 200°C. Further evaluations of the strain gage epoxy will be made to ascertain that these observations are real and not artifacts of the test setup. It is also possible that some mineralogical changes might be associated with expansion. Evidence of this could be obtained from petrographic and x-ray diffraction analyses.

The strain gages also indicate anisotropic behavior of the concrete. Again, additional testing will be performed to verify the strain gage temperature corrections and to further assess the efficacy of the strain gage epoxy. Anisotropy could result from preferred orientation of the steel fibers in the concrete. This may be evaluated from systematic observations of the specimens and from measurements of ultrasonic velocities. These tests will be performed for the final report.

6.0 Summary and Conclusions

A suite of creep tests has been initiated on CIP concrete specimens that were cast at the time that the CIP concrete liner was emplaced in the Heated Drift in Yucca Mountain. Preliminary data have provided coefficients of thermal expansion in the range of 13–17 $\mu\text{e}/^\circ\text{C}$. Creep has been measured at 30% of unconfined compressive strength and at temperatures of 20 and 200°C.

7.0 References

- ASTM (American Society for Testing and Materials). 1993. *Standard Test Method for Creep of Concrete in Compression*, ASTM C512-87. Philadelphia, Pennsylvania: American Society for Testing and Materials.
- ASTM (American Society for Testing and Materials). 1993. *Standard Practice for Making and Curing Concrete Test Specimens in the Laboratory*, ASTM C192-90A. Philadelphia, Pennsylvania: American Society for Testing and Materials.
- ASTM (American Society for Testing and Materials). 1993. *Standard Test Method for Determining the Mechanical Properties of Concrete under Triaxial Loads*, ASTM C801-91. Philadelphia, Pennsylvania: American Society for Testing and Materials.
- Brodsky, N. 1998. "Unconfined Compression Tests on Cast-in-Place Concrete Specimens from the Drift Scale Test Area of the Exploratory Studies Facility at Yucca Mountain, Nevada." Data Tracking Number (DTN) SNL23030598001.001. Technical Data Information Form (TDIF) No. 306714. MOL.19980518.0273-.0276.
- CRWMS M&O. 1998. "Civilian Radioactive Waste Management & Operating Contractor, Procurement Document for Procurement of Quality Affecting Laboratory Testing of Concrete Properties at Elevated Temperatures." BCAA00000-01717-1300-00001, Rev. 00. Las Vegas, Nevada: TRW Environmental Safety Systems. MOL.19980213.0345.
- Neville, A.M. 1997. *Properties of Concrete*, Fourth Edition. New York, New York: John Wiley and Sons, Inc. 454. TIC Catalog Number: 236567.
- Oland, C.B.; Naus, D.J.; Robinson, G.C. 1980. "Final Report of Comprehensive Testing Program for Concrete at Elevated Temperatures." ORNL/BRP-80/5. Oak Ridge, Tennessee: Oak Ridge National Laboratory 36 and 40. TIC Catalog Number: 233096.

Item Description:	Drift Scale Test Draft Status Report #1: Evaluation and Comparative Analysis of the Drift Scale Test Thermal and Thermomechanical Data (Results of 12/3/1997 Through 5/31/1998)
Availability:	<input checked="" type="checkbox"/> Publicly Available <input type="checkbox"/> Non-Publicly Available
Sensitivity:	<input checked="" type="checkbox"/> Non-Sensitive <input type="checkbox"/> Non-Sensitive-Copyright <input type="checkbox"/> Sensitive <input type="checkbox"/> Sensitive-Copyright
Electronic Media Type: (If applicable)	Microfiche CD-Rom Non-ADAMS compliant
Contact:	US Nuclear Regulatory Commission Office of Nuclear Materials Safety and Safeguards Yucca Mountain Project Manager
Storage/File Location:	US Nuclear Regulatory Commission Office of Nuclear Materials Safety and Safeguards Two White Flint North Room T7- E34 11545 Rockville Pike Rockville, Maryland 20852-2738